BIBLIOGRAPHIC DATA SHEET	1. Report No. BuMines OFR 74-73	2.	

4. Title and Subtitle
Influence of Mine Fires on the Ventilation of Underground Mines

5. Report Date
July 6, 1973

6. Performing Organization Code

7. Author(s)
Rudolf E. Greuer

8. Performing Organization Rept. No.

9. Performing Organization Name and Address
Michigan Technological University
College of Engineering
Department of Mining Engineering
Houghton, MI

10. Project/Task/Work Unit No.

11. Contract/Grant No.
S 0122095

12. Sponsoring Agency Name and Address
Office of Assistant Director--Mining
Bureau of Mines
U.S. Department of the Interior
Washington, DC 20240

13. Type of Report & Period Covered
University grant research, 1972-73

14. Sponsoring Agency Code

15. Supplementary Notes
Approved for release by Director, Bureau of Mines, November 28, 1973.

16. Abstracts
A comprehensive report was prepared dealing with the influence of accidental fires in underground mines on the ventilation of underground mines. The primary objective of the study was to obtain and evaluate all available information (mostly from foreign sources) dealing with methods of prediction of disturbances in a ventilation system by a mine fire. Particular aspects considered are: properties of mine fires, temperatures of fumes behind the fire zone, forces developed by fumes, qualitative and quantitative prediction of disturbances caused by fires. The compilation of results indicates that the interaction of ventilation flows and fires can be predicted with more accuracy than was previously assumed. The organized study and theoretical review contained in the report should be of great interest to mining engineers.

17. Key Words and Document Analysis. 17a. Descriptors

Mining
- Aerodynamic forces
- Analysis
- Air flow
- Coal mines
- Combustion products
- Computer programs
- Evaluation
- Flame propagation
- Fire fighting
- Mine fires
- Mine ventilation
- Reviews
- Smoke abatement
- Underground mining

17b. Identifiers/Open-Ended Terms

Mining and safety research

17c. COSATI Field/Group 08I

18. Distribution Statement
Release unlimited by NTIS.

19. Security Class (This Report) UNCLASSIFIED

20. Security Class (This Page) UNCLASSIFIED

21. No. of Pages

22. Price

USBM Contract No. S0122095

INFLUENCE OF MINE FIRES ON THE VENTILATION OF UNDERGROUND MINES

Rudolf E. Greuer

Principal Investigator

Michigan Technological University

College of Engineering

Department of Mining Engineering

USBM CONTRACT REPORT NO. S0122095

July 6, 1973

Bureau of Mines Open File Report 74-73

DEPARTMENT OF THE INTERIOR

BUREAU OF MINES

WASHINGTON, D. C.

ia

FOREWORD

This report was prepared by Michigan Technological University, College of Engineering, Department of Mining Engineering, Houghton, Michigan, under USBM Contract No. S0122095. The contract was initiated under the Coal Mine Health and Safety Program. It was administered under the technical direction of PM&SRC with Mr. R. Chaiken acting as the technical project officer. Mr. F. Pavlich was the contract administrator for the Bureau of Mines.

This report is a summary of the work recently completed as part of this contract during the period June 13, 1972 to June 13, 1973. This report was submitted by the author on June 8, 1973.

This technical report has been reviewed and approved.

It is hereby certified that no inventions have been made on this project.

The views and conclusions contained in this document are those of the author and should not be interpreted as necessarily representing the official policies of the Interior Department's Bureau of Mines or of the U.S. Government.

Contents

I. Introduction

Every mine contains inflammable materials, either in form of the minerals mined or in the form of brought-in supplies. Although great efforts are made to make mines as far as possible fireproof and to prevent ignition sources, the possibility of mine fires, like that of other accidents, will always continue to exist.

Detailed statistics are available for coal mines. They show (65,112) that the number of major mine fires in the USA over the last 20 years has remained more or less constant with approximately 50 per year. The same number is reported (26) for the British coal mines. Other countries (147) report about 1 major fire for every 10 million tons of coal production.

Conflicting data are published on the number of fatalities caused by fires, presumably because frequently deviating opinions on the cause of death exist. On the average (82,99) 4 miners are killed per year in the US and in the British coal mines. Although this number is much smaller than that for several other causes of fatalities, one must keep in mind that almost every small fire can develop into a large disaster.

The greatest hazards of mine fires are the poisonous and sometimes explosive products of combustion, carried by the ventilation through the mine. To combat this hazard, the paths the combustion products take must be known for the proper designation of escape routes and the safe and economic performance of fire fighting activities.

Predictions of the airflow distribution in a mine at fire are, however, complicated by the fact that the fire itself can cause, by the forces it develops, considerable ventilation disturbance. How large these disturbances are depends very much on the local circumstances. In some mining areas they are considered to be a very serious threat. Since they are frequently encountered and some larger mine disasters were due to unexpected airflow reversals, their determination is an integral part of all fire emergency plans. In other mining areas, mainly those where the mines have no large vertical extension, they are considered to be negligible compared with the disturbances caused by physical changes of the airways such as destroyed seals, ventilation doors or air blockage due to roof fall. It must, however, be admitted that the degree of necessity seen for taking into account ventilation forces developed by fires in emergency plans is also frequently a question of the accuracy expected from these plans.

Mining engineers have studied the interaction between ventilation and mine fires for several decades. The results are a greater number of methods to assess the ventilation forces developed by fires and their influence on a given ventilation system. Work in this direction has been revived by the wide use that computers have found in mine ventilation planning. Where ventilation network calculations with an hitherto unknown accuracy became routine, fire emergency plans based on network calculations soon became routine, too.

It can be expected that in the near future in the USA more emphasis than in the past will be placed on fire emergency plans which take the influence of fires on the ventilation into account. This report is an evaluation of all accessible information pertinent to this problem. It attempts to be a complete description of what has been done, not what the author thinks was necessary to do. Consequently, it contains little critique although the author has tried to group together those theoretical approaches and planning procedures which share a common concept, and to compare the results. The number of publications evaluated is considerably larger than indicated in the bibliography. Of publications with similar contents only one sample was usually listed.

There will, of course, be different opinions as to what information is pertinent. With as wide a field as this the report had to be limited to that information either coming from mining sources or being the common fund of all engineering branches.

As indicated above this report concentrates on the prediction of ventilation disturbances caused by mine fires for fire emergency plans. This finds it expression in the parts into which the report has been divided.

Following the first part, the introduction, the second part deals with the properties of mine fires and in particular with their dependence on ventilation conditions. Contrary to technical combustion processes, not too much is known about accidental mine fires. Research by mining engineers has concentrated mainly on investigating the effectiveness of fire fighting equipment and measures. In emergency plans usually fires of the worst possible state with the highest temperature ever observed are assumed. Still, some systematic research has been done and the results are presented. They can perhaps serve as the basis for fire simulations in future emergency plans.

Since the forces developed by mine fires are mainly thermal forces, the third part deals with the temperatures of air and combustion products (fumes) behind the fire. They are mainly influenced by the heat exchange with the airway walls. For their determination the considerable work done on the precalculation of temperatures due to heat flow from the walls to the air can be of help and this work, as far as applicable, is reviewed, too.

The fourth part then deals with the ventilation forces developed by the fumes. They are theoretically derived and the results compared with experimental observations.

In the fifth part the ventilation disturbances which can be caused by these forces are qualitatively discussed. The different types of ventilation plans and their usefulness for the prediction of ventilation disturbances are demonstrated. Examples of observed disturbances in accidental mine fires are given.

The sixth part describes the different approaches which are used

by ventilation engineers to make quantitative predictions. At first the methods, which require no network calculation and take into account only the airway at the fire and neighboring airways are explained. Then criteria to judge the stability of ventilation currents and rules to improve it are discussed. Finally the present practice of using analog and digital computers for the design of fire emergency plans is described and their potential investigated.

II. Properties of Mine Fires

The propagation of flames over the surface of combustible solids is an extremely complex process. In spite of the high sophistication the two competent disciplines, combustion and fire protection engineering and their auxiliary sciences, have reached, they still mainly rely on experimental evidence, at its best arranged in simplified semiempirical theories. Their applicability to mine fires is therefore very limited. Combustion engineering is not concerned with accidental fires and fire protection engineering deals with fires of different natures than the mine fires, which are distinguished by a restricted air supply and a usually uniform composition and arrangement of the combustible material, giving them unique properties. This report will therefore limit itself to the evaluation of literature dealing specifically with fires in mines or under conditions similar to those in mines.

A) Modes of fire propagation

The most systematic work on this problem has been done by Roberts and colleagues (103, 104, 105, 106). According to them, mine fires can display two different modes of propagation:

1) through localized heat feedback from the flames;
2) through all over heat feedback from the fumes.

The resulting mine fires are of distinct different types.

Fires of the first type are controlled by the same mechanisms as unconfined fires in the open. Propagation occurs by radiation and convection from the flames and hot gases, which heat the combustible material in the immediate vicinity of the fire, before they are mixed with the general airstream. The latter is not heated to temperatures high enough to generate gaseous fuel from combustible material or to light it. Due to the fact that combustion takes place only in the immediate neighborhood of the combustible material, considerable quantities of oxygen can pass through the fire without being consumed. Fires of this type are therefore frequently called unconfined or oxygen rich fires.

The second type of fire propagation occurs where the general air stream has become hot enough to generate gaseous fuel from the combustible material, along which it passes. In this case the fire extends until all available oxygen is being consumed, which limits the heat development. The generation of gaseous fuel continues for a considerable distance downstream of the area, where the last oxygen reacted. The fire extension is thus limited by the supply of oxygen. The high temperatures required for this type of fire propagation are, outside of mines, usually reached only in confined passages. Fires of this type are therefore frequently called confined or fuel rich fires.

Although most accidental mine fires, being started by relatively small ignition sources, develop into oxygen rich fires and stay

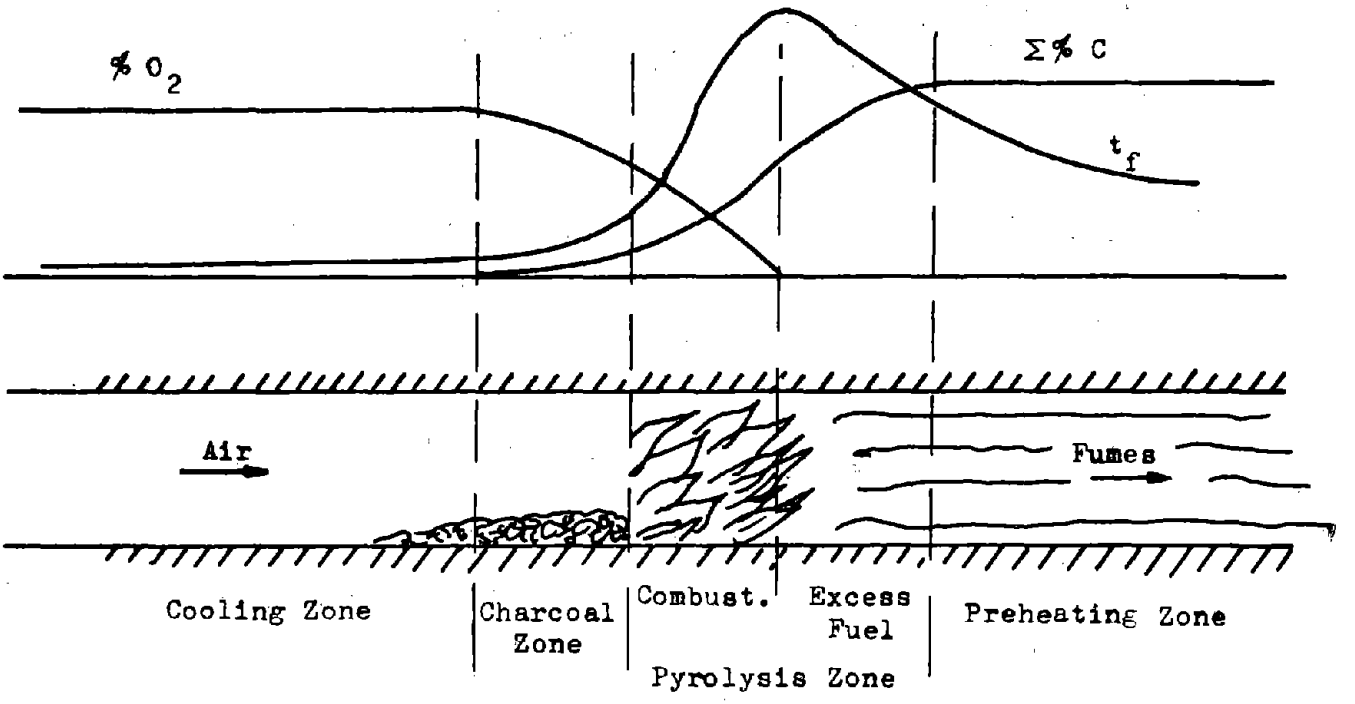

Fig. 1. Zones Developed by Fuel Rich Fires(103)

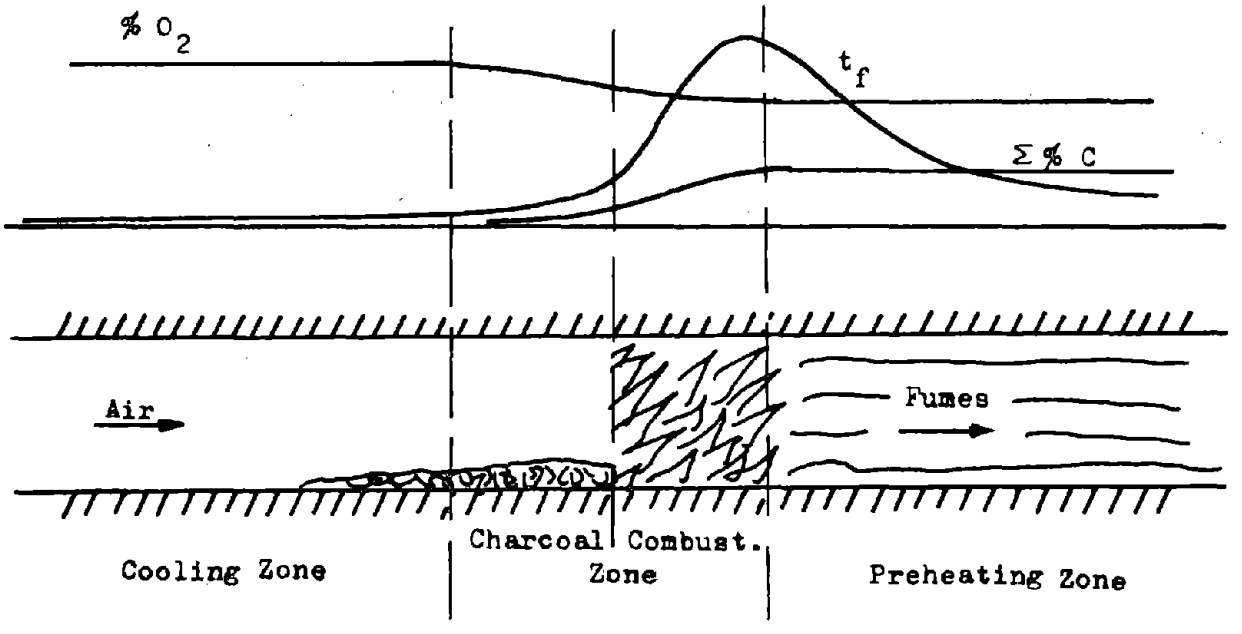

Fig. 2. Zones Developed by Oxygen Rich Fires

oxygen rich, fuel rich fires have been much more thoroughly studied. The reason may be that fuel rich fires are a much greater hazard because of their greater flame advance, heat release, toxicity and, if mixed with air, explosibility of their combustion products and because of the fact that most oxygen rich fires can by spontaneous growth become fuel rich. Another reason may be that fuel rich fires render themselves better to a systematic analysis.

Schematic representations of fuel rich timber fires have been published by Roberts and colleagues (100, 101, 103, 104, 105) and by Baltajtis and Markovic (7). As shown in fig. 1 they distinguish several zones, which are, in the direction of the air flow, the cooling and the charcoal zone, the pyrolysis zone with the combustion and the excess fuel section, and the preheating zone. The average temperatures of the gas stream and its content of oxygen and carbonaceous constituents are also indicated.

The cooling zone is a zone through which the fire has already passed and in which it is now extinct. Only heat transfer processes due to forced convection take place, the walls of the airway are cooled and the air is heated.

In the charcoal zone the carbonized residue of the fuel which is still hot enough to react with the oxygen of the air is burned. The heating of the ventilation air continues, its oxygen content is reduced.

In the combustion section of the pyrolysis zone the volatiles produced by the decomposition of the combustible material are burned in the ventilating air. The gas temperatures rise to a maximum and the oxygen content is reduced to zero. In the excess fuel section of the pyrolysis zone the fumes are sufficiently hot to cause pyrolysis of the combustible material. The absence of oxygen will, however, prevent combustion and the pyrolysis products remain as excess fuel in the fumes. The heat consumption of the pyrolysis causes the temperatures of the fumes to drop.

The final cooling of the fumes takes place in the preheating zone, which gets its name from the preheating and drying of the airway section towards which the fire is moving. The heat transfer from the fumes to the airway takes place mainly by forced convection, although close to the pyrolysis zone radiation should be involved, too.

No equivalent schematic representations for oxygen rich fires have been published, but it can be assumed that for timber they would appear as shown in fig. 2. Due to the fact that evolution of volatiles occurs only in the immediate vicinity of flames, no pyrolysis zone exists. The drop in oxygen and the increase in carbon content of the air stream as well as its temperature increase in the combustion zone will be lower than for fuel rich fires.

B) Controlling mechanisms and equilibrium states

The controlling mechanisms of unconfined and confined fires have been visualized by Roberts (106). The behavior of the former is more easily umderstood when explained by the example of fires in the open first. If in such a fire with one dimensional spread of flame the rate of flame advance is called V and the width of the fire L (fig. 3), the relation between V and L will be similar as shown by curve 1 in fig. 4. For $L<L_o$ no propagation of the fire takes place due to inadequate heat transfer ahead of the flames. For $L>L_o$ V will increase with L as the emissivity and height of the flames increase until the extension of the fire L has reached such a magnitude that V is no longer influenced by L. If D is the depth of the fuel bed consumed by the fire, γ its specific weight and B the velocity with which the fire penetrates the fuel bed, the rate of fuel added to the fire (per unit width of flame front) is $V*D*\gamma$ and the rate of fuel consumption is $L*B*\gamma$. In a fully developed fire V and L are constant with respect to time and it is $V*D*\gamma = L*B*\gamma$ or $V = (B/D)\ L$, represented by curve 2 fig. 4. Possible values of L and V are indicated by the two intersections of curves 1 and 2. Of these, the point L_1,V_1 is however, not a stable condition, since for $L<L_1$ the curve 1 shows that $V<(B/D)\ L$, which indicates a decreasing fire and for $L> L_1$ it shows $V>(B/D)\ L$, which indicates and increasing fire. In other words, if a fire is initiated with $L<L_1$ it will die out, if it is initiated with $L> L_1$ it will adjust itself to the condition $L = L_2$.

For fires in mine roadways or ducts it is advantageous to express the rate of fuel added to the fire by the dimensionless parameter $V^+ = C*V*D*\gamma*P*f/(V_a*\gamma_a*A)$

where C = mass of air required for complete combustion of unit mass of fuel
P = perimeter of roadway
f = fraction of perimeter which is covered with combustible materials
V_a = air velocity
γ_a = specific weight of air
A = cross section of roadway

Analogously, the rate of fuel consumption is expressed by

$$L^+ = C*L*B*\gamma*P*f/(V_a*\gamma_a*A)$$

A fire in a mine roadway or duct is in its early stages controlled by local heat transfer effects close to the fuel surface and behaves therefore similar to a fire in the open. However, as the fire increases, additional heat transfer from the fumes will occur and provide an additional increase of V^+ with L^+ which becomes very large when the temperature of the fumes exceeds the threshhold beyond which pyrolysis of the fuel becomes rapid. This increase in V^+ is finally limited by the heat development of the fire, which reaches a peak at $L^+ = 1$, when all oxygen in the air supply is consumed. A further increase in L^+ results in a decreasing V^+, since excess fuel causes dropping temperatures of the fumes. The relationship between V^+ and

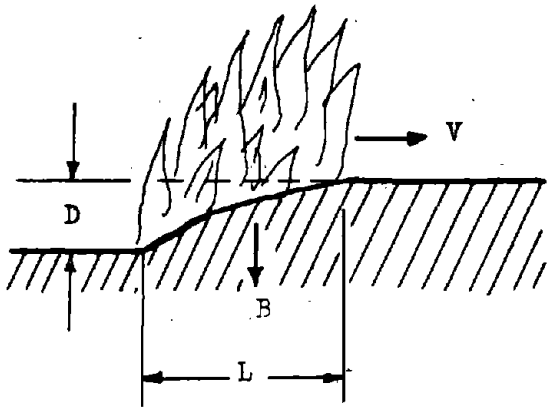

Fig. 3. Model of Onedimensional Spread of Fire (106)

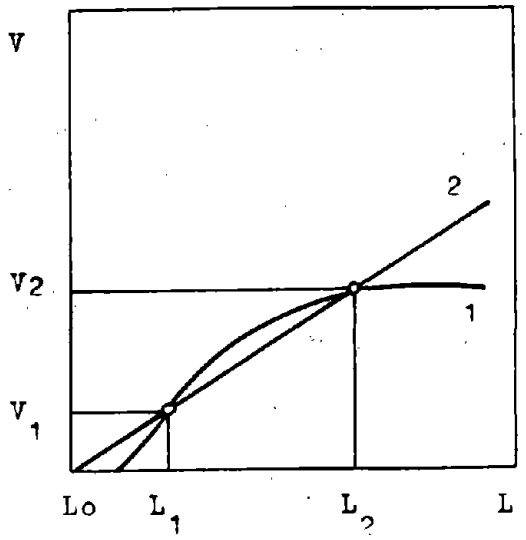

Fig. 4. Relationship between V and L in Unconfined Fires (106)

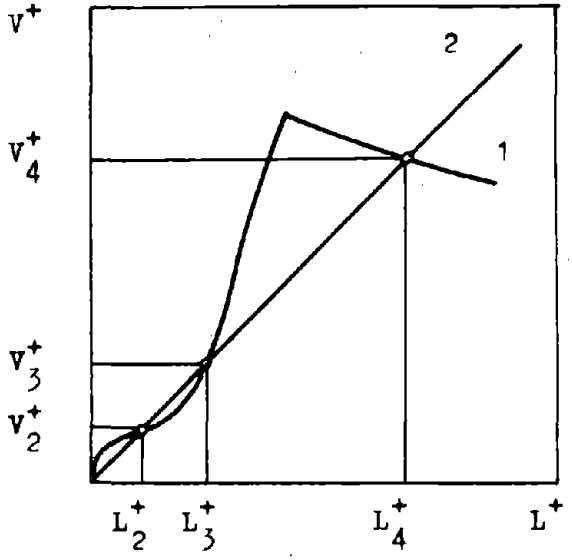

Fig. 5. Relationship between V^+ and L^+ in Confined Timber Fires (106)

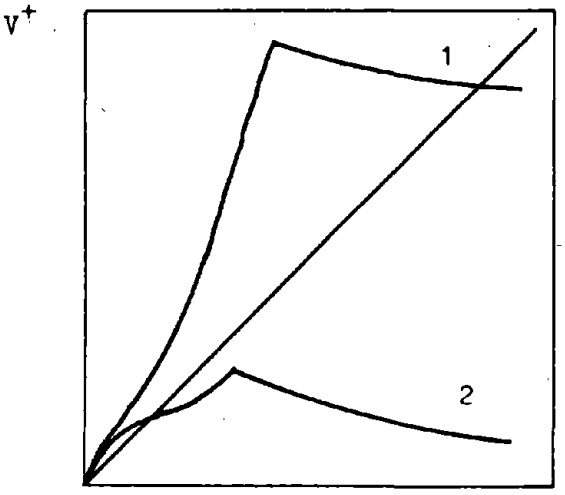

Fig. 6. Easy and Difficult Ignitable Fuels in Confined Fires (106)

and L^+ will therefore be similar shown by curve 1 in fig. 5. (The initial portion of this curve, which is similar to the initial portion of curve 1 in fig. 4 has been simplified by making $L^+_1 = 0$). The fire is fully developed when the rate of fuel added is equal to the rate of fuel consumed, or when $V^+ = L^+$ (curve 2 in fig. 5). Three possible pairs of V^+ and L^+, indicated by the intersections of curves 1 and 2, exist. In a similar way, as for fires in the open, it can be reasoned that L^+_3, V^+_3 represent an unstable condition, whereas the other two points are stable. L^+_2, V^+_2 represent the unconfined, oxygen rich type of a fire, L^+_4, V^+_4 the confined, fuel rich type. If a fire is initiated with $L^+ < L^+_3$ it will assume values of L^+_2, V^+_2. If it is initiated with $L^+ > L^+_3$ it will assume values of L^+_4, V^+_4.

From the definition of L^+ it is obvious that L^+_3 is mostly readily exceeded:
the smaller - the air velocity V_a
and
the larger - the initial length of the fire L,
the penetration velocity B,
the fuel density γ',
the fracture of the perimeter covered with combustible material, and the ratio P/A (or the smaller the roadway).
Furthermore, if the air supply of a developed fire in the state L^+_2, V^+_2 is reduced to such an extent that L^+_3 is exceeded, a rapid growth of the fire to the state L^+_4, V^+_4 will result. The reverse, to move a fire from the state L^+_4, V^+_4 to the state L^+_2, V^+_2 would require a very large and sudden increase in the air supply or a limitation in the fuel available for the fire so that L^+ becomes smaller than L^+_3.

Curve 1 in fig. 5 is characteristic for fuels like timber. A more easily ignitable fuel than timber will show a steeper increase of V^+ with L^+ (curve 1 in fig. 6) and give rise to a state $L^+ > 1$ or a fuel rich fire from any size of initial L, V_a, P/A or f. A less easily ignitable fuel will stay in the region $L^+ < 1$ and always burn as an oxygen rich fire (curve 2 in fig. 6).

Roberts and Clough (103) have provided a heat balance for the pyrolysis zone (comprising combustion and excess fuel section) of a confined fire in a timber lined duct. They can clearly prove that under the assumption of rapid mixing of the hot combustion products with the airstream two equilibrium states (corresponding to L^+_3, V^+_3 and L^+_4, V^+_4 in fig. 5) exist, of which only the one with the fuel rich fumes (L^+_4, V^+_4) is stable. As will be shown later this is in qualitative agreement with all experimental observations made so far with timber fires in mine roadways. They yield either fumes containing more than 15 - 16% O_2 or containing no O_2.

As a parameter to describe the state of mine fires and as criterium for equilibrium states Roberts and colleagues (100, 103, 104, 105, 106) suggest the use of the fuel/air ratio

$$R = \frac{\text{air required for complete combustion}}{\text{air supplied}}$$

which correspondents to the air ratio coefficient in combustion engineering. The justification for the name is that the numerator can be divided into two factors: fuel supply * air required for complete combustion per unit fuel. Roberts and colleagues suggest in principle 3 different methods to determine R for timbered roadways, namely (104):

$$R = \frac{5 * V_f * W * F}{V_a * \rho_a * A}$$

where 5 = mass of air required per unit mass timber for complete combustion
V_f = fire velocity
W = timber loading per unit length of roadway
F = fraction of timber burnt away by fire
$V_a * \rho_a * A$ = massflow of air through roadway

$$R = \frac{5 * P * L_f * m_v}{V_a * \rho_a * A}$$

where P = surface area of timber per unit length of roadway
L_f = length of firezone
m_v = mass rate of volatile formation per unit surface area

or, for R<1

$$R = \frac{\%CO_2 \text{ in moisture free fumes}}{21}$$

From a great number of experiments Robert and colleagues conclude that fully developed oxygen rich timber fires have fuel/air ratios R<0.3 (105, 106) or maximal R<0.4 (104). Fully developed fuel rich timber fires have ratios R ∿ 3 (100) or minimal R ∿ 2 - 3 (106). Fires with fuel/air ratios R > 0.4 are unstable and will spontaneously grow to the fuel rich condition. It should be noted that fuel/air ratios of R ∿ 0.3 would correspond to oxygen consumptions of ∿6% or oxygen concentrations of ∿15% in the fumes, the lowest observed values for oxygen rich timber fires.

Unfortunately, these critical fuel/air ratios for equilibrium states have been established thus far for timber fires only.

a) Conditions for the development of fuel rich fires

As outlined above it depends on:
the type of combustible material,
its quantity,
the mine roadway size,
the ventilation,
and the ignition source
whether an oxygen or a fuel rich fire develops.

The higher the ignition quality of a combustible material the greater the probability that the fire becomes fuel rich. Mineral oil has been observed to give rise always to fuel rich fires (104),

when the ratio oil surface A (ft^2) and air quantity Q_a (ft^3/sec) was $A/Q_a > 0.153$. Polyurethane foam lining applied to 75% of the roadway perimeter always caused fuel rich fires, too (106). Timber can, however, burn in oxygen rich or fuel rich fires, depending on quantity, roadway size, ventilation and ignition (7, 94, 103, 104, 118). The few data published on unsealed coal fires (86,87) suggest that these are usually oxygen rich.

A prerequisite for fuel rich fires is that enough combustible material along the path the fumes take is available for the development of a pyrolysis zone. If only isolated fire objects (118) or shorter lengths of timber lining are set afire (104) this condition is not met and oxygen rich fires will result.

It has been derived above (106) that the larger the ratio roadway perimeter/ cross section, or the smaller the roadway is, the greater the probability of fuel rich fires. This has been confirmed by Roberts (106) who observed that timber fires in model ducts (1 ft^2) always developed spontaneously to the fuel rich state.

The lower the air velocity V_a, the larger the fuel/ air ratio R and the higher, therefore, the possibility of fuel rich fires. An oxygen rich fire can develop into a fuel rich fire by reduction of the ventilation (104). With the practical feasible increases in ventilation there has been, however, so far no tendency for fuel rich fires observed to revert to the oxygen rich state, until the fuel supply is limited.

If an ignition source starts a fuel rich fire, it must be capable of producing a pyrolysis zone. This requires that the temperature of the total gas stream passing along the combustible material be raised to a temperature which allows significant pyrolysis. How high this temperature has to be depends on the type of combustible material and the time of exposure. For timber pyrolysis Roberts and Clough (103) give a surface value of 527°F, which requires average air temperatures between 900 and 1250°F, depending on the magnitude of the heat transfer coefficient, which is a function of the air velocity. Klinger (68) gives a surface temperature of 527°F too, and Wilde (142) a range of 536 - 608°F. The lowest ignition temperatures for 9 different types of wood as a function of their exposure time are shown in fig. 7 (75).

The temperature increase Δt which the air experiences from an ignition source can be calculated from

$$\Delta t = \frac{Q_h}{Q_a * \rho_a * c_{pa}}$$

where Q_h = heat development of ignition source
Q_a = volume flow of air
c_{pa} = specific heat of mine air

Following a graph given by Maas and Sadée (75) for the ignition of oxygen rich timber fires the relationship between Q_h and Q_a has been plotted in fig. 8 for Δt = 333°F and 263°F under the assumption of ρ_a = 0.075 lb/ft^3 and c_{pa} = 0.24 Btu/lb°F. 263° F is the temperature increase necessary to heat air from 68°F to 331°F,

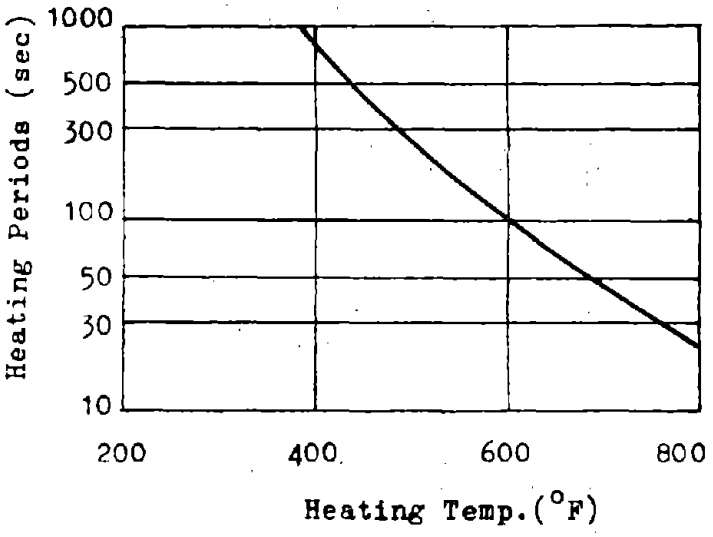

Fig. 7. Mean Ignition Temperatures of Wood (75)

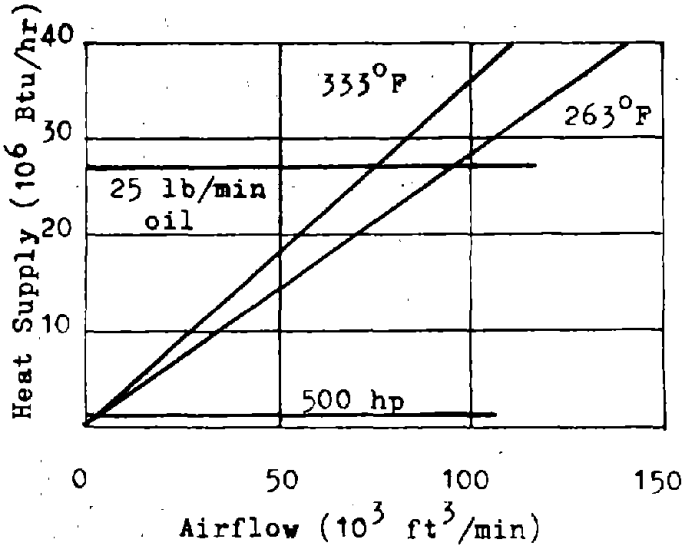

Fig. 8. Relation between Heat Supply and Airtemperature Increase

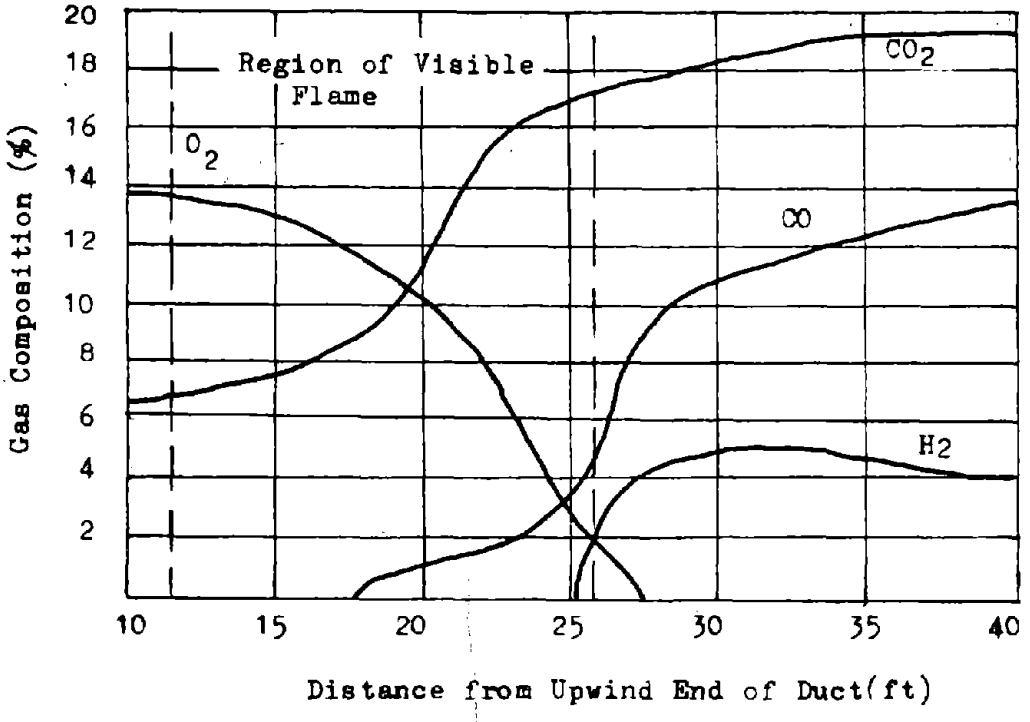

Fig. 9. Variation of Gas Composition along a Duct with a Fuel Rich Timber Fire (100)

the assumed lowest ignition temperature after long preheating and 333°F is the increase to 401°F, the ignition temperature after 15 minutes of preheating. In the same figure are indicated the heats developed when 500 hp are completely converted into heat and by an oilfire burning at the rate of 25 lbs/min. For the latter complete combustion in an oxygen rich atmosphere is assumed.

Since for fuel rich fires the pyrolysis zone has to have a certain length and considerable cooling of the fumes due to heat transfer to the walls occurs and since a considerable temperature difference between combustible material and air must exist to facilitate heat transfer, the heat quantities needed to ignite a fuel rich fire are most probably much higher than those shown in fig. 8. Roberts and Blackwell (104) report that a burning rate of 40 lb/min of mineral oil over 10 minutes in a ventilation current of 22,000 ft^3/min were about the minimum to start a fuel rich timber fire. A more detailed discussion of the temperature distribution in fuel rich fires is given in chapter II.C.e.

C) Observations in accidental and experimental mine fires

Because timber played a prominent role in most larger mine fires of the past, nearly all published observations on the properties of accidental fires deal with timber fires and systematic experimental investigations have concentrated on them, too. This is rather unfortunate and much work certainly remains to be done. However, the fire controlling mechanisms and the relationship of the dominating parameters do not depend on the type of combustible material so that the insights gained from timber fires can be used for other fires, too.

The great number of fire experiments conducted routinely by experimental mines all over the world usually aim at testing the inflammability or fire resistance of materials and equipment used underground or at measuring the efficiency of fire extinguishing devices. Since the fires have usually no opportunity to develop fully to an equilibrium state, the results obtained from these test have therefore little general validity.

All observations discussed in the following chapters deal with unsealed fires.

a) Composition of combustion products

The composition of combustion products can be calculated when the fuel composition and the air/fuel ratio is known. For industrial fuels in particular charts exist which relate CO_2, CO and O_2 concentrations in the fumes with the fuel/air ratio. Their discussion exceeds the scope of this report, however.

Roberts and colleagues (104) conclude that most accidental mine fires are oxygen rich fires since they are started by relatively small ignition sources. The large scale experiments evaluated by

them in a tunnel of 45 ft^2 cross section showed generally the features of oxygen rich fires, too, since limited lengths of timber lining (up to 135 ft) were used. Only with large igniting sources or with a reduction of the air velocity after the timber had been ignited could fuel rich fires be generated. Table 1 shows the gas analyses of the combustion products from 6 experimental timber fires and 3 accidental mine fires involving timber lagging. All the small scale experiments in a duct of 1 ft^2 cross section gave rise, however, to fuel rich fires in all the conditions studied (106). As an example the variation in gas composition along the duct is shown in fig. 9 (100). As average values Roberts and colleagues state for oxygen rich timber fires (106):
3 - 5 %CO_2, 0.1 - 0.5 % CO, 16 -18 % O_2,
for fuel rich timber fires (104)
18 - 20 % CO_2, 5 - 8 % CO, 2 - 5 % H_2, 0 - 1 % O_2.

Egorov and Kondratenko (31) evaluated about 10,000 gas samples taken in Russian coal mines. They were taken 70 - 1000 ft behind unsealed fires. Since most CO determinations were done with an outdated and unreliable method, they suspect that the CO concentrations were considerable higher than stated. The results of their evaluation is compiled in table 2. Since larger open fires usually require sealing, it can be assumed that most samples came from concealed or smaller open fires. Examples for typical gas concentrations behind large open fires, as given by the authors, are shown in table 3.

Baltajtis and Markovic (7) give in table 4 as an example of their experiments (in a tunnel of 46.3 ft^2 cross section, timbered over 614 ft with props and bars of 6 - 7 " diameter and lagging of 1 - 2 " thickness) the total concentration of carbonaceous gases (CO_2 + CO + CH_4) as a function of time and location. One sees clearly the movement of the flamezone. Irregularities in the gas composition are attributed by the authors to air leakage from the outside into the tunnel.

Voskobojnikov (131) calculated table 5 for the composition of fumes from wood with different moisture contents. Although not stated by him this table is obviously based on the assumption that dry wood produces fumes with the composition given in the last column of the table.

Fig. 10 is an example from the 130 experiments conducted by Schmidt and Grumbrecht (118) in a raise with 22 ft^2 cross section. Since they used as fire objects only wood piles of up to 700 lb weight, all the fires they obtained remained oxygen rich.

b) Fuel consumption of timber fires

Extension and propagation of mine fires depend on the rate at which the combustible material is consumed. Maas and Sadée (75) give the maximal rate of burning for round timbers of different cross sections in fig. 11. If from this figure the thickness of the

Table 1. Combustion Products of Large Scale Timber Fires (104)

Fire	% CO	% CO_2	% O_2
Experiment No 1	0.30	4.1	16.6
No 2	0.18	2.5	18.3
No 3		6.9	14.1
No 4	0.15	3.2	17.6
No 5	0.24	4.8	16.0
No 6	0.20	4.5	16.3
Accidental Fires			
Creswell Colliery	0.23	5.6	14.1
Haford Colliery	0.96	4.8	14.8
Blackwell B Colliery	0.58	4.3	15.0

Table 2. Results of 10,000 Gas Samples Taken Behind Unsealed Fires (31)

	Number of Samples with Volume Concentrations (%) of:								
	0 - 0.5	0.5 - 1	1 - 2	2 - 3	3 - 5	5 - 10	10 - 15	15 - 20	20 - 100
O_2			28	30	68	100	220	8554	
CO_2	8765	475	230	198	152	124	60		
CO	9966	24	10						
CH_4	8870	324	170	143	125	116	102	85	64
H_2		17	13	3					

Table 3. Combustion Products of Larger Accidental Open Fires (31)

	Volume Concentration (%)				
Name of Mine	O_2	CO_2	CO	CH_4	H_2
Sredazugol No 1/5	5.0	14.0		0.08	
Kapitalnajy, Primorskugol	2.2	12.0	1.0	0.42	
Zeljinskincev, Donezkugol	3.6	12.5	5.2	1.0	
Kalinin, Kizelugol	2.8	9.95	2.8	0.07	2.65

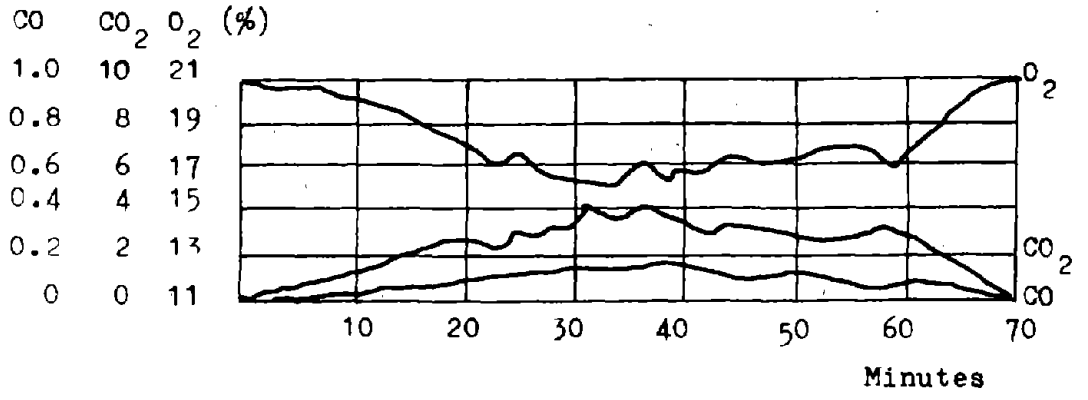

Fig. 10. Example of an Oxygen Rich Timber Fire (118)

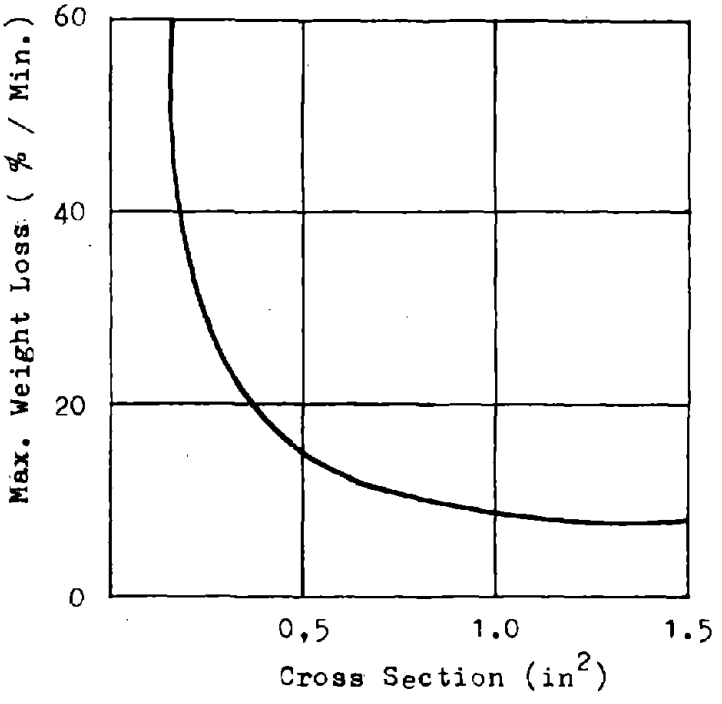

Fig. 11. Maximal Rate of Burning for Round Timbers (75)

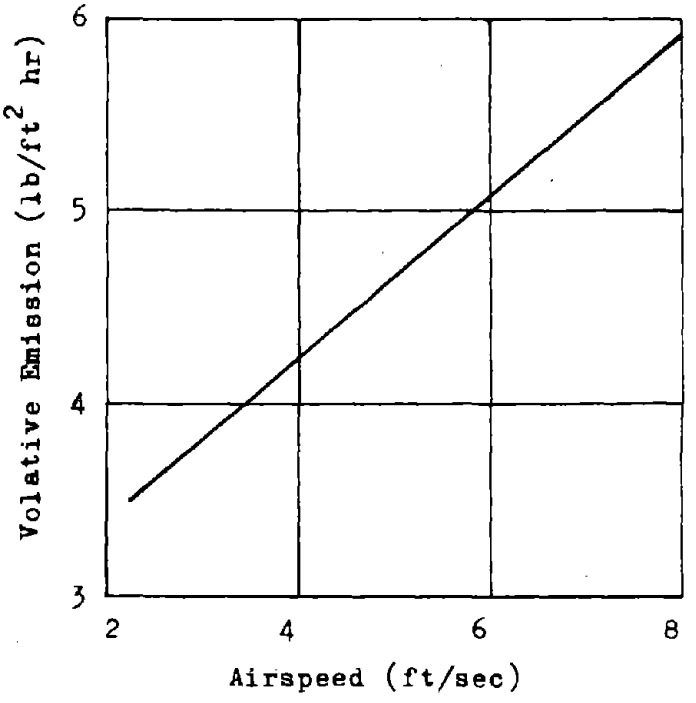

Fig. 12. Volatile Emission of Burning Timber (104)

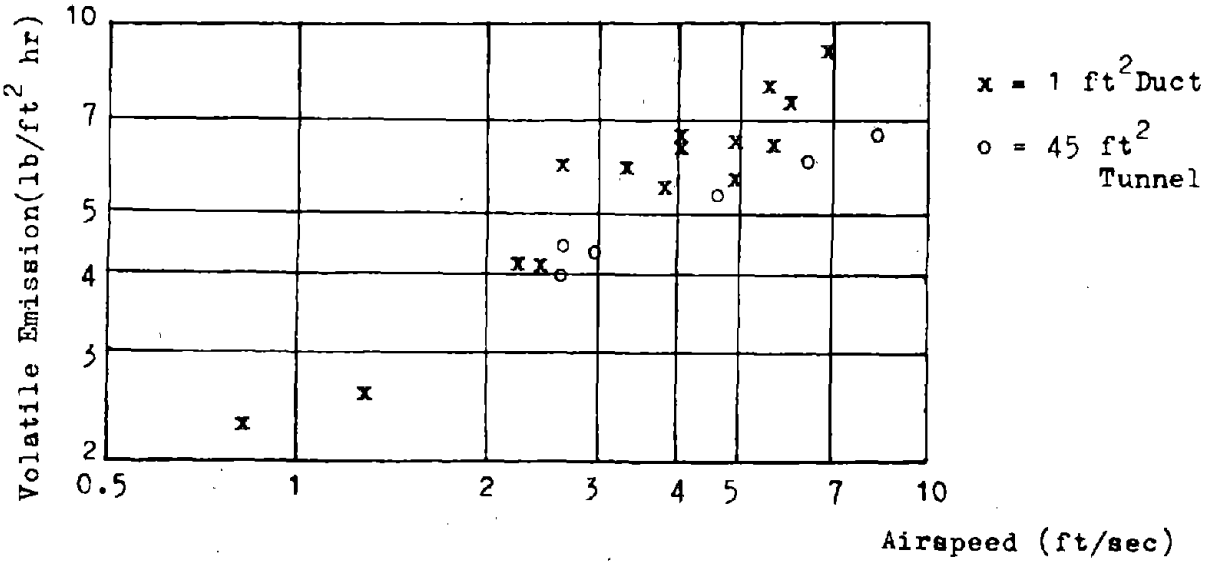

Fig. 13. Volatile Emission of Burning Timber (105)

burnt layer of timber at its perimeter is calculated, one sees that it approaches asymptotically 0.03 in/min. This is the same order of magnitude as the rate of penetration of the pyrolysis front B (fig. 3) given by Roberts (106) for timber as
B = 0.014 - 0.052 in/min
For polyurethane foam he measured
B = 0.78 - 1.9 in/min
B depends on the air velocity which most probably explains the spread between the high and low values.

The rate of pyrolysis m_v, expressed as a mass rate of fuel evolution per unit surface area has been observed by Roberts (106) for timber to be
$m_v = 2.29 - 8.5$ lb/ft^2 hr
and for polyurethane foam to be
$m_v = 7.38 - 20$ lb/ft^2 hr.
The dependence of m_v on the air velocity, as published by Roberts and Blackwell (104), for a tunnel of 45 ft^2 cross section is shown in fig. 12 and as published by Roberts (105) for two tunnels of 45 and 1 ft^2 cross section in fig. 13.

Baltajtis and Markovic (7) give as the average fuel consumption in pyrolysis and charcoal zone combined a value of $m_v = 2$ lb/ft^2 hr.

In oxygen rich fires all fuel is burned and the oxygen concentration drops to approximately 15%. Maas and Sadée (75) therefore suggest to calculate the amount of timber burnt by

$$M_F = \frac{6 * Q_a * 3{,}600}{100 * 11.9} = 18.15\ Q_a \text{ lb/hr}$$

where 6 = volume % O_2 consumed in an oxygen rich fire
Q_a = airflow (ft^3/sec)
11.9 = ft^3 oxygen required to burn 1 lb of wood

Baltajtis and Markovic (7) give a formula, which is valid for oxygen rich as well as for fuel rich fires. The volume of the dry gas stream leaving a fire can be determined from

$$Q_{dg} = \frac{378}{12} C_F / \Sigma C_p \quad (\text{ft}^3/\text{lb})$$

where 378 = volume of 1 lb mole (ft^3 /lb-mole)
12 = molecular weight of carbon
C_F = mass % C in fuel
ΣC_p = volume % C in combustion products

Under the assumption that the airstream entering the fire Q_a is approximately equal to the gas stream leaving the fire $M_F * Q_{dg}$, the fuel consumption can be calculated from

$$M_F = Q_a / Q_{dg} = 0.0317 \frac{\Sigma C_p}{C_F} Q_a$$

The same approach is suggested by Both (14).

Table 4. Total Concentration of Carbonaceous Gases (Vol. %) in an Experimental Large Scale Timber Fire (7)

Time since Ignition (min)	Distance From Source of Ignition (ft)						
	64.5	82	147.5	213	311	442	475
10	24.6	27.1	24.2	23.7	24.5	25.2	27.2
30	7.5	11.5	27.9	24.9	23.7	27.9	29.8
50	2.7	4.8	17.2	24.0	26.6	28.1	27.2
70	1.2	2.1	15.7	22.5	23.0	23.2	26.0
90	1.1	2.4	7.3	18.1	22.7	25.3	27.4
110	0.5	1.0	7.0	14.9	22.3	23.4	26.5
130	0.3	0.9	2.4	8.6	19.7	21.8	22.9

Table 5. Calculated Composition of Fumes for Timber with Different Moisture Contents (131)

	Moisture Content of Timber (Mass %)				
	7	10	20	30	0
CO_2 (vol. %)	9.62	9.61	9.41	9.24	9.80
O_2 "	3.17	3.15	3.09	3.04	3.22
N_2 "	76.18	75.65	73.85	71.84	77.00
CO "	1.21	1.20	1.18	1.15	1.23
H_2O "	9.82	10.39	12.47	14.73	8.75
volume of fumes per lb timber (standard cft)	124.8	121.2	110.0	98.2	
air consumption per lb timber (standard cft)	118.8	114.4	101.5	88.5	
volume ratio fumes/air	1.05	1.057	1.082	1.11	
specific weight ratio fumes/air	0.9891	0.9882	0.9781	0.9682	

c) Minimum extension of timber fires

Maas and Sadée (75) estimate the flamezone length of oxygen rich timber fires with the formula

$$L_f = \frac{MF*100}{W*1*60} \quad (ft)$$ where M_F = timber burnt by fire (lb/hr)

W = timber load of roadway (lb/ft)
1 = weightloss of timber due to fire (%/min)

Roberts and Blackwell mention (104) that the extension of timber fires can be calculated from their definition of the fuel/air ratio

$$R = \frac{5*P*L_f*m_v}{V_a*\gamma_a*A}$$

or, with P and L_f in ft, A in ft^2, V_a in ft/sec, γ_a in lb/ft^3 and m_v in $\frac{lb}{ft^2 hr}$

$$L_f = \frac{R*3,600}{5} * \frac{V_a*\gamma_a*A}{P*m_v} \quad (ft)$$

As outlined above they suggest R∿0.3 for fully developed oxygen rich timber fires and R∿3 for fully developed fuel rich timber fires. Values for m_v as a function of V_a have been given in chapter II-C-b. L_f indicates the length of the flamezone for oxygen rich fires, for fuel rich fires the length of the pyrolysis zone.

A comparison of this formula, written with $\gamma'_a = 0.075$ lb/ft^3 and R = 0.3 as

$$L_f = \frac{R*\gamma_a*60}{5} * \frac{Q_a*60}{P*m_v} = 0.27\ Q_a \frac{60}{P*m_v}$$

with the formula from Maas and Sadée, written as

$$L_f = \frac{M_F*100}{W*1*60} = \frac{18.15}{60} * \frac{Q_a*100}{W*1} = 0.303\ Q_a \frac{100}{W*1}$$

shows good agreement since W*1/100 as well as $P*m_v/60$ specify the amount of timber burnt per foot of roadway and minute.

Baltajtis and Markovic (7) give for the first stage of a timber fire, before any extended charcoal zone has formed, the formula

$$L_{f1} = \frac{M_F}{P*m_v} = 0.0317*3600* \frac{\Sigma C_p}{C_F} * \frac{Q_a}{P*m_v} \quad (ft)$$

with Q_a in ft^3/sec, P in ft and m_v in lb/ft^2hr. If this formula is written in the form

$$L_{f1} = 0.0317*60* \frac{\Sigma C_p}{C_F} * \frac{Q_a*60}{P*m_v}$$

and for an oxygen rich fire $\Sigma C_p = 5\%$ and for timber $C_F = 35\%$ are inserted, one obtains

$$L_{f1} = 0.0317*60* \frac{5}{35} * \frac{Q_a*60}{P*m_v} = 0.272\ Q_a\ \frac{60}{P*m_v}$$

which is in good agreement with the previous formulas, too.

If in a second stage a charcoal zone starts forming, the total length of charcoal and pyrolysis zone can be calculated from

$L_{f2} = L_{f1} + V_f*\tau$ where V_f = velocity of pyrolysis zone advance

τ = time elapsed since begin of the second stadium

When in a third stage finally an equilibrium has been reached and charcoal zone and pyrolysis zone move at the same speed, Baltajtis and Markovic suggest use of the formula

$$L_{f2} = 0.0317*3600* \frac{\Sigma C_p}{C_F} * \frac{Q_a}{P*m_v}$$

with an average value of m_v for both zones. As its value they suggest $m_v = 2\ lb/ft^2\ hr$.

d) Velocity of fire propagation

Fire propagation along a roadway is due to heat transfer by radiation and convection. The latter takes place as natural convection, caused by air movement as the result of buoyancy forces of the hot fumes and as forced convection, caused by the ventilating air current. Since the air movements creating the convection provide the fire at the same time with fresh oxygen, heat transfer by convection has a larger influence on the propagation of fires than radiation. And since the air velocities as the result of buoyancy forces are quite low, forced convection in the direction of the ventilating air current is usually considerably larger than natural convection.

A fire in an unventilated or little ventilated airway will therefore spread in both directions, upwind and downwind. Since the oxygen supply upwind is better, the propagation velocity in this direction may even be higher than downwind. The higher the velocity of the ventilating air current becomes, however, the stronger the tendency of a fire to spread downwind.

Buoyancy forces developed by hot fumes are directed vertically

upwards. The fumes therefore have a tendency to form a layer along the roof. In unventilated or laminar ventilated airways this layer is dispersed by molecular motion only, which is a very slow process. Turbulent dispersion requires that the kinetic energy of the turbulent particles, formed by the ventilating air current is high enough to overcome the buoyancy forces. Since this kinetic energy is proportional to the air velocity, a certain minimum velocity is required for the turbulent dispersion of such layers.

In little-ventilated airways the fumes will therefore mainly travel and the fire will propagate along the roof. In inclined descensionally ventilated airways air can flow into the fire downhill along the floor whereas the fumes are travelling and the fire is spreading uphill along the roof.

The velocities with which mine fires spread in unventilated airways or with which they spread in ventilated airways upwind against the air current are small compared with those in other directions. Their propagation is easier to control, too. Backing of smoke can be fought by local air velocity increases with transverse brattice or shields, blocking the lower cross section of the airway (29,82). No systematic investigations on fire propagation velocities against air currents and few (33) on the extension of backed smoke layers are known although many of the insights gained from the studies of gas layers would be transferrable to these problems.

Some typical examples for observations made shall be quoted. Both (13) reports that the fire propagation as well as the backing of smoke against the airflow has so far always been negligible in West German coal mines. The reason is most probably the high air velocities associated with longwall mining. Only a few cases are known where the backed smoke reached extensions of up to 100 ft. Fires propagating along the roof against the ventilating air current could always be extinguished easily.

Mitchell (82) reports that in the experimental coal mine of the USBM the length of the backed smoke layer was 100 ft with an air velocity of 120 ft/min, 50 ft with 180 ft/min and 10 ft with 230 ft/min. Eisner and Smith (33) mention the best known instance of backed smoke which was in 1910 at Whitehaven Colliery in Great Britain with 372 yards against an intake ventilation speed of some 325 ft/min; 86 men were lost. In this case, however, the ventilation must have been descensional and one can suspect that intermittent airflow reversals occurred.

Osipov and Zadan (94) state that in their fire experiments in timbered tunnels the fire velocity against the airflow did not exceed 20 ft/hr. Dougherty (29) remarks however that " in high volatile coals the rate of propagation outward can be both rapid and extensive whereas its rate of travel inby is fairly slow or negligible". On occasion the rate of spread was 150 ft/hr against a ventilation speed of 150 ft/min.

The systematic work done so far deals with fire propagation in the direction of airflow at ordinary airspeeds. All of this work has again been done in timbered roadways.

Maas and Sadée (75) estimate the velocity with which the flamezone of an oxygen rich fire moves along a timbered roadway by

$$V_f = \frac{M_F}{W} = \frac{18.15\ Q_a}{W} \quad \text{(ft/hr)}$$

Where M_F = amount of timber burnt (lb/hr)

W = timber loading of roadway (lb/ft)

Q_a = air quantity (ft^3/sec)

Baltajtis and Markovic (7) suggest the same approach with the formula

$$V_f = \frac{M_F}{W} = 0.0317*3{,}600*\frac{\Sigma C_p}{C_F} * \frac{Q_a}{W} \quad \text{(ft/hr)}$$

With C_F = 35 % and ΣC_p = 5 % for an oxygen rich fire this becomes

$$V_f = 16.3\ \frac{Q_a}{W}$$

If the formula $V_f = 0.0317*3{,}600*\frac{\Sigma C_p}{C_F} * \frac{Q_a}{W}$ suggested by Baltajtis and Markovic is applied to fuel rich timber fires with $\Sigma C_p \sim 30$ % and $C_F \sim 35$ %, it becomes

$$V_f = 98.8\ \frac{Q_a}{W}$$

A comparison of calculated with measured velocities, obtained for fuel rich fires in a timbered tunnel of 34.3 ft^2 cross section and 614 ft length is shown in table 6.

Apparently the same tunnel was used by Osipov and Zadan (94) for a larger number of experiments whose results they express in the formula

$$V_f = \frac{P_a}{8.89 + 0.0027*P_a} \quad \text{(ft/hr)}$$

where P_a = airflow/timberloading

$= Q_a*60/v_t\left(\frac{ft^3/min}{ft^3/ft}\right)$

v_t = timber loading (ft^3/ft)

All the fires studied by them were obviously fuel rich. If a specific weight of 40 lb/ft^3 is assumed for timber, the above formula by Osipov and Zadan gives for values of $Q_a/W = 2$ or $P_a = 4{,}800$ approximately the same velocities as one obtains with $V_f = 98.8\ Q_a/W$. For smaller values of P_a, however, it gives greater velocities and for larger values of P_a smaller velocities and the deviations can become considerable.

Since Osipov and Zadan feel that the ratio airway cross section / timberloading is fairly constant for Russian mines, which makes P_a proportional to the air velocity, they suggest as the evaluation of

their results a second formula

$$V_f = \frac{V_a}{0.0111 + 0.00275\ V_a} \quad \text{(ft/hr)} \qquad \text{where } V_a = \text{air velocity (ft/sec)}$$

As examples of observed fire velocities Osipov and Zadan give the values for 5 accidental and 9 experimental fires (table 7).

Roberts and colleagues found that an approximately linear relation between air and fire velocities exists. As an example, fig. 14 shows the rate of spread of fuel rich fires (R = 3) measured in a square duct of 1 ft^2 cross section plotted against the air velocity (100,103,104).

A possibility to calculate V_f offers the definition of the fuel/air ratio

$$R = \frac{5 * V_f * W * F}{V_a * \gamma_a * A}$$

With R = 0.3, γ_a = 0.075 lb/ft^3 and F = 1.0 one obtains for oxygen rich fires

$$V_f = \frac{0.3 * 0.075 * 3,600}{5} * \frac{Q_a}{W} = 16.2\ \frac{Q_a}{W} \quad \text{(ft/hr)}$$

which agrees well with the above formulas by Maas and Sadée and Baltajtis and Markovic. For fuel rich fires one obtains

$$V_f = \frac{3 * 0.075 * 3,600}{5} * \frac{Q_a}{W} = 162 * \frac{Q_a}{W} \quad \text{(ft/hr)}$$

which is not in as good agreement with the formula of Baltajtis and Markovic.

Roberts and Blackwell (104) report that in an accidental mine-fire 1200 ft of timber lagging were consumed in 40 hours. The estimated averages of fire velocity for a further 8 accidental fires were in the range of 66 - 330 ft/hr. If mixing of the fumes with fresh air from other airways gives rise to secondary fires, the rate of spread can, of course, be considerably higher. Mc Crodan (77) reports that in the fire at the McIntyre Porcupine Mine 1965 the path of the fire extended vertically through 1190 ft and horizontally through 7,155 ft within one week.

e) Temperatures developed by timber fires

The highest temperature a fire can reach is its adiabatic flame temperature. It can be determined from a heat balance which requires that the enthalpy of the reactants (air and fuel) plus the heat of reaction be equal to the enthalpy of the

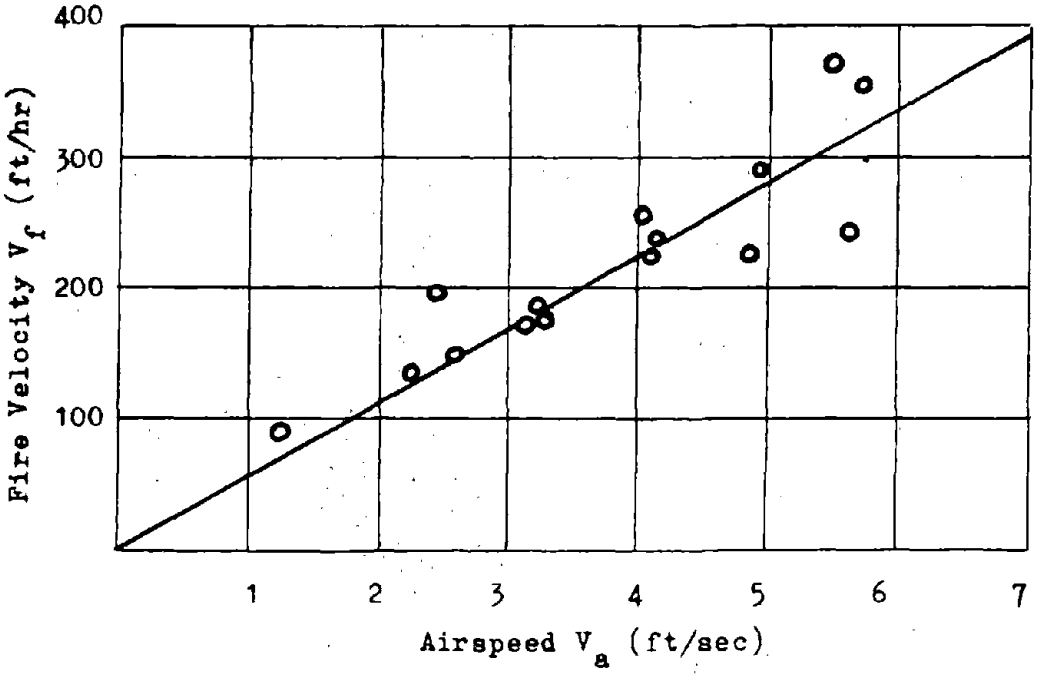

Fig. 14. Rate of Spread of a Fuel Rich Timber Fire (100)

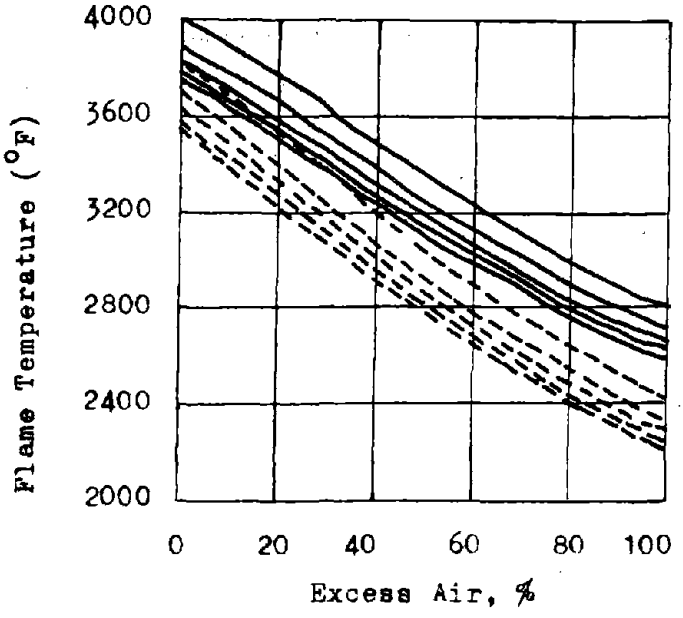

Fig. 15. Adiabatic Flame Temperature as a Function of the Hydrogen-to-Air Ratio of the Fuel and of the Excess Air(Solid Lines: 600°F of Excess Air, Dotted Lines: 100°F) (85)

Table 6. Comparison of Calculated and Measured Propagation Velocities of Timber Fires (7)

Test No	Air Velocity (ft/sec)	Timber Loading (lb/ft)	Propagation Velocity (ft/hr) Calculated	Measured
1	3.9	83.3	190	184
2	5.9	83.3	285	269
3	9.8	83.3	471	492
4	13.1	83.3	600	586

Table 7. Observed Fire Velocities of Accidental and Experimental Fires (94)

Mine		Cross Section (ft^2)	Air Veloc. (ft/sec)	Time since Ignition (hr)	Extension of Fire (ft)	Average Fire Veloc. (ft/hr)
Neshdannaja, Combinat Rostov		92.6	4.26	2.3	426	185
Choladnaja Balka, Group Makejevka		53.9	4.91	6	1050	175
Proletarian Dictatorship, Combinat Rostov		81.9	2.13	10	1230	123
October Revolution Group Schachtjorsk		61.4	3.28	18	2490	138
Astern No 10, Group Kommunarsk		48.5	6.56	2	426	213
	Test No					
CNIL VGSC Donbassa (Central Scientific Research Laboratory of the Mine Rescue Teams of the Donezk Basin)	1	32.3	3.28	0.5	98	196
	2	32.3	1.97	2.3	311	135
	3	32.3	5.74	1	229	229
	4	3.23	3.28	1.2	207	173
	5	32.3	3.28	0.5	66	132
	6	32.3	3.28	1.1	197	179
	7	32.3	6.89	2.5	531	213
	8	32.3	10.15	2.2	531	241
	9	32.3	17.06	1.8	531	295

combustion products. The heat of reaction for complete combustion is equal to the lower calorific value of the fuel. For incomplete combustion it must be corrected by subtracting the heat of combustion of any unburnt fuel due to lack of oxygen or dissociation. One has to consider, furthermore, that the products of combustion can include solids as well as gases.

The calculation of the adiabatic flame temperature is relatively cumbersome, since in addition to the specific heat variations of the combustion products their composition changes with temperature, due to dissociation, must be considered. Besides trial and error methods the use of charts is therefore advisable. As an example fig. 15 shows adiabatic flame temperatures calculated by Myers, Goldberg and Smith (85) for fuels of different carbon/hydrogen atomic ratios ranging from zero to four. Two sets of curves for air preheat temperatures of 100 and 600°F are plotted as functions of excess air or fuel/air ratios.

Calculations of adiabatic flame temperatures are based on the assumption of a perfectly mixed gas stream passing through the fire. As described above, this assumption holds for fuel rich fires but not for oxygen rich fires. Therefore, one can for the latter expect a wide range of flame temperatures being present in one and the same fire.

It is, however, possible to estimate the highest temperature the fumes can theoretically reach after the combustion products have been mixed with the excess air. Maas and Sadée (75) state that in oxygen rich timber fires a temperature increase higher than 1692°F has never been observed. They derive this figure by dividing the heat generation of the fire Q_h by the heat content of the gases passing through the fire. The former can be determined from

$Q_h = h_u * M_F$ (Btu/hr) where h_u = lower calorific value of timber (Btu/lb)
M_F = fuel consumption (lb/hr)

If the mass flow of the gas stream passing through the fire is considered to be approximately constant, its temperature increase is

$$\Delta t_f = \frac{Q_h}{Q_a * \rho_a * c_{pa}} = \frac{h_u * M_F}{Q_a * \rho_a * c_{pa}}$$

With the above quoted relation

$M_F = 18.15\ Q_a$ (lb/hr) and $\rho_a = 0.078$ lb/ft^3, $c_{pa} = 0.24$ Btu/lb°F, $h_u = 6,300$ Btu/lb one obtains

$$\Delta t_f = \frac{6,300 * 18.15}{3,600 * 0.078 * 0.24} = 1695\ ^{\circ}F$$

Baltajtis and Markovic mention that for incomplete combustion (as in fuel rich fires) the heat generated by the fire per unit mass fuel is smaller than the lower calorific value. For combustion products containing CO, H_2 and CH_4 they suggest to use the formula

$$Q_h = h_u * M_F - Q_g \, (3.21\, C_{CO} + 2.75\, C_{H_2} + 9.11\, C_{CH_4})$$

where Q_g = volume flow of fumes at standard conditions per hr (Sft^3/hr)

$C_{CO}, C_{H_2}, C_{CH_4}$ = volume % of CO, H_2 and CH_4 in fumes

3.21;2.75;9.11 = heat of combustion for CO, H_2 and CH_4 (Btu/ (Sft^3/100))

To determine from this heat the temperature of the fumes requires the same calculations which are necessary for the calculation of the adiabatic flame temperatures. An additional aggravation is that many pyrolysis products enter the fumes between the flame-zone and the point, where the gas samples are taken.

Experience shows that the temperatures of the fumes behind oxygen rich timber fires are considerably lower than 1700°F. If they were this high, a pyrolysis zone would develop and the fire would become fuel rich. Behind fuel rich fires the temperatures are equally much lower than the adiabatic flame temperatures. The reasons for are this the large heat transfer from the flames to the walls of the airway, caused by the high flame temperatures and the addition of gaseous pyrolysis products at temperatures lower than those of the gas stream.

Roberts and Clough (103) derived a function for the gas temperature in the pyrolysis zone of fuel rich timber fires, which takes these factors into account. The highest temperature can be expected where all the oxygen has been consumed and is, according to this function

$$t_{fmax} = \left[\frac{23{,}700}{\beta_1} + t'_w\right](1 - 1.262^{-\beta_1}) + 32 \quad (°F)$$

t'_w is the surface temperature at which significant pyrolysis of the timber begins, which according to Roberts and Clough is at t'_w = 527°F. β_1 is defined by

$$\beta_1 = 1 + h/(m * c_F * f)$$

where h = gas-to-wall heat transfer coefficient

m = volatile emission rate per unit wood surface area

c_F = specific heat of volatiles

f = fraction of roadway perimeter lined with wood

The term $m * c_F * f$ is the heat content of the volatiles emitted per unit roadway surface area and time. It is more or less proportional to the heat transfer coefficient h with the result that β_1 is more or less constant for larger velocities. Values for β_1 determined in a square model duct of 1 ft sidelength with f = 0.75 and plotted over Reynolds Numbers calculated with air viscosities at 1832°F are

shown in figure 16.

At the end of the pyrolysis zone, where the wood surface temperature is $t'_w = 527^oF$, the gas temperature t'_f can be described by

$$\frac{t'_f - t'_w}{t_{fmax} - t'_w} = \left[\frac{1 + 0.262*R}{1.262}\right]^{-\beta_2}$$

The fuel/air ratio for fuel rich timber fires can be assumed to be R = 3. Values for β_2 are shown in fig. 16.

Measured maximal gas stream temperatures in the combustion zone t_{fmax} and estimated gas temperatures at the end of the pyrolysis zone t'_f, determined by Roberts and Clough (103) in their model duct are shown as function of the air velocity in fig. 17. A consideration of scaling laws for fires (105) shows that the gas temperature - air velocity relationship is approximately the same in small scale model tests and large scale fires. One, however, can expect the maximum gas temperature in large scale fires to be about 100-200°F lower than in model tests, due to the greater importance of radiation.

As an example from the many experiments conducted by Roberts and colleagues in their model duct fig. 18 shows the typical variation of gas temperature in a fuel rich timber fire with distance 2, 5, 8, and 11 minutes after the start of the fire (102). The temperature reaches a peak of about 2000°F in the flamezone. Because of the greater effect of radiation at higher temperatures and because of the addition of pyrolysis products, which are due to the lack of oxygen no longer burned, a rapid temperature decrease to about 1000°F takes place. From there on no further pyrolysis products are added and the temperatures decrease more or less exponentially with distance.

Temperature curves measured by other researchers in fuel rich timber fires are very similar. Fig. 19 shows experimental results published by Osipov and Zadan (94). The temperatures were measured in the center of a horizontal rectangular tunnel of 45 ft^2 cross section at the distances and times indicated in the figure. The same tunnel was used by Baltajtis and Markovic (7) for fire experiments and the observed temperatures published by them are given in table 8.

Voskobojnikov (131) describes a fire experiment in a square, timbered tunnel of 43 ft^2 cross section, ascending with 16.5°. After 20 minutes the fire was so far developed that the whole cross section was filled with flames. Fig. 20 shows the observed temperatures along the tunnel 20, 24, 28, and 32 minutes after the fire had been ignited.

Fewer observations exist for oxygen rich fires than for fuel

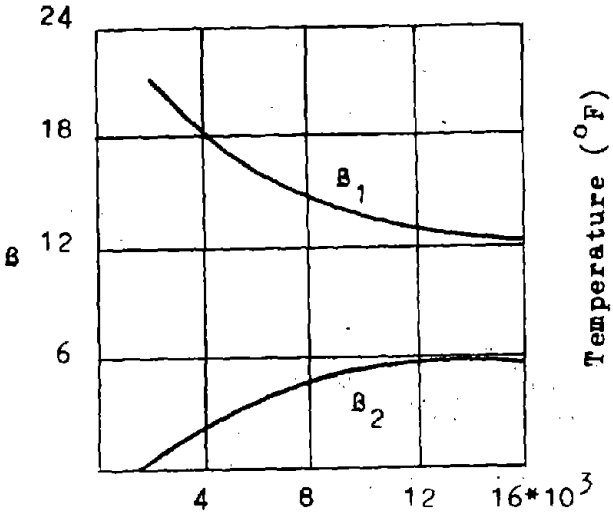

Fig. 16. Values of Functions β from Model Tests (103)

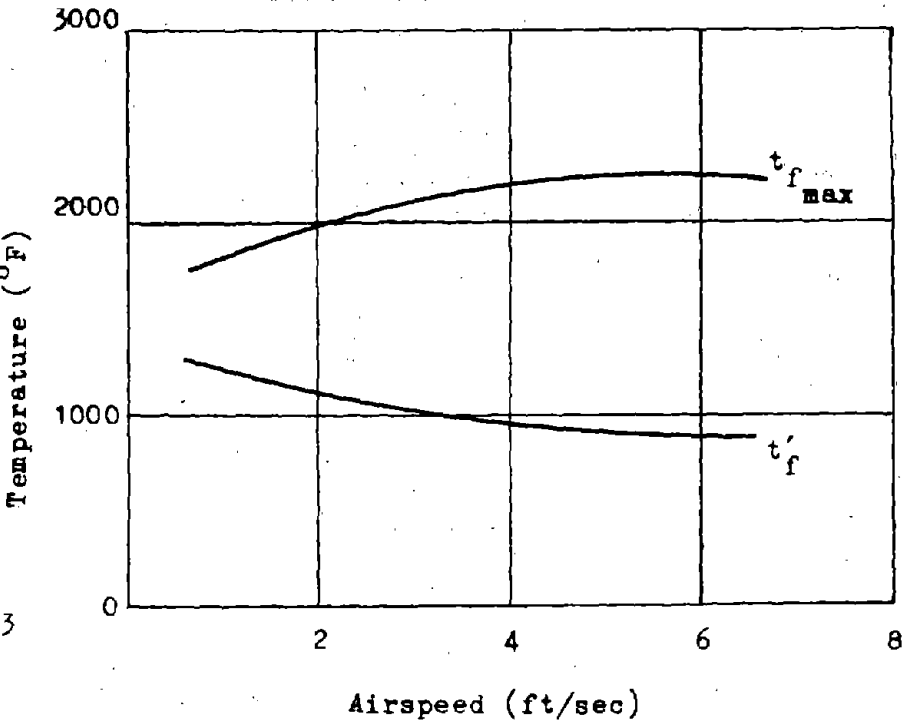

Fig. 17. Gas Temperature at End of Pyrolysis Zone t'_f and Maximal Gas Temperature in Combustion Zone $t_{f_{max}}$ of Timber Fire (103)

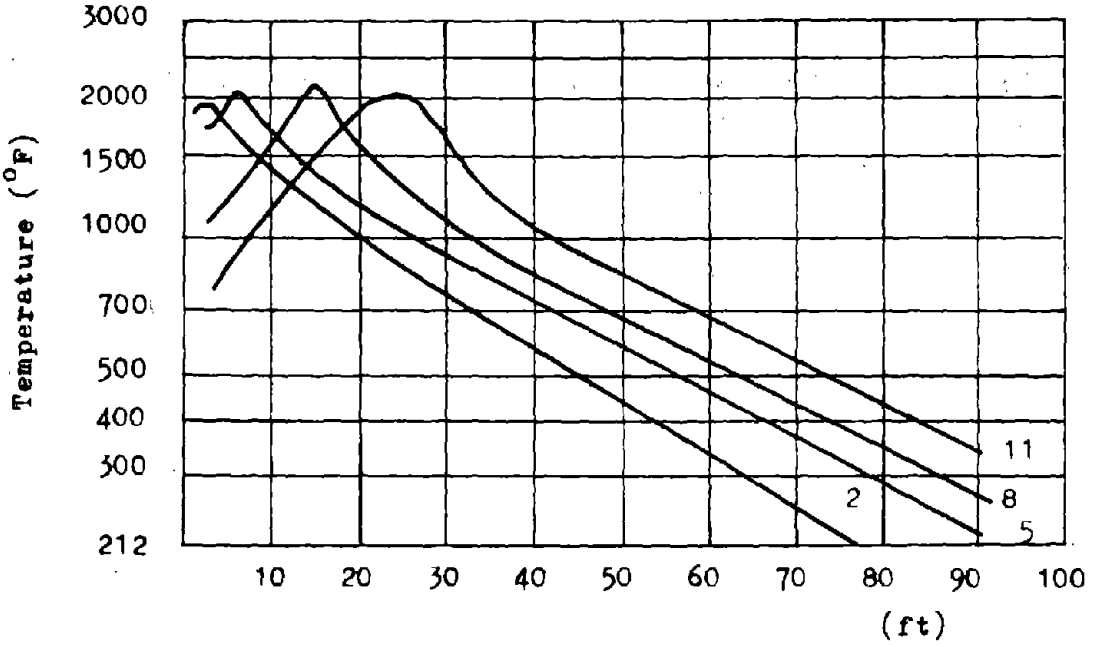

Fig. 18. Variation of Temperature along Model Duct with Fuel Rich Timber Fire 2-11 Minutes after Start of the Fire (102)

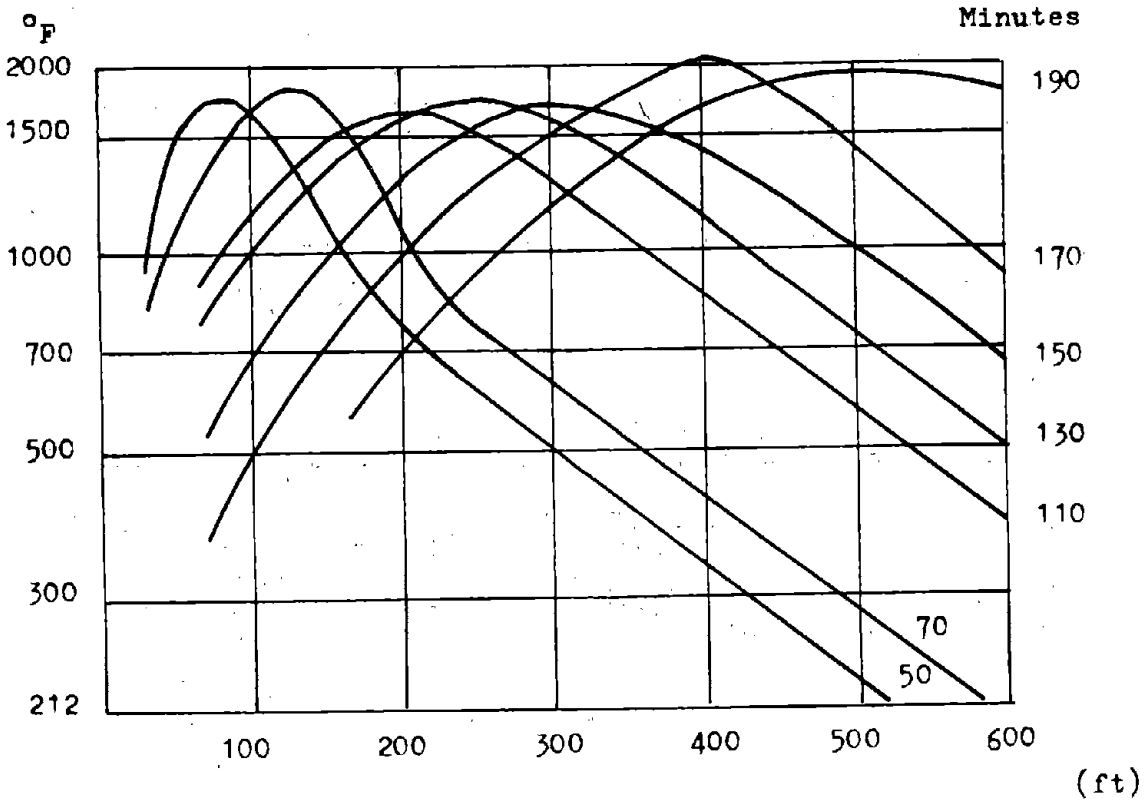

Fig. 19. Temperature along Tunnel of 45 ft^2 Cross Section with Timber Fire (94)

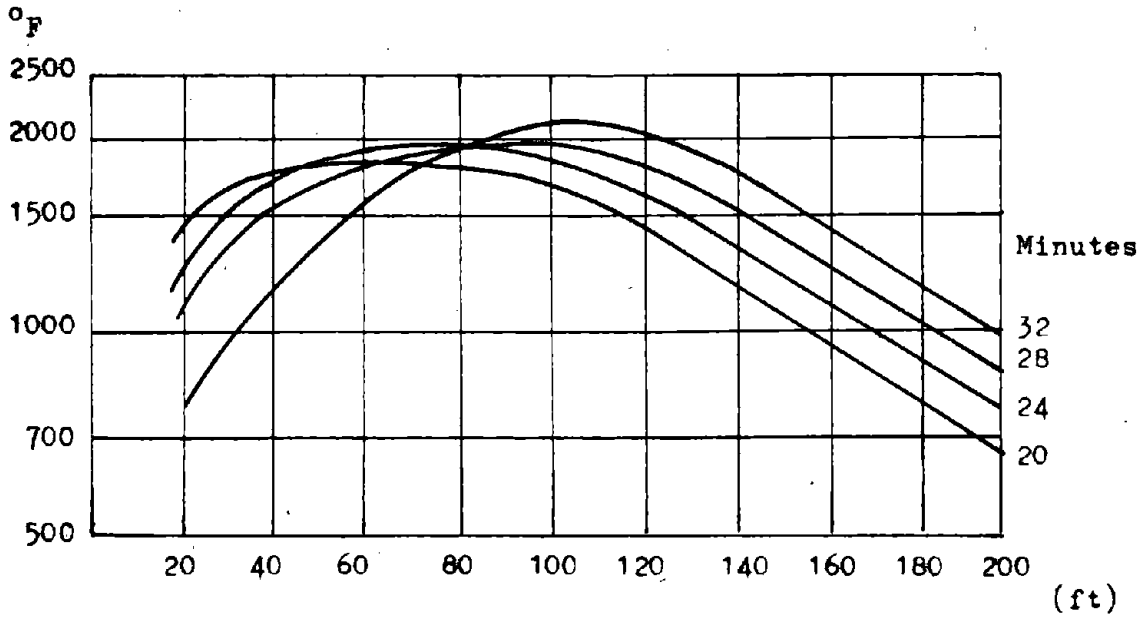

Fig. 20. Temperature along Tunnel with Timber Fire (43 ft^2 Cross Section) (131)

Table 8. Gas Temperatures (°F) Measured in a Large Scale Timber Fire (7)

Time since Ignition (min)	Distance from Source of Ignition (ft) 65.5	82	147.5	213	311	410	475
10	1796	1706	1174	752	392	248	221
30	1412	1562	1743	1330	752	464	402
50	1112	1112	1581	1634	1050	662	572
70	752	878	1203	1787	1454	896	752
90	652	716	860	1922	1996	1094	932
110	518	562	1022	1670	1868	1184	1050
130	419	464	572	1400	1472	1526	1131

Table 9. Materials Burned in Open Fires in British Coal Mines (26)

Year	Coal	Coal Dust	Wood	Oil or Grease	Hydraulic Fluid	Conveyor Belt
1966	11	36	13	14	3	10
1967	10	23	14	10	0	6
1968	8	27	12	21	5	4
1969	3	29	13	19	0	7
1970	5	34	15	14	2	8
Total	37	149	67	78	10	35

Table 10. Maximal Observed Temperatures in Experimental Coal Fires (45,87)

Location of Coal	Floor			Floor and Rib		
Quantity (lb)	3650	24350	7500	7500	12500	12500
Time since Ignition (min)	180	310	130	285	135	250
Maximal Temperature (°F)	1400	1490	1550	1600	1550	1650

Location of Coal	Floor, Rib and Roof							
Quantity (lb)	17000	18000	15550	18550	14250	12250	17850	19330
Time since Ignition (min)	215	195	190	165	220	180	255	225
Maximal Temperature (°F)	1800	1550	1560	1200	1200	1290	1530	1790

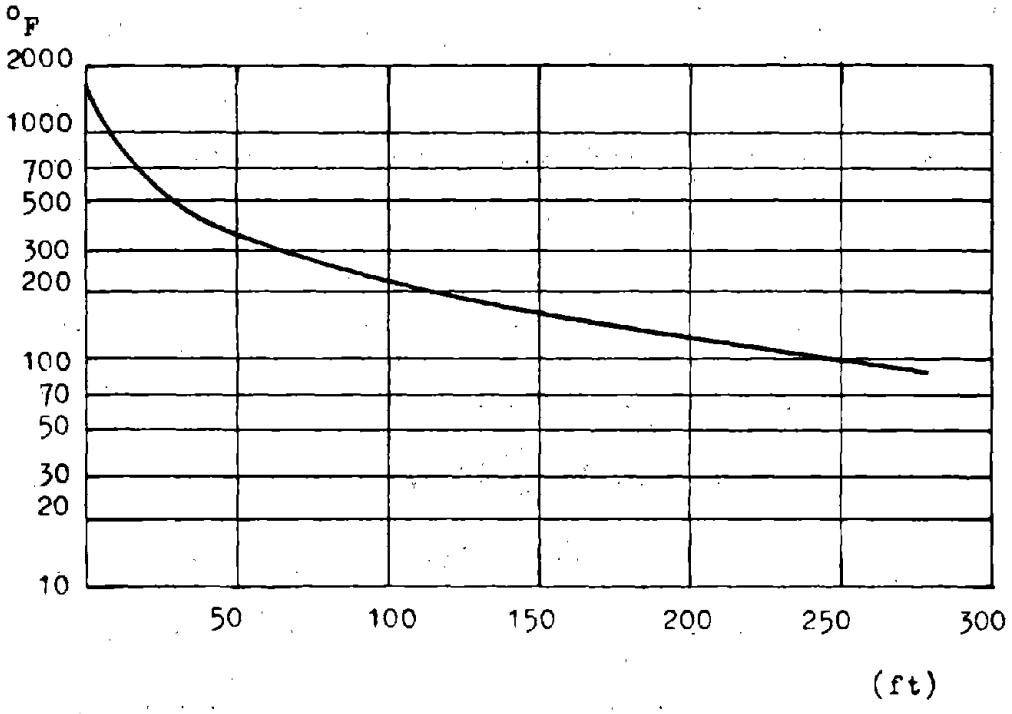

Fig. 21. Temperature along a Descensionally Ventilated Raise with a Woodpile as Fire Object (118)

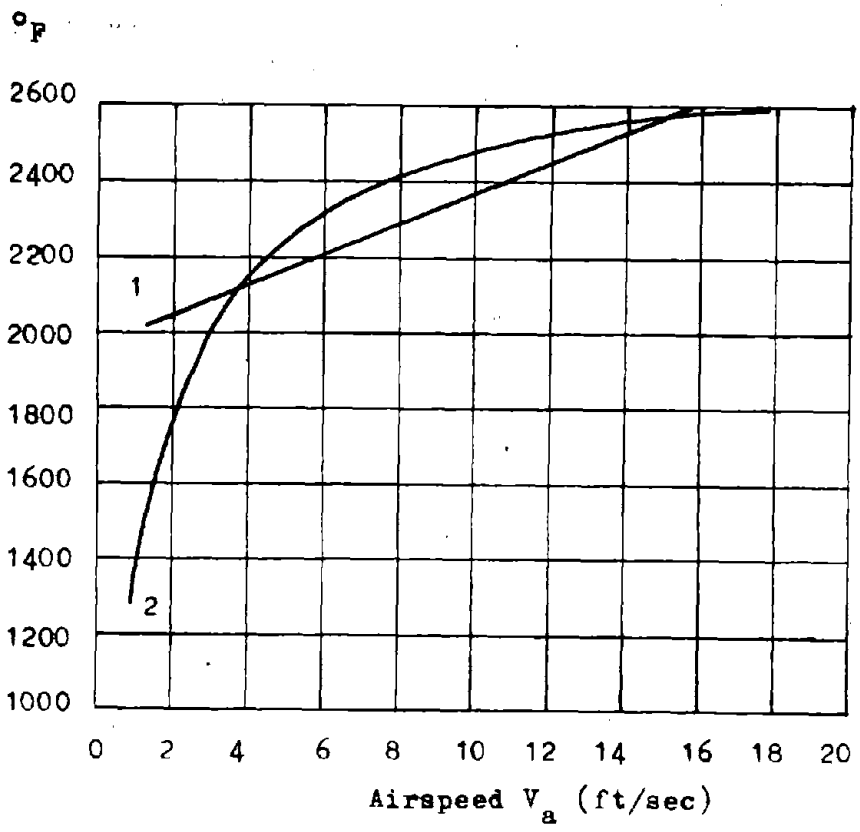

Fig. 22. Maximal Gas Temperatures of Timber Fires Calculated with Formulas Suggested by Osipov and Zadan (94)

rich fires. Schmidt and Grumbrecht (118) conducted 130 large scale fire tests in a 72° raise of 22 ft^2 cross section, in which centrally located wood piles of 250 - 700 lb weight were ignited. All their fires remained oxygen rich (fig. 10). Since the purpose of their experiments was to find the largest possible ventilation disturbance, all observed temperatures were entered into a single graph and an upper envelope curve was plotted (fig. 21). Although most temperatures are considerable lower than this envelope curve, one sees clearly that in oxygen rich fires the flame temperatures can be in the same order of magnitude as in fuel rich fires. The temperature decrease immediately behind the fire is due, however, to the mixing of combustion products with excess air much more rapid.

Osipov and Zadan (94) made the same observations as Roberts and Clough (fig. 17) that the temperatures increase with air velocity. From their experiments in a timbered tunnel of 45 ft^2 cross section they conclude that the maximal temperature of fully developed fires can be described by the formulas

$$t_{fmax} = 1975 + 40 * V_a \quad (^\circ F) \text{ for } 1.6 < V_a < 16 \text{ (curve 1 in fig. 22) or by}$$

$$t_{fmax} = 32 + \frac{V_a}{0.000419 + 0.000361 * V_a} \quad (^\circ F) \text{ for } 0 < V_a < 26 \text{ (curve 2 in}$$

figure 22). The air velocity V_a is measured in ft/sec. Expressed as a function of the ratio P_a = airflow/timberloading (ft^3 / min air per ft^3 /ft timber) they obtain

$$t_{fmax} = 32 + \frac{P_a}{0.257 + 0.000381 * P_a} \quad (^\circ F)$$

These temperatures were reached about 1 hour after the ignition of the fire and then remained constant. The temperatures in the original stages of the fire are slightly lower, since less preheating of the air in the burnt out heated sections of the duct takes place.

f) Coal fires

Coal fires, especially coal dust fires, are more frequent than timber fires. (table 9). However less attention is given them in the literature and very few results on systematic fire experiments have been published. The reason may be that they are less dangerous than timber fires. Although coal dust is a material with one of the lowest ignition temperatures encountered underground (fig. 23), the rate of growth of a fire in coal dust is low. It is in the order of magnitude of 3 1/2 inches/hr, dropping to 2 in/hr when the coal dust is mixed with stone dust (32). Coal dust fires, therefore, do not pose any serious threat to life or production. The danger of coal dust is instead to act as a igniter and fuse to other more flammable materials.

Lump or solid coal fires are usually not too serious a risk to life either, especially in their early stages. Coal,

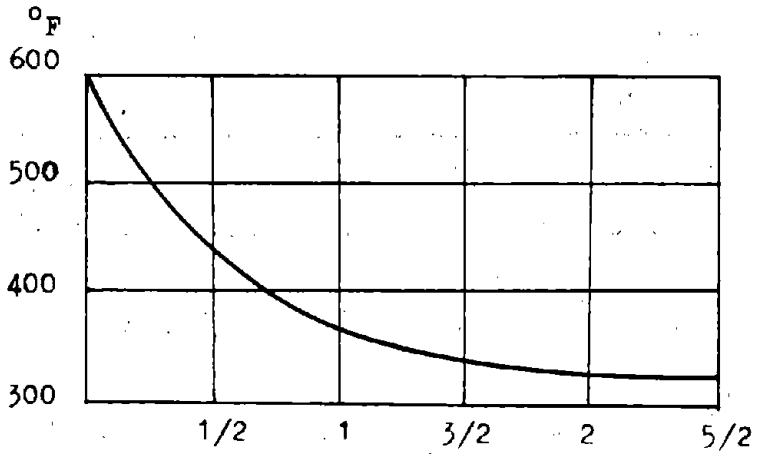

a) Minimum Surface Temperature for Ignition

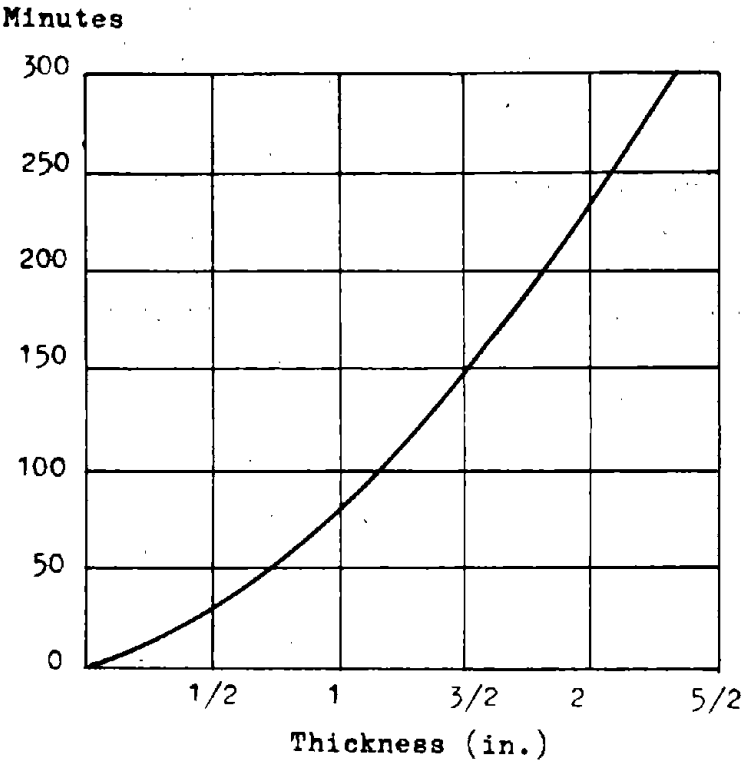

b) Maximum Delay before Ignition at Minimum Ignition Temperature

Fig. 23. Smouldering of Silkstone Coal Dust with 34-36% Volatiles (32)

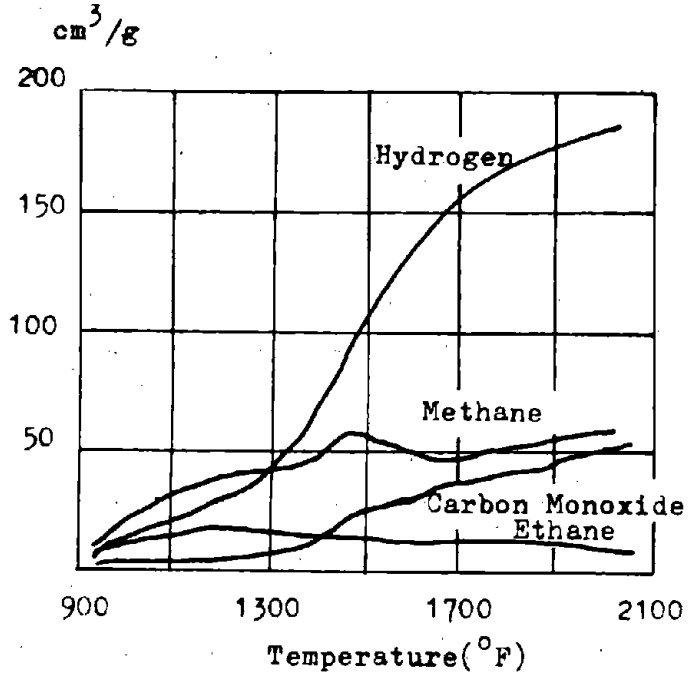

Fig. 24. Example for Volume of Gases Evolved from Coal

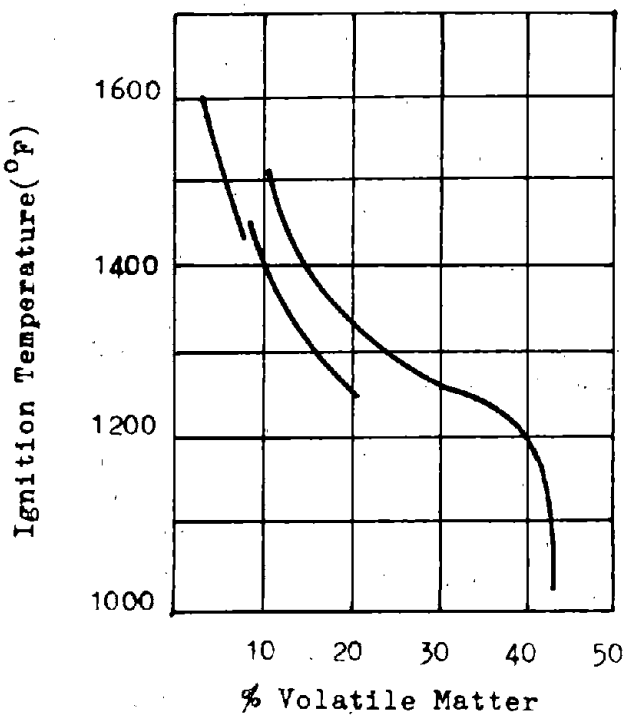

Fig. 25. Ignition Temperature of Coal (29)

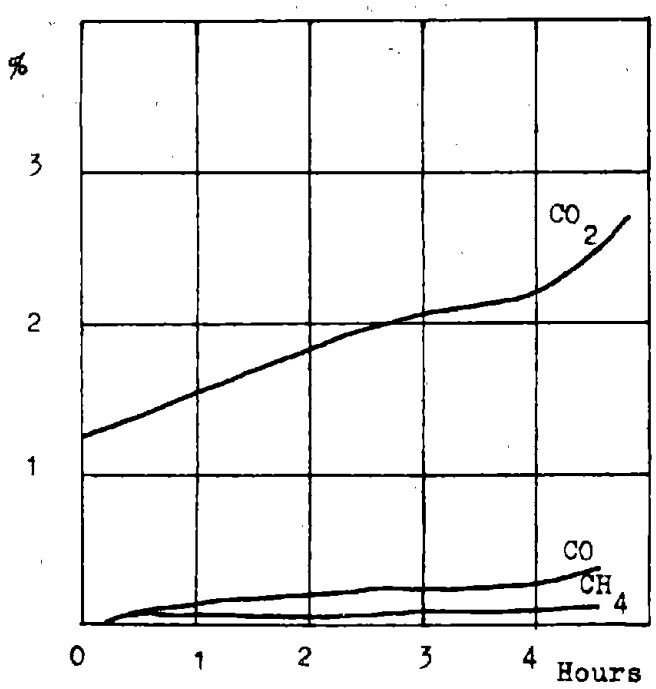

Fig. 26. Observed Composition of Fumes behind a Coal Fire (87)

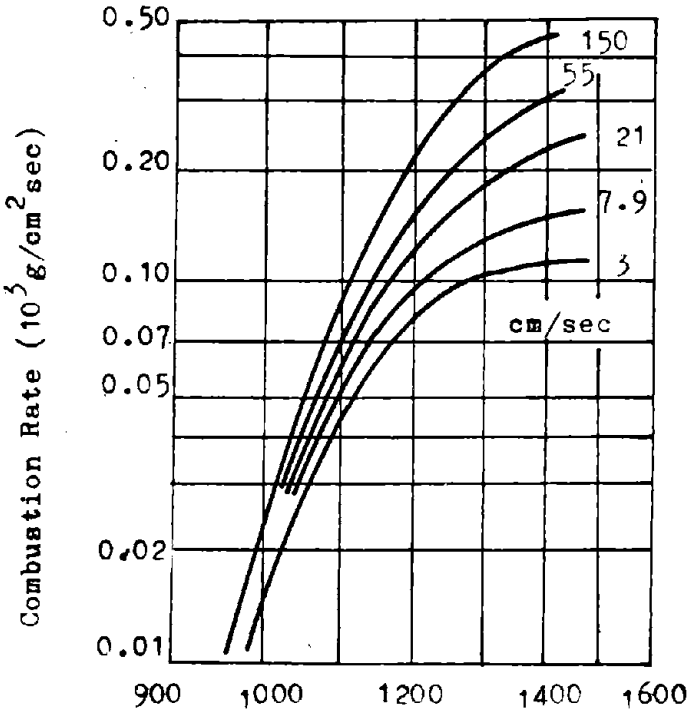

Fig. 27. Combustion Rate of Brush Coal as a Function of Temperature(°K) and Air Velocity(cm/sec) (96)

with approximately 5 % for anthracite and 40 % for high volatile C bituminous coal has a much lower volatile content than wood with 75 - 85 %. Substantial distillation of volatile matter begins only at about 600°F and becomes rapid at about 1300°F (fig. 24), whereas the corresponding temperatures for wood are approximately 400 and 550°F. Also the ignition temperatures are higher, although the latter are not constants but depend on oxygen concentrations, exposure times, mineral contents, etc. Fig. 25 (29) shows the order of magnitude.

Due to its economic importance as one of the principal energy sources, the combustion of coal in industrial processes has been the subject of a vast number of investigations. This does not however apply to the accidental combustion of coal in underground mines, where, except for fire extinguishing equipment, no systematic work seems to have been done. Due to the complexity of fire it would be risky to try to develop a model for such fires. It would exceed the scope of this report, being a literature evaluation, too.

The controlling mechanisms of fire propagation for coal fires should in principle be the same as those described in chapter II-B. Since coal is a difficult ignitable fuel one can expect coal fires, at least for higher ranking coals, to be oxygen rich fires. Fuel rich fires will mainly occur as a temporary phenomenon after a reduction in ventilation.

Few data have been published on the composition of combustion products of open underground coal fires. All deal with oxygen rich fires, probably due to the limited extension of the fuel beds provided. Nagy, Hartmann and Howarth (86) report that in 35 experiments with coal fires of 20 ft length and air velocities between 2.8 and 5 ft/sec the fumes contained 0.02 - 2.6 % CO_2, 17.55 - 20.61 % O_2, 0.01 - 0.12 % CO, 0.0 - 0.04 % CH_4, no H_2, and N_2 as the balance. Nagy, Murphy and Mitchell (87) give, for a fire of 24,350 lb of coal spread over a length of 15 ft along the floor, the CO_2, CO and CH_4 contents shown in fig. 26.

Temperature observations were published by Nagy, Murphy, Mitchell (87) and Hartmann, Nagy, Barnes, Murphy (45). Their coal fires had a length of 15 ft, the air velocities were in the range of 50 - 100 ft/min, the coal covered either the floor, floor and rib, or floor, rib and roof. Coal quantity, location, burning time and maximal observed temperatures in the fuel bed are compiled in table 10. A timber fire of 1100 lb in the same tunnel after 10 minutes rose to a temperature of 1600°F. Air temperatures were in the range of 700°F.

No data have been published so far on fuel consumption, extension and velocity of coal fires. To estimate the order of magnitude one could proceed as follows, although, due to the lack of experimental confirmation, the results have to be accepted with caution. The fuel consumption can be determined as derived in chapter II-C-b with the formula

$$M_F = 0.0317 \frac{\Sigma C_p}{C_F} * 3{,}600 * Q_a \quad (lb/hr)$$

where C_F = mass % C in fuel

ΣC_p = volume % C in combustion products

Q_a = airflow (ft^3/sec)

If one assumes that in oxygen rich fires, where the fire propagation takes place through local heat transfer from the flames along the walls, the volatiles as well as the fixed carbon is consumed, and that ΣC_p is not higher but most probably lower than in timber fires, one obtains for anthracite

$$M_{Fmax} = 0.0317 * \frac{6}{85} * 3{,}600 * Q_a = 8.05\ Q_a$$

and for high volatile C bituminous coal

$$M_{Fmax} = 0.0317 * \frac{6}{70} * 3{,}600 * Q_a = 9.78\ Q_a$$

Fuel rich fires are mainly fed by the gas generated from the coal by the hot fumes. Judging from the products obtained in high-temperature coke ovens the gas composition changes with coal but its carbon content remains from low volatile to high volatile C bituminous coal in the range of 50 %. Under the assumption that all carbon is burned to CO and all oxygen has been consumed, one obtains for ΣC_p values between 12 and 20 %. Consequently

$$M_{Fmax} = 0.0317 * \frac{20}{50} * 3{,}600 * Q_a = 45.6\ Q_a \quad (lb/hr)$$

The maximal extension for oxygen rich fires of the fire zone can be determined under the assumption that all fuel consumed is fixed carbon. The combustion rate of brush coal (probably lower than that of underground coal and therefore leading to the calculation of too large fire zones) has been determined by Parker and Hottel (96) and is shown in fig. 27 as a function of temperature and air velocity. If the temperature in the fuel bed is 1500°F, the average combustion rate is $m_v = 0.06 * 10^{-3}$ $g/cm^2 * sec$. or $m_v = 0.45$ $lb/ft^2 sec$. With $M_F = m_v * P * L_f$, where P = perimeter of airway and L_f = length of fire zone one obtains for anthracite

$$L_{fmax} = \frac{8.05}{0.45} * \frac{Q_a}{P} = 17.9\ \frac{Q_a}{P} \quad (ft)$$

and for high volatile C bituminous coal

$$L_{fmax} = \frac{9.78}{0.45} * \frac{Q_a}{P} = 21.7\ \frac{Q_a}{P} \quad (ft)$$

For fuel rich fires one can make the assumption that per hour a layer of 1/2 inch thickness of the coal is carbonized (72). This results in a volatile emission of

$M_F = P * L_f * \frac{1}{24} * \gamma'_C * C_v$ where γ'_C = specific weight of coal

C_v = mass % volatile matter of coal

With $\gamma'_C = 80$ lb/ft^3, $C_v = 40$ % and $M_F = 45.6\ Q_a$ one obtains

$$L_f = \frac{45.6 * 24}{80 * 0.40} * \frac{Q_a}{P} = 34.2\ \frac{Q_a}{P} \quad \text{(ft)}$$

The velocity with which a coal fire spreads is hard to predict. Due to the unlimited availability of fuel it will be strongly influenced by such factors as diffusional resistance of the slag formed along the walls. It will certainly be much smaller than that of timber fires but how large it is has to be answered by accidental or experimental evidence.

III. Temperature of Fumes Behind the Fire Zone

All major forces exerted by mine fires on the ventilation can be considered as thermal forces. For their determination the knowledge of the temperature changes, caused by the fires, is indispensable. This applies less to flame- or pyrolysis zones, which are comparatively short, than to the much longer airway sections downwind of the fire which can experience considerable temperature changes, too.

The temperature of the fumes leaving a flame- or pyrolysis zone is changed by mixing with other air currents and by heat exchange with the airway walls. The effects of mixing are easy to describe. Except for the entropy, each individual property of the mixture is equal to the mass-weighted arithmetic mean of the same properties of the constituents. No further detailed discussion of mixing processes is therefore necessary.

Less simple to describe are the heat exchange processes. The different approaches applied by ventilation engineers where applicable will therefore fill the whole following part III of this report.

A. Steady state heat exchange with airway walls

The assumption of an infinite heat capacity of the rock surrounding an airway leads to constant rock temperatures and to a steady heat exchange process between air and rock. If the rock, before exposed to the fumes with the temperature t_f, had assumed the average temperature t_a of the ventilating air, the heat transfer d_q from the fumes to the rock can be described by

$$dq = \alpha\ (t_f - t_a)\ P\ dL$$

where α = heat transfer coefficient
P = perimeter of airway
L = length of airway

This will cause a change of temperature in the fumes by

$$dt_f = -\frac{dq}{G * c_p}$$

where G = mass flow rate of fumes
c_p = constant pressure specific heat of fumes

With
t_{fo} = temperature of fumes at the begin of the airway ($L = 0$)
one obtains

$$t_f = t_a + (t_{fo} - t_a)\ \exp\left(-\frac{\alpha\ P\ L}{G * c_p}\right) \qquad \text{equ. 3.1}$$

The mean temperature of the fumes in the airway, which is frequently used for the determination of thermal forces, is

$$t_{fm} = \frac{1}{L} \int t_f\ dL = t_a + \frac{t_{fo} - t_a}{L} * \frac{G * c_p}{\alpha P}\left(1 - \exp\left(-\frac{\alpha P * L}{G * c_p}\right)\right)$$

The mean of the squares of the absolute temperatures, which is sometimes used for the same purpose, is

$$(T_{msq})^2 = \frac{\int T_f^2 dL}{L} = T_a^2 + \frac{t_{fo} - t_a}{L} * \frac{G*c_p}{\alpha P} \left[2T_a\left(1 - \exp\left(-\frac{\alpha P*L}{G*c_p}\right)\right) + \frac{t_{fo} - t_a}{2}\left(1 - \exp\left(-\frac{2\alpha P*L}{G*c_p}\right)\right)\right]$$

In nonhorizontal airways the change of the original rock temperature with depth and of the air temperature due to pressure changes (autocompression) has to be taken into account. If the original rock temperature is decribed by the formula

$$t_{RV} = t_{RVo} - gr*L*\sin\beta$$

where t_{RVo} = original rock temperature at begin of airway
gr = geothermal gradient
β = angle of airway inclination (positive for ascensional, negative for descensional airways)

and if the pressure changes with depth cause the temperature change

$$dt_a = -\frac{\sin\beta}{I*c_p} dL = -ga*\sin\beta*dL$$

where I = mechanical heat equivalent = 778.26 ft-lb/Btu

the combined effect of heat exchange between fumes and rock and autocompression can be described by

$$dt_f = -ga*\sin\beta*dL - (t_f - t_{RVo} + gr*\sin\beta*L)\frac{\alpha P}{G*c_p} dL$$

With $t_f = t_{fo}$ for $L = 0$ integration results in

$$t_f = t_{RVo} - gr*L*\sin\beta + \left(t_{fo} - t_{RVo} - \frac{G*c_p*\sin\beta}{\alpha P}(gr-ga)\right)\exp\left(-\frac{\alpha P*L}{G*c_p}\right) + \frac{G*c_p*\sin}{\alpha P}(gr-ga) \qquad \text{EQU. 3.2}$$

Under the assumption that for older airways the heat exchange between air and rock had become negligible before the fire started and that the rock had assumed the temperature of the air ($t_{RVo} = t_{ao}$, $gr = ga$) this equation can be reduced to

$$t_f = t_{ao} - ga*L*\sin\beta + (t_{fo} - t_{ao})\exp\left(-\frac{\alpha P*L}{G*c_p}\right) \qquad \text{EQU. 3.3}$$

Mean temperatures t_{fm} and mean square absolute temperatures $(T_{msq})^2$ can be calculated without difficulties.

A later comparison with the results obtained for non-steady heat exchange processes shows that the assumption of a steady state process is a good approximation for small air quantities and for the first minutes, during which the heat exchange takes place.

B) Non steady state heat exchange with airway walls

A more accurate treatment has to take into account the limited heat capacity of the rock surrounding the airways. Whenever a heat exchange between the air and the walls occurs, a gradually thickening layer of rock with temperatures between the original rock temperature and the air builds up. This layer forms an insulation and lets the heat exchange decline with time.

Due to the importance of accurate temperature precalculations in deeper mines with climatic difficulties, many attempts for the calculation of the non-steady state heat exchange between air and rock have been made. Within the scope of this report it is impossible to quote every single paper which exists on this topic. Only those, which became better known because they suggested an improvement of existing solutions and whose results are applicable to mine fires shall be discussed.

The non-steady state heat exchange between rock and air is a very complex problem since it comprises
the heatflow by conduction within the rock,
the heat transfer by convection and radiation from the rock to the air or vice versa,
the heat transfer associated with mass flow.
Heat flow by conduction can be determined with the help of Fourier's equation of heat conduction

$$\frac{\partial t}{\partial \tau} = a\ \nabla^2 t + \frac{1}{c * \gamma'} W$$

where t = rock temperature
τ = time
$a = \frac{k}{c\gamma'}$ = thermal diffusivity of rock
k = heat conductivity of rock
c = specific heat of rock
γ' = specific weight of rock
W = heat generation per unit volume inside rock

In applying this equation on the heat exchange in mine airways the following assumptions are usually made:
the rock is homogeneous and isotropical,
the temperature of the rock surrounding the airway is uniform at the beginning of the heat exchange,
the airway has a circular cross section,
the heatflow parallel to the airway is negligible,
no heat sources or sinks exist in the rock,
no change of phase of the rock humidity occurs.
Fourier's equation of heat conduction can then be expressed in cylinder coordinates in the following form:

$$\frac{\partial t}{\partial \tau} = a \left(\frac{\partial^2 t}{\partial r^2} + \frac{1}{r} * \frac{\partial t}{\partial r} \right)$$

Under the additional assumptions:
the original rock temperature remains preserved at a sufficient distance from the airway,
the wall temperature is equal the air temperature (heat transfer coeff. $\alpha = \infty$),
the air temperature along the airway does not change with time,

general solutions with numerical applications have been provided by Nicholson (90), Smith (119), Carslaw and Jaeger (21) and de Braaf (15), extensive numerical solutions by Carrier (24), Goch and Patterson (37), Jaeger and Clark (60), Wiles (143), Koenig (69), Batzel (8) and Boldizsar (11,12). Simplified solutions assuming an insulating mantle of constant thickness were derived by Heise and Drekopf (50,51) and Stokes and Cernik(123).

Solutions with a variable heat transfer coefficient α were published by Jaeger (59), Scott (111), Scerban and Kremnev (107), Starfield (122), Nottrot and Sadée (91) and Amano and Shigeno (4). A set of 2500 solutions has been calculated by the West German coal mines and is part of their computer library (135). Numerical procedures for temperature precalculations, which allow accommodation of a great variety of boundary conditions were recently developed by Jordan and colleagues (61,62,63). They do not attempt to obtain solutions in closed form.

Fourier's equation of heat conduction describes the temperature distribution in the rock. The heat exchange between rock and air per unit time and wall area is for a circular airway with the radius r_o

$$h_R = k\left(\frac{\partial t_R}{\partial r}\right)_{r=r_o}$$

or, with the wall temperature t_w

$$h_R = \alpha \ (t_w - t_a)$$

Most solutions of the Fourier equation for the heat exchange in mine air make use of or can be related to the use of a dimensionless function

$$K(\alpha) = \frac{\alpha\, r_o}{k} * \frac{t_w - t_a}{t_{RV} - t_a} = r_o \frac{(\partial t/\partial r)_{r=r_o}}{t_{RV} - t_a}$$

A comparison between

$$h_R = k\,(t_{RV} - t_a)\,\frac{1}{r_o}\,K(\alpha)$$

and the equation for a hypothetical steady state heatflow between the temperatures t_{RV} and t_a through a layer of rock with the thickness y

$$h_R = k\,(t_{RV} - t_a)\ \frac{1}{y}$$

delivers: $K(\alpha) = r_o/y$. $K(\alpha)$ can therefore be visualized as a dimensionless scale for the thickness of the insulating layer of rock surrounding airways and increasing with age. It is therefore frequently called: "Coefficient of age". The advantage of its use is that, with proper values of $K(\alpha)$, non-steady state heatflow processes can be treated as steady state processes.

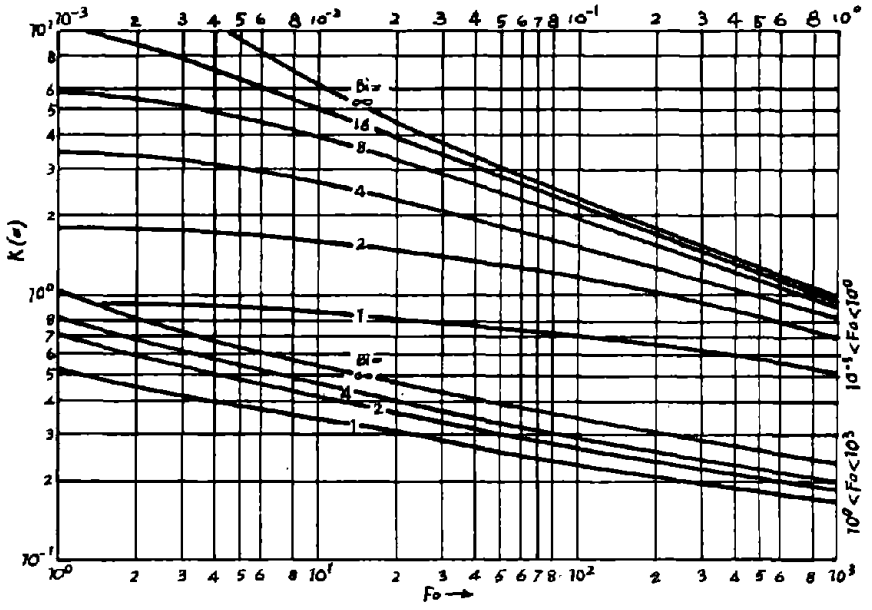

Fig. 28. Coefficients of Age $K(\alpha) = f(Fo, Bi)$ according to Scerban and Kremnev (107)

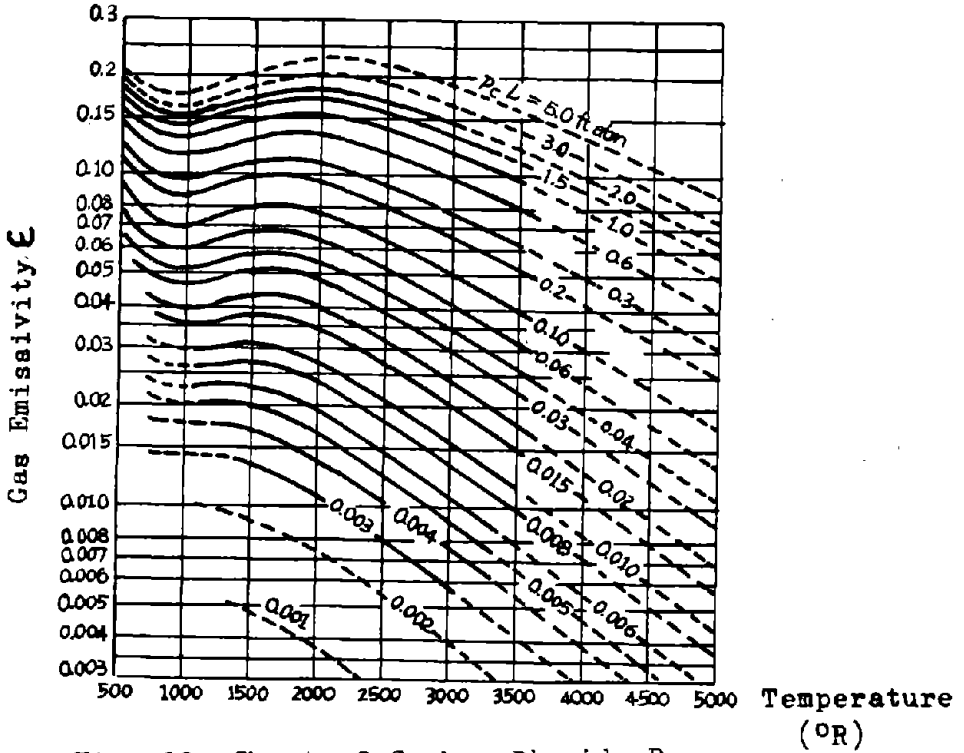

Fig. 29. Chart of Carbon Dioxide Radiation (58)

The coefficient of age K(α) is a function of the dimensionless numbers $Fo = \frac{a\tau}{r_o^2}$ and $Bi = \frac{\alpha r_o}{k}$, frequently called Fourier and Biot numbers. A comparison shows that the values obtained for K(α) by the different authors agree well with each other. An example are the results of Jaeger and Clark (60) for $F_o = 10^{-2} - 10^3$ and Bi = ∞ (α = ∞) given in table 11, the results of Nottrot and Sadée (91) for Fo = 0.0004 - 1000 and Bi = 0.1 - ∞ in table 12 and the results of Scerban and Kremnev (107) for Fo = 10^{-3} - 10^3 and Bi = 1 - ∞ in fig. 28. Table 12 a contains dimensionless wall temperatures, calculated by Nottrot and Sadée(91).

Several of the above quoted authors provide solutions of the Fourier equation for short periods of heat exchange. Numerical solutions have been published by Scerban and Kremnev (107) and Scott (111). If the terminology of this report is used, Scerban and Kremnev's results for K(α) are

$$K(\alpha) = Bi - \frac{Bi^2}{0.375+Bi}\left[1 - \exp(z^2)\left(1 - \frac{2}{\sqrt{\pi}}\int_0^z \exp(-z^2)dz\right)\right]$$

where $z = (0.375 + Bi)\sqrt{Fo}$

If the term in brackets is called f(z), this equation can be written as

$$K(\alpha) = Bi - \frac{Bi^2}{0.375 + Bi} f(z)$$

Values for f(z) are given in table 13. According to the authors, for values Bi>10 and Fo>0.005 an approximation

$K(\alpha) = 0.375 + \frac{r_o}{\sqrt{\pi a \tau}}$ is justified.

Scott (111) suggests for time periods < 6 weeks (again in the terminology of this report)

$$K(\alpha) \sim Bi - 2\left(\frac{Fo}{\pi}\right)^{1/2} (Bi)^2$$

Since the coefficient of age K(α) is based on circular cross sections, corrections for noncircular airways have been determined by Koenig (69). According to his recommendations an equivalent radius $r_o = \frac{P}{\delta}$ should be applied, where δ has the following values for equilateral cross sections:

shape	δ	shape	δ	shape	δ
triangle	7.108	hexagon	6.521	decagone	6.374
quadrangle	6.778	octagon	6.421	circle	6.283

For rectangular shapes with different side ratios he recommends:

side ratio	δ	side ratio	δ	side ratio	δ
0.1	7.40	0.4	6.92	0.7	6.81
0.2	7.15	0.5	6.87	0.8	6.80
0.3	7.00	0.6	6.83	0.9	6.78

Table 11. Coefficient of Age for Bi = ∞ (60)

Fo	0	1	2	3	4	5	6	7	8	9
0,0	∞	6,129	4,471	3,736	3,297	2,997	2,774	2,602	2,462	2,347
0,1	2,249	2,164	2,090	2,026	1,967	1,915	1,868	1,825	1,785	1,749
0,2	1,715	1,684	1,655	1,628	1,602	1,578	1,556	1,534	1,514	1,495
0,3	1,476	1,459	1,442	1,427	1,411	1,397	1,383	1,369	1,357	1,344
0,4	1,333	1,321	1,310	1,299	1,289	1,279	1,269	1,260	1,251	1,242
0,5	1,234	1,225	1,217	1,209	1,202	1,194	1,187	1,180	1,173	1,166
0,6	1,160	1,154	1,147	1,141	1,136	1,130	1,124	1,119	1,113	1,108
0,7	1,102	1,097	1,092	1,087	1,082	1,078	1,073	1,069	1,064	1,060
0,8	1,056	1,052	1,047	1,043	1,039	1,035	1,031	1,028	1,024	1,020
0,9	1,017	1,013	1,010	1,006	1,003	1,000	0,997	0,993	0,990	0,987
1,	0,984	0,955	0,930	0,908	0,888	0,870	0,854	0,838	0,825	0,812
2,	0,800	0,790	0,779	0,770	0,761	0,752	0,744	0,737	0,730	0,723
3,	0,716	0,710	0,704	0,698	0,693	0,688	0,682	0,678	0,673	0,669
4,	0,664	0,660	0,656	0,652	0,648	0,645	0,641	0,638	0,635	0,631
5,	0,628	0,625	0,622	0,619	0,616	0,614	0,611	0,608	0,606	0,604
6,	0,601	0,599	0,596	0,594	0,592	0,590	0,587	0,585	0,583	0,581
7,	0,579	0,577	0,575	0,573	0,572	0,570	0,568	0,567	0,565	0,563
8,	0,562	0,560	0,558	0,557	0,555	0,554	0,552	0,551	0,550	0,548
9,	0,547	0,546	0,544	0,543	0,541	0,540	0,539	0,537	0,536	0,535
1	0,534	0,523	0,513	0,504	0,497	0,489	0,483	0,477	0,471	0,466
2	0,461	0,457	0,453	0,449	0,445	0,441	0,438	0,435	0,432	0,429
3	0,426	0,424	0,421	0,419	0,416	0,414	0,412	0,410	0,408	0,406
4	0,404	0,402	0,400	0,399	0,397	0,396	0,394	0,393	0,391	0,390
5	0,388	0,387	0,385	0,384	0,383	0,382	0,381	0,379	0,378	0,377
6	0,376	0,375	0,374	0,373	0,372	0,371	0,370	0,369	0,368	0,367
7	0,366	0,366	0,365	0,364	0,363	0,362	0,362	0,361	0,360	0,359
8	0,358	0,358	0,357	0,356	0,355	0,355	0,354	0,353	0,353	0,352
9	0,352	0,351	0,351	0,350	0,349	0,348	0,348	0,347	0,347	0,346
Fo	00	10	20	30	40	50	60	70	80	90
1	0,346	0,341	0,336	0,332	0,328	0,325	0,322	0,319	0,316	0,314
2	0,311	0,309	0,307	0,305	0,303	0,301	0,300	0,298	0,297	0,295
3	0,294	0,292	0,291	0,290	0,289	0,287	0,286	0,285	0,284	0,283
4	0,282	0,281	0,280	0,280	0,279	0,278	0,277	0,276	0,276	0,275
5	0,274	0,274	0,273	0,272	0,272	0,271	0,270	0,270	0,269	0,268
6	0,268	0,267	0,267	0,266	0,265	0,265	0,264	0,264	0,263	0,263
7	0,263	0,262	0,262	0,261	0,261	0,260	0,260	0,259	0,259	0,258
8	0,258	0,258	0,257	0,257	0,256	0,256	0,256	0,256	0,255	0,255
9	0,254	0,254	0,254	0,254	0,253	0,253	0,252	0,252	0,252	0,252
10	0,251									

Table 12. Coefficient of Age for Variable Fo and Bi (91)

Fo \ Bi	0,1	0,3	0,5	1,0	2,5	5,0	10,0	25,0	∞
0,0004	0,100	0,298	0,495	0,980	2,368	4,490	8,114	15,482	
0,008	0,099	0,292	0,477	0,912	1,997	3,277	4,723	6,104	
0,014	0,099	0,289	0,471	0,887	1,874	2,941	4,003	4,865	
0,02	0,098	0,287	0,465	0,868	1,788	2,717	3,569	4,197	4,472
0,08	0,097	0,276	0,437	0,772	1,400	1,873	2,188	2,375	2,463
0,14	0,097	0,270	0,422	0,724	1,233	1,578	1,786	1,907	1,967
0,20	0,096	0,265	0,411	0,691	1,138	1,412	1,573	1,667	1,715
0,80	0,093	0,244	0,361	0,557	0,803	0,924	0,995	1,033	1,056
1,40	0,092	0,235	0,340	0,506	0,698	0,788	0,839	0,870	0,888
2,00	0,091	0,228	0,326	0,475	0,640	0,716	0,759	0,785	0,800
8,00	0,087	0,203	0,276	0,375	0,472	0,515	0,540	0,553	0,562
14,00	0,085	0,193	0,258	0,343	0,424	0,459	0,477	0,489	0,496
20,00	0,084	0,187	0,248	0,325	0,397	0,427	0,444	0,455	0,461
80,00	0,079	0,167	0,213	0,269	0,317	0,336	0,348	0,355	0,358
120,00			0,205	0,256		0,316	0,326		0,336
1000,00									0,251

Table 12a. Dimensionless Wall Temperature $(t_w - t_a)/(t_{RV} - t_a)$ (91)

Fo \ Bi	0,1	0,3	0,5	1,0	2,5	5,0	10,0	25,0	∞
0,0004	0,998	0,994	0,990	0,980	0,947	0,898	0,811	0,619	0,000
0,008	0,991	0,972	0,954	0,912	0,799	0,656	0,472	0,244	0,000
0,014	0,988	0,964	0,941	0,887	0,750	0,588	0,400	0,195	0,000
0,02	0,986	0,958	0,930	0,868	0,715	0,543	0,357	0,168	0,000
0,08	0,973	0,921	0,874	0,772	0,561	0,375	0,219	0,095	0,000
0,14	0,965	0,901	0,843	0,724	0,495	0,316	0,179	0,076	0,000
0,20	0,960	0,886	0,821	0,691	0,455	0,282	0,157	0,067	0,000
0,80	0,931	0,815	0,722	0,557	0,321	0,185	0,100	0,041	0,000
1,40	0,917	0,782	0,679	0,506	0,279	0,158	0,084	0,035	0,000
2,00	0,907	0,760	0,651	0,475	0,256	0,143	0,076	0,031	0,000
8,00	0,865	0,675	0,551	0,375	0,189	0,103	0,054	0,022	0,000
14,00	0,847	0,643	0,515	0,343	0,169	0,092	0,048	0,020	0,000
20,00	0,835	0,623	0,495	0,325	0,159	0,085	0,044	0,018	0,000
80,00	0,792	0,555	0,426	0,269	0,127	0,067	0,035	0,014	0,000
120,00			0,409	0,256		0,063	0,033		0,000

a) Solutions for heat flow from rock to air

Far more solutions for the change of air temperatures due to heat flow from the rock to the air have been published than for heat flow from fumes to the rock. Since there exists in principle no mathematical difference and these relations can be used for the temperature precalculation of fumes, they shall be discussed, too.

The common method to determine the air temperature is to describe the heat flow per unit time by

$$dq = h_R \, dA = k \, (t_{RV} - t_a) \, \frac{1}{r_o} \, K(\alpha) \, P \, dL$$

and the air temperature change by

$$dt_a = \frac{dq}{G^* c_p}$$

With $t_a = t_{ao}$ for $L = 0$ one obtains

$$t_a = t_{RV} - (t_{RV} - t_{ao}) \exp\left(- \frac{P \, k \, K(\alpha) \, L}{G \, c_p \, r_o}\right) \qquad \text{EQU. 3.4}$$

This procedure is not quite correct. The coefficient of age has been calculated under the assumption of a time-constant air temperature in the airway. Since the coefficient of age changes with time, the air temperature will, however, change with time, too.

More accurate solutions of the Fourier equation for air temperatures, which follow periodic or logarithmic changes with time have been provided by Scerban and Kremnev (107), for linear, periodic or exponential changes with time by Kremnev and Koslov (70). Van Heerden (49), Hiramatsu and Kokado (52) and Kappelmayer and Mundry (64), the latter in form of extensive tables, have solved the Fourier equation and the differential equation for the air temperature simultaneously. A comparison, however, shows that the deviations of the results obtained with the assumption of time constant and time variable temperatures are not very large, especially for older airways.

A larger number of authors have investigated the influence of periodic temperature changes around a constant average temperature at the begin of an airway (4,8,11,12,15,42,50,51,69,107). These temperature variations are propagated with the air along the airway although with decreasing amplitude and increasing phase shift. The average temperatures in every point of the airway are not influenced, however.

Since solutions of linear differential equations can be added to obtain the desired boundary conditions, modifications of the above equation for t_a are not too difficult. Where no source is indicated these modifications have been derived by the author to allow a uniform presentation.

Table 13. Values of f(z) for the Determination of K(α) (107)

z	f(z)	z	f(z)	z	f(z)
0,0	0,0000	5,0	0,8872	22	0,9744
0,1	0,1036	5,5	0,8974	24	0,9765
0,2	0,1910	6,0	0,9060	26	0,9783
0,3	0,2654	6,5	0,9132	28	0,9799
0,4	0,3202	7,0	0,9194	30	0,9812
0,5	0,3843	7,5	0,9248	35	0,9839
0,6	0,4323	8,0	0,9295	40	0,9859
0,7	0,4741	8,5	0,9336	45	0,9875
0,8	0,5109	9,0	0,9373	50	0,9887
0,9	0,5435	9,5	0,9406	60	0,9906
1,0	0,5724	10	0,9436	70	0,9919
1,2	0,6214	11	0,9487	80	0,9929
1,4	0,6614	12	0,9530	90	0,9937
1,6	0,6975	13	0,9566	100	0,9944
1,8	0,7217	14	0,9597	110	0,9949
2,0	0,7434	15	0,9624	120	0,9953
2,5	0,7928	16	0,9647	130	0,9957
3,0	0,8207	17	0,9668	140	0,9960
3,5	0,8454	18	0,9686	160	0,9964
4,0	0,8634	19	0,9703	180	0,9968
4,5	0,8777	20	0,9718	200	0,9971

In nonhorizontal airways geothermal gradient and autocompression have to be taken into account. For vertical airways with the elevation change Z (positive for upcast, negative for downcast shafts) the equation

$$t_a = t_{RVo} - gr\ Z - [t_{RVo} - t_{ao} \pm \frac{G\ c_p\ r_o}{P\ k\ K(\alpha)}\ (gr - ga)]$$

$$* \exp(-\frac{P\ k\ K(\alpha)}{G\ c_p\ r_o}(\pm Z)\ \pm \frac{G\ c_p\ r_o}{P\ k\ K(\alpha)}\ (gr - ga) \qquad \text{EQU. 3.5}$$

have been suggested (69,11,42), where the plus signs have to be used for upcast and the mines signs for downcast shafts. For inclined airways with the slope angleβ(positive for ascending, negative for descending airways) one would correspondingly obtain

$$t_a = t_{RVo} - gr\ L \sin\beta + [t_{ao} - t_{RVo} - \frac{G c_p r_o \sin\beta}{P\ k\ K(\alpha)}\ (gr - ga)]$$

$$*\exp(-\frac{P\ k\ K(\alpha)\ L}{G\ c_p\ r_o}) + \frac{G\ c_p\ r_o \sin\beta}{P\ k\ K(\alpha)}(gr - ga) \qquad \text{EQU. 3.6}$$

For the case that the air temperature at the beginning of an airway is at the time τ_1 changed from a constant value t_{ao1} to a constant value t_{ao2}, Koenig (69) gives a solution for the temperature field of the rock. From this the resulting airtemperature along the airway can be derived. For $\tau<\tau_1$ the air temperature is, as in equation 3.4

$$t_a = t_{RV} - (t_{RV} - t_{ao1})\exp(-\frac{P\ k\ K(\alpha)_1\ L}{G\ c_p\ r_o})$$

For $\tau>\tau_1$ it becomes

$$t_a = t_{RV} - (t_{RV} - t_{ao1})\exp(-\frac{P\ k\ K(\alpha)_1\ L}{G\ c_p\ r_o}) + (t_{ao2} - t_{ao1})$$

$$*\exp\ (-\frac{P\ k\ K(\alpha)_2\ L}{G\ c_p\ r_o}) \qquad \text{EQU. 3.7}$$

$K(\alpha)_1$ has to be determined from the Fourier number of the time τ and $K(\alpha)_2$ of $(\tau - \tau_1)$.

The equivalent equation for nonhorizontal airways and $\tau>\tau_1$ is

$$t_a = t_{RVo} - gr\ L \sin\beta - [t_{RVo} - t_{ao1} + \frac{G\ c_p\ r_o \sin\beta}{P\ k\ K(\alpha)_1}(gr - ga)]$$

$$* \exp(-\frac{P\ k\ K(\alpha)_1\ L}{G\ c_p\ r_o}) + \frac{G\ c_p\ r_o \sin\beta}{P\ k\ K(\alpha)_1}\ (gr - ga) + (t_{ao2} - t_{ao1})$$

$$* \exp(-\frac{P\ k\ K(\alpha)_2\ L}{G\ c_p\ r_o} \qquad \text{EQU. 3.8}$$

If in addition to the heat exchange with the rock a heat source emits the heat quantity Q evenly along an airway, the resulting air temperature is (8,12):

$$t_a = t_{RV} + \frac{Q\ r_o}{P\ k\ K(\alpha)\ L} - (t_{RV} - t_{ao} + \frac{Q\ r_o}{P\ k\ K(\alpha)\ L}) \exp(-\frac{P\ k\ K(\alpha)\ L}{G\ c_p\ r_o})$$

EQU. 3.9

An equivalent formula for nonhorizontal airways can be derived from calculations of Boldizsar (12)

$$t_a = t_{RVo} - gr\ L \sin\beta - [t_{RVo} - t_{ao} + \frac{G\ c_p\ r_o \sin\beta}{P\ k\ K(\alpha)}(gr - ga) + \frac{Q\ r_o}{P\ k\ K(\alpha) L}]$$

$$*\exp(-\frac{P\ k\ K(\alpha)\ L}{G\ c_p\ r_o}) + \frac{G\ c_p\ r_o \sin\beta}{P\ k\ K(\alpha)}(gr-ga) + \frac{Q\ r_o}{P\ k\ K(\alpha)\ L}$$

EQU. 3.10

Both equations are only valid when the heat source has been active over the whole life of the airway.

If the air quantity in an airway is changed, equation 3.4 suggests that for the new air quantity an "effective age" of the airway should be used, which, with the new air quantity, would give the same temperature distribution along the airway as the old air quantity did within the "real age". The condition for the same temperature distribution is

$$K(\alpha)_{eff} = K(\alpha)_{rel} \frac{G_{new}}{G_{old}}$$

from which the Fourier number and τ can be determined.

Influence of water

Experience with temperature precalculations show that even in seemingly dry airways the influence of water should not be neglected.

If more water flows from the rock towards an airway than evaporates, the walls of this airway remain wet. Under the assumption that the amount of water evaporated is proportional to the airway length, the evaporation process can be considered as a heat sink evenly distributed along the airway. This approach has been chosen by Batzel (8), Boldizsar (12), Koenig (69), Mosin and Kremnev (71) and Abramov, Mosin and Kremnev (2). Their formulas for the temperature changes are those for evenly distributed heat sinks. If condensation takes place one would have to deal with heat sources; the theory or formulas do not change.

The assumption that the water vapor content of the air changes proportional to the airway length is a gross simplification.

The amount of water vapor absorbed depends on the relative humidity of the air. A solution for the change of humidity ratio and temperature of air along an airway for steady state heatflow was comparatively early derived by Stokes and Cernik (123) and de Braaf (51).

Under the assumption that the part P_w of the perimeter is covered with water, they describe the heat balance of the airway by

$$P\ K\ (t_{RV} - t_a)\ dL = G\ c_p\ dt_a + G\ r\ d\omega$$

$$G\ d\omega = \beta P_w\ (p_w - p_a)\ dL$$

where K = heat transfer coefficient
ω = humidity ratio = lb water vapor/lb air
β = mass transfer coefficient
p_w = water vapor pressure at t_a
p_a = partial pressure of water vapor in air
r = heat of evaporation per unit weight of water

The heat transfer coefficient K is a function of k, a, α, r_o and τ and serves the same purpose as the term $k*K(\alpha)/r_o$ in the equations for non steady state heat exchanges.

With $\delta = \frac{Ra}{Rv - Ra} = 1.64$ and $\sigma = \frac{p_b * Rv}{Rv - Ra}$

where Ra, Rv = gas constants of air and water
p_b = air pressure

de Braaf's solutions as for practical purposes satisfying approximations are:

$$\omega = \frac{\delta}{\sigma} p_b - \left(\frac{\delta}{\sigma} p_b - \omega_o \right) \exp\left(- \frac{\beta P_w \sigma}{G \delta} L\right)$$

$$t_a = t_{RV} - (t_{RV} - t_{ao}) \exp\left(- \frac{P\ K\ L}{G\ c_p}\right) - \frac{\beta\ p_w\ r(\delta P_w - \sigma \omega o)}{\sigma\ c_p\ \beta\ P_w - \delta\ P\ K}$$

$$* \left[\exp\left(- \frac{P\ K\ L}{G\ c_p}\right) - \exp\left(- \frac{\beta P_w \sigma}{G \delta} L\right) \right] \qquad \text{EQU. 3. 11}$$

Under the assumption that the walls are covered with layers of saturated air, Koenig (69) and Mundry (84) derive sets of equations for the change of humidity ratios and temperatures along horizontal and vertical airways. Their simultaneous solution requires considerable mathematical effort, which limits the practical application. A further disadvantage is that condensation cannot be considered by their formulas.

The same applies to the large set of equations derived by Wiles (144, 145) to describe the heat and moisture transfer in mine airways, where the floor is wet and the walls are dry.

If less water flows from the rock towards an airway than evaporates, the rock surrounding this airway is gradually dried.

An equilibrium is reached when the water quantity flowing towards the airway is equal the water vapor quantity which by diffusion migrates through the insulating layer of dry rock into the airway. This is the state of, to Scott (111) nearly all seemingly dry airways in the British and, according to Voss, (132) the majority of all dry airways in the German coal mines. Since the evaporation of water consumes heat, Scott (111) sets up the following equation:

$$q_R = q_V + q_W = q_V + \alpha\ (t_w - t_a)$$

where q_R = heat flow from rock
q_V = heat consumed for evaporation of water
q_W = heat transferred from wall to air

As solution for q_R he obtains

$$q_R = \frac{k}{r_o}\ (t_{VR} - t_a + \frac{q_V}{\alpha})\ K(\alpha)$$

Scott does not use this equation to derive the resulting air temperature changes, but it is not difficult to do this. The heat balance between air and rock is

$$G\ c_p\ dt_a = q_W\ P\ dL = (q_R - q_V)\ P\ dL = \frac{k\ P\ K(\alpha)}{r_o}(t_{RV} - t_a)\ dL$$

$$+ (\frac{k\ K\ (\alpha)}{r_o} - 1)\ q_V\ P\ dL$$

$$= \frac{k\ P\ K(\alpha)}{r_o}\ (t_{RV} - t_a)\ dL + (\frac{K(\alpha)}{Bi} - 1)\ q_V\ P\ dL$$

The solution, with ta = tao for L =0 is:

$$t_a = t_{RV} - [t_{RV} - t_{ao} + (\frac{K(\alpha)}{Bi}) - 1)\ \frac{q_V\ r_o}{k\ K(\alpha)}\ ]\ \exp(-\frac{P\ k\ K(\alpha)\ L}{G\ c_p\ r_o})$$

$$+ (\frac{K(\alpha)}{Bi} - 1)\ \frac{q_V\ r_o}{k\ K(\alpha)} \qquad \text{EQU. 3.12}$$

Since the heat quantity q_V is extracted from the rock, internal evaporation of water increases the heatflow from the virgin rock towards the airway in the manner, as an increased heat conductivity k. Voss (132) suggests, therefore that the heatflow from the rock to the air per unit time be expressed by

$$Q_R = k_{equ}\ (t_{RV} - t_a)\ \frac{1}{r_o}\ K(\alpha)\ P\ dL$$

where $k_{equ} = k\ \frac{dh}{c_p * dta} = k\ /\eta$ and dh = enthalpy change of air

Of this heatflow the fraction η will increase the air temperature by

$$dt_a = \frac{Q_R\ \eta}{G\ c_p}$$

With $t_a = t_{ao}$ for L = 0 the solution for t_a is equation 3.4 but $K(\alpha)$ is now a function of a changed Fourier number Fo determined by

$$Fo = \frac{k_{equ}}{c^* \gamma'} * \frac{\tau}{r_o^2} = \frac{k}{\eta^* c^* \gamma'} * \frac{\tau}{r_o^2} = \frac{a_{equ}\tau}{r_o^2}$$

The Biot number, calculated with the heat transfer coefficient for the total, wet and dry transferred heat $\alpha_{equ} = \alpha/\eta$ and k_{equ} remains due to

$$Bi = \frac{\alpha_{equ} * r_o}{k_{equ}} = \frac{\alpha\, r_o}{k}$$ the same as for dry rock.

The factor η for existing airways can be determined from psychrometric measurements and for planned airways experience figures can be used(132). Since the amount of water evaporation depends on the state of the air and the latter changes along an airway, Voss (135, 136) refined his method by calculating the wall temperatures, the evaporation and η sectionwide over short lengths. Computer programs have been written to allow the handling of the considerable numerical work involved.

b) Application of these solutions on mine fires

All of the equations 3.4 - 3.12 can in one way or the other be utilized for the calculation of temperatures behind a fire. This applies in particular to equ. 3.7 and 3.8, which take into account the combined effect of original heat exchange between ventilating air and rock and subsequent heat exchange between fumes and rock. In these equations t_{ao_1} would be the airtemperature at the location of the fire t_{ao} before the fire starts and t_{ao_2} the temperature of the fumes leaving the fire. A closer inspection of equation 3.8 shows that for the small values of

$\frac{P\, k\, K(\alpha)_1}{G\, c_p\, r_o}$, which are usually encountered in shafts, it

can be approximated by

$$t_a = t_{ao_1} - g_a\, L \sin\beta + (t_{ao_2} - t_{ao_1}) \exp\left(-\frac{P\, k\, K(\alpha)_2\, L}{G\, c_p\, r_o}\right) \qquad \text{EQU. 3.13}$$

With the assumption that the rock surrounding an airway had before the fire started itself adjusted to the temperature of the air passing through this airway and that consequently no heat exchange had any longer taken place equation 3.4 becomes

$$t_f = t_a + (t_{fo} - t_a) \exp\left(-\frac{P\, k\, K(\alpha)\, L}{G\, c_p\, r_o}\right) \qquad \text{EQU. 3.14}$$

and equation 3.6, with gr = ga, becomes

$$t_f = t_{ao} - g_a\, L \sin\beta + (t_{fo} - t_{ao}) \exp\left(-\frac{P\, k\, K(\alpha)\, L}{G\, c_p\, r_o}\right) \qquad \text{EQU. 3.15}$$

If a heat source (burning conveyor belt, condensing water) or heat sink (evaporating water) is evenly distributed along an airway, equ. 3.9 and 3.10 can be used. For younger airways an average rocktemperature at the time of the fire has to be determined. For older airways the assumption $t_a = t_{VR}$ AND gr = ga leads to

$$t_f = t_a + \frac{q\ r_o}{P\ k\ K(\alpha)} - (t_a - t_{fo} + \frac{q\ r_o}{P\ k\ K(\alpha)})\exp(-\frac{P\ k\ K(\alpha)\ L}{G\ c_p\ r_o})$$

EQU. 3.16

for horizontal and to

$$t_f = t_{ao} - ga\ L \sin \beta + \frac{q\ r_o}{P\ k\ K(\alpha)} - (t_{ao} - t_{fo} + \frac{q\ r_o}{P\ k\ K(\alpha)})$$

$$*\exp(-\frac{P\ k\ K(\alpha)\ L}{G\ c_p\ r_o})$$ EQU. 3.17

for nonhorizontal airways.

A comparison between equation 3.1 for the steady state heat exchange and equation 3.4 for the non-steady state process shows that both give the same results as long as

$$\frac{K(\alpha)\ k}{r_o} = \alpha \quad \text{or} \quad K(\alpha) = \frac{r_o}{k} = Bi$$

Table 12 shows that this is the case for small Fourier numbers (short times) and small Biot numbers (small α caused by small air velocities).

If an equilibrium between evaporating water and water flow towards the airway has been established, Scott's (111) approach of an internal heat sink or Voss' approach of an equivalent heat conductivity (132) could be used, too. Both methods, however, are semiempirical methods and rely on the experimental determination of q_V or k_{equ} under the conditions of mine fires.

c) Solutions especially derived for mine fires

Several authors have published equations for the temperatures of fumes behind mine fires, which were especially derived for this purpose. As can be expected they agree widely with the equations already discussed.

Woropajew (146) considers the heat exchange between fumes and rock as a steady state process and arrives consequently at equation 3.1. Osipov and Zadan (94) modify this equation. If L is the distance from the origin of the fire to the point under consideration, the progress of the fire towards this point has to be taken into account, too, so that

$$t_f = t_a + (t_{fo} - t_a)\ \exp(-\frac{\alpha P}{G\ c_p}(L - V_f \tau))$$ EQU. 3.18

They give mathematical expressions for t_{fo}, α and V_f which are contained in the pertinent chapters of this report.

Maas and Sadée (75) make the assumption of a non-steady state heat exchange process and recommend an equation which can be converted into equation 3.14. For $K(\alpha)$ they use values published by Carslaw and Jaeger (22), which are the same as published earlier by Jaeger (59).

Roberts and Kennedy (100) derive the temperature distribution in airways whose walls are considered to be semi infinite solids. Their solution can not be written explicitely. For the case that $K(\alpha)$ is no longer time dependent and the fire has reached a quasi-steady-state, where the temperature distribution is not changing with respect to a point moving with the velocity of the fire, Roberts and Clough (103) can give the equation

$$\frac{tf}{t_{fo}} = \exp\left(-\frac{\alpha P L}{G c_p} * \frac{t_{fo} - t_{wo}}{t_{fo}}\right) \qquad \text{EQU. 3.19}$$

where t_{wo} is the wall temperature at the point of the gas temperature t_{fo}. For the ratio gas temperature to wall temperature they derive (102) for a square duct with the side-length 1

$$\frac{t_f}{t_w} = \frac{1}{2} + \left(\frac{1}{4} + \frac{1}{K}\right)^{0.5}$$

where $K = \dfrac{\alpha G c_p 1}{4 V_f (k \gamma' c)_R}$; k, γ', c are wall properties.

Kremnev and Mosin (71) investigate the non-steady state heat exchange between fumes and rock in cooperation with heat sources and heat sinks under the assumption of an original uniform rock temperature t_{RV} and an even distribution of the heat sources and sinks along the airway. Heat sources (oxydation processes) develop the heat quantity q_A per unit wall area and time, heat sinks (evaporation of water) consume the heat quantity $r*W_1$ per unit weight of air and unit length of airway (r = heat of evaporation per unit weight of water = 1030 Btu/lb, W_1 = weight of evaporated water (lb water per lb of air and ft of airway length)). The heat balance of the airway is under these assumptions

$$-G c_p dt_f + q_A P dL = (t_f - t_{RV}) \frac{P k K(\alpha)}{r_o} dL + W_1 r G dL$$

If the temperature of the fumes at the begin of the airway is described by

$$t_{fo} = t_b + b\tau$$

the temperature of the fumes along the airway is

$$t_f = t_{RV} + \left[(t_b + b\tau - t_{RV}) + \frac{r_o W_1 G r}{P k K(\alpha)} - \frac{q_A r_o}{k K(\alpha)}\right] \exp\left(-\frac{P k K(\alpha) L}{G c_p r_o}\right)$$

$$- \frac{r_o W_1 G r}{P k K(\alpha)} + \frac{q_A r_o}{k K(\alpha)} \qquad \text{EQU. 3.21}$$

If the temperature of the fumes at the beginning of the airway is described by

$$t_{fo} = t_b * \exp(b\tau)$$

the temperature of the fumes along the airway is

$$t_f = t_{RV} + [(t_b * \exp(b\tau) - t_{RV}) + \frac{r_o W_l G r}{P k K(\alpha)} - \frac{q_A r_o}{k K(\alpha)}] * \exp(-\frac{P k K(\alpha) L}{G c_p r_o}) - \frac{r_o W_l G r}{P k K(\alpha)} + \frac{q_A r_o}{k K(\alpha)}$$

EQU. 3.22

Under the assumption of a constant temperature at the begin of the airway and a combination of heat sources and sinks to $q = q_A P - r W_l G$ the equations 3.21 and 3.22 would become equation 3.16.
For the calculation of r_o in noncircular airways the formuls $r_o = 0.564 \sqrt{A}$ and for the calculation of $K(\alpha)$ the above quoted formulas for short periods of heat exchange are recommended.

In another paper (2) Abramov, Mosin and Kremnev give an equation based on constant temperatures at the airway beginning and not heat sources, only heat sinks:

$$t_f = t_{RV} + (t_{fo} - t_{RV} + \frac{r_o W_l G r}{P k K(\alpha)}) \exp(-\frac{P k K(\alpha) L}{G c_p r_o}) - \frac{r_o W_l G r}{P k K(\alpha)}$$

EQU. 3.23

This equation seems to follow directly from equ. 3.16 or equ. 3.21. The authors suggest use of heat conductivities k, which are functions of the rock temperature. This resembles Voss' approach (132) of introducing an equivalent heat conductivity k_{equ} which takes into account the heat consumption for water evaporation inside the rock. Without discussing the reasons, the authors give a few recommendations for thermal diffusivities as functions of temperatures (table 14). As rock temperature they suggest using the mean between the wall temperature t_w and the original rock temperature t_{RV}. For the estimation of the wall temperature they make use of the condition that the heat transferred from the fumes to the wall must be equal the heat carried away into the rock:

$$\alpha(t_f - t_w) = \frac{k K(\alpha)}{r_o} (t_f - t_{RV}) \text{ or}$$

$$t_w = t_f - \frac{k K(\alpha)}{\alpha r_o} (t_f - t_{RV})$$

C) The heat transfer coefficient α

Following Newton's law of cooling the heat transfer coefficient α is defined by

$G \Delta h = \alpha (t_f - t_w) A$ where h = enthalpy of air per unit mass
G = mass flow rate of air

Heat transfer from a gas to a solid wall or vice versa comprises:
conduction through the laminar boundary layer at the wall,
convection by the movement of turbulent particles,
transfer by mass exchange between gas and wall,
radiation.

Since every turbulent flow has a laminar sublayer it has become general practice to consider the first two processes together and to relate the heat quantity Q_c transferred by their combined action with the convection coefficient α_c to the temperature difference between gas and wall.

$$Q_c = \alpha_c \, (t_f - t_w) \, A$$

a) Convection

Since thickness of laminar sublayer and turbulent movement depend on flow conditions one must, as in fluid mechanics, rely on semiempireal theories for the determination of α_c. The dimensional analysis obtains for incompressible gas and enforced flow (forced convection):

$$\alpha_{cf} = \frac{k}{l} * \text{function } (N_R, N_{Pr})$$

where l = characteristic length

N_R = Reynolds number = $V_a \, l/\nu$

N_{Pr} = Prandtl number = ν/a

V_a = gas velocity

ν = gas kinematic viscosity

for compressible gas and unenforced, natural flow (natural convection):

$$\alpha_{cn} = \frac{k}{l} * \text{function } (N_{Gr}, N_{Pr})$$

where N_{Gr} = Grashof number = $\dfrac{g\beta \, t \, l^3}{\nu^2}$

g = gravitational acceleration

β = thermal expansion $\Rightarrow \dfrac{1}{v} * \dfrac{dv}{dt}$

v = specific volume

A vast amount of literature exists on convection coefficients. This report has to limit itself to those convection coefficients obtained for or applicable to mine airways. The majority of them have been determined for heat transfer from the wall to the air. However, they should be applicable to the preheating zone of fires, too, since no combustion processes with the development of buoyant products occur any longer.

Table 14. Variation of Thermal Diffusivity with Temperature (71)

Material	Mean Temperature (°F)	Thermal Diffusivity (ft^2/hr)
Clay	395	0.0078
	1580	0.0191
Clay	286	0.0072
	1385	0.0171
Sandy Shale	262	0.0086
	1240	0.0173
Coking Coal	227	0.0051
	1190	0.0172
Gas Coal	320	0.0054
	540	0.0073
Gasflame Coal	295	0.0052
	543	0.0066

Table 15. Increase of Convection Coefficients with Wall Roughness (108)

Support Diameter d_s/d	Support Spacing s/d_s	Wall Conditions Relativ. Smooth	Rough e/d = 0.03	Rough e/d = 0.05
no support		1.0	1.65	1.75
0.06	14	1.85	2.10	2.20
	7	2.00	2.20	2.30
	3.5	2.15	2.40	2.50
0.09	7	2.30	2.50	2.60
	3.5	2.50	2.65	2.75
0.12	7	2.60	2.85	2.95
	3.5	2.80	3.00	3.10

d = hydraulic diameter of airway; d_s = diameter of supports;
s = spacing of supports; e = roughness elevations of wall

Table 16. Comparison of Observed and Calculated Temperatures Behind a Fire (71)

Distance from Fire (Sect. No)	V	VI	VII	VIII	IX	X	XI	XII
Calculated Temperature (°C)	87	44	38	33	29	27	25	24
Measured Temperature (°C)	84	42	38	32	28	27	23	21
Deviation (%)	+3.6	+4.8	0	+3.1	+3.6	0	+8.7	+14

Little information from mining sources exists for natural convection, since unventilated airways are usually sealed off. Scott (111) recommends

$\alpha_{cn} = 0.30\ (t_w - t_a)^{0.5}$ with α_{cn} in Btu/ft^2 hr ^{o}F and t in ^{o}F,

and for the combined effect of natural and forced convection α_{cf}

$\alpha_c = \alpha_{cn} + \alpha_{cf}$

Voss (134) recommends

$\alpha_{cn} = 0.39\ (t_w - t_a)^{0.25}$ and $\alpha_c = (\alpha_{cn}^2 + \alpha_{cf}^2)^{0.5}$

Coefficients of forced convection were formerly understood to have a linear relationship to the air velocity. The more accurate the methods of their determination became, the more the results started to follow the relation, obtained by dimensional analysis,

$$\alpha_c = \text{factor} * \frac{k}{l} * N_R^{\ m} * N_{Pr}^{\ n}$$

Since k and N_{Pr} of air do not change much, they are quite frequently combined with the factor.

A linear relationship between α_c (Btu/ft^2 hr ^{o}F) and V_a (ft/sec) is assumed by de Braaf (15) with

$\alpha_c = 1 + 0.212\ V_a$,

Kappelmeyer and Mundry (64) with

$\alpha_c = 1.13 + 0.225\ V_a$

and Osipov and Zadan (94,95) with

$\alpha_c = 0.9 + 0.221\ V_a$.

An exponent of V_a with a value <1 is assumed by Stokes and Cernik (123) with

$\alpha_c = 0.41 + 0.695\ V_a^{0.67}$,

Budryk(17) with

$\alpha_c = 0.41 + 0.79\ V_a^{0.5}$,

Batzel (8) with

$\alpha_c = 0.72 + 0.555\ V_a^{0.8}$ for smooth airways without supports and

$\alpha_c = 0.512 + 0.652\ V_a^{0.6}$ for airways with steel supports,

Woropajew (146) with

$\alpha_c = 0.397\ V_a^{0.8}$

Scott (111) with

$\alpha_c = 0.34\ h^{-0.25} V_a^{0.75}$ for airways with supports where h = profile height of supports (ft.). Since the coefficient of friction decreases with increasing V_a for smooth airways, the following two formulas are based on exponents of $V_a < 1$ too. Hiramatsu and Kokado (52) suggest

$$\alpha_c = \frac{k\ f\ V_a}{8\nu} \quad \text{with f = coefficient of friction}$$

Scott (111) recommends for roadways without supports

$$\alpha_c = 28\ V_a\ f.$$

Closer to the relationship obtained by dimensional analysis are the next expressions for α_c. Scerban, Kremnev and Zuravlenko (108) suggest

$\alpha_c = 0.0195 \frac{k}{l} \varepsilon N_R^{0.8}$ or, using average values for k and the dynamic viscosity ν and substituting the hydraulic diameter d = 4A/P for l,

$$\alpha_c = 1.85 \frac{\varepsilon\ V_a^{0.8}\ \gamma_a^{0.8}\ p^{0.2}}{A^{0.2}}$$

where γ_a = specific weight of air (lb/ft^3)

ε is a factor indicating the influence of the wall roughness on the convection process. For round timber supports use of the values compiled in table 15 is recommended. For square supports the authors suggest these values be increased by 8%.

Abramov, Mosin and Kremnev (2) suggest a modification of the last formula when applied to mine fires by multiplying numerator and denominator by $A^{0.8}$ and taking into account the change of k and μ with temperature:

$$\alpha_c = B\varepsilon \frac{G^{0.8}\ p^{0.2}}{A} \qquad (G \text{ in lb/sec})$$

For the factor $B = \frac{0.0195\ k}{4^{0.2}(\mu\ g)^{0.8}}$ they suggest

t (°F)	32	212	572	932	1292	1652
B	1.85	2.04	2.77	2.50	2.59	2.64

Voss (134) finds in dry airways good agreement of his measurements with a formula

$$\alpha_c = \alpha_{co} \left(\frac{f}{f_o}\right) (100/N_R)^{1/8}$$

where f = coefficient of friction of airway
f_o = coefficient of friction of hydraulically smooth wall at the same Reynolds number
α_{co} = convection coefficient of hydraulically smooth wall which can be determined from

$$\alpha_{co} = \frac{k}{d}\ 0.106\ N_R^{2/3}$$

By using average values for k and ν Voss modifies this formula to

$$\alpha_{co} = 5.24 \frac{V_a^{2/3}}{d^{1/3}}$$

For rough walls he recommends multiplication of α_{co} with the factors ε of Scerban, Kremnev and Zuravlenko (108), which he finds confirmed by his measurements. His formula for rough walls is consequently

$$\alpha_c = 5.24 \frac{V_a^{2/3}}{d^{1/3}} \varepsilon$$

Roberts and colleagues (100, 102) measured the heat transfer in the preheating zone of a square duct of 1 = 1 ft sidelength. Expressed in Stanton numbers

$$N_{St} = \frac{\alpha c}{V_a \rho c}$$

they obtained with

$$N_R = \frac{V_a l}{\nu}$$

for the smooth duct

$$N_{St} = 0.025\ N_R^{-0.2}$$

for the electrically heated duct, lined with model timber supports

$$N_{St} = 0.10\ N_R^{-0.31}$$

and for the model duct at fire

$$N_{S_t} = 0.106\ N_R^{-0.214}$$

The experiments could not answer the question if the increase of the heat transfer from the electrically heated to the fire heated duct was caused by radiation or by secondary flows due to incomplete mixing of buyoant combustion products.

b) Mass transfer

In the preheating zone of a fire, where no significant pyrolysis or other chemical reactions take place any longer, are the main sources for heat transfer by mass transfer the condensation and evaporation of water. Principally, heat transfer by mass transfer cannot be considered separately from heat transfer by convection at the surface and from heat flow by conduction in the interior of a wall, since the mass transfer changes the thermal properties of both, surface and interior. Due to its technical importance a vast amount of research has been done on this problem. Once again, this report has to limit itself to such work done on mine airways.

The different methods to take into account condensing or evaporating water in temperature precalculations have been discussed. It is common practice to use a heat transfer coefficient α, which is the sum of the dry convection coefficient α_c and a wet convection coefficient α_w defined by

$$\alpha_w = \frac{Q_w}{P\ L\ (t_f - t_w)} = \frac{W\ r}{P\ L\ (t_f - t_w)}$$

where W = weight of water exchanged per unit time
r = heat of evaporation per unit weight

Stokes and Cernik (123), de Braaf (15) and Mosin and Kremnev (71) suggest to calculate W for wet walls from

$$W = \beta\ (p_w - p_a)\ P\ L$$

where β = mass transfer coefficient
p_w = water vapor pressure at wall temperature
p_a = partial pressure of water vapor in air

The mass transfer coefficient can be determined from Lewis' law

$$\beta = \frac{\alpha\ c}{c_p\ \gamma\ R_v\ T}$$ where R_v = gass constant of water vapor

For moist walls Scerban, Kremnev and Zuravlenko (108) recommond the use of the following experience values:

shafts:	= 0.000740 (1/hr)
mainroads and haulage ways:	= 0.00110 (1/hr)
coal faces:	= 0.00220 (1/hr)

Voss (134) introduces for moist but not water-covered walls an effective mass transfer coefficient

$\beta' = \eta\beta$ (η has been defined in chapter III-B.a)
He reports the results of a large number of underground measurements according to which η is in the range 0.02 - 0.14 with an average of about 0.05 for the German coal mines. For more accurate temperature precalculations he (133,135,136) derives an iteration method where the mutual dependent wall temperatures and humidity ratios are matched. This method is applied sectionwise along an airway. The considerable work can only be handled with the help of computers. As a rough approximation Voss (134) recommends $\alpha = \alpha_c(2.1 - \eta)$

A very general approximation is recommended by Bogajavlensky (10) for coal faces

$$\alpha = \alpha_c + \alpha_w = 2.5\alpha_c$$

c) Radiation

Nonpolar, symmetric molecules such as O_2, N_2 and H_2 are relatively transparent to thermal radiation. Heat transfer by radiation is therefore neglected under ordinary ventilation conditions with few exceptions (134) by ventilation engineers. Polar, unsymmetric molecules, such as CO_2, H_2O, CO, SO_2 and many hydrocarbons can enter into thermal radiation exchange appreciably at the temperatures encountered in mine fires. Their contribution to the heat exchange between fumes and airway walls should therefore be assessed and if necessary taken into account.

The only attempts in this direction which could be found in the literature were made by Roberts (105). He states as a typical example from his model tests with a square duct of 1 ft sidelength that the ratios of heat transfer by radiation to heat transfer by convection were equal to 4.6 in the combustion section and equal to 0.88 in the excess fuel section of a fuel rich timber fire.

The order of magnitude of heat transfer by radiation from a gas to a black surrounding can be calculated by

$$Q_r = \sigma A (\varepsilon_g T_g^4 - \alpha_b T_w^4) = \sigma^{*}10^8 A \left[\varepsilon_g \left(\frac{T_g}{100}\right)^4 - \alpha_b \left(\frac{T_w}{100}\right)^4\right]$$

where $\sigma^{*}10^8$ = constant = 0.1723 Btu/ft^2 $^{\circ}$R^{4}hr

A = area of black surrounding

ε_g = emissivity of gas at temperature T_g

α_b = absorptivity of gas at temperature T_g for radiation from a black body at temperature T_w

If the surrounding is not black but gray with the emissivity ε_{gr}, the net heat transfer can be found by considering successive absorptions and reflections. Hottel and Egbert (56) performed a calculation for ε_{gr} = 0.8 - 0.9, the range most frequently encountered. They suggest the use of a factor ε_{eff} to take into account the deviation of a gray from a black surrounding and find that this factor can be approximated by

$$\varepsilon_{eff} = \frac{\varepsilon_{gr} + 1}{2} .$$

The emissivity ε_g is a function of the gas concentration, the thickness of the gas body and the temperature. Because concentration and thickness complement each other in their effects on the radiation, it is possible to consider the emissivity as a function of their product. It has become customary to express the concentration by the partial pressure p_c of the radiating gas measured in atmospheres and the thickness by the average length of paths for the radiant beams, measured in feet. Fig. 29 (58) shows as an example a diagram for the emissivity ε of CO_2 as a function of the product p_c L and the temperature T_g.

The absorptivity α_b would be equal the emissivity ε, if gas

and wall had the same temperature. For $T_g > T_w$ the term T_w^4 becomes very small so that the approximation $\alpha_b \sim \varepsilon_w$ causes no large errors. The complete formula for the radiant heat transfer in then

$$Q_r = \sigma * 10^8 \; A \; \varepsilon_{eff} \left[\varepsilon_g \left(\frac{T_g}{100}\right)^4 - \varepsilon_w \left(\frac{T_w}{100}\right)^4\right]$$

For a more accurate solution, Hottel and colleagues (55,56), based on experiments, recommend to determine ε_w from the pertinent wall temperature T_w but for a parameter $p_c \; L/(T_w/T_g)$ and to obtain α_b (for CO_2) from

$$\alpha_b = \varepsilon_w \left(\frac{T_g}{T_w}\right)^{0.65}$$

For approximations, diagrams based on the formula

$Q_r = A \; (E_g - A_w)$ where E_g = emission from gas to black surrounding

A_w = absorption by gas of radiation by black surrounding

and the parameters p_c L and T have been developed (55,56).

The heat quantities transferred by radiation and convection can be added. There is little mutual interdependence. When a heat transfer coefficient

$$\alpha_r = \frac{Q_r}{A \; (t_g - t_w)}$$

shall be used, one must be aware that α_r is a function of not only $(t_g - t_w)$ but of t_g resp. t_w, too.

Roberts (105) found that the calculated emissivity due to non-luminous radiation from CO_2, CO and H_2O for his tests was in the range of 0.22. The measured emissivities were considerably higher- 0.6 for the combustion section and 0.5 for the excess fuel section. The balance being most probably due to radiation from the smoke and droplet content of the combustion products.

D) Temperature observations

Many researchers seem to feel that for the accuracy, presently expected from fire emergency plans, sufficient theoretical knowledge for the calculation of gas temperature changes behind fires exists. Not too many systematic temperature observations downwind of fires are therefore performed.

a) Stationary fires

Roberts and Kennedy (100) observed air and wall temperatures in a square duct of 1 = 2.5 inches sidelength with the fire simulated by a stationary electric heater. Fig. 30 shows the one example of their results published by them. Plotted over the dimensionless distance from the fire x/1 are ratios

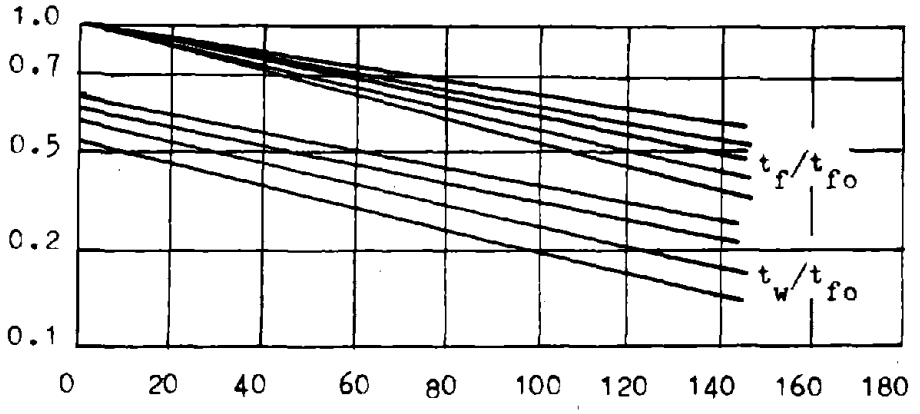

Fig. 30. Temperature Decline in a Model Duct behind a Stationary Heat Source (100)

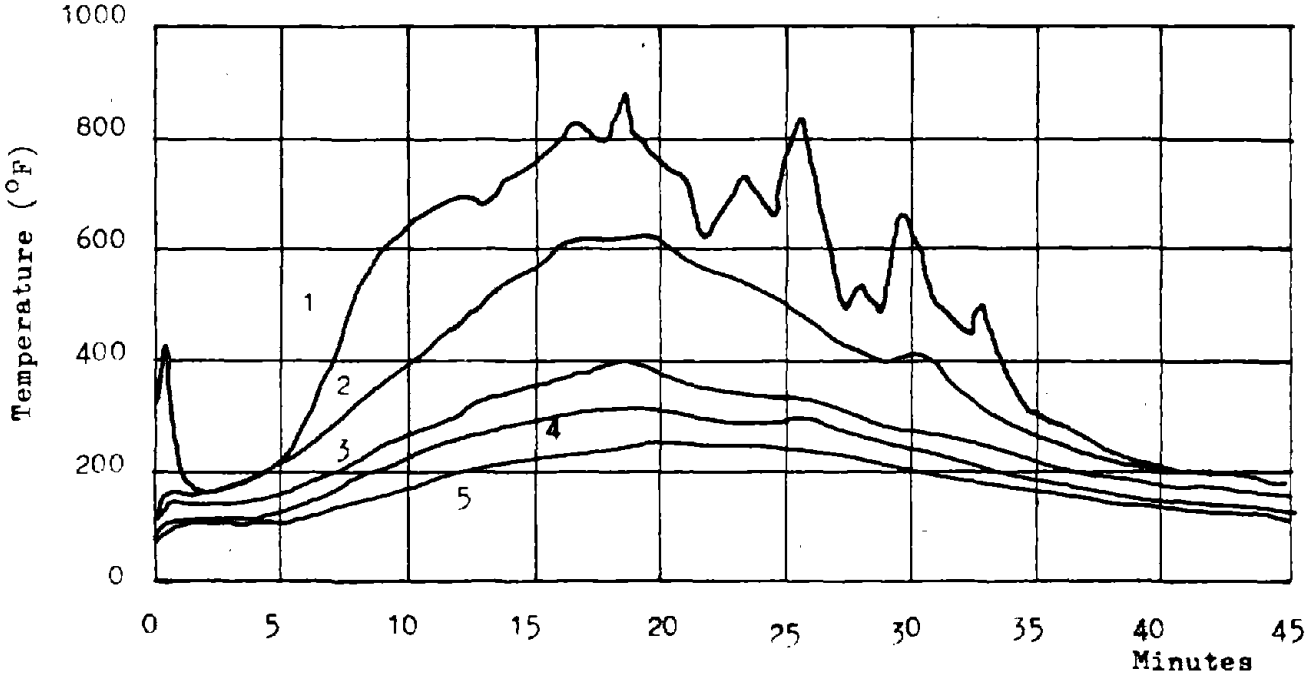

Fig. 31. Temperature Variation in an Ascensionally Ventilated Raise with Time and Distance from Fire (118)

t_f/t_{fo} for (bottom to top) 475, 900, 1300, 2200, and 3100 seconds after the fire started. Equally the ratios t_w/t_{fo} for 475, 900, 1300, and 2200 seconds have been entered. One sees that the temperatures decrease exponentially with distance but increase with time, as can be expected from the theory.

Kremnev and Mosin (71) report that their experimental observations in a model duct of 124 ft length with a thick clay insulation agreed well with results obtained from the equation

$$t_f = t_{RV} + (t_{fo} - t_{RV}) \exp(- \frac{P\ k\ K(\alpha)\ L}{G\ c_p\ r_o}).$$

For a comparison they give table 16 (without stating to which distances the section numbers refer).

The highest temperatures observed by Schmidt and Grumbrecht (118) in 130 large scale fire experiments in a 72° raise of 2 ft height and 11 ft width are shown in fig. 21. Of these experiments 117 were conducted with descensional ventilation to study the airflow fluctuations and reversals caused by fires. The one temperature observation along the raise reported for ascensional ventilation is shown in fig. 31. Curves 1 -5 refer to the fire zone and distance of 10, 30, 62, and 110 ft downwind of the fire. The fire object was a woodpile of 265 lb and 1 ft width in the middle of the airway. The airflow varied between 6,350 ft^3/min and 10,930 ft^3/min. The temperatures were measured in the airway centers only, which explains the rugged temperature curve for the fire zone.

Fig. 32 shows the band(curves 1) formed by the ratios $(t_f - t_{RV})/(t_{fo} - t_{RV})$ for the temperatures from fig. 31 with $t_{RV} = 59°F$. Obviously it takes approximately 30 ft before the fumes from the fire and the air bypassing the fire mixed. The temperatures then follow the expected exponential decrease with distance. For a comparison the same ratios have been calculated from

$$t_f = t_{RV} + (t_{fo} - t_{RV}) \exp(- \frac{\alpha\ P\ L}{G\ c_p})$$

for Q_a = 6350 ft^3/min (curve 2) and 10,930 ft^3/min (curve 3) with

$$\alpha = 5.24 \frac{V_a^{2/3}}{d^{1/2}} \epsilon, \qquad \text{where } \epsilon = 2.7 \text{ for the raise with 3 rows of supports and } \rho_a = 0.078 \text{ lb/ft}^3.$$

The slopes of the calculated and measured curves are quite similar.

Schmidt (114) gives as the results of earlier tests in horizontal or ascensionally ventilated inclined airways as a basis for emergency plans the following temperature - distance relations, without discussing airways or air quantities:

distance from fire (ft)	0	131	262	393	524	655
temperature (°F)	1472	626	320	209	140	112
mean temperature (°F)	1472	1004	924	572	482	392

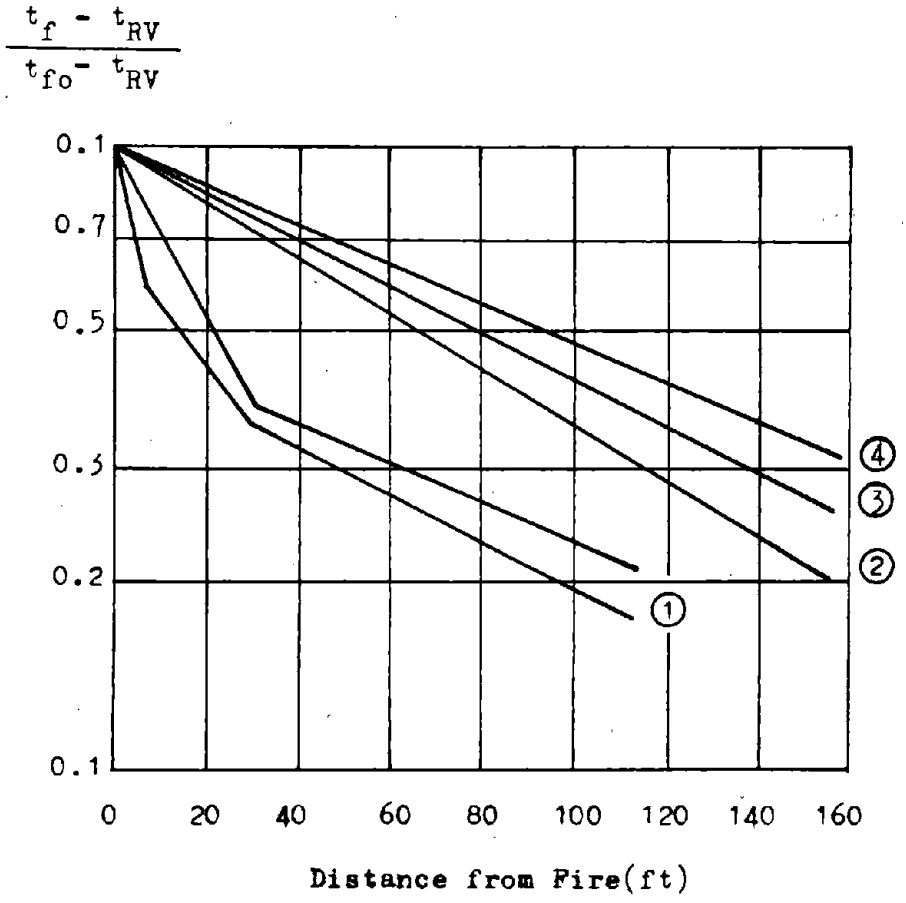

Fig. 32. Relative Temperature behind a Fire

Under the assumption of $t_{RV} = 86^{\circ}F$ as an average value for older airways in German coal mines, the ratio $(t_f - t_{RV})/(t_{fo} - t_{RV})$ has been plotted as curve 4 in fig. 32 too.

Klinger reports (68) that with an air velocity of 10 ft/sec he measured 22 minutes after the start of a timber fire temperatures of:

in the fire zone:	1472 °F
90 ft downstream:	860 °F
128 ft downstream:	608 °F

which indicates an exponential temperature-distance relation, too.

Nagy, Hartmann and Howarth (86) report 60 ft inby a coal fire an air temperature of 770 °F.

b) Moving fires

The temperature observations on moving fires, which are contained in the literature, have already been discussed (fig. 18, 19, 20, table 8). Although the theory predicts that the fumes behind moving fires should cool faster than behind stationary fires; the difference does not seem to be too large. The reason is that the coefficient of age $K(\alpha)$, at least for smaller air velocities, does not change too much with time.

IV. Forces Developed by Fumes

Temperature changes of the ventilating air, caused by mine fires, have two major effects on the ventilation:
a throttling effect,
a natural draft effect.
Before both effects are numerically assessed it seems advisable to define the energy scales in which they are measured.

Energies in mine ventilation are either expressed per unit weight of air (ft-lb/lb) and then called heads (h) or per unit volume of air ($ft\text{-}lb/ft^3 = lb/ft^2$) and then called pressures (p). Since the relationship between unit weights and volumes is the specific weight γ (lb/ft^3), heads and pressures are related by the specific weight, too: $h = p/\gamma$.

Within a ventilation system γ can undergo considerable changes. This has the consequence that equal energy quantities must sometimes be expressed by considerably different pressures, a fact which complicates the application of energy balances. To overcome this difficulty but still to maintain the use of the familiar units of pressures, heads are frequently expressed as pressures by multiplying them with a constant conversion factor, based on a standard specific weight of $\gamma_s = 0.075$ lb/ft^3 and the factor 1/5.194 inches WG/(lb/ft^2)

$$h\ (ft) * \frac{0.075}{5.194} = h\ (in.WG)$$

Unfortunately, the difference between heads and pressures in neglected by many ventilation engineers or not too well understood and considerable confusion exists in the literature on this subject.

To distinguish in this report the "energy quantity pressure" from the physical pressure, the former is always used with a subscript.

A) Throttling effect

The headloss h_L of air currents, due to airway resistances, can be described by Darcy's equation

$$dh_L = f \frac{dL}{D} * \frac{V_a^2}{2g} = f \frac{dL\ P}{4\ A} * \frac{V_a^2}{2g}$$ with f = coefficient of friction

The velocity V_a of an air current passing through a fire is changed by: mass flow increases due to addition of combustion products and evaporated water,
volume changes due to temperature changes.

Mass flow increases have been discussed in chapter 2 of this report. They can be calculated from the composition of the fumes: (see chapter VI-D.b.1) according to Voskobojnikov (131) they are in the range of 5 - 11 %, according to Schmidt (116) they are around 10 %.

Temperature changes can be considered in the following way. With $G = Q * \gamma$ and $Q = V_a * A$, Darcy's equation can be written as

$$dh_L = f \frac{dL\ P}{8\ g\ A^3} * \frac{1}{\gamma^2} * G^2$$

If pressure changes are neglected, the equation of state $p/\gamma = R\ T$ delivers $\gamma\ T$ = constant = $\gamma_a\ T_a$, with the subscript a indicating the original state of the air before the fire started. Then

$$dh_L = f \frac{dL\ P}{8\ g\ A^3} * \left(\frac{T}{T_a \gamma_a}\right)^2 G^2$$

If an average temperature $(T_{msq})^2 = \int \frac{T^2 dL}{L}$ is introduced and as well G as f, P and A are considered to be constant, this becomes

$$h_L = f \frac{L\ P}{8\ g\ A^3} * \left(\frac{Tmsq}{\gamma_a T_a}\right)^2 G^2.$$

The pertinent pressure loss p_L is , with $p_L = h_L * \gamma$

$$dp_L = f \frac{dL\ P}{8\ g\ A^3} * \left(\frac{T}{\gamma_a T_a}\right) G^2$$

If an average temperature $T_m = \int \frac{T\ dL}{L}$ is introduced, this becomes with G, f, P, and A kept constant

$$p_L = f \frac{L\,P}{8\,g\,A^3} * \left(\frac{T_m}{\rho_a T_a}\right) G^2.$$

The additional headloss, caused by the mass flow increase from G_a to $F * G_a$ and the temperature increase from T_a to T_{msq} is

$$\Delta h_L = h_{La} \left(F \frac{T_{msq}}{T_a}\right)^2 - 1)$$

the additional pressure loss is

$$\Delta p_L = p_{La} \left(F^2 \frac{T_m}{T_a} - 1\right)$$

These additional head- and pressure losses are called the throttling effect. Fig. 33 - 35 indicates the order of magnitude of throttling effects caused by temperature increases.

Fig. 33 shows the additional headloss Δh_L in percent of the original headloss (or the factor $\left(\frac{T_{msq}}{T_a}\right)^2 - 1$) as function of the ratio T_{fo}/T_a for constant parameters $\alpha P\ L/G\ c_p$). A value of $\alpha P\ L/(G\ c_p) = 0.5$ would apply to a short airway with a large air quantity, a value of 10 to a long airway with a small air quantity. Fig. 34 shows the additional pressure loss Δp_L (or the factor $\frac{T_m}{T_a} - 1$). T_m and T_{msq} were determined by using the formulas given in chapter III-A.

By comparing fig. 33 and 34 one sees that Δh_L is much larger than Δp_L. The reason is that the pressure loss p_L, being energy per unit volume, is based on an increased volume flow instead, like the headloss h_L, on a constant mass flow.

The fact that the throttling effect will occur mainly in the immediate vicinity of the fire is demonstrated in fig. 35. Here the additional headlosses, caused by the volume expansion are plotted for every 100 ft of airway length with an assumed fire temperature of $T_{fo}/T_a = 4$. For $\alpha P/G * c_p$ the values 0.001 (large airflow), 0.0025, and 0.005 (small airflow) have been chosen. One should be aware that α increases with G too. If α is assumed to be proportional to $V_a^{0.8}$, a doubling of $\alpha P/(G\ c_p)$ would correspond to an decrease of G by a factor 32.

A certain additional throttling effect is caused by the changes in kinetic energy of the air current. If the kinetic energy is expressed per unit weight as velocity head h_v, the change in kinetic energy content is

$$\Delta h_v = \frac{V_{a2}^2}{2g} - \frac{V_{a1}^2}{2g}$$

or, under the assumption of constant mass flow and constant cross sections

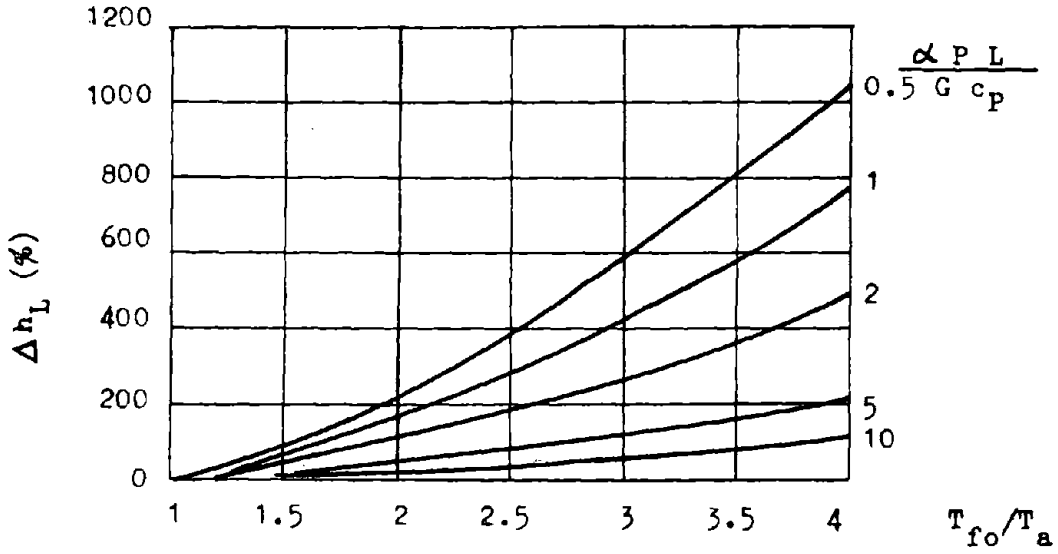

Fig. 33. Additional Headloss Caused by Throttling Effect

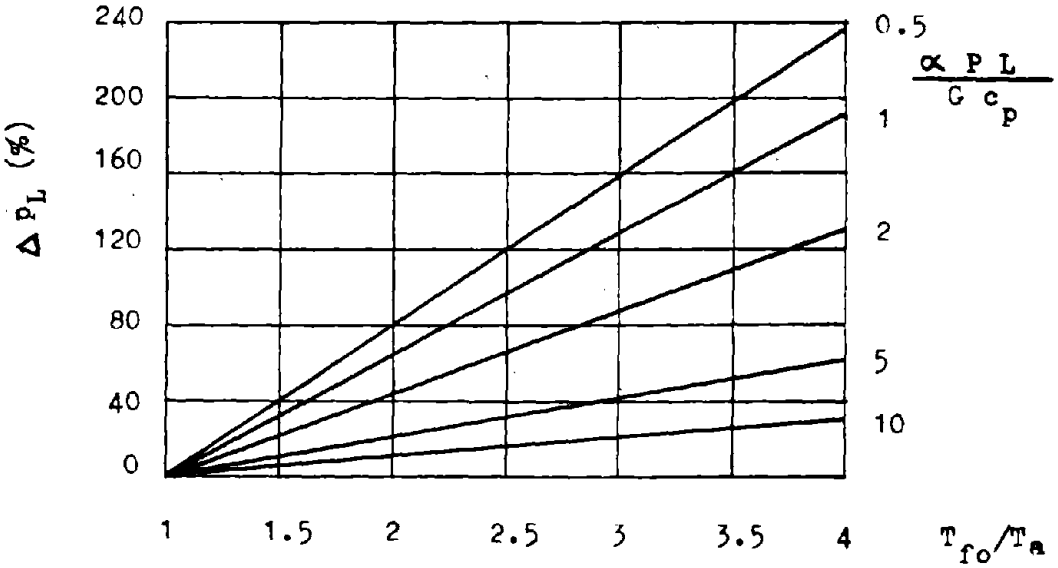

Fig. 34. Additional Pressure Loss Caused by Throttling Effect

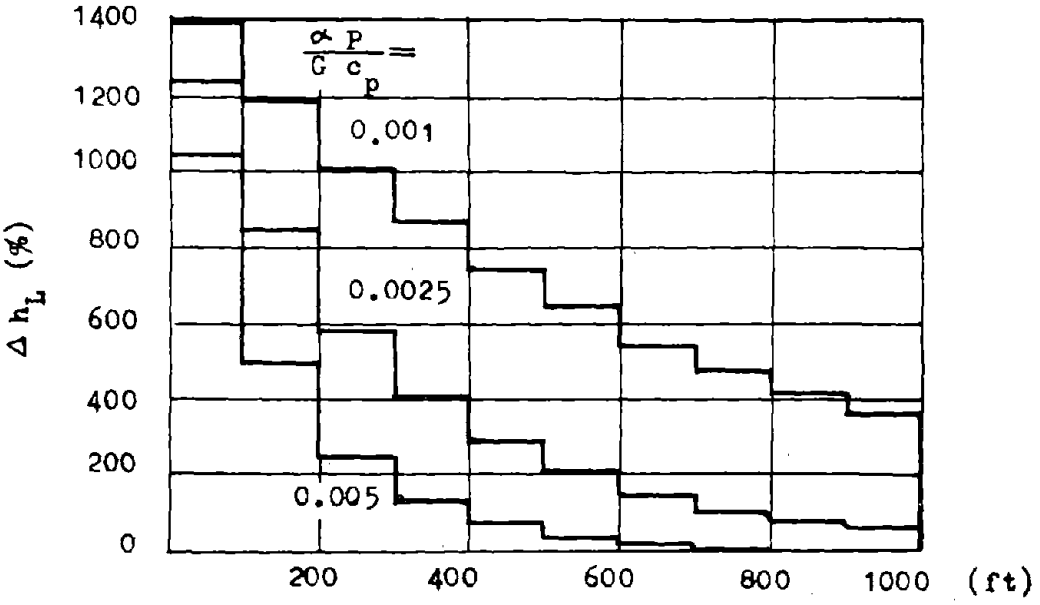

Fig. 35. Additional Headloss Plotted over Airway Length

$$\Delta h_v = \frac{V_{a1}^2}{2g} \left(\left(\frac{T_2}{T_1}\right)^2 - 1\right)$$

If the kinetic energy is expressed per unit volume as velocity pressure p_v, the change is

$dp_v = \gamma \frac{V_a \, dV_a}{g}$. From $G = Q\gamma = A\, V_a \gamma$ follows for the assumption of G = constant and A = constant that $V_a \gamma$ = constant, too. Consequently

$$\Delta p_v = \gamma V_a \int \frac{dV_a}{g} = \frac{\gamma V_a (V_{a2} - V_{a1})}{g} = \frac{\gamma_2 V_{a2}^2 - \gamma_1 V_{a1}^2}{g} \quad \text{or}$$

$$\Delta p_v = \frac{\gamma_1 V_{a1}^2}{g} \left(\frac{T_2}{T_1} - 1\right).$$

It is a very common mistake that ventilation engineers assume for the change of p_v caused by volume changes

$$\Delta p_v = \frac{\gamma_2 V_{a2}^2 - \gamma_1 V_{a1}^2}{2g}$$

This formula is correct for velocity changes caused by changes of A or G but not for compressibility effects.

A positive Δh_v or Δp_v, as observed when air passes through a fire and is heated has a throttling effect ($T_2 > T_1$) on the airflow. A negative Δh_v or Δp_v, as observed when the fumes cool down ($T_2 < T_1$), will support the airflow.

A large number of ventilation engineers prefer to base ventilation calculations on pressure losses and to convert Darcy's equation into the resistance equation

$$p_{Lm} = R_m * Q_m^2 \quad \text{where } R_m = f \frac{L\,P}{4\,A^3} * \frac{\gamma_m}{2g}$$

With $\gamma_m / \gamma_a = T_a / T_m$ and $Q_m / Q_a = T_m / T_a$ it follows that

$$R_m = R_a \frac{T_a}{T_m} \quad \text{and} \quad Q_m = Q_a \frac{T_m}{T_a}.$$

An airway with the original pressure loss p_{La} at the temperature T_a will therefore at the temperature T_m have the pressure loss

$$p_{Lm} = R_a \frac{T_a}{T_m} \left(Q_a \frac{T_m}{T_a}\right)^2 = R_a Q_a^2 \frac{T_m}{T_a} = p_{La} \frac{T_m}{T_a}$$

Voskobojnikov suggests an equivalent resistance factor, which also takes into account the changes of velocity pressures. It contains a factor of 1.11 for the increased mass flow behind the fire.

$$R_{equ} = \frac{p_{Lm}}{Q_a^2} = 1.11^2 \left[R_a \frac{T_m}{T_a} + \frac{\gamma_a}{2gA^2} \left(\frac{T_m}{T_a} - \frac{1}{1.11^2}\right)\right]$$

According to the derivations performed above the factor $\frac{\gamma a}{2gA^2}$ should rather read $\frac{\gamma a}{g A^2}$

B) Natural draft effects

a) Definition and determination of natural drafts

The great number of misleading statements found in the literature concerning the natural draft makes it advisable to discuss its definition and the more popular methods for its determination first.

Natural draft is caused by the conversion of heat into mechanical energy, which is then available to propel the air and to overcome friction losses. For such a conversion under steady state conditions cyclic processes are necessary, which are provided by every loop of the ventilation network. The amount of heat converted in a cyclic process into mechanical work is indicated by the area enclosed by this process in a p-v diagram. This statement can easily be proved by applying the first law of thermodynamics, in ventilation frequently called the energy equation, in the form

$$v\,dp + dV_a^2/2g + dZ + dh_L = 0 \qquad Z = \text{elevation}$$

for airways without fans to a loop, which results in

$$-\oint v\,dp = \oint dh_L .$$

$\oint dh_L$ is the sum of all friction losses experienced by the air, flowing through this loop, $\oint v\,dp$ is the energy necessary, to balance these losses.

If, in the airways of the loop, mechanical energy dw is exchanged between air and surrounding (fans, dropping water, etc.), one obtains

$$-\oint v\,dp + \oint dw = \oint dh_L$$

In this case both, the heat energy $\oint v\,dp$ and the mechanical energy $\oint dw$ have to balance the losses.

The natural draft expressed as energy per unit weight of air is called the natural ventilation head h_N and its magnitude is consequently

$$h_N = -\oint v\,dp$$

Natural draft is always tied to a cyclic process, to a loop. Statements on natural draft without specifying the loop where it is

developed are not too meaningful.

The natural draft expressed as energy per unit volume flowing through the loop can be derived by multiplying the energy equation in the above used form by the specific weight γ :

$$dp + \frac{\gamma}{2g} dV_a^2 + \gamma dZ + \gamma dh_L = 0$$

Application to a loop results in

$$- \oint \gamma dZ = \oint \gamma dh_L = \oint dp_L$$

$\oint dp_L$ is the sum of all pressure losses experienced by the air in the loop. If mechanical work dp_F is exchanged between air and surrounding, one obtains

$$- \oint \gamma dZ + \oint dp_F = \oint dp_L$$

The term $- \oint \gamma dZ$ is called the natural ventilation pressure

$$p_N = - \oint \gamma dZ$$

p_N and h_N are related by the average specific weight γ_m of the air in the loop through $p_N = \gamma_m h_N$, where, for loops without fans

$$\gamma_m = \frac{\oint \gamma dh_L}{\oint dh_L} = \frac{\oint dp_L}{\oint dh_L}$$

and for loops with fans

$$\gamma'_m = \frac{\oint \gamma dh_L - \oint \gamma dh_F}{\oint dh_L \quad \oint dh_F} = \frac{\oint dp_L - \oint dp_F}{\oint dh_F \quad \oint dh_F}$$

In using the natural ventilation pressure p_N one must be aware that even in loops without a natural draft but with a fan, p_N has a value $\neq 0$. Despite $\oint dh_L = \oint dh_F$ as the condition for no natural draft, one obtains usually $\oint \gamma dh_L \neq \oint \gamma dh_F$ since the specific weights of the air while overcoming friction and while passing through the fan are different. Consequently one finds from the energy equation

$$\oint \gamma dZ + \oint \gamma dh_L - \oint \gamma dh_F = 0$$

$$- \oint \gamma dZ = p_N \neq 0$$

This is a common experience. In mines ventilated by fans there is for instance always a difference in the specific weights of the air in the intake and return airways, even if no temperature difference exists, which according to $p_N = \oint \gamma dZ$ produces a natural ventilation pressure. If the fans are switched off, the difference in specific weight disappears and p_N becomes zero (40).

The formula $p_N = - \oint \gamma dZ$ applied to a loop formed by two

vertical and two horizontal airways with the elevation difference ΔZ delivers with γ_{mD} AND γ_{mU} as the mean specific weights in the downcast and upcast airways

$$p_N = (\gamma_{mD} - \gamma_{mU})\ \Delta Z$$

This result has led to the explanation of the natural draft as caused by the different weight of corresponding air columns. As the above discussion on the nature of the natural draft has shown, these different weights are an attendant symptom of natural drafts but not its cause.

Since the determination of specific weights or volumes is tedious, approximation formulas are widely used for $h_N = - \oint v\, dp$ and $p_N = - \oint \gamma\, dZ$. The more popular ones are based on temperatures and elevations, both easy to determine. Woropajew (121) suggests calculating the amount $\oint v\, dp$ from the area enclosed by the loop in a T-Z diagram. His derivations, published shortly after WW II, were not available to the author of this report but his method can be explained as follows (42). Volume changes are in mine ventilation mainly caused by temperature changes

$$v \sim T\,(\frac{R}{p})_{\text{average}}$$

Pressure changes are mainly caused by elevation changes, pressure losses and fan pressures

$$dp \sim \frac{1}{v_{\text{average}}}(\,dZ - dh_F + dh_L)$$

The natural ventilation head can then be approximated by

$$h_n = - \oint v\, dp \sim (\frac{R}{p * v})_{\text{average}} * \oint T\,(\,dZ - dh_F + dh_L)$$

If, as is usually the case, the friction losses in the non horizontal airways are fairly evenly distributed, replacing $\oint T\,(dZ - dh_F + dh_L)$ by $\oint T\, dZ$ changes the shape of the area enclosed by the loop in the T-Z diagram but does not change the size of its area significantly. One can therefore approximate

$$h_n \sim \frac{1}{T_{ml}} \oint T\, dZ$$

where $T_{ml} = (\frac{R}{p\ v})_{\text{average}}$ is the average temperature of the air in the loop. The errors accepted in using this formula are shown in fig. 36 (42) under the assumption that the friction losses in the nonhorizontal airways are equal and that the loop shows a parallelogram shape in a p-v diagram. One sees that the errors of this handy approximation are within tolerable limits.

The formula $p_N = (\gamma_{mD} - \gamma_{mU})\Delta Z$ is frequently approximated by

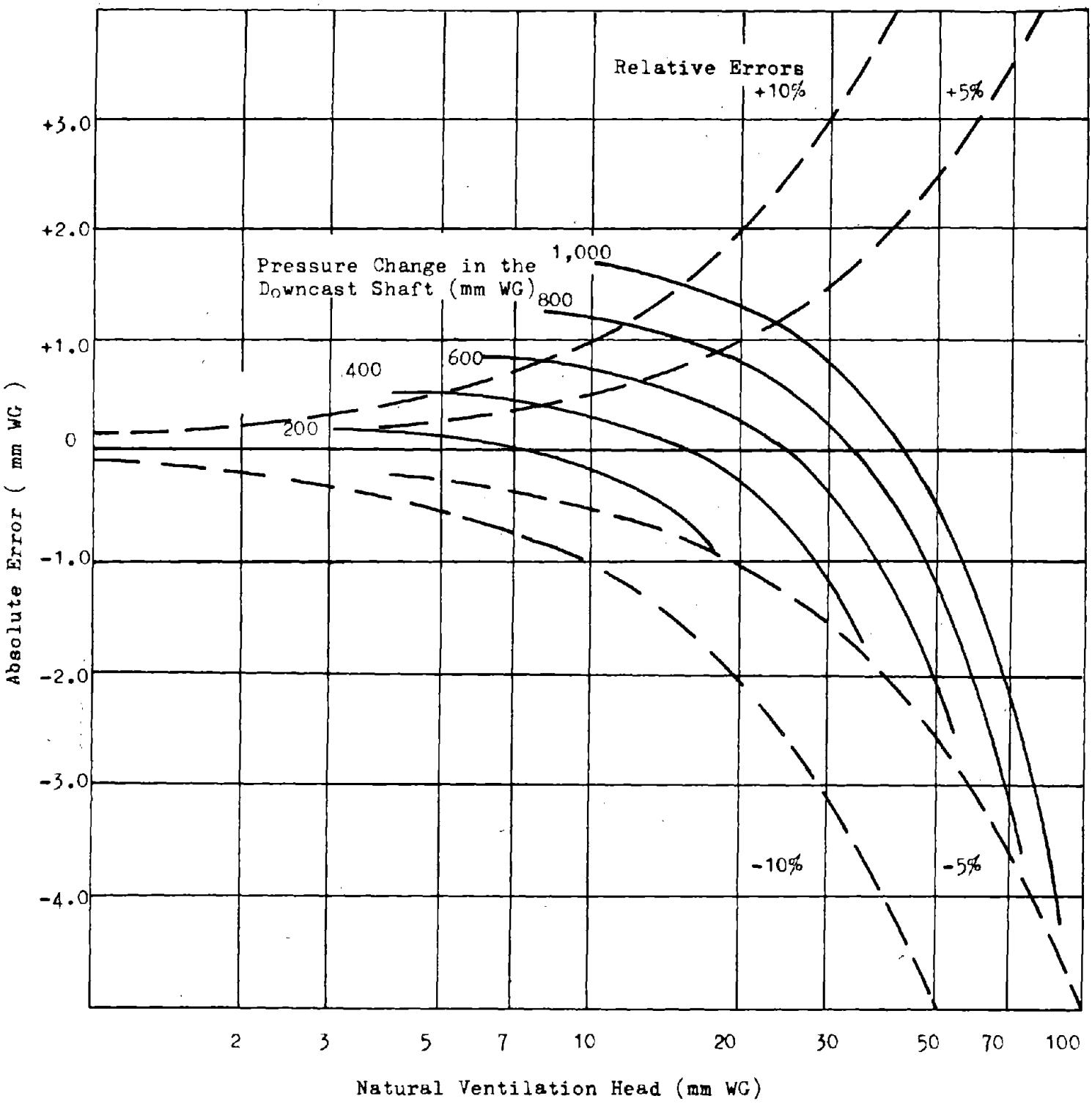

Fig. 36. Error of the Approximation $h_N \approx \frac{1}{T_{ml}} \oint T \, dZ$ (42)

$$p_N = \frac{p}{R}\left(\frac{1}{T_{mD}} - \frac{1}{T_{mU}}\right)\Delta Z = \frac{p}{R}\left(\frac{T_{mU} - T_{mD}}{T_{mU} * T_{mD}}\right)\Delta Z =$$

$$\frac{\gamma_{mD}}{T_{mU}}\left(T_{mU} - T_{mD}\right)\Delta Z.$$

For the calculation of the natural draft, which is caused by a mine fire in excess of the previously already existing natural draft, the differences

$$h_N = -\oint v_f\, dp + \oint v_a\, dp = -\oint (v_f - v_a)dp$$

or

$$p_N = -\oint \gamma_f dZ + \oint \gamma_a dZ = -\oint (\gamma_f - \gamma_a)\, dZ$$

have to be determined. Subscript f and a indicate the condition during and before the fire.

If one considers an individual airway, whose specific volume or weight have been changed by the fire, the additional natural draft caused by the fire in a loop, formed by this airway and other airways without any changes is

$$h_N = -\oint (v_f - v_a)\, dp$$

or

$$p_N = -\oint (\gamma_f - \gamma_a)\, dZ$$

It should be noted that the integral has to be calculated only for the airway with the changes. In this context one can speak of natural draft in individual airways, although one understands that for the development of natural draft loops are necessary.

b) Combination of throttling and natural draft effects

The last two equations contain only data for one individual airway. They can therefore be used to demonstrate the combined result of throttling and natural draft effects in one individual airway, when its temperature changes. To avoid unnecessary lengthy discussions, only pressure effects will be investigated.

If the temperature changes in the airway from a uniform T_a along the airway to a uniform T_m, the natural draft can be calculated from

$$p_N = (\gamma_a - \gamma_m)\Delta Z = \gamma_a\left(1 - \frac{T_a}{T_m}\right)\Delta Z = \gamma_a\left(1 - \frac{T_a}{T_m}\right) L \sin\beta$$

(slope angle β positive for ascending, negative for descending ventilation)

The throttling effect is

$$\Delta p_L = p_{La}\left(\frac{T_m}{T_a} - 1\right)$$

The combined pressure effect is

$$p_T = p_N - \Delta p_L = \gamma'_a (1 - \frac{T_a}{T_m}) L \sin\beta - p_{La} (\frac{T_m}{T_a} - 1)$$

A positive p_T has a tendency to increase the airflow, a negative p_T to reduce it.

One sees from this equation that p_N is positive for ascensional, negative for descensional ventilation and zero for horizontal airways. Its magnitude depends on γ'_a and T_a of the original state, the new temperature T_m and the elevation change L sin β only. It will be zero for $T_m = T_a$ and approach asymptotically $p_N = \gamma'_a$ L sin β with increasing T_m.

The throttling effect p_L is proportional to the pressure loss in the original state

$$p_{La} = f \frac{L P}{8 g A^3} * \frac{1}{\gamma'_a} * G^2$$

and the term $(\frac{T_m}{T_a} - 1)$. It has always a tendency to reduct the airflow.

Fig. 37 shows as an example p_T for an ascensionally ventilated vertical airway (L = 300 ft, P = 40 ft, A = 100 ft^2, γ'_a = 0.075 lb/ft^3) as a function of T_m/T_a with the airflow as parameter. One sees the increase of the throttling effect with air quantity and that a maximum for p_T exists. At which temperature this maximum occurs can be determined from

$$\frac{dp_T}{dp_m} = + \frac{T_a}{T_m^2} \gamma'_a L \sin\beta - p_{La} \frac{1}{T_a} = 0$$

which delivers

$$\frac{T_m}{T_a} = (\frac{\gamma'_a L \sin\beta}{p_{La}})^{1/2} = \frac{\gamma'_a}{G} (\frac{\sin\beta \; 8 g A^3}{f P})^{1/2}$$

c) Natural draft values recommended in literature

The literature contains a few recommendations on the magnitude of natural drafts in fire emergency plans. Osipov and Zadan (95) give a chart for p_N in a vertically ascending airway of 86 ft^2 cross section for airway lengths between 0 and 4590 ft and air velocities between 3.3 and 33 ft/sec (fig. 40). This chart is based on the formula

$$p_N = \gamma'_a \frac{T_m - T_a}{T_m} L \sin\beta, \; \gamma'_a = 0.078 \text{ lb/ft}^3, \; \alpha = 0.9 + 0.221 \, V_a,$$

$$T_m = T_a + \frac{G \, c_p}{\alpha P \, L} (t_{fo} - t_a) (1 - \exp(-\frac{\alpha P \, L}{G \, c_p})) \text{ and}$$

$$t_{fo} = V_a/(0.000419 + 0.000361 \, V_a) + 32$$

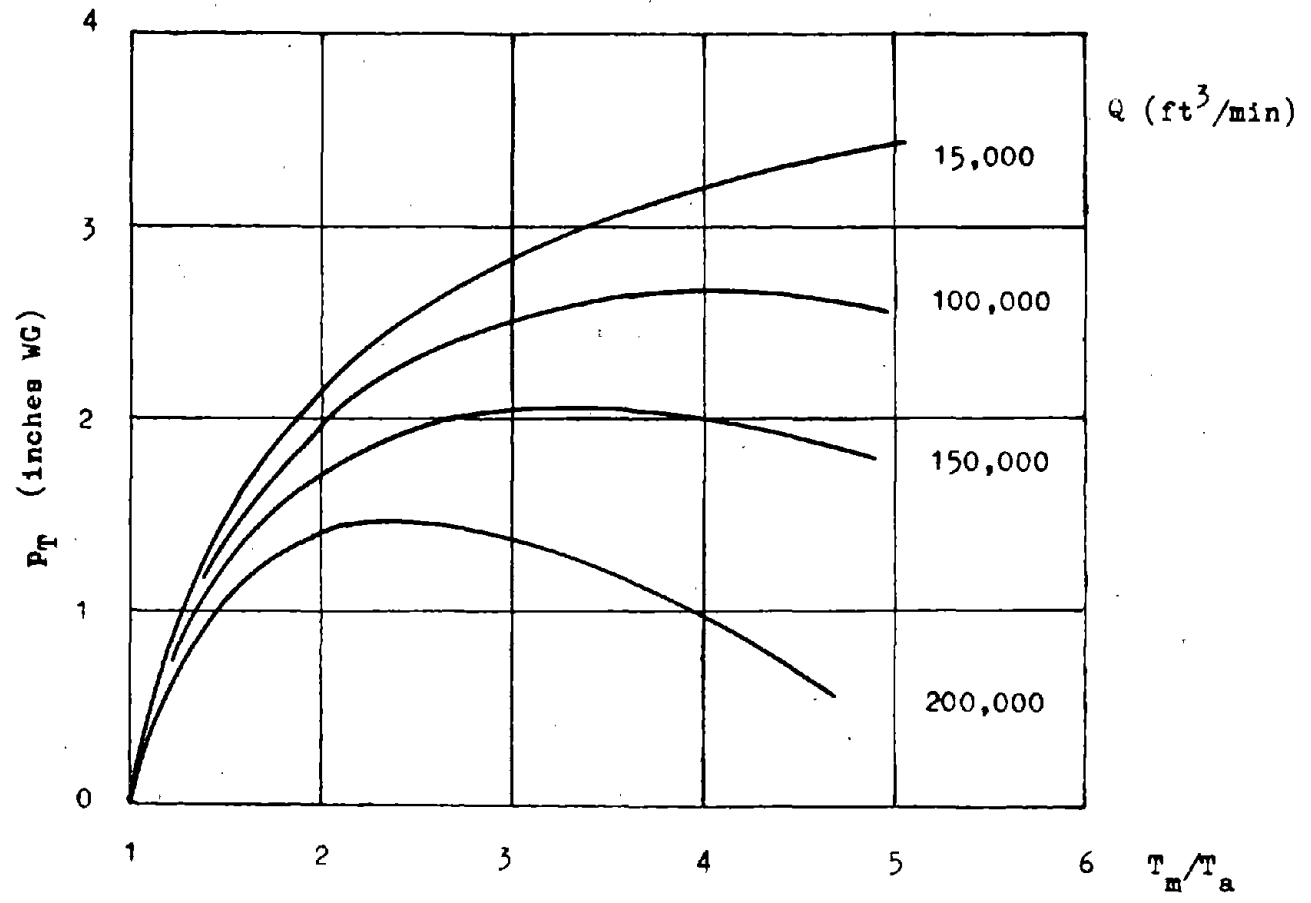

Fig. 37. Combined Pressure of Throttling and Natural Draft Effects

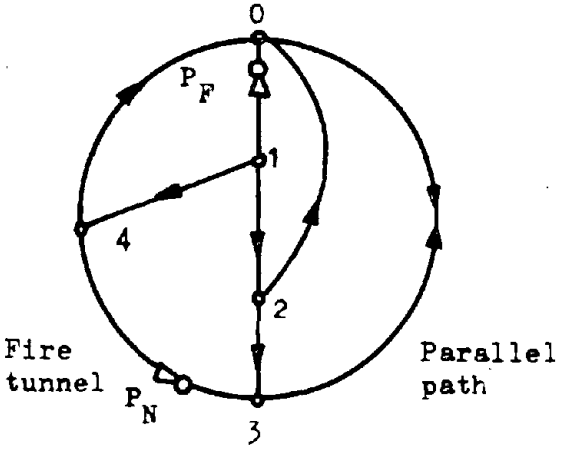

Fig. 38. Ventilation Plan of Fire Tunnel Used by Voskobojnikov (131)

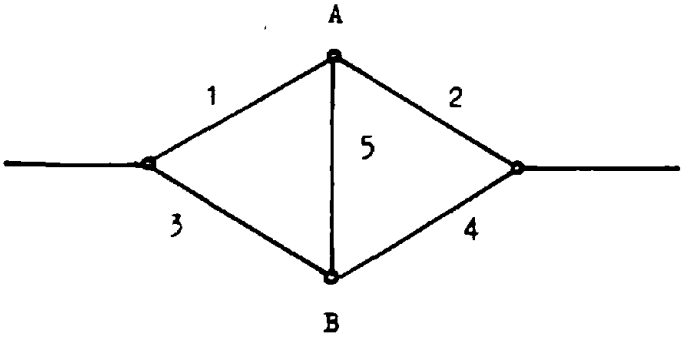

Fig. 39. Example for a Diagonal Airway

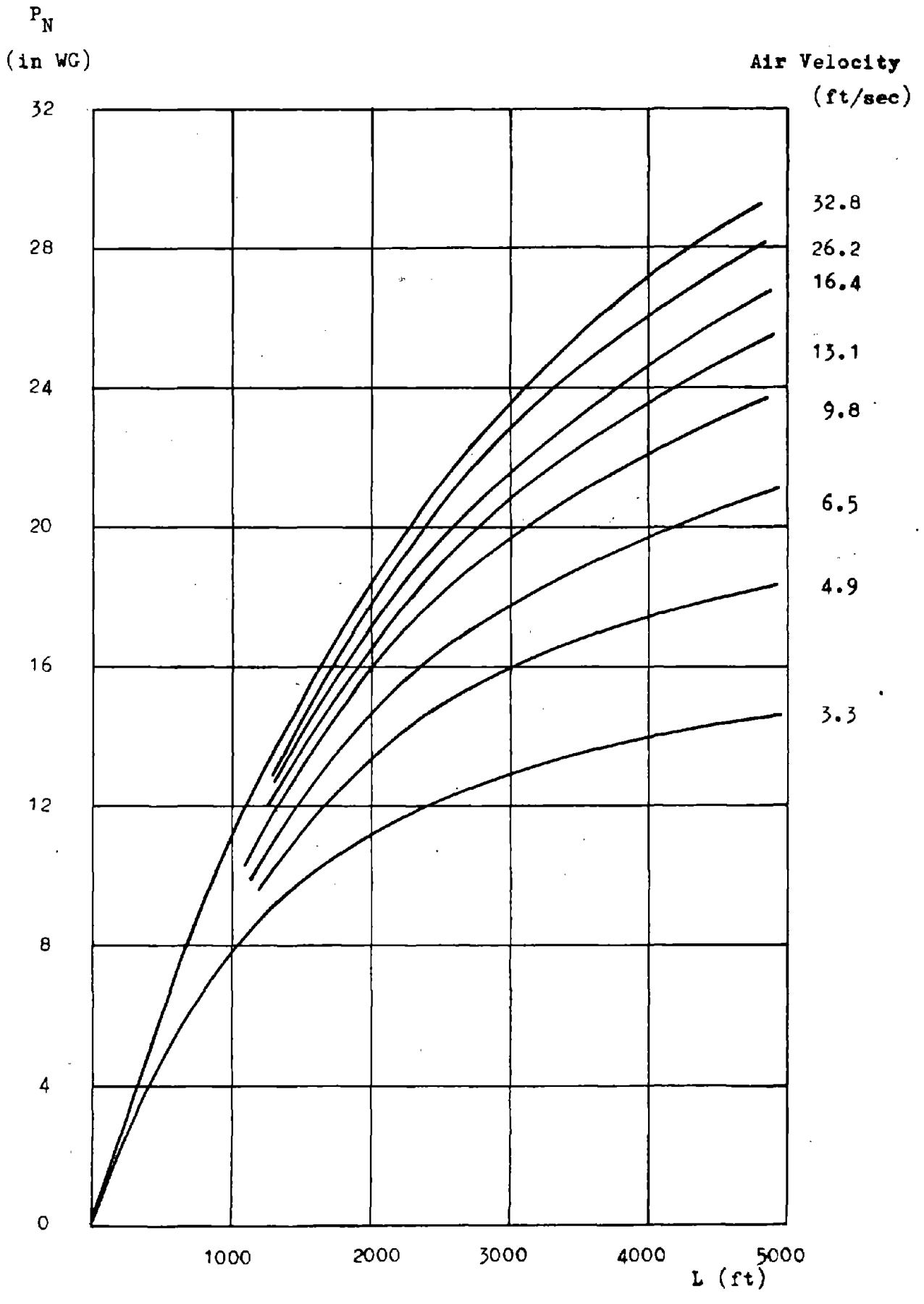

Fig. 40. Chart for Natural Ventilation Pressures (95)

For inclined airways of other cross sections the authors recommend the application of two correction factors to the chart value p_{NC}

$$p_N = p_{NC} * k_1 * k_2$$

where k_1 takes the slope into account and is the sin function of the slope angle β and k_2 considers the influence of the cross section on T_m. Values for k_2 are contained in table 17.

Hrbac and Tesar (57) design from the formulas

$$p_N = \gamma_a \frac{T_m - T_a}{T_m} L \sin \beta \quad \text{and}$$

$$t_f = t_a + (t_{fo} - t_a) \exp(- \frac{\alpha P L}{G c_p})$$

under the assumption of $t_a = 78\ ^oF$, $\gamma_a = 0.078\ lb/ft^3$ and

$$\alpha = 0.41 + 0.79 V_a^{0.5}$$

a chart, which allows for given values of P/A, V_a, t_{fo}, ΔZ and L the determination of the temperature at the end of the airway t_{f2}, the average temperature t_m and the natural ventilation pressure p_N.

Trutwin (]28) discusses the numberical solution of

$$p_N = - \oint (\gamma_f - \gamma_a)\, dZ$$

Under the assumption that the change of specific weight $\Delta\gamma = \gamma_f - \gamma_a$ is mainly caused by the temperature change $\Delta T = T_f - T_a$ and that other influences can be neglected, he obtains from the equation of state $p/\gamma = R\,T$ and its partial derivative $\partial\gamma/\partial T = - p/R\,T^2$

$$\Delta\gamma = \int_{T_a}^{T_a + \Delta T} \frac{p}{R\,T^2}\, dT = - \frac{p}{R\,T_a} * \frac{\Delta T}{T_a + \Delta T} = - \gamma_a \frac{\Delta T}{T_a + \Delta T}$$

The same result could have been obtained directly from the definition of $\Delta\gamma$

$$\Delta\gamma = \gamma_f - \gamma_a = - \gamma_a \left(1 - \frac{T_a}{T_a + \Delta T}\right) = - \gamma_a \frac{\Delta T}{T_a + \Delta T}$$

The assumption of a steady state heat exchange between fumes and the airway walls delivers with $\Delta T_o = T_{fo} - T_a$ and $\Delta T = \Delta T_o$ for L = 0

$$\Delta T = \Delta T_o * \exp(- \frac{\alpha P L}{G c_p})$$

With this expression being inserted into

$$p_N = - \int (\gamma_f - \gamma_a)\, dZ = \int \gamma_a \frac{\Delta T}{T_a + \Delta T}\, dZ$$

and with $dZ/dL = \sin \beta$ and with the abbreviation $A = \frac{\alpha P}{G c_p}$ one obtains

$$p_N = \sin\beta \, \gamma_a \int_{L_1}^{L_2} \frac{\Delta T_o \exp(-AL)}{T_a + \Delta T_o \exp(-AL)} \, dL$$

and, after executing the integration

$$p_N = \frac{\sin\beta \, \gamma_a}{A} \ln\left(\frac{T_a + \Delta T_o \exp(-AL_1)}{T_a + \Delta T_o \exp(-AL_2)} \right)$$

If a function

$$LN(L) = \ln\left(\frac{T_a + \Delta T_o}{T_a + \Delta T_o \exp(-AL)} \right)$$

is introduced, p_N CAN be calculated from

$$p_N = \frac{\sin\beta \, \gamma_a}{A} \left(LN(L_2) - LN(L_1)\right)$$

In his paper (128) Trutwin provides a table and 3 graphs which show LN(L) for values of AL between 0.001 and 17.0 and for values of T_o between 100°K. and 1000°K. T_a is assumed to be equal 300°K.

Voskobojnikov (131) describes tests which he conducted with fires in a tunnel of 16.5° slope, 43 ft² cross section and 144 ft length. This tunnel was part of the ventilation system shown in fig. 38. Its resistance was expressed by

$R_{equ} = 1.11^2 \left(R_a \frac{T_m}{T_a} + \frac{\gamma_a}{2 g A^2} \left(\frac{T_m}{T_a} - \frac{1}{1.11^2}\right)\right)$, the natural ventilation pressure was calculated from

$$p_N = \gamma_a \left(\frac{T_m - T_a}{T_m}\right) \Delta Z.$$

With the help of an analog computer it was determined at which temperatures T_m and the pertinent p_N the airflow in the parallel path 0-3 would be reversed. During the fire the temperature in the tunnel was measured in 5 cross sections with 5 thermocouples per cross section and T_m was calculated as the average of all thermocouple readings. In all fire tests a good agreement (3 - 5 %) was achieved between the calculated T_m, at which the airflow reversal was to be expected and the measured T_m, at which the reversal took actually place.

Schmidt and Grumbrecht (118) performed direct meassurements of the natural ventilation pressure p_N developed by fires in a descensionally ventilated raise. For this purpose they connected the upper and lower end of the raise over a manometer with a hose laid out in adjacent airways with undisturbed temperatures. If standstill of the airflow occurs in the raise, the energy equation applied to the raise is

$$\gamma_f \, dZ + dp = 0$$

and the energy equation for the hose is

Table 17. Correction Factors to Fig. 38 for Variable Cross Sections (95)

Airway Length (ft)	Airway Cross Section (ft^2) 21.6	43.3	86.4	108	216	433	Air Speed (ft/sec)
164	0,97	0,99	1,00	1,00	1,01	1,02	3.3 - 32.8
328	0,94	0,98	1,00	1,01	1,03	1,04	3.3 - 32.8
984	0,75	0,90	1,00	1,04	1,20	1,27	3.3 - 6.6
	0,80	0,92	1,00	1,03	1,11	1,15	9.8 - 13.1
	0,81	0,93	1,00	1,02	1,08	1,12	16.4 - 32.8
1640	0,61	0,81	1,00	1,06	1,32	1,46	3.3
	0,64	0,82	1,00	1,05	1,26	1,38	4.9
	0,67	0,84	1,00	1,04	1,21	1,30	6.6
	0,70	0,87	1,00	1,04	1,16	1,25	9.8 - 13.1
	0,73	0,88	1,00	1,03	1,15	1,20	16.4 - 32.8
2300	0,58	0,79	1,00	1,07	1,40	1,62	3.3
	0,60	0,80	1,00	1,06	1,35	1,55	4.9
	0,62	0,82	1,00	1,05	1,29	1,43	6.6
	0,65	0,83	1,00	1,05	1,24	1,35	9.8 - 13.1
	0,67	0,85	1,00	1,04	1,21	1,30	16.4 - 19.7
	0,69	0,85	1,00	1,04	1,20	1,27	26.3 - 32.8
3280	0,55	0,77	1,00	1,08	1,47	1,78	3.3
	0,57	0,79	1,00	1,08	1,43	1,70	4.9
	0,59	0,81	1,00	1,07	1,37	1,60	6.6
	0,61	0,81	1,00	1,06	1,33	1,50	9.8 - 13.1
	0,62	0,82	1,00	1,06	1,30	1,42	16.4 - 19.7
	0,62	0,83	1,00	1,05	1,26	1,40	26.3 - 32.8
4920	0,52	0,75	1,00	1,09	1156	1,06	3.3
	0,54	0,76	1,00	1,08	1,50	1,81	4.9
	0,55	0,77	1,00	1,08	1,46	1,76	6.6
	0,57	0,78	1,00	1,08	1,43	1,74	9.8 - 13.1
	0,59	0,79	1,00	1,07	1,40	1,60	16.4 - 19.7
	0,60	0,79	1,00	1,06	1,36	1,56	26.3 - 32.8

Table 18. Factors α for the Determination of Natural Ventilation Pressures in Descensinally Ventilated Airways (118)

Factor α (in WG/100 ft ^{o}F) $*10^3$	Frequency (%)
0.4	9
0.400 - 0.533	10
0.533 - 0.667	35
0.667 - 0.800	32
0.800 - 0.933	7
0.933 - 1.067	7

$$\gamma_a \, dZ + dp = 0$$

For the loop formed by the raise and the hose one obtains

$$- \oint (\gamma_f - \gamma_a) \, dZ = \int dp$$

and since $- \int (\gamma_f - \gamma_a) \, dZ = p_N$ and $\oint dp$ is the reading of the manometer, the latter indicates p_N. Schmidt and Grumbrecht arranged the data they collected in 60 fires for p_N and ΔZ with the formula

$$p_N = \alpha \frac{\Delta Z}{100} (T_m - T_a),$$

from which they determined the factor α. They felt that with the airflow fluctuations preceding a standstill, a representative T_m was too difficult to establish for every individual experiment, and they used the values from fig. 21 for T_m. Since the time at which the airflow standstill occurred and, therefore, the extension of the fire depended on the ventilating pressure, acting on the raise, and the latter was changed for the observation of other factors during the tests, the calculated values of α show a considerable spread. A statistical evaluation is compiled in table 18.

V. Qualitative Prediction of Ventilation Disturbances Caused by Fires

Throttling and natural draft effects can cause considerable changes in the quantity of ventilating air currents and sometimes even reverse their direction. These changes are not limited to the airway at fire but can occur in neighboring airways as well.

The dangers caused by air quantity reductions can in non-gassy mines be neglected. In gassy mines they can, however, lead to formation of explosive mixtures with all their pertinent dangers, which are especially obvious when the explosive mixture travels through the firezone.

Airflow reversals can be the cause of even more severe hazards. CO-laden air can enter the intake airways and poison large sections or all of the mine. In gassy mines explosive mixtures can be formed since every airflow reversal is preceded by a period of airflow reduction. Even in non-gassy mines explosions can be caused by explosive fumes, which after a reversal of airflow reach the firezone again.

Ventilation disturbances in the form of smoke layers have been discussed in chapter II-C.d. Since they are an easy to survey local phenomenon and can always be fought by local air velocity increases, no further comments seem to be necessary.

A) Horizontal airways

Open fires in horizontal airways, with only negligible temperature changes in following non-horizontal airways, have a throttling but no natural draft effect. The result is an airflow decrease in the airway at fire and all airways being in series with it. Due to smaller friction losses in these airways, the ventilating pressure of the airway at fire will increase and counteract the throttling effect. Air quantity decreases of up to 30 % were observed (13), however, rockfall may have been at least partially responsible.

A reversal of airflow in the airway at fire and the pertinent airway in series cannot occur. It is, however, possible in diagonal airways, which are connections between parallel airways, whose airflow direction is determined by the resistance ratios of the parallel airways. A simple example is shown in fig. 39. If the original airflow in the diagonal airway 5 is from A to B, it could be reversed by a fire in airways 1 or 4.

B) Ascensionally ventilated airways

Open fires in ascensionally ventilated airways also cause a throttling as a natural draft effect. If the temperatures or the elevation changes behind the fire are not too small, or, as the example of fig. 37 for vertical airways shows, the air quantities are not too large, the natural draft will usually be stronger than the throttling effect and increase the airflow. If enough combustible material is present, the increased oxygen supply will then intensify the fire so that considerable natural drafts are finally developed.

The increase in airflow in the airway at fire is accompanied by a decrease in parallel airways. If the original ventilating pressures for the parallel airways are small, even airflow standstills and reversals with all their dangerous consequences can occur. Remedies for stabilizing the airflow in parallel airways are an increase of the resistance of the airway at fire, which would at the same time reduce the oxygen supply and fire intensity, and an increase in the ventilating pressures. The latter aim can be accomplished by increasing the fan pressure or by lowering the resistance in the intake and return airways to the parallel airways.

Fig. 41 shows an example of how the airflow changed in a 72^{0} raise of 262 ft length, when at its bottom a fire object of 265 lb of timber was lit.

C) Descensionally ventilated airways

Open fires in descensionally ventilated airways cause, besides the ever present throttling effect, a natural draft, which is opposed to the original ventilating pressure and has

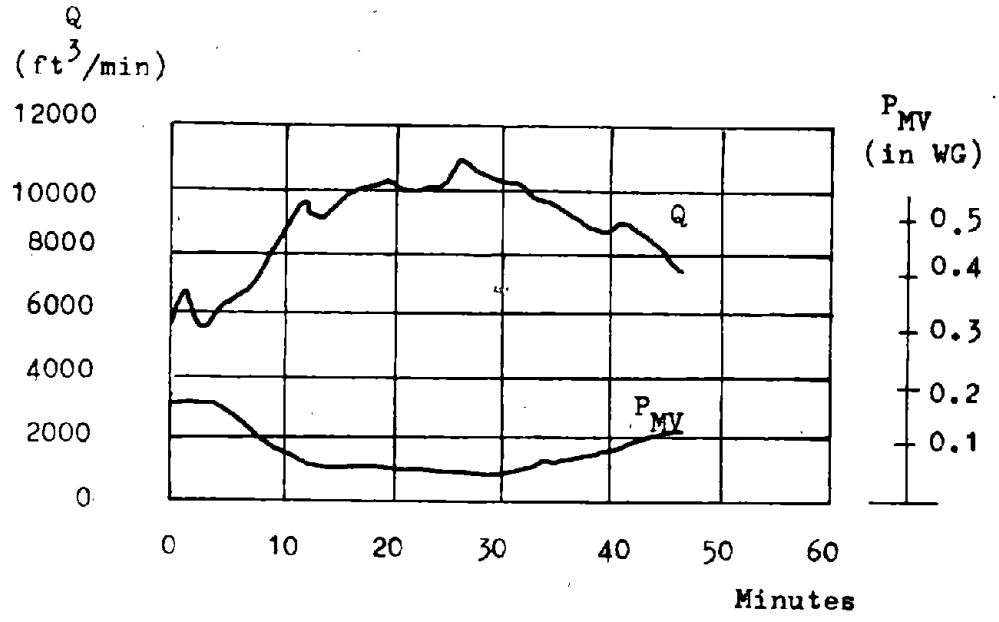

Fig. 41. Airflow and Ventilating Pressure Changes in an Ascensionally Ventilated Raise at Fire (118)

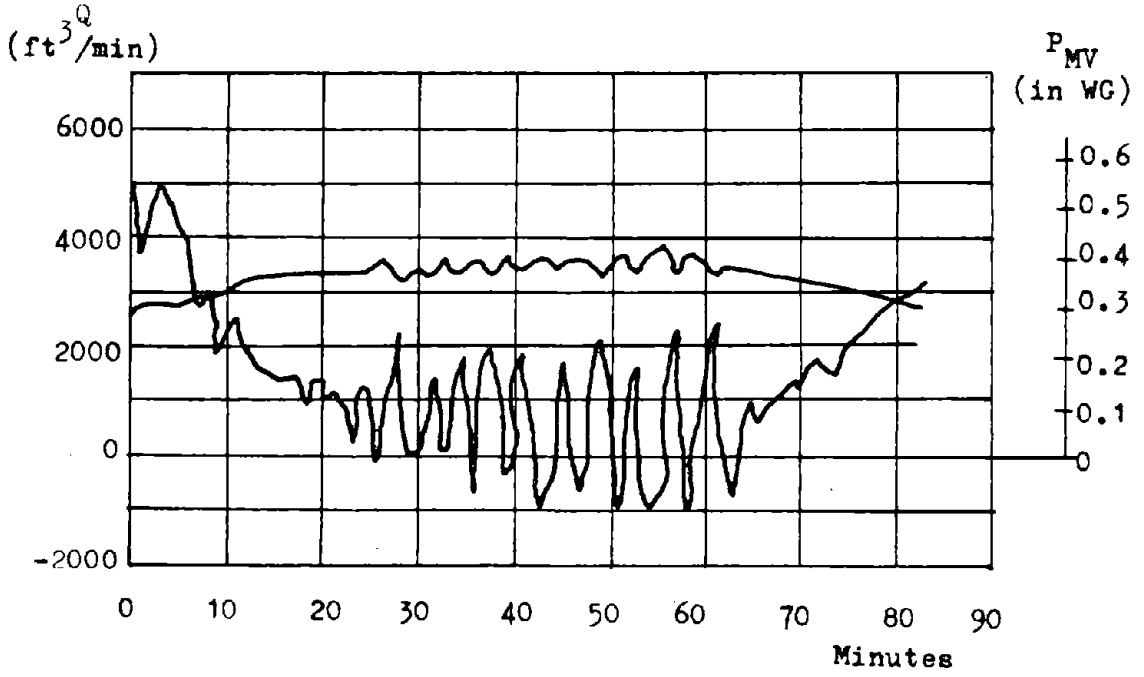

Fig. 42. Airflow and Ventilating Pressure Changes in a Descensionally Ventilated Raise at Fire (115)

a tendency to decrease or even reverse the airflow. A decrease in airflow usually decreases the intensity of the fire, too. The reduced natural draft, again permits a larger air supply, which in turn increases fire intensity and draft. Except for the case of limited natural drafts due to small elevation changes behind the fire and a lack of combustible material or for the case of very high original ventilating pressures, one can expect a violent fluctuation of the airflow in descensionally ventilated airways at fire. An example, measured by Schmidt (115) in a 72° raise, if given in fig. 42.

Whether a permanent airflow reversal takes place depends on several factors. There have to be sufficient elevation changes for the fumes on both sides of the fire. A fire at the bottom of a shaft or raise will not develop enough natural draft to initiate a reversal, a fire at the top not enough, to maintain it.

The oxygen content of the fumes is usually considerably lower than that of the fresh air. It is especially low behind fires of high intensities. If these high intensities effect an airflow reversal, the fire is at first ventilated with oxygen-poor air, which will reduce the fire intensity. If the plug of oxygen-poor fumes, travelling back through the fire, is long enough, no permanent reversible will be possible. When decrease of airflow, standstill or reversal take place as early as possible permanent reversible may occur. This can be supported by a low original ventilating pressure acting on the airway, or by a fire developing fast to a high intensity.

Fig. 43 (115) shows the airflow changes caused by such a fast developing fire in the same raise, for which fig. 42 was obtained.

Permanent reversal after a longer fire duration can occur, when the fire is supplied with oxygen from damaged compressed air lines or from other airways, joining the return airway of the fire. Fig. 44 a and b (117) compare fires in the same descensionally ventilated raise without (a) and with a fresh air current of 177 ft^3/ min mixed below the fire with the fumes (b).

While in ascensional ventilation airways parallel to the airway at fire are endangered by airflow standstills and reversals, in descensional ventilation the airway at fire itself is endangered most. The decrease in air quantity in the descensionally ventilated airway causes, like the throttling effect in horizontal airways, an increase in the ventilating pressure of parallel airways. This is clearly visible from the recorded ventilating pressures for parallel airways in fig. 42 and 43.

The means to stabilize the airflow in the descensionally ventilated airway is to increase the ventilating pressure acting on this airway. This can be done by increasing the fan pressure and by throttling parallel airways. By applying the latter measure

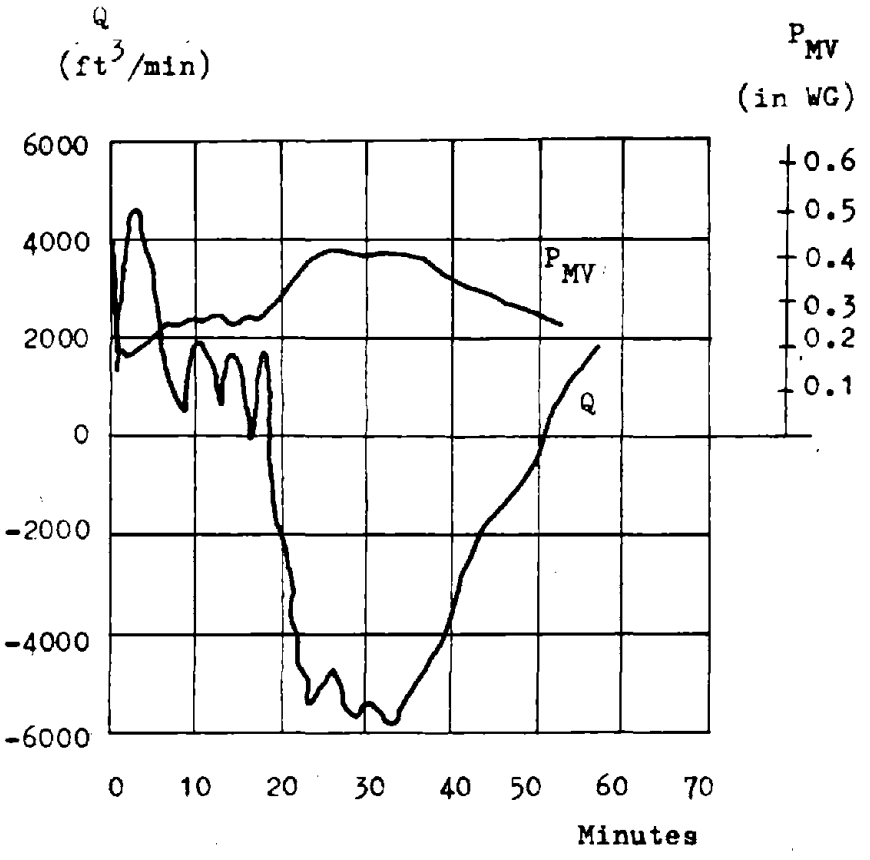

Fig. 43. Fast Developing Fire in a Descensionally Ventilated Raise (115)

Fig. 44a

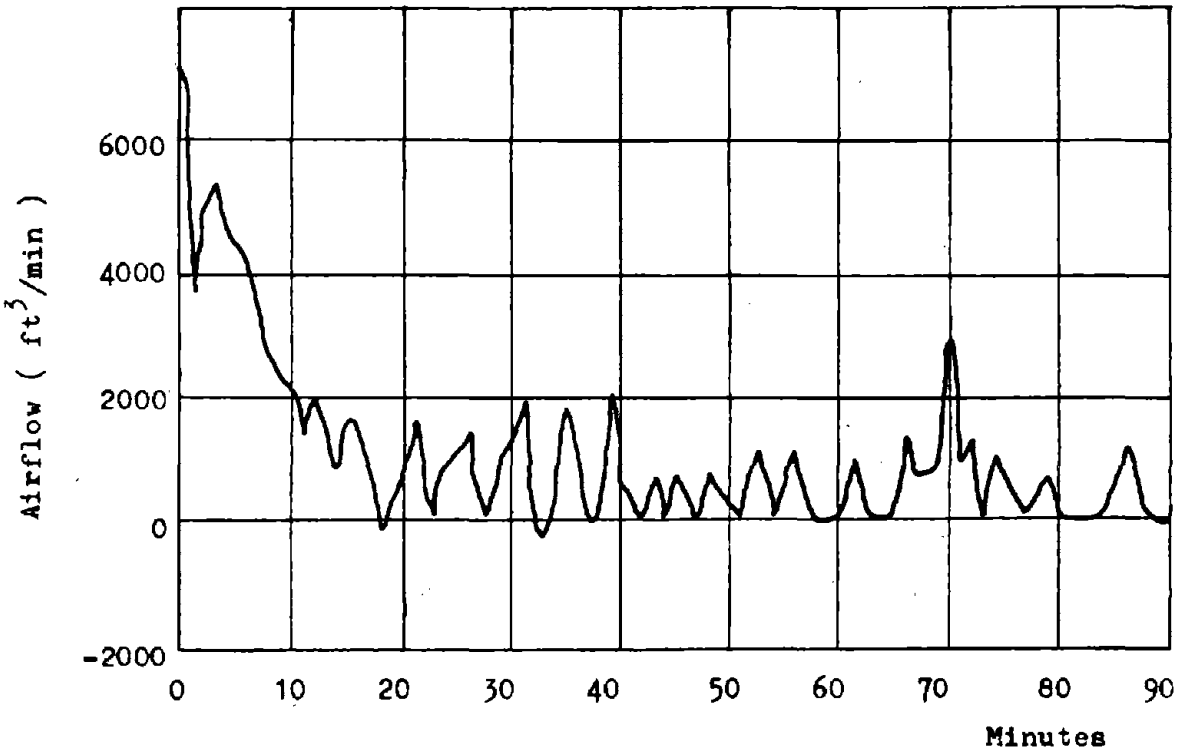

Fig. 44b

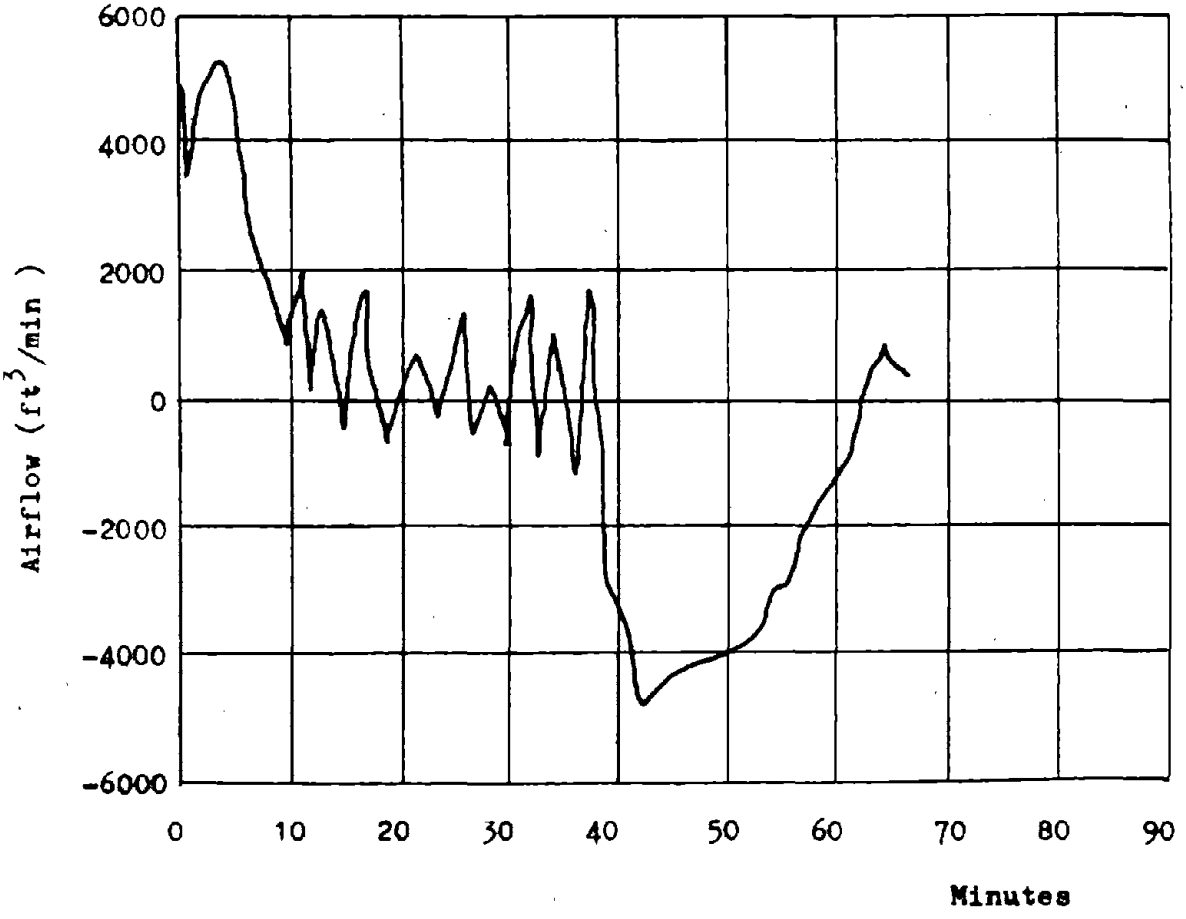

Fig. 44. Airflow in a Descensionally Ventilated Raise at Fire without (a) and with (b) Fresh Air Mixed with the Fumes (117)

one has to make sure that in gassy mines no explosive mixtures can result from the airflow reductions.

Since the throttling effect as well as the natural draft have a tendency to reduce the airflow, fires in descensionally ventilated airways usually don't reach the intensity of fires in ascensional ventilation and propagate with a considerably slower velocity. Schmidt (117) emphasizes as the result of his 117 large scale tests that the combined throttling and natural draft effects of these fires in the past have been quite frequently overestimated. He recommends (118) that German ventilation engineers should replace the formula

$$\Delta p_N = 0.0018 \frac{\Delta Z}{100} (T_m - T_a) \quad \text{(in WG)}$$

so far used in emergency plans for the combined throttling and natural draft effect by

$$\Delta p_N = 0.00133 \frac{\Delta Z}{100} (T_m - T_a)$$

D) Examples of airflow reversals

For each of the three possibilities discussed above, fires in horizontal, ascensionally and descensionally ventilated airways, one example of an airflow reversal in a mine fire is given below.

Horizontal airway

At the mine Dukla (CSR) two parallel ventilation splits were connected by a diagonal airway. The throttling effect of a fire (July 7, 1961) in one of the splits reversed the airflow in the diagonal airway and allowedfumes to flow into the intake airways of the other split. As a result 108 miners were killed (35, 125).

Ascensionally ventilated airway

Fig. 45 shows part of the ventilation plan of the mine Roche-la-Moliere as it existed on June 30, 1928, when a fire in the raise 3 - 4 close to junction 4 occurred. The developed natural draft at first caused an airflow reversal (broken arrows) in airways 8 - 7 - 5 - 2, 7 - 6 - 3 and 6 - 5. Here, 48 miners were killed. Later, after the fire had moved down the raise away from 4 towards 3, the airflow normalized again in these airways but a short reversal in airway 4 - 1 occurred (6,35).

Descensionally ventilated airway

Woropajew (146) describes a fire in a Russian coal mine, working a dipping seam. The fire started in the descensionally ventilated raise 2 - 3 - 4 at point 3 (fig. 46). The natural draft reversed the airflow in the raise and finally became so strong that even in the intake airway 1 - 2 a reversal occurred.

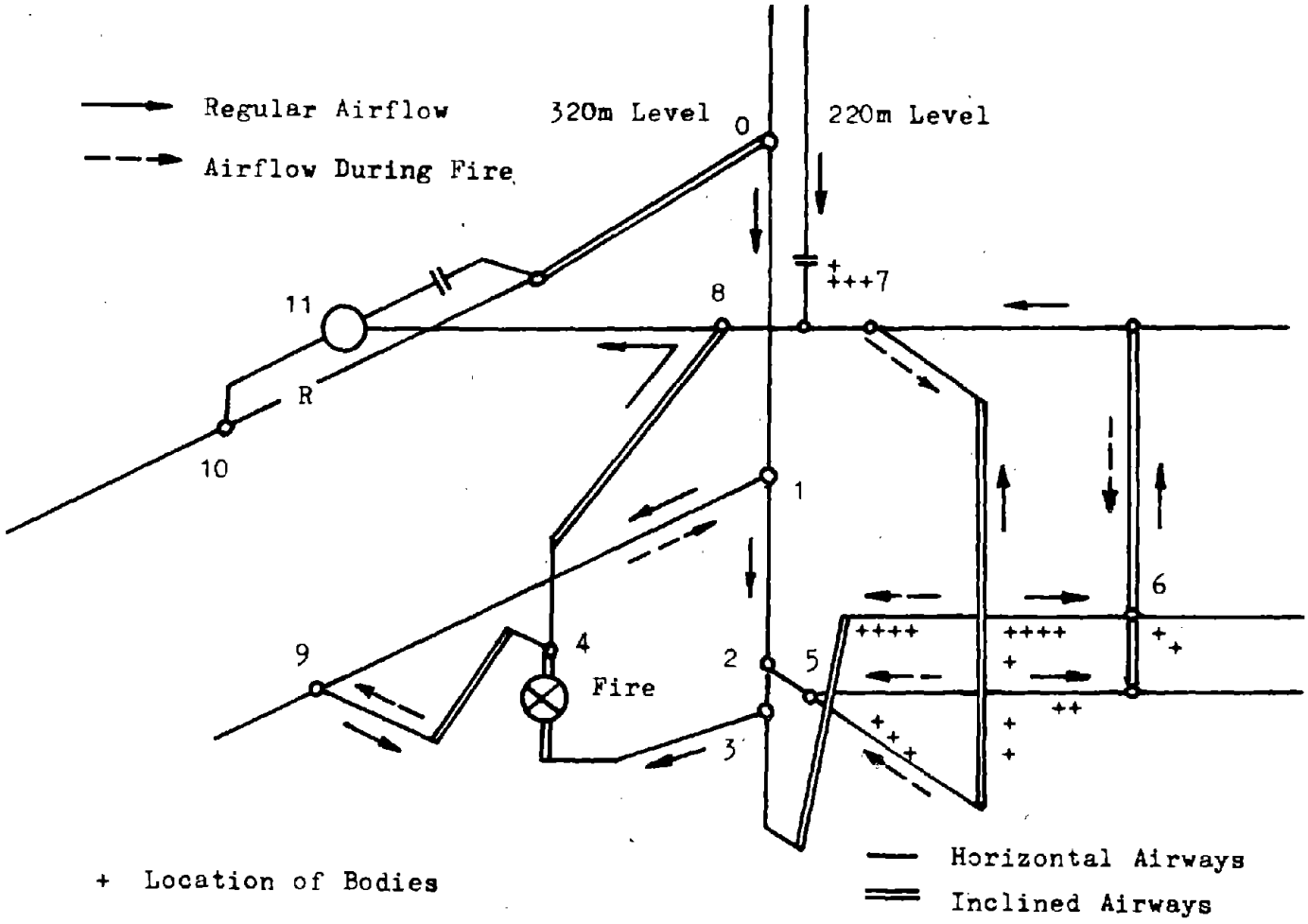

Fig. 45. Fire at the Mine Roche-la-Molière (35)

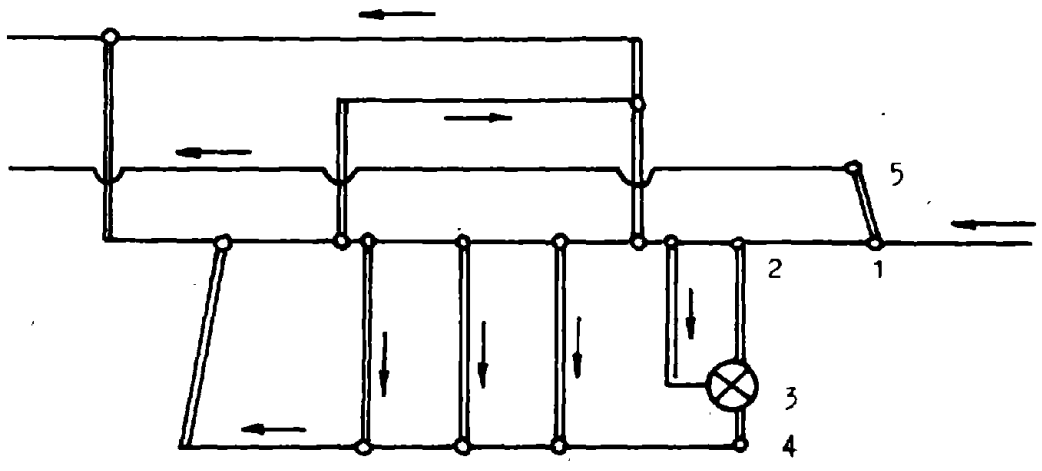

Fig. 46. Example for a Fire in a Descensionally Ventilated Airway Given by Woropajew (146)

E) Suitable ventilation plans

Suitable ventilation plans are of great help for every type of ventilation planning and, therefore, for the prediction of ventilation disturbances caused by mine fires, too. They should contain the main features of the ventilation system without confusing details and the significant ventilation data. The former should comprise the airways, location of fans, ventilation doors, regulators, seals and dams, ventilation curtains and ducts, crossings, explosion barriers, production workings, trolley and Diesel haulage roads. The latter should include direction and magnitude of air currents, concentrations of hazardous gases, measuring stations, elevations of airways, fan heads or pressures and mine ventilating heads or pressures for the individual airways. If it is found too difficult to enter these data into the plans, they should be kept in up to date reference files, which can be used in conjunction with the ventilation plans. That such plans are possible is proved by the fact that they are required by law (35, 92) in several countries.

For the planning of fire fighting measures additional plans should be provided, which contain information on the water and compressed air pipeline systems, stored fire fighting and survival equipment, telephone lines etc. They should be plotted in the same scale and perspective as the ventilation plans to ease simultaneous use.

a) Plans in use

The ventilation plans actually used vary widely. The simplest type is based on plan maps, which in many cases suffice, especially when all mine workings are more or less situated in one plane.

For more complex layouts of openings, as results from mining more than one coal seam or ore deposits with a larger vertical extension, plan maps become too confusing and perspective plans are preferred. The type of projection, if not prescribed by law, is usually a compromise between clarity of the map and the ease with which horizontal and vertical distances can be read from the map.

Occasionally, but not too frequently, models are used as a three dimensional image of a ventilation system. The Dutch coal mines favored these, built from wires of different colors to indicate the function of airways. The work involved in changing the models and the prohibitive costs of keeping records for certain time periods and providing copies required that the models be used only in addition to other ventilation plans.

Quite frequently simplified ventilation plans are derived which show only the more important airways of a ventilation system. This

is especially the case when ventilation network calculation are performed and one tries to keep the number of airways going into the calculation as small as possible. Another reason is to gain a better understanding of the mutual interaction of the airways comprising the system. Several types of such simplified plans are in use.

When ventilation network calculations were still mainly performed manually, with many ventilation engineers it became popular to represent ventilation plans in an abstract form resembling electric wiring diagrams. In these plans the configuration of the network is more conspicuous than in map plans or perspective drawings. Airways in series or parallel can be grouped together and replaced by equivalent resistors. In controlled splitting the number and location of the necessary regulators to enforce the wanted airflow distribution is more easily found. In natural splitting the diagonal airways, which cause difficulties in network calculations, are more easily detected.

An even clearer picture of the network configuration is obtained when in schematic ventilation plans the crossing of airways or the overlapping of loops are as far as possible avoided. Since plans of this type are most widely used in Poland (where they are required by law for every mine) they are usually known by their Polish name as "canonical plans" (18). They are however, gaining increasing popularity in other countries as the basis of emergency plans, too, since they are especially suited to detect possible instabilities in ventilation systems.

As an example fig. 47 shows the ventilation plan from fig. 45 converted into a canonical plan (35). The natural draft developed during the first stage of the fire in airway 4 - 8 and during the second stage in airway 3 - 4 is indicated by the pressure sources a and b. Both pressure sources have a tendency to circulate the air in those loops, of which they are a part and the stronger this tendency, the closer the loops are to the fire. The larger pressure source a succeeds in circulating the air in the loops 4-8-7-6-3-4, 4-8-7-6-5-2-3-4, and 4-8-7-5-2-3-4. The weaker source b succeeds only in the loop 3-4-9-1-2-3.

To judge the influence of several pressure sources in a ventilation network on the stability of the airflow in selected airways qualitatively and, as far as possible, quantitatively the Polish engineer Budryk (35) suggested the use of a so called " closed schematic plan" nowadays more frequently called "Budryk plan". Characteristic for this plan is that the airway, whose stability is to be judged, forms the boundary between those parts of the network which are dominated by one of the pressure sources. Although quantitative predictions about the stability of an airway are only possible for comparatively simple networks, the Budryk plan allows valuable conclusions

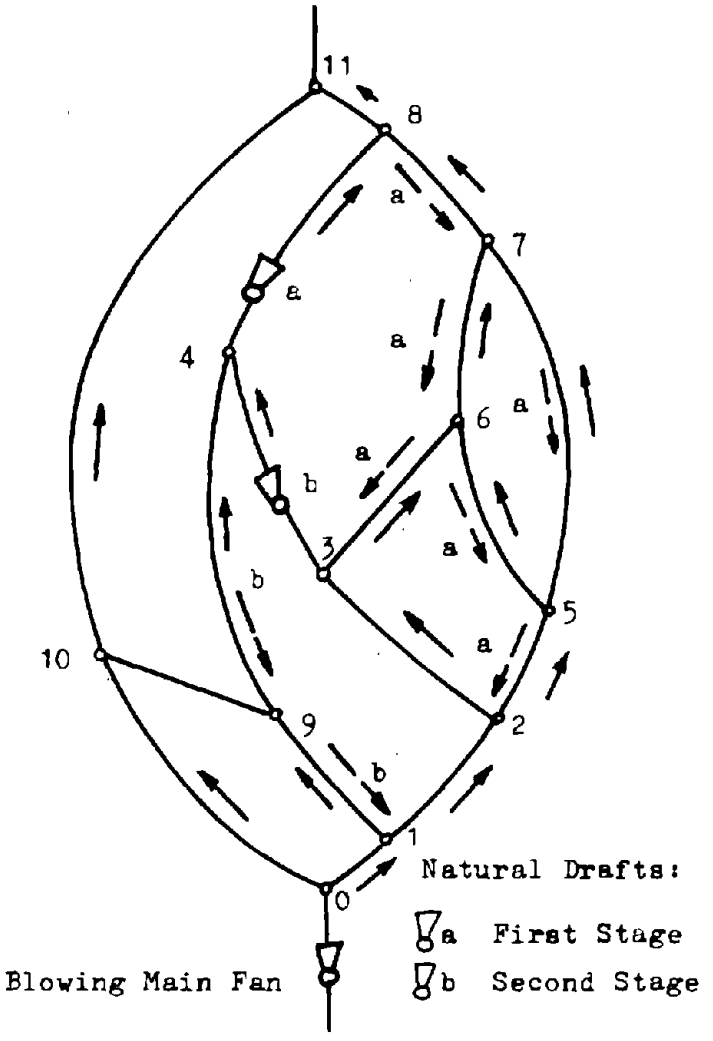

Fig. 47. Canonical Plan of Ventilation Plan Shown in Fig. 45 (35)

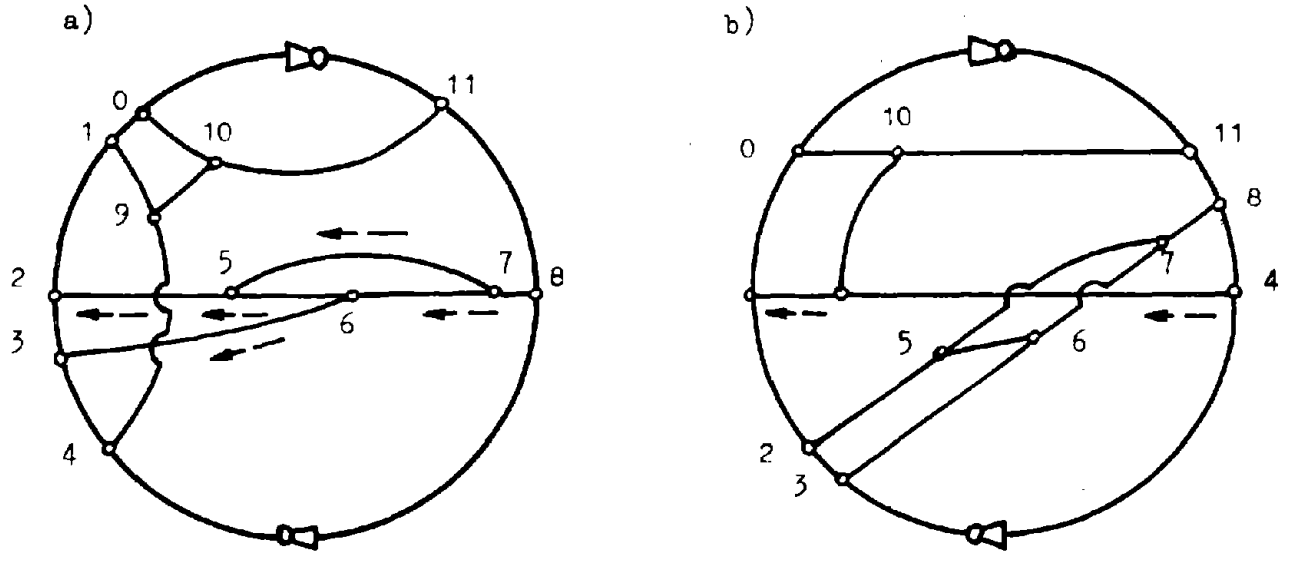

Fig. 48. Budryk Plan of Ventilation Plan from Fig. 45 (35)

as how to increase the stability of this airway. The name "closed plan" originates from the fact that every air current is thought to be short circuited through the atmosphere (which in fact it is).

Every airway or group of airways, whose stability must be investigated and every new location of a pressure source leads theoretically to a different Budryk plan. In the practice of fire emergency plans ventilation engineers usually limit the airways to escape routes or stability boundaries, beyond which no airflow reversal should occur and the location of the pressure sources to airways where natural drafts can be created by fires. Even if no actual Budryk plans have been plotted, familiarity with the principles on which they are based can be of considerable help in selecting the right measures to stabilize the airflow in critical airways. A special chapter of this report (chapter VI-B) will therefore bring a more detailed discussion of the Budryk plans and their use.

As examples, fig. 48 a and b show the ventilation plan from fig. 45 converted into two Budryk plans with the natural draft of the fire developed in airway 4-8 and airway 3-4.

b) Definition of ventilating heads and pressures

It has been mentioned that the data contained in ventilation plans should include mine ventilating heads or pressures. These are differences in the energy content of the air between two points of the network or, when the two points are the begin and end of an airway, changes in the energy content of the air when moving through this airway. Since they indicate the stability and economy of existing airflow as well as the direction of potential airflow, their use has become very popular with ventilation engineers.

According to the above definition of heads and pressures, mine ventilating heads h_{MV} are energy differences per unit weight and mine ventilation pressures p_{MV} per unit volume of air. Being differences in energy contents they can be determined from the energy equation in the following form:

$$v\,dp + dZ + \frac{dV_a^2}{2g} + dh_{MV} = 0$$

$$dp + \gamma\,dZ + \frac{\gamma}{2g}\,dV_a^2 + dp_{MV} = 0$$

A comparison with the energy equation in the form

$$v\,dp + dZ + \frac{dV_a^2}{2g} + dh_L - dh_F = 0 \qquad h_F = \text{fan heads}$$

$$dp + \gamma\,dZ + \frac{\gamma}{2g}\,dV_a^2 + dp_L - dp_F = 0 \qquad p_F = \text{fan pressures}$$

and integration along airways with an exchange of mechanical energy yields

$$h_{MV} = h_L - h_F$$

$$p_{MV} = p_L - p_F$$

Integration along airways without exchange of mechanical energy results in

$$h_{MV} = h_L$$

$$p_{MV} = p_L$$

By applying the above energy equations on a loop one obtain

$$\oint_{airway} \left(v\,dp + dZ + \frac{dV_a^2}{2g} + dh_{MV}\right) + \oint_{restloop} \left(v\,dp + dZ + \frac{dV_a^2}{2g} + dh_L - dh_F\right) =$$

$$\oint_{loop} (v\,dp) + h_{MV} + \oint_{restloop} (dh_L - dh_F) = 0$$

or, with $h_N = -\oint v\,dp$ = natural head in the loop

$\Sigma h_L = \oint dh_L$ = sum of headlosses in the airways of the restloop

$\Sigma h_F = \oint dh_F$ = sum of fanheads in restloop

$$h_{MV} = \Sigma h_F + h_N - \Sigma h_L$$

which is actually Kirchhoff's second rule or the mesh equation of ventilation networks. Similarly one obtains

$$p_{MV} = \Sigma p_F + p_N - \Sigma p_L$$

To avoid an unnecessary lengthy discussion only the problems associated with the mine ventilating pressures will be discussed. A similar discussion of the mine ventilating heads would be completely analogous.

Fig. 49 shows how the ventilating pressure between two points, connected by two parallel airways, can be calculated by using the above derived formulas. It shows, furthermore, that one can definitely determine the ventilating pressure between any two points, when the locations of pressure sources and pressure losses are known. The result is not influenced by the path used between the two points.

It is therefore possible to calculate for all points of the network their ventilating pressure against a common reference point

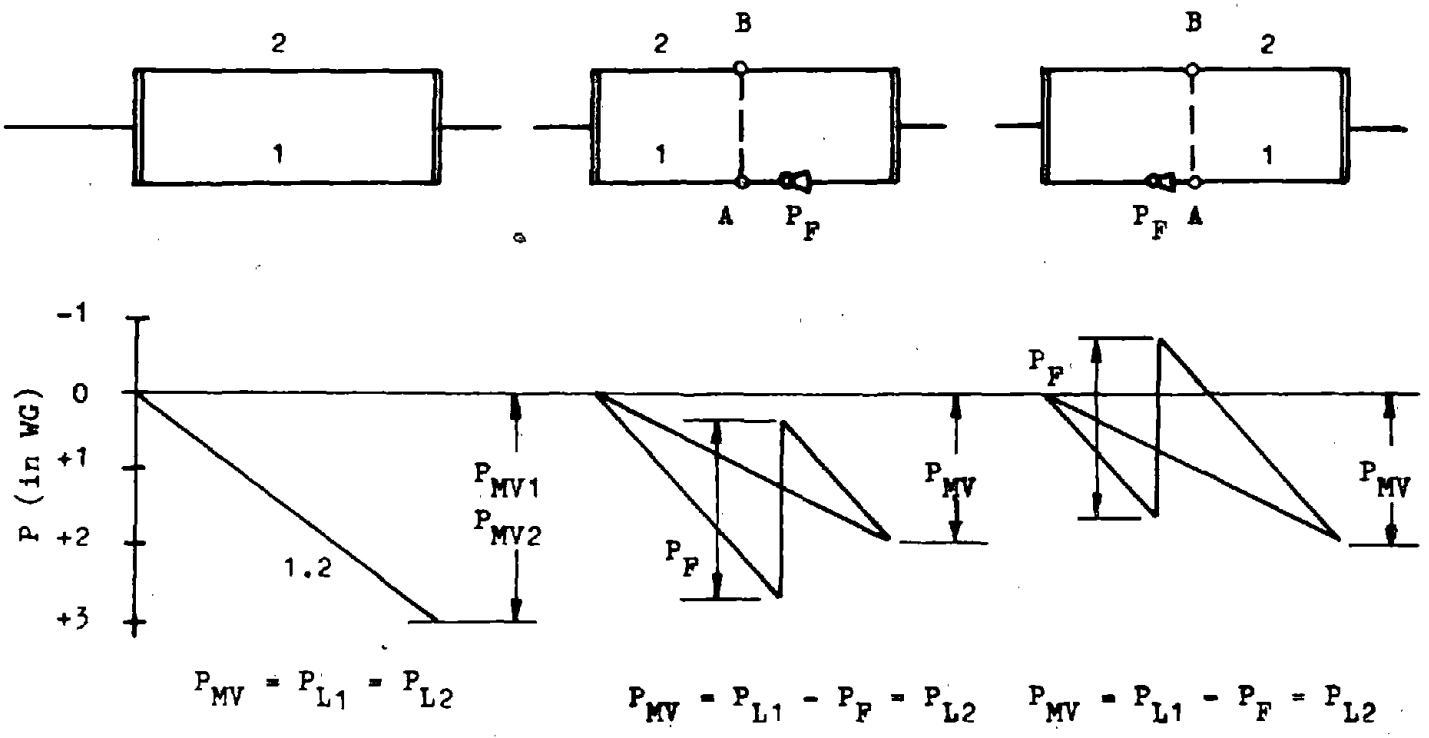

Fig. 49. Ventilating Pressures of Two Parallel Airways

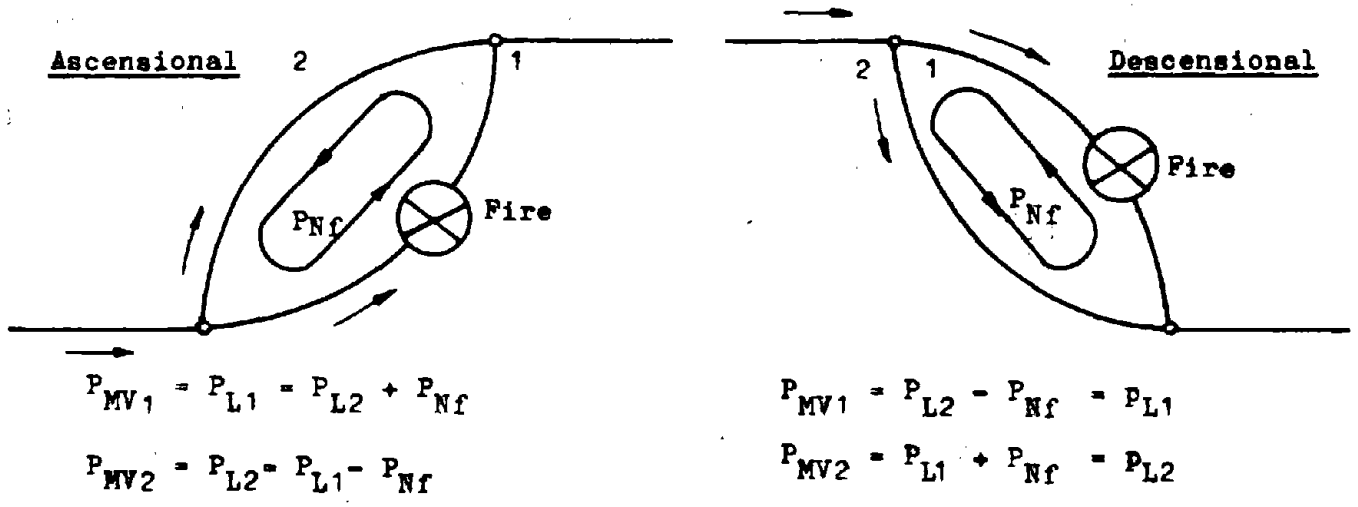

Fig. 50. Ventilating Pressures of Two Inclined Parallel Airways with Natural Drafts

and in this way to obtain a kind of ventilating potential P for them. If in fig. 49 the begin of airways 1 and 2 are made the reference point, the plotted pressure curves would at the same time indicate these potentials.

One of the most valuable advantages the use of ventilating potentials offers is the prediction of airflow directions in planned airways or suspected leakage paths. In fig. 49 it is quite obvious that in a connection A-B the air would flow from B to A with the booster fan at the end and from A to B with the booster fan at the begin of airway 1.

Things become more complicated if natural drafts are developed in the loops of a network. Fig. 50 shows two parallel airways, ventilated ascensionally and descensionally. Due to a fire a natural ventilation pressure is generated in the loop. The calculation of p_{MV} shows that the ventilating pressures for the two parallel ^{MV}airways are no longer the same. This is not surprising since the energy equation defining p_{MV} contains the path function $\int \gamma dZ$. If a ventilation network ^{MV}contains loops with natural ventilation pressure it is therefore theoretically impossible to define an unambiguous potential for most of its points.

Ventilation engineers frequently overcome this difficulty in their practical work by considering the natural drafts as imaginary fans. If the fans are arranged in such a way that Kirchhoff's second rule or the mesh equations are satisfied, network calculations will deliver the correct answers. As discussed in chapter VI-D.b.3, however, there exists a great number of possibilities to imitate the natural draft with fans arranged in different airways and still to satisfy the mesh equations. Every different fan arrangement delivers different ventilating pressures.

Fig. 51 shows as an example the two parallel airways ascensionally and descensionally ventilated within a simple network. The ordinary natural ventilation for the loops going through the shafts and either of the two parallel airways is p_{No}. If a fire develops in the loop formed by the two parallel airways the natural draft p_{Nf}, this can be imitated by an imaginary fan in either of the two airways 1 or 2. A network calculation would give the same air quantity distribution for both arrangements. Different ventilating pressures are, however, obtained for airways 1 and 2 and these ventilating pressures are the same as those derived in fig. 50.

c) Representation of ventilating heads and pressures in ventilation plans

The fact that, whenever natural drafts exist in a ventilation system, mine ventilating heads and pressures and ventilating potentials are path functions, leads to difficulties in their representation in ventilation plans. The most frequent method used by ventilation engineers to avoid these difficulties

Ascensional

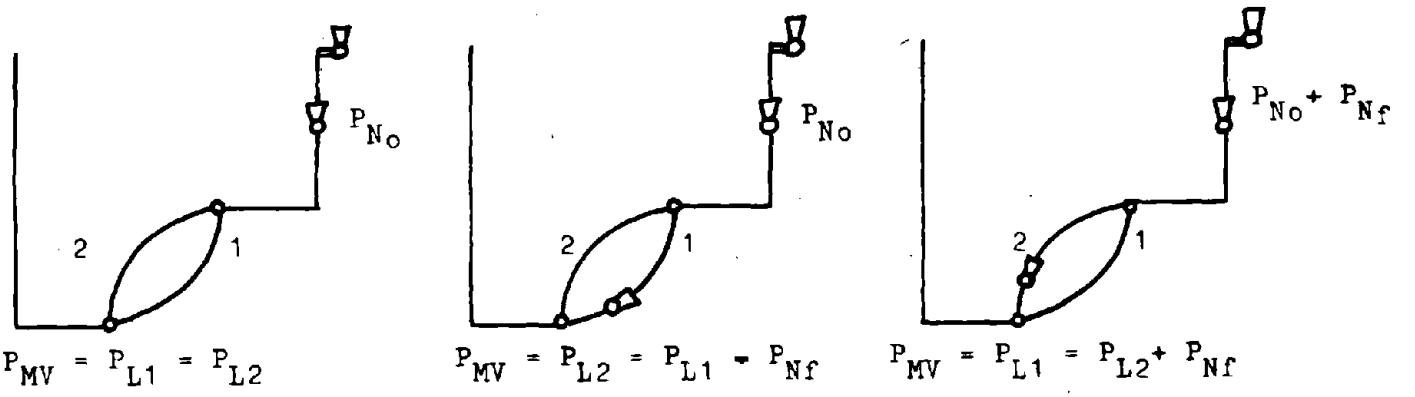

Descensional

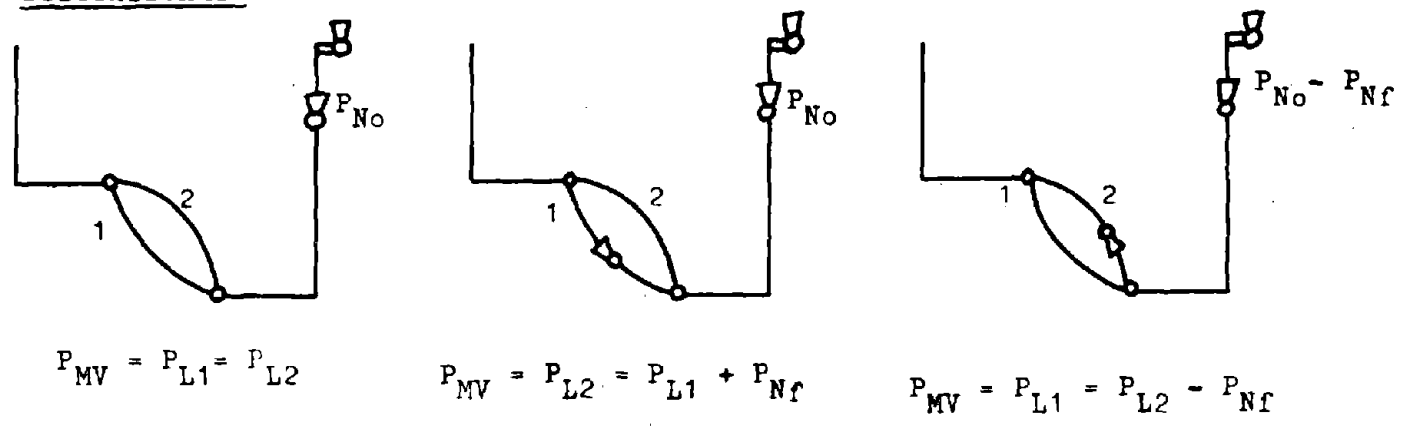

Fig. 51. Possibilities for the Simulation of Natural Drafts

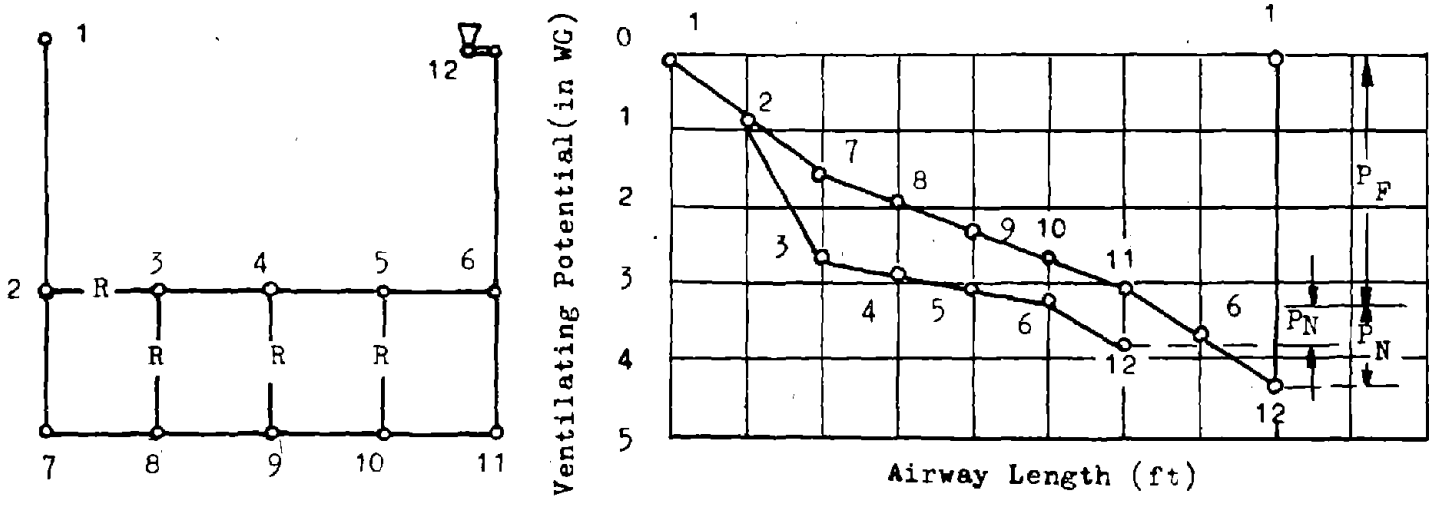

Fig. 52. Ventilating Potential Plotted over Airway Length

is to calculate ventilating potentials separately for individual loops, which run from the intake airways through the mine to the return airways. They are obtained by summing up the head or pressure losses in the airways of the loops and are usually plotted over the airway length. Fig. 52 shows a simple example. Since different loops can have different natural drafts one must be careful in using these potentials for the prediction of airflow directions in planned connections between two points in different loops, at least as long as the difference in potential is not larger than the difference in the natural drafts of the two loops.

Another popular method is to use equivalent resistances for the airways in loops with natural drafts, which give the same airflow distribution as the genuine resistances and the draft combined. The natural drafts can then be neglected and a definite potential can be assigned to every junction of the network, which is then usually entered in to the ventilation plan. However, no generally recognized method as how to determine the equivalent resistances exists. Usually a sequence of network calculations is performed and the airway resistances are, by a trial and error method, manually altered until the desired flow distribution is achieved.

Since the pitfalls of the last method are obvious, many ventilation engineers apply it only to small natural drafts. In loops with larger natural drafts they still assign a potential to every junction by adding up the head or pressure losses, but at the junction where the loops are closed and for which two different potentials would result, only the potential obtained along the more important airways is indicated, together with the natural draft in the loop. Figure 53 shows a simplified example for this procedure.

The pressure potentials have been calculated by adding up the pressure losses from the shaft collar of the intake shaft along the upper and lower level. The natural draft in the internal loop formed by the two levels and the lower portions of the two shafts is 0.5 in.WG. For the potential of upper level landing of the upcast shaft, consequently, two values, 0.5 in.WG. apart, could be obtained. Only 3.65 in.WG, resulting from the path along the lower level are, however, entered but the natural draft of 0.5 in.WG is marked, too, at the upper level. This is done to draw the attention of the plan user to the fact that the potential of the upper level might have been determined to be up to 0.5 in. WG higher, if a path going along the lower level had been chosen for the calculation.

Polish ventilation engineers frequently design their canonical plans in such a way that the location of airway junctions in the plan indicate their potential. Figure 54 shows as an example the canonical plan from figure 47 plotted against a ventilating potential scale (20,35). It is assumed that this type of plan will shortly be required by law in Poland.

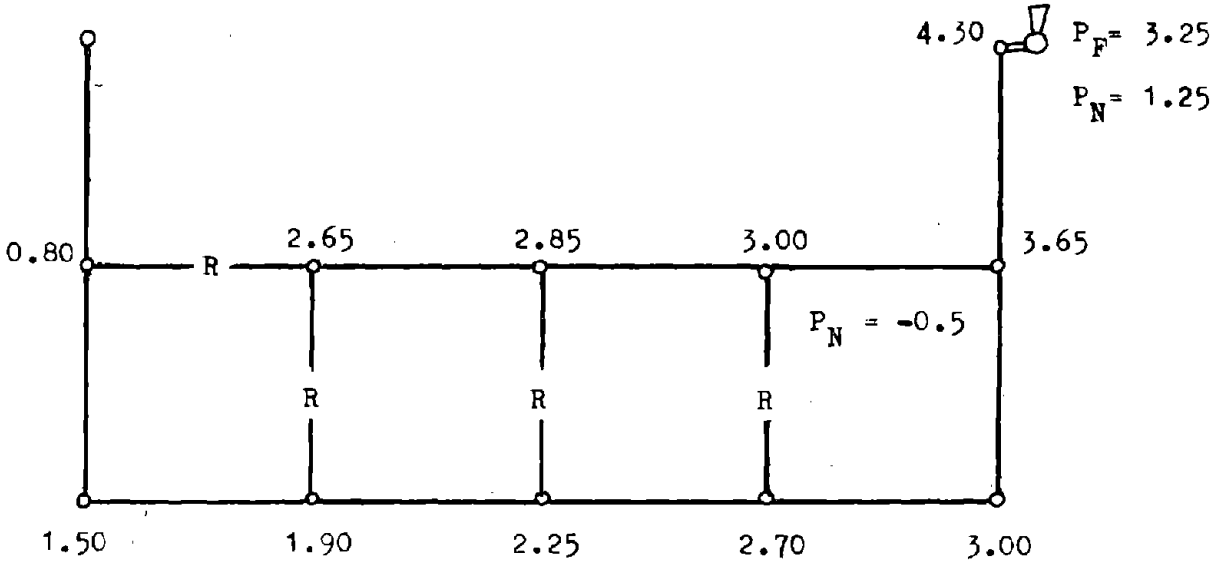

Fig. 53. Ventilation Potentials Entered in Ventilation Plan

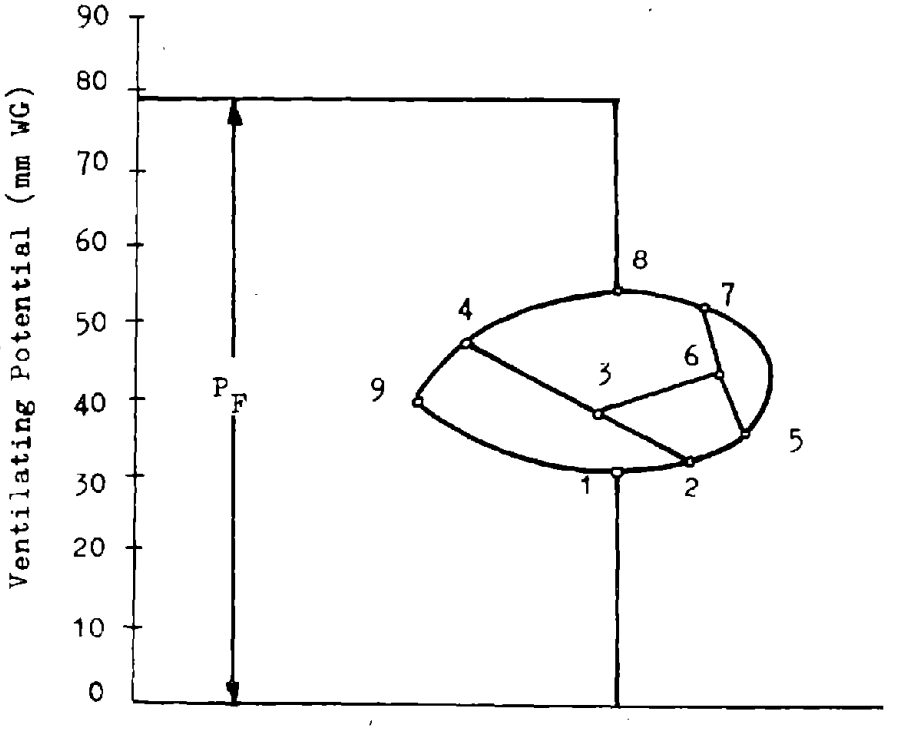

Fig. 54. Canonical Plan of Fig. 47 Combined with a Scale of Ventilating Potentials (35)

VI. Quantitative Predictions of Ventilation Disturbances Caused by Fires

A) Numerical solutions without computer aid

If the natural and throttling effects are known or can be calculated from other data, the influence of a fire on the airflow distribution in a ventilation system can be determined in a ventilation network calculation. If sufficient data on the network as the basis of the network calculation and a computer for the execution of the calculation are available, this is no great effort.

Where this is not the case and the calculations have to be done manually, ventilation engineers in investigating the influence of a fire must quite frequently to be content with abridged and simplified network calculations for the immediate vicinity of the fire. Since it is usually here that the fire has the greatest influence on the ventilation, these calculations can be very useful. The accuracy expected from the results determines the extent of permissible simplifications. To keep the manual work in tolerable limits, ventilation engineers, moreover, limit the network calculations frequently to the investigation of especially critical states, like the criteria for airflow standstills and reversals.

Network calculations for the vicinity of the fire are usually based on pressures, since the specific weight of the air in a limited area, except for the changes caused by the fire itself, remains fairly constant. As pointed out above, it makes no difference in principle if ventilation calculations are based on energies per unit weight (heads) or energies per unit volume (pressures) and ventilation engineers traditionally prefer the pressure approach.

To demonstrate the capacity as well as the work requirement, of conventional analytical network calculations, this method shall be applied to several simple examples first. A literature evaluation follows. It will then be shown that even with manual calculations some very valuable numerical solutions and rules for the airflow behavior in more complicated networks can be obtained.

a) Conventional analytical method

Conventional analytical methods are easy to apply in network calculations when the network contains airways in series and parallel only. But even here the amount of work necessary can be a serious handicap. It usually becomes unsurmountable or a direct analytical solution is altogether impossible, when diagonal airways occur in the network.

The network chosen here as an example for the vicinity of

the fire comprises one airway in parallel and two in series with the airway at fire. It is assumed that the resistances of all airways, the throttling and natural draft effects of the fire and the ventilating pressures acting on these 4 airways are known (fig. 55a).

To reduce the number of equations describing the network the airways 3a and 3b are combined to airway 3 and the throttling and natural draft effect to the pressure effect of the fire p_{Nf} (fig. 55b). With the indicated airflow directions the 3 resistance equations are

$p_{L1} = R_1 Q_1^2$ (equ. 6.1); $p_{L2} = R_2 Q_2^2$ (equ. 6.2);

$p_{L3} = R_3 Q_3^2$ (equ. 6.3)

Under the assumption that the air, after leaving the airway at fire has again assumed its original volume, the junction equations are

$Q_1 + Q_2 = Q_3$ (equ. 6.4); $Q_3 = Q_{total}$ (equ. 6.5)

The two mesh equation are

$p_{L1} - p_{Nf} = p_{L2}$ (equ. 6.6); $p_{L2} + p_{L3} = p_{MV}$ (equ. 6.7)

Combining 6.2 and 6.4 yields

$$p_{L2} = R_2 (Q_3 - Q_1)^2 \qquad \text{equ. 6.8}$$

Adding 6.6 and 6.7 and combining with 6.1 and 6.3 results in

$$Q_3^2 = \frac{p_{MV} + p_{Nf}}{R_3} - \frac{R_1}{R_3} Q_1^2 \qquad \text{equ. 6.9}$$

combining 6.8, 6.6 and 6.1 in

$p_{Nf} + R_2(Q_3 - Q_1)^2 = R_1 Q_1^2$ or

$$\frac{p_{Nf}}{R_2} + Q_3^2 - 2 Q_3 Q_1 + Q_1^2 - \frac{R_1}{R_2} Q_1^2 = 0 \qquad \text{equ. 6.10}$$

Substituting 6.9 for Q_3 in 6.10 delivers

$$\frac{p_{Nf}}{R_2} + \frac{p_{MV} + p_{Nf}}{R_3} - \frac{R_1}{R_3} Q_1^2 - 2 Q_1 \sqrt{\frac{p_{MV} + p_{Nf}}{R_3} - \frac{R_1}{R_3} Q_1^2} + Q_1^2 - \frac{R_1}{R_2} Q_1^2 = 0$$

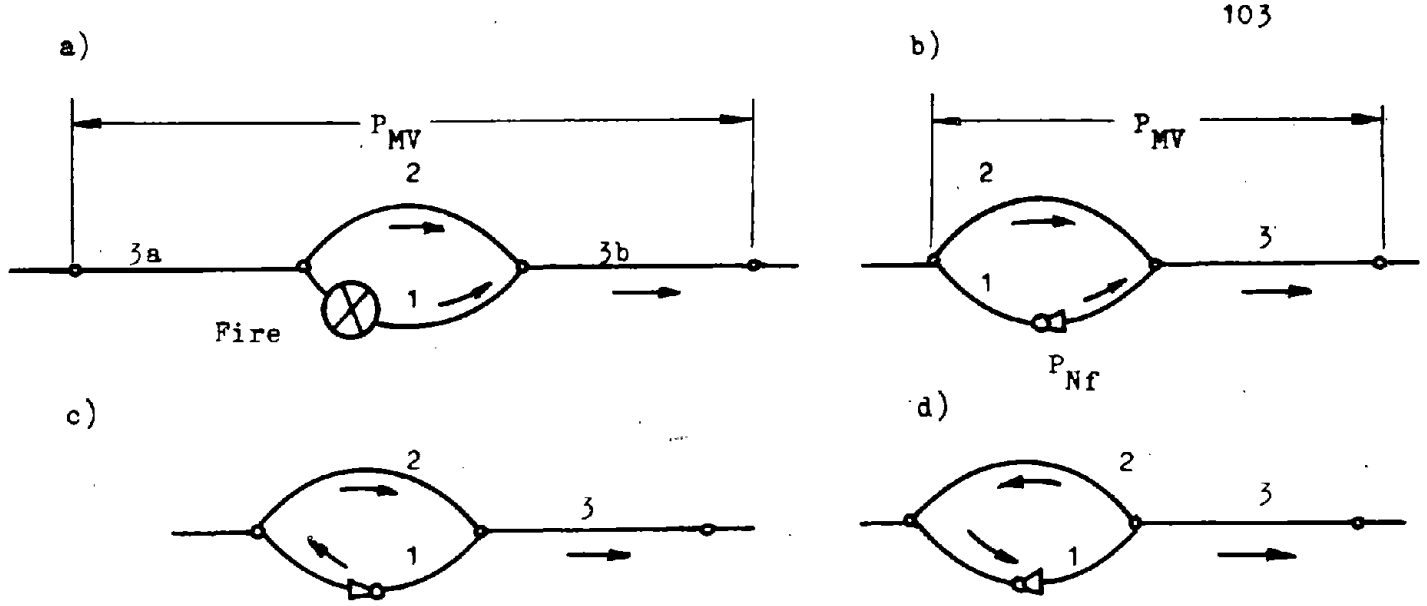

Fig. 55. Simple Network for the Demonstration of Conventional Analytical Methods of Network Calculations

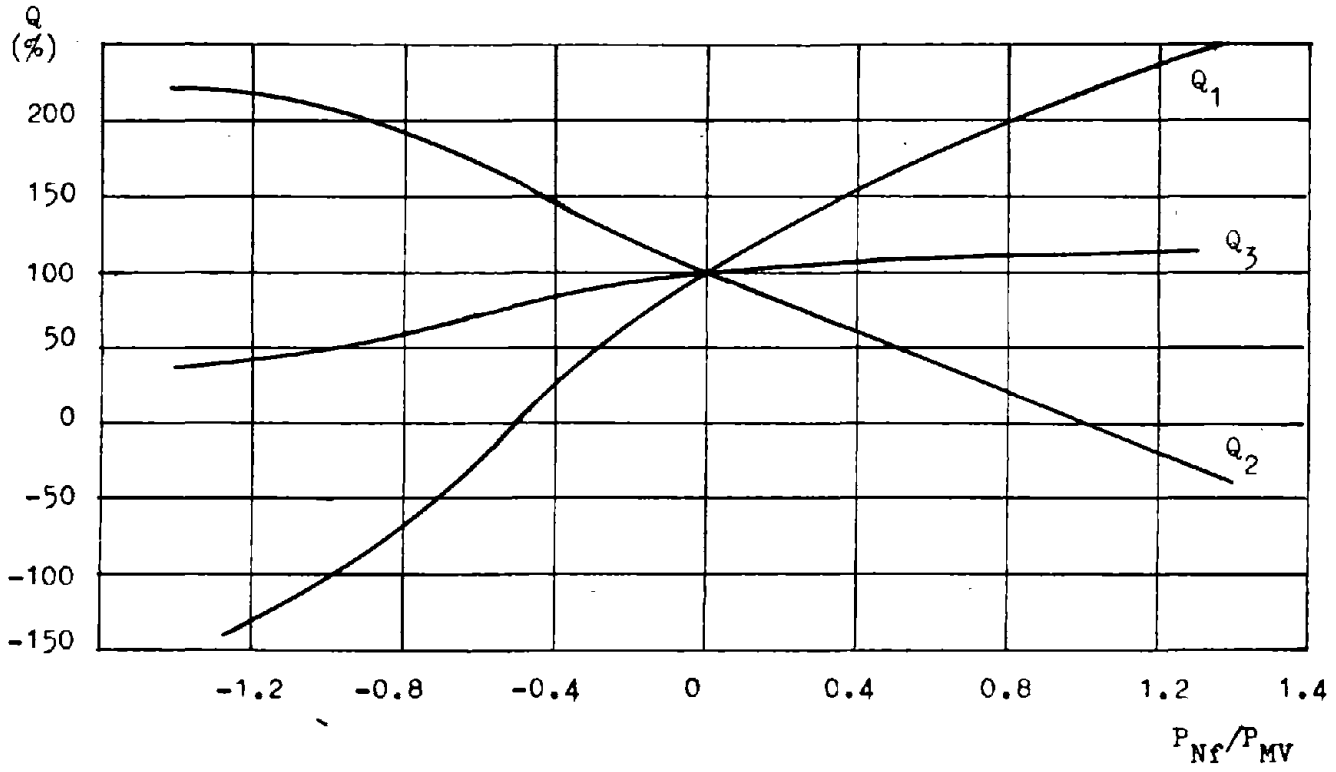

Fig. 56a. Airflow Variation in the Network of Fig. 55 with Variable P_{Nf} ($R_1 = R_2 = R_3$, $P_{MV}/R_3 = 0.2$ (10^5 cfm)^2)

$$\left(1 - \frac{R_1}{R_3} - \frac{R_1}{R_2}\right) Q_1^2 + \left(\frac{p_{MV} + p_{Nf}}{R_3} + \frac{p_{Nf}}{R_2}\right) = 2\sqrt{\frac{p_{MV} + p_{Nf}}{R_3} Q_1^2 - \frac{R_1}{R_3} Q_1^4}$$ equ. 6.11

If the contents of the two parenthesis are called A and B this can be written as

$$A Q_1^2 + B = 2\sqrt{\frac{p_{MV} + p_{Nf}}{R_3} Q_1^2 - \frac{R_1}{R_3} Q_1^4}$$ equ. 6.12

Squaring this equation results in

$$A^2 Q_1^4 + 2 A B Q_1^2 + B^2 = 4\left(\frac{p_{MV} + p_{Nf}}{R_3} Q_1^2 - \frac{R_1}{R_3} Q_1^4\right) \quad \text{or}$$

$$\left(A^2 + 4\frac{R_1}{R_3}\right) Q_1^4 + \left(2 A B - 4\frac{p_{MV} + p_{Nf}}{R_3}\right) Q_1^2 + B^2 = 0$$ equ. 6.13

If again the contents of the two parenthesis are called C and D this can be written as

$$C Q_1^4 + D Q_1^2 + B^2 = 0$$ equ. 6.14

Solved for Q_1 one obtains

$$Q_1 = \sqrt{-\frac{D}{2C} - \sqrt{\frac{D^2}{4C^2} - \frac{B^2}{C}}} = \sqrt{\frac{1}{2C}\left(-D - \sqrt{D^2 - 4CB^2}\right.}$$

equ. 6.15

With Q_1 known Q_3 can be calculated from 6.9 and Q_2 from 6.4.

If a large negative p_{Nf} reverses the airflow in airway 1 (fig. 55c) the junction equation 6.4 changes to $Q_2 - Q_1 = Q_3$ and the mesh equation 6.6 changes to $- p_{L1} - p_{Nf} = p_{L2}$. This changes the factors A and C to

$$A = \left(1 + \frac{R_1}{R_3} + \frac{R_1}{R_2}\right) \quad \text{and} \quad C = \left(A^2 - 4\frac{R_1}{R_3}\right)$$

If a large positive p_{Nf} causes an airflow reversal in airway 2 (fig. 55d) the junction equation 6.4 changes to $Q_1 - Q_2 = Q_3$ and the mesh equations 6.6 and 6.7 change to $p_{L1} - p_{Nf} = - p_{L2}$ and $p_{L3} - p_{L2} = p_{MV}$. This changes the factors A and B to

$$A = \left(\frac{R_1}{R_3} - \frac{R_1}{R_2} - 1\right) \text{ and } B = \left(\frac{p_{Nf}}{R_2} - \frac{p_{MV} - p_{Nf}}{R_3}\right)$$

and equation 6.15 to

$$Q_1 = \sqrt{\frac{1}{2C}\left(-D + \sqrt{D^2 - 4CB^2}\right)}$$

These unfortunate modifications of junction and mesh equations would be avoided if ventilation engineers would in manual network calculations, write the resistance equation as $p_L = R \mid Q \mid Q$ as they do in their digital computer programs.

Figure 56a shows as an example of the derived equations how the airflow distribution changes as a function of the ratio p_{Nf}/p_{MV}. It has been assumed that $R_1 = R_2 = R_3$ and that $p_{MV}/R_3 = 0.2\ (10^5\ ft^3/min)^2$ (e.g. $p_{MV} = 2$ in.WG, $R_3 = 10 * 10^{-10}$ in.WG/$(ft^3/min)^2$.) Figure 56b shows the distribution in the same network when R_1 has been increased to $R_1 = 2R_2 = 2R_3$. One sees that the stability of airway 2 has been improved. The stability of airway 1 has, however, remained the same for negative p_{Nf}. It can be increased by throttling airway 2. Figure 56c shows the results for $R_1 = 0.5\ R_2 = R_3$.

In judging the effectiveness of installing regulators to stabilize the airflow in the neighborhood of the fire one should keep in mind that every regulator will decrease the airflow passing through the mine and, therefore, have a tendency to increase the ventilating pressure p_{MV} acting on this neighborhood. For a given p_{Nf} the ratio p_{Nf}/p_{MV} will consequently decrease.

The pressure p_{Nf} at which airflow standstill occurs can be easily calculated (116). In the case of a positive pressure p_{Nf} (fig. 55b, ascensional ventilation) in airway 1 airflow standstill in airway 2 changes equ. 6.4 to $Q_1 = Q_3$ and equ. 6.6 and 6.7 to $p_{L1} = p_{Nf}$ and $p_{L3} = p_{MV}$. This delivers as condition for airflow standstill in airway 2

$$\frac{p_{Nf}}{p_{MV}} = \frac{p_{L1}}{p_{L_3}} = \frac{R_1\ Q_1^2}{R_3\ Q_3^2} = \frac{R_1}{R_3}$$

For $\frac{p_{Nf}}{p_{MV}} < \frac{R_1}{R_3}$ the original airflow direction will be maintained, for

$\frac{p_{Nf}}{p_{MV}} > \frac{R_1}{R_3}$ reversal will occur. This can be seen from figure 56 a, b, c, where R_1/R_3 has values of 1, 2, 1 and the airflow standstill is shown at $p_{Nf}/p_{MV} = 1, 2, 1$.

In the case of a negative pressure p_{Nf} (fig. 55c, descensional ventilation) airflow standstill in airway 1 changes equation 6.4 to $Q_2 = Q_3$ and equ. 6.6 $p_{L2} = - p_{Nf}$. This delivers as condition for airflow standstill in airway 1

$$\frac{-p_{Nf}}{p_{MV}} = \frac{p_{L2}}{p_{L2} + p_{L3}} = \frac{R_2\ Q_2^2}{R_2\ Q_2^2 + R_3\ Q_3^2} = \frac{R_2}{R_2 + R_3}$$

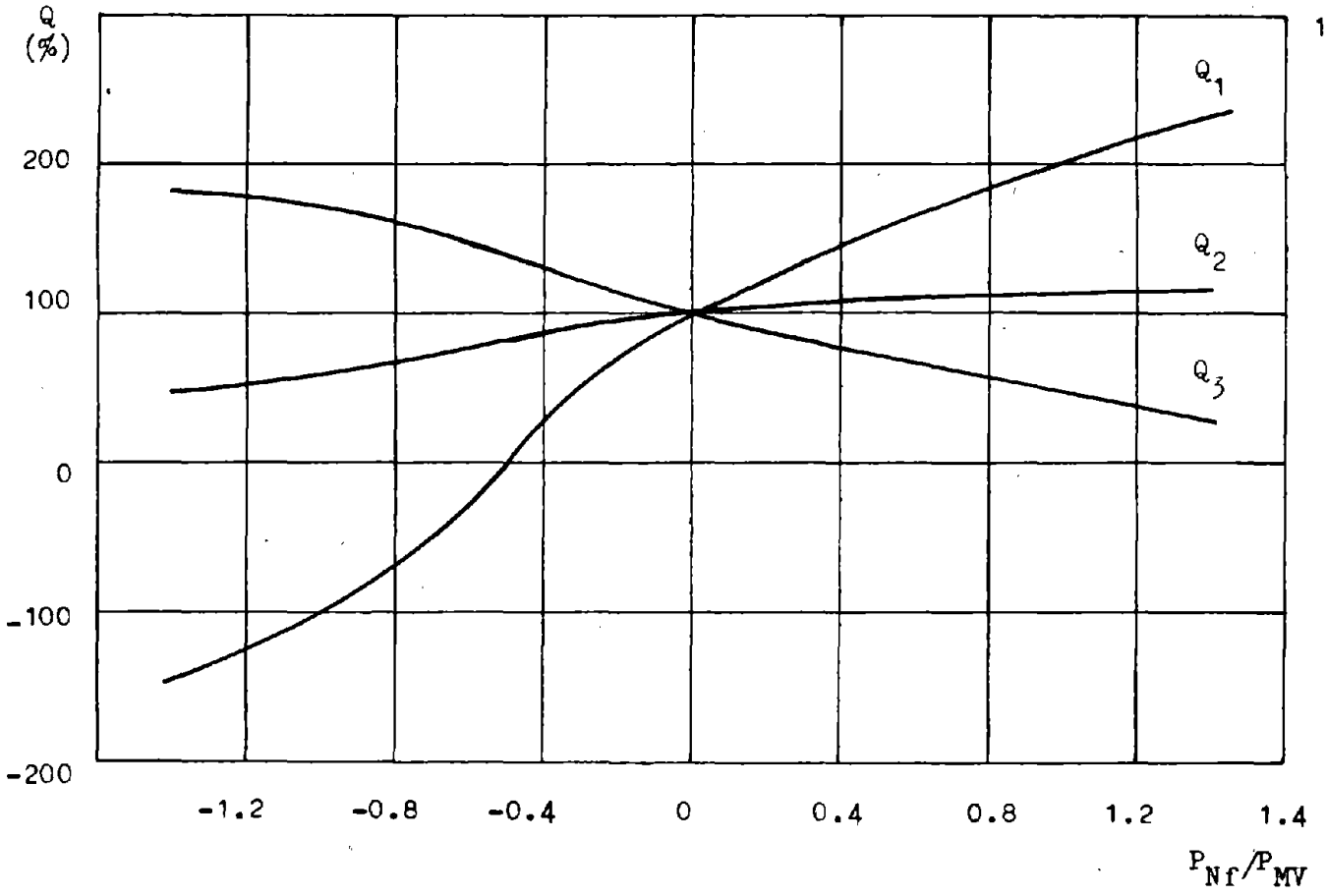

Fig. 56b. Airflow Variation ($R_1 = 2R_2 = 2R_3$, $P_{MV}/R_3 = 0.2\ (10^5 \text{cfm})^2$)

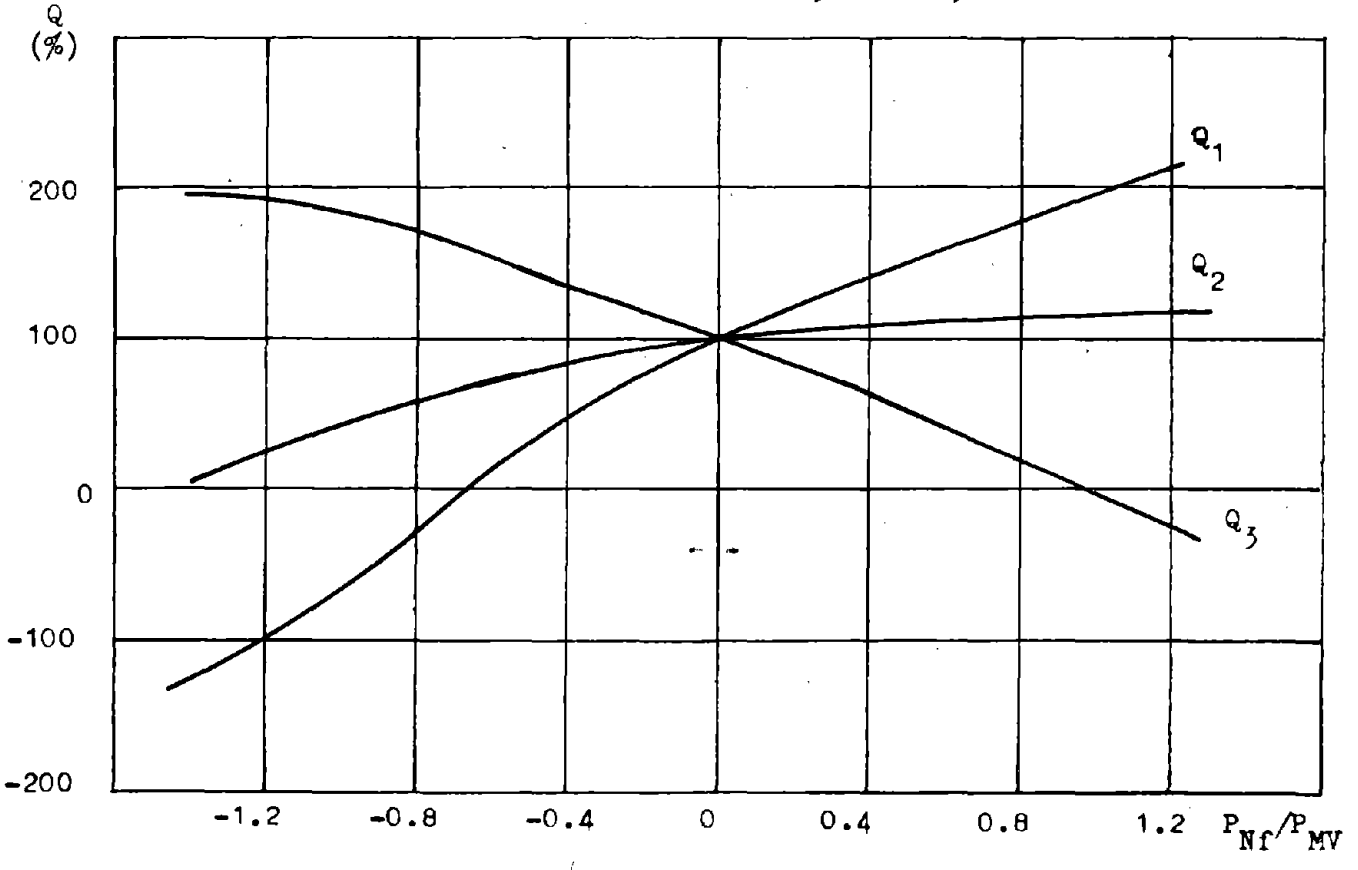

Fig. 56c. Airflow in the Network of Fig. 55 with Variable P_{Nf}

($R_1 = 0.5\ R_2 = R_3$, $P_{MV}/R_3 = 0.2\ (10^5\ \text{cfm})^2$)

as condition for reversal

$$\frac{-p_{Nf}}{p_{MV}} > \frac{R_2}{R_2 + R_3}$$

and as condition for the maintainance of the original airflow direction

$$\frac{-p_{Nf}}{p_{MV}} < \frac{R_2}{R_2 + R_3}$$

This can again be seen from fig. 56 a, b, c where $R_2/(R_2 + R_3)$ has values of 1/2, 1/2 and 2/3 and the airflow standstill in airway 1 is shown at p_{Nf}/p_{MV} = 1/2, 1/2 and 2/3. One sees furthermore that even after the total blocking of airway 2 to $R_2 = \infty$ at $p_{Nf}/p_{MV} = -1$ a standstill cannot be prevented.

Literature Evaluation

Woropajew (146) investigates the stability criteria of networks comprising two parallel airways only. If the fire develops the pressure p_{Nf} and the ventilating pressure acting at the two parallel airways is p_{MV}, the mesh equation for 2 descensionally ventilated airways with a fire in airway 1 (fig. 57a) can be written as

$$p_{MV} = p_{L2} = p_{L1} + p_{Nf}$$

Air standstill in airway 1 is consequently caused by $p_{MV} = p_{Nf}$. If the airways are ascensionally ventilated, Woropajew assumes for the pressure developed by the fire not a positive p_{Nf} in the airway at fire but a negative p_{Nf} in the parallel airway 2 (fig. 57b). This is correct, too, since the direction in which the natural draft tries to circulate the air in the loop of its origin remains the same. He obtains as mesh equations $p_{MV} = p_{L1} = p_{L2} - (-p_{Nf})$ and as conditon for air standstill in airway 2 $p_{MV} = p_{Nf}$.

The other possibility, assuming for airway 1 a positive p_{Nf} would lead to $p_{MV} = p_{L1} - p_{Nf} = p_{L2}$ and to the standstill condition $p_{MV} = 0$. As explained above (fig. 50) there are in both cases different values obtained for p_{MV} and the difference is p_{Nf}.

Osipov and Zadan (95) follow Woropajew's derivations and suggest a method to determine p_{MV} at standstill conditions. They define p_{MV} as the pressure loss in the airway under consideration, which can be measured by the conventional barometric or manometric methods. If the resistance R of the airway is increased, p_{MV} will increase too. If the relation between p_{MV} and R is approximated by the function

$$p_{MV} = \frac{a\ b\ R}{1 + b*R}$$

p_{MV} at standstill conditions would be obtained for $R = \infty$ (fig. 58). Since an actual standstill in an airway can be hazardous, Osipov and Zadan suggest the airway be throttled only to different extents. If p_{MVi} is the ventilating pressure measured at the pertinent resistance R_i of the throttled airway and if n measurements are performed, $p_{MV_{max}}$ at air standstill can be obtained from

$$p_{MV_{max}} = \frac{(\sum R_i^2)\, n - (\sum R_i)^2}{(\sum \frac{R_i^2}{p_{MVi}})\, n - \sum R_i \sum \frac{R_i}{p_{MVi}}}$$

Maas and Sadée (75) derive stability criteria as functions of air temperatures for a small network comprising two shafts and two ascensionally ventilated parallel airways. This can be converted into the network shown in fig. 55b. Natural draft and throttling effect are not combined, however, but treated separately.

If the natural draft is p_{Nf} one obtains for airflow standstill in airway 2

$$\frac{p_{Nf}}{p_{MV}} = \frac{p_{L1}}{p_{L3}}$$

Since airways 1 and 3 carry the same massflow but not the same volume flow, p_{L1} and p_{L3} have to be based on massflow. Darcy's equation

$$p_L = f \frac{L\,P}{4\,A} \frac{\gamma}{2g} V_a^2 = f \frac{L\,P}{8\,g\,A^3} \gamma\, Q^2 = R\, Q^2$$

becomes with $Q = G/\gamma$

$$p_L = f \frac{L\,P}{8\,g\,A^3} \frac{1}{\gamma} G^2$$ and with the average specific weight of the air γ_a and the temperature T_a before the fire started, under the assumption

$$\gamma_a T_a = \gamma T : \quad p_L = f \frac{L\,P}{8\,g\,A^3} \frac{1}{\gamma_a T_a} T\, G^2 = S\, T\, G^2$$

The condition for airflow standstill in airway 2 is

$$p_{MV} = p_{L3} = S_3\, T_3\, G^2 \text{ or } p_{Nf} = p_{L1} = S_1\, T_1\, G^2 \text{ or } \frac{p_{Nf}}{p_{MV}} = \frac{S_1\, T_1}{S_3\, T_3}$$

with T_1 and T_3 being the average temperatures in airways 1 and 3.

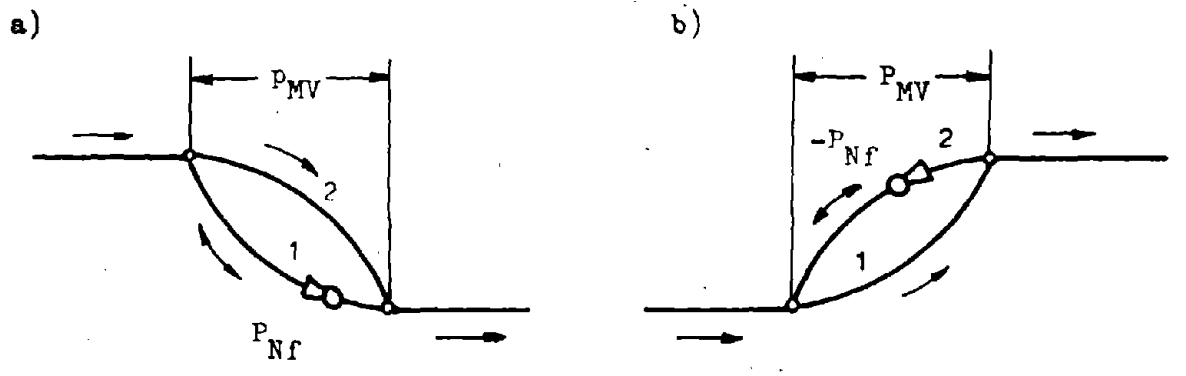

Fig. 57. Woropajew's Stability Criteria (146)

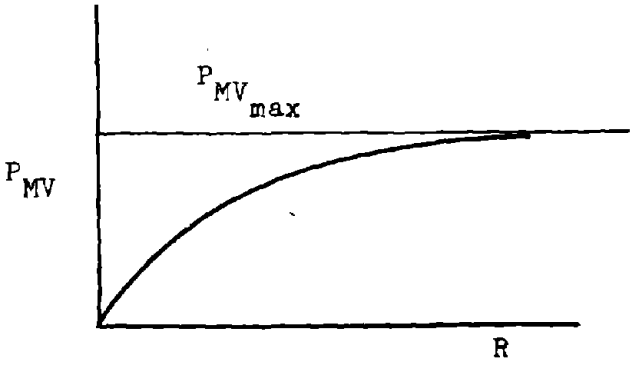

Fig. 58. Variation of P_{MV} with R for an Airway within a Network (95)

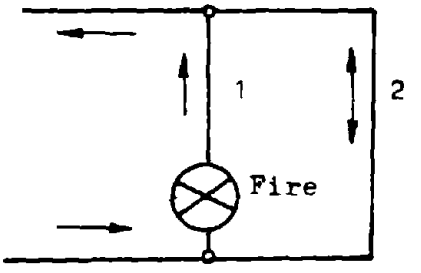

Fig. 59a. Example of a simple Network (35)

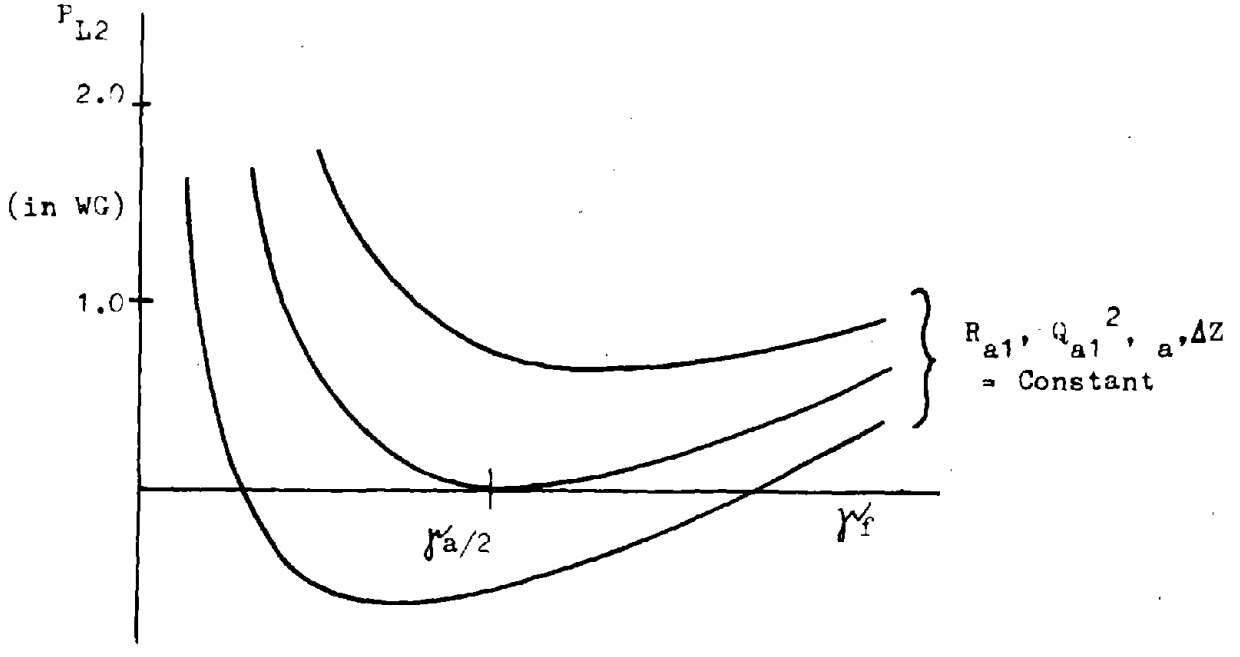

Fig. 59b. Relation between Pressure Loss in Airway 2 of Fig. 59a and the Specific Weight of the Air γ_f in Airway 1 (35)

The natural draft can be determined from

$$p_{Nf} = (\gamma_2 - \gamma_1)\Delta Z = \left(\frac{T_a}{T_2} - \frac{T_a}{T_1}\right)\gamma_a \Delta Z = \left(\frac{T_1 - T_2}{T_1 T_2}\right) T_a \gamma_a \Delta Z$$

Combination of the two last equations yields with the approximation $T_2 = T_3$

$$\frac{T_1 - T_2}{T_1^2} \quad \frac{T_a \gamma_a \Delta Z}{p_{MV}} = \frac{S_1}{S_3}$$

From $d\left(\frac{T_1 - T_2}{T_1^2}\right)/dT_1 = 0$ one obtains that the term $\frac{T_1 - T_2}{T_1^2}$ has a maximum for $T_1 = 2\,T_2$. This means that the fire has its largest influence on the airflow of airway 2 for $T_1 = 2\,T_2$. This value inserted into the above equation results in

$$\frac{\Delta Z}{p_{MV}} = \frac{S_1}{S_3} \quad \frac{4\,T_2}{T_a \gamma_a}$$

With the approximation $T_2 = T_a$ and the assumption of $\gamma_a = 0.075$ lb/ft^3 one obtains

$$\frac{\Delta Z}{p_{MV}} = \frac{4}{0.075} \frac{S_1}{S_3}$$ and, if p_{MV} is measured in in. WG

$$\frac{\Delta Z}{p_{MV}} = \frac{4 * 5.194}{0.075} \frac{S_1}{S_3} = 277 \frac{S_1}{S_3}$$

This means that for $S_1 = S_3$ and a ventilating pressure of 1 in.WG an elevation change of at least 277 ft. for the hot fumes is needed to facilitate an airflow standstill in the parallel airway 2. Or that for an elevation change of 100 ft. and a ventilating pressure of 1 in. WG, S_3 must be 2.77 times larger than S_1.

b) Approximation methods of the ECSC for ascensionally ventilated airways

As part of a larger study, the Committee on Mine Ventilation of the ECSC investigated the airflow in ascensionally ventilated airways parallel to airways at fire (35, appendix 3). Their conclusions are not at all only of theoretical interest, as the first impression may be. They make it possible to find those airways where the possibility of airflow standstills or reversals does not exist and which, therefore, can be exempted from a detailed investigation in emergency plans.

Since the conclusions of the Committee are hard to understand without any reference to how they were obtained, the employed derivations shall be outlined, too.

1) Two airways, fire at beginning of one of them

The assumed ventilation system is shown in fig. 59a.

If kinetic energy changes are neglected the energy equation can be written as

$$dp + \gamma dZ + dp_L = 0$$

If R and Q are described by the values R_a and Q_a they would have for air of the original state before the fire started, the resistance equation is

$$p_L = R\,Q^2 = R_a \left(\frac{\gamma_f}{\gamma_a}\right) Q_a^2 \left(\frac{\gamma_a}{\gamma_f}\right)^2 = R_a\, Q_a^2 \left(\frac{\gamma_a}{\gamma_f}\right)$$

With the assumption of a constant γ in every airway one obtains

$$\Delta p_1 = \gamma_f \Delta Z + R_{a1}\, Q_{a1} \frac{\gamma_a}{\gamma_f}$$

$$\Delta p_2 = \gamma_a \Delta Z + p_{L2}$$

$$p_{L2} = -(\gamma_a - \gamma_f)\Delta Z + R_{a1}\, Q_{a1}^2 \frac{\gamma_a}{\gamma_f}$$

p_{L2} as a function of γ_f is consequently a hyperbola with the parameters

γ_a, ΔZ, $R_{a1}Q_{a1}^2$. From $dp_{L2}/d\gamma_f = 0$ one obtains that p_{L2} has a minimum at

$$\gamma_{f_{min}} = \gamma_a \sqrt{\frac{R_{a1}\, Q_{a1}^2}{\gamma_a\, \Delta Z}}$$

The pertinent p_{L2} would be

$$p_{L2_{min}} = -\gamma_a \Delta Z + 2\gamma_a \Delta Z \sqrt{\frac{R_{a1}\, Q_{a1}^2}{\gamma_a\, \Delta Z}} = -\gamma_a \Delta Z + 2\Delta Z\, \gamma_{f_{min}}$$

For $\gamma_{f_{min}} = 0.5\gamma_a$ one obtains $p_{L2} = 0$ (fig. 59b). This means that the hyperbola, which has its minimum at $\gamma_{f_{min}} = 0.5\gamma_a$ touches with its minimum the abscissa and is the critical hyperbola separating those, for which airflow standstill or reversal occurs from those, where it does not occur. If any standstill or reversal in airway 2 could be caused by a fire in airway 1 at all, this standstill or reversal will occur at $\gamma_f = 0.5\gamma_a$ too.

With $p_{L2} = 0 = -(\gamma_a - \gamma_f)\Delta Z + R_{a1}\, Q_{a1}^2 \frac{\gamma_a}{\gamma_f}$ and $\gamma_f = 0.5\gamma_a$ one obtains as the standstill condition for airway 2

$$R_{a1}\, Q_{as}^2 = \frac{1}{4}\gamma_a \Delta Z$$

No reversal will occur for $R_{a1}\, Q_{as}^2 > \frac{1}{4}\gamma_a \Delta Z$

Q_{as} is the airflow in airway 1 at the moment of airflow standstill

in airway 2. It is not known and can be determined only by a network calculation, comprising the whole ventilation system. For a first estimate one can replace Q_{as} by the normal airflow without the fire Q_{n1}. The stability criterion then is

$$R_{a1}\, Q_{n1}^2 > \frac{1}{4}\, \gamma_a\, \Delta Z$$

or, with the normal pressure loss in airway 1 $p_{Ln1} = R_{a1}\, Q_{n1}^2$

$$p_{Ln1} > \frac{1}{4}\, \gamma_a \Delta Z$$

Since Q_{as} is larger than Q_{n1} these formulas contain a considerable if not excessive safety. How Q_{a1} changes with p_{L2} can be estimated by assuming

$$p_{L2} = p_F - \mathcal{R}\, Q_{a1}^2 \quad \text{or} \quad Q_{a1}^2 = \frac{p_F - p_{L2}}{\mathcal{R}}$$

where p_F is the fan pressure acting on the network and $\mathcal{R}$ is a hypothetical equivalent resistance for the rest of the network. From the energy equation applied to the two airways 1 and 2 one obtains then

$$p_{L2} = -(\gamma_a - \gamma_f)\Delta Z + \frac{(p_F - p_{L2})R_{a1}}{\mathcal{R}}\, \frac{\gamma_a}{\gamma_f} \quad \text{or}$$

$$p_{L2} = \frac{p_F \frac{R_{a1}}{\mathcal{R}}\, \frac{\gamma_a}{\gamma_f} - (\gamma_a - \gamma_f)\Delta Z}{1 + \frac{R_a}{\mathcal{R}}\, \frac{\gamma_a}{\gamma_f}}$$

p_{L2} as a function of γ_f is again a hyperbola with the parameters γ_a, ΔZ and $\frac{p_F R_{a1}}{\mathcal{R}}$ for which at $\gamma_f = 0.5\,\gamma_a$ as well $p_{L2} = 0$ as $\frac{dp_{L2}}{d\gamma_f} = 0$.

That means there exists again a critical hyperbola which touches the abscissa with its minimum at $\gamma_f = 0.5\,\gamma_a$ and separates those hyperbolas with the airflow standstill or reversal from those without. The possibility of airflow standstill in airway 2 can again be detected by inserting $\gamma_f = 0.5\,\gamma_a$ into the above equation for p_{L2}. Standstill will occur at

$$R_{a1}\, \frac{p_F}{\mathcal{R}} = \frac{1}{4}\, \gamma_a \Delta Z$$

If one assumes for $p_{L2} = 0$ $\frac{p_F}{\mathcal{R}} = Q_{as}^2$, one obtains again

$$R_{a1}\, Q_{as}^2 = \frac{1}{4}\, \gamma_a \Delta Z$$

One can visualize Q_{as} as the air quantity which the network is able to force through a short circuit with the resistance zero connecting

the ends of airways 1 and 2. Q_{as} is at least as large as the sum of the originally flowing

Q_{n1} and Q_{n2}

$$Q_{as}^2 > (Q_{n1} + Q_{n2})^2$$

There is consequently no danger of airflow standstill or reversal as long as

$$R_{a1}\, Q_{as}^2 > R_{a1}\, (Q_{n1} + Q_{n2})^2 > \frac{1}{4}\, \gamma_a \Delta Z$$

Under the assumption of $Q_{n1} = Q_{n2} = Q_n$ this becomes

$$R_{a1}\, Q_n^2 = p_{Ln1} > \frac{1}{16}\, \gamma_a \Delta Z$$

For two parallel airways to a third airway at fire this would become

$$p_{Ln1} > \frac{1}{36}\, \gamma_a \Delta Z \quad \text{etc.}$$

2) Two airways, fire at different locations in one of them

In the previous chapter it has been assumed that the throttling effect acts over the total length of the airway 1 and that the total height ΔZ is used for the development of a natural draft. In this chapter, stability criteria are developed for two parallel airways 1 and 2, where the airway at fire 1 has a horizontal intake and return section and the fire has different locations within the nonhorizontal section (fig. 60).

The energy equation delivers

$$p_{L2} = -(\gamma_a - \gamma_f)\Delta Z_f + R_{a1.1}\, Q_{a1}^2 + R_{a1.2}\, Q_{a1}^2 \frac{\gamma_a}{\gamma_f}$$

With the following abbreviations

$$k = \frac{R_{a1.1}}{R_{a1.1} + R_{a1.2}} \qquad x = \frac{\Delta Z_f}{\Delta Z} \qquad y = \frac{(R_{a1.1} + R_{a1.2})\, Q_{a1}^2}{\Delta Z}$$

this equation becomes

$$\frac{p_{L2}}{\Delta Z} = -x(\gamma_a - \gamma_f) + k\, y + (1 - k)\, y \frac{\gamma_a}{\gamma_f}$$

p_{L2} as a function of γ_f is again a hyperbola with a minimum $\left(\frac{dp_{L2}}{d\gamma_f} = 0\right)$

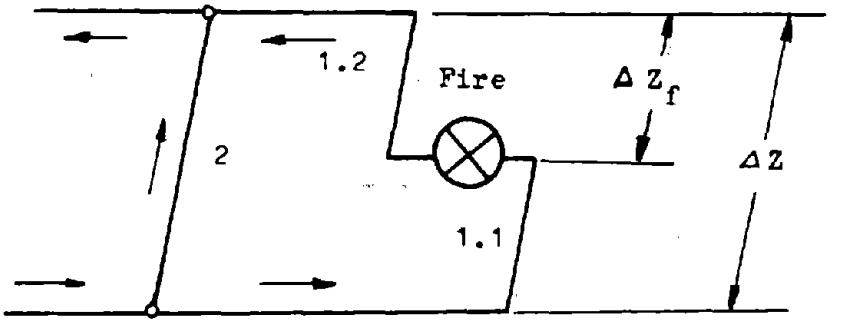

Fig. 60.

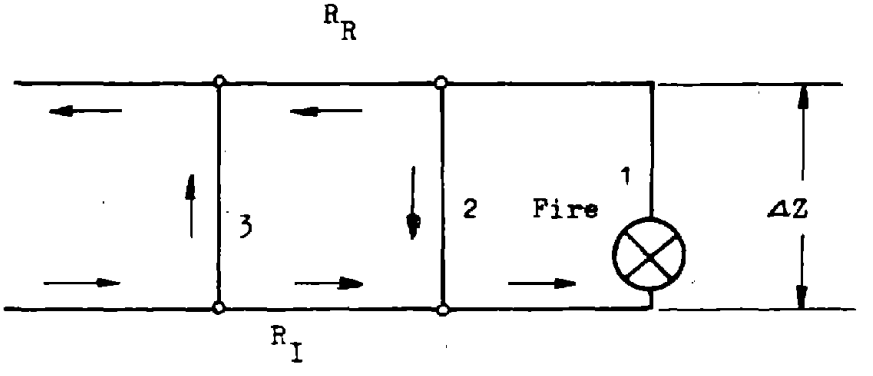

Fig. 61.

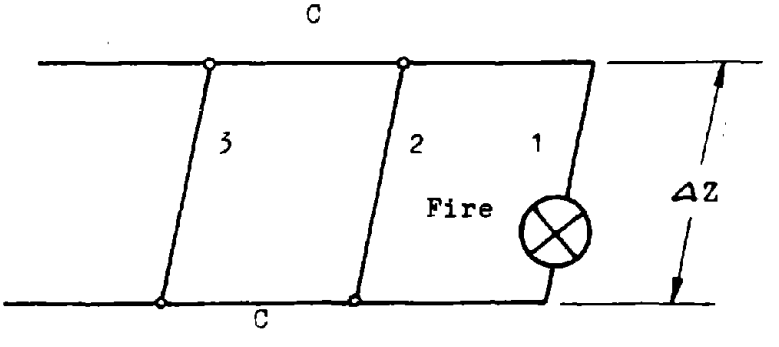

Fig. 62.

Fig. 60 - Fig. 62. Airways in the Vicinity of a Fire for the Judgement of Which Stability Approximation Formulas Were Derived (35)

for

$$x = \frac{y\,(1-k)\,\gamma_a}{\gamma_f^2}$$

This inserted into the last equation for $p_{L2}/\Delta Z$ yields

$$\frac{p_{L2\,min}}{\Delta Z} = x\left(2\gamma_f - \gamma_a + \frac{k\,\gamma_f^2}{(1-k)\,\gamma_a}\right)$$

The value γ_f where the critical hyperbola (separating those with and without air standstill) touches with its minimum the abscissa can be found from

$$p_{L2\,min} = 0$$

which results in

$$\gamma_{f_{min}} = \gamma_a\,\frac{\sqrt{1-k} - (1-k)}{k}$$

This for not too high values of k developed into a series results in

$$\gamma_{f_{min}} = \gamma_a\left(\frac{1}{2} - \frac{k}{8} - \frac{k^2}{16} - \frac{5\,k^2}{128} \ldots\right)$$

This shows that $\gamma_{f_{min}}$ is close to $0.5\,\gamma_a$ and is a variable of the ratio k = intake airway resistance/total resistance for the airway at fire. It is only over k influenced by the location of the fire, not by $x = \frac{\Delta Z_f}{\Delta Z}$.

The possibility of standstill can be detected by inserting $\gamma_{f_{min}}$ into the minimum condition for the hyperbola

$$x = \frac{y\,(1-k)\,\gamma_a}{\gamma_f^2}$$

For the worst case, a fire at the foot of the nonhorizontal airway section $(x = \Delta Z_f/\Delta Z = 1)$ and with the approximation $\gamma_f = 0.5\,\gamma_a(1 - \frac{k}{4})$ for not too high values of k, one obtains

$$y = \frac{\gamma_f^2}{(1-k)\,\gamma_a} = \frac{(R_{a1.1} + R_{a1.2})\,Q_{as}^2}{\Delta Z} \approx \frac{0.25\,\gamma_a\,(1 - \frac{k}{2})}{1-k} = \frac{\gamma_a}{4\,(1 - \frac{k}{2})}$$

$$(R_{a1.1} + R_{a1.2})\,Q_{as}^2\,(1 - \frac{k}{2}) \approx \frac{1}{4}\,\gamma_a \Delta Z$$

and with the used definition of k

$$R_{a1.2}\, Q_{as}^2 + \frac{1}{2} R_{a1.1}\, Q_{as}^2 \approx \frac{1}{4} \gamma_a \Delta Z$$

Q_{as} is again not known but the assumption $Q_{as} = Q_{n1} + Q_{n2} = 2\, Q_n$ delivers

$$(R_{a1.2} + \frac{1}{2} R_{a1.1})\, Q_n^2 \approx \frac{1}{16} \gamma_a \Delta Z$$

Consequently there is no danger of airflow standstill or reversal as long as

$$(R_{a1.2} + \frac{1}{2} R_{a1.1})\, Q_n^2 > \frac{1}{16} \gamma_a \Delta Z$$

If, for example, the resistance of the intake airway $R_{a1.1}$ is $\frac{1}{3}$ of the total resistance R_{a1} of airway 1, no danger of standstill or reversal exists as long as

$$(\frac{2}{3} R_{a1} + \frac{1}{6} R_{a1})\, Q_n^2 > \frac{1}{16} \gamma_a \Delta Z$$

or

$$R_{a1}\, Q_n^2 > \frac{1}{13} \gamma_a \Delta Z$$

One sees that the lacking throttling effect in the intake airway increases the possibility of standstills or reversals.

3) Three airways, one at fire, one with reversed airflow

Three airways 1, 2, and 3 are parallel. Airway 1 is at fire, the airflow in airway 2 has already been reversed (fig. 61). The possibility of airflow reversal in airway 3 shall be investigated.

If the intake airway R_I and the return airway R_R for airways 1 and 2 are combined to

$$R_C = R_I + R_R$$

energy and resistance equation deliver

$$p_{L3} = R_C\, Q_C^2 + R_{a1} Q_{a1}^2 \frac{\gamma_a}{\gamma_f} - (\gamma_a - \gamma_f) \Delta Z$$

With $Q_{a1} = Q_2 + Q_C$ and and

$$\frac{Q_2^2}{Q_C^2} = \frac{R_C}{R_2} \left(1 - \frac{p_{L3}}{R_C\, Q_C^2}\right)$$, obtained from $p_{L3} = R_C\, Q_C^2 - R_2\, Q_2^2$,

this becomes

$$p_{L3} = Q_C^2 \left(R_C + R_{a1}\left(1 + \sqrt{\frac{R_C}{R_2}\left(1 - \frac{p_{L3}}{R_C\, Q_C^2}\right)}\right)^2 \frac{\gamma_a}{\gamma_f}\right) - (\gamma_a - \gamma_f)\Delta Z$$

This implicit function of p_{L3} is difficult to handle. Since only the neighborhood of $p_{L3} = 0$ is of interest for stability criteria, the term

$$\frac{p_{L3}}{R_C\, Q_C^2}$$ is neglected. Then

$$p_{L3} = Q_C^2 \left(R_C + R_{a1}\left(1 + \sqrt{\frac{R_C}{R_2}}\right)^2 \frac{\gamma_a}{\gamma_f}\right) - (\gamma_a - \gamma_f)\Delta Z$$

If the abbreviation

$$R_S = R_C + R_{a1}\left(1 + \sqrt{\frac{R_C}{R_2}}\right)^2$$ is introduced, this becomes

$$\frac{p_{L3}}{\Delta Z} = \frac{Q_C^2}{\Delta Z}\left(R_C + (R_S - R_C)\frac{\gamma_a}{\gamma_f}\right) - (\gamma_a - \gamma_f)$$

and with $k = \frac{R_C}{R_S}$ and $y = \frac{R_S\, Q_C^2}{\Delta Z}$

$$\frac{p_{L3}}{\Delta Z} = k\, y + y\,(1 - k)\frac{\gamma_a}{\gamma_f} - (\gamma_a - \gamma_f)$$

This is again a hyperbola which intersects the abscissa ($p_{L3} = 0$) at

$$k\, y + y\,(1 - k)\frac{\gamma_a}{\gamma_f} - (\gamma_a - \gamma_f) = 0 \quad \text{or}$$

$$\gamma_f^2 + (k\, y - \gamma_a)\gamma_f + (1 - k)\, y\, \gamma_a = 0 \quad \text{or}$$

$$\gamma_f = 0.5\left(\gamma_a - k\, y \pm \sqrt{(k\, y - \gamma_a)^2 - 4\,(1 - k)\, y\, \gamma_a}\right)$$

For the critical hyperbola, which touches the abscissa only in one point and which separates those hyperbolas, for which standstill or reversal in airway 3 is possible from those, where it is not, one obtains

$$\gamma_{f_{min}} = 0.5\,(\gamma_a - k\, y) \quad \text{and}$$

$$y = \gamma_a \frac{2 - k - 2\sqrt{1 - k}}{k^2} \quad \text{or}$$

$$\gamma_{f_{min}} = \gamma_a \frac{\sqrt{1 - k} - (1 - k)}{k}$$

From the above formula for p_{L3} one sees that the danger of airflow standstill or reversal is not only influenced by k, γ_f and ΔZ but by

$$y = \frac{(R_C + R_{a1}\,(1 + \sqrt{R_C/R_2}\,)^2\,)\,Q_C^2}{\Delta Z}$$

as well and is the smaller the larger R_C, R_{a1} and Q_C and the smaller R_2 are. The standstill condition

$$y = \gamma_a \frac{2 - k - 2\sqrt{1 - k}}{k^2}$$ developed into a series yields

$$y = \frac{\gamma_a}{4}\left(1 + \frac{k}{2} + \frac{5\,k^2}{16} \quad ....\right)$$

For not too large values of k one can approximate

$$y = \frac{\gamma_a}{4} \quad \frac{1}{(1 - \frac{k}{2})}$$

Equated with the definition of y one obtains

$$\frac{(R_C + R_{a1}\,(1 + \sqrt{R_C/R_2}\,)^2\,)\,Q_C^2}{\Delta Z} = \frac{\gamma_a}{4} \quad \frac{1}{(1 - \frac{k}{2})}$$ or, with the

definition of k:

$$\frac{1}{2} R_C\, Q_C^2 + R_{a1}\,(1 + \sqrt{R_C/R_2}\,)^2\, Q_C^2 = \frac{1}{4}\gamma_a\, \Delta Z$$

From $R_C\, Q_C^2 = R_2\, Q_2^2$ for the moment of airflow standstill in airway 3 and

$$Q_{a1} = Q_C + Q_2$$ one obtains

$$(1 + \sqrt{R_C/R_2}\,)^2\, Q_C^2 = Q_{a1}^2$$ and consequently

$$\frac{1}{2} R_C\, Q_C^2 + R_{a1}\, Q_{a1}^2 = \frac{1}{4}\gamma_a\, \Delta Z$$

The air quantities Q_C and Q_{a1} are unknown. A safe assumption is to substitute for Q_C and Q_{a1} the total air quantity

$$Q_t = Q_{n1} + Q_{n2} + Q_{n3}$$

which normally flows through the three parallel airways. Under this assumption no danger of airflow reversal in airway 3 exists when

$$(\frac{1}{2} R_C + R_{a1}) (Q_{n1} + Q_{n2} + Q_{n3})^2 > \frac{1}{4} \gamma_a \Delta Z$$

4) Recommendations for test procedures

All the above derivations are based on the assumptions that the kinetic energy changes can be neglected and that the mass-flow of gases, while passing through the fire, does not change. Neglect of kinetic energy changes have, under ordinary ventilation conditions on the derived relations the same effect as an error of up to 3 ft. in the assumption of ΔZ. If the massflow of the air passing through the fire is increased by ε %, one has to multiply the resistance of the airways behind the fire by a factor $(1 + \varepsilon/100)^2$ Since the size of ε is disputed, it is suggested this factor be dropped as an additional safety. The assumption of a constant specific weight in the airways can be met by determining these specific weights from the average temperature

$$T_m = \int \frac{T \, dL}{L}$$

The committee condenses its findings into two sets of simple rules. The first set is easier to apply and has a very high built-in safety factor. If its application shows instabilities, a check should be made with the second set of rules. If the instability is confirmed, an accurate calculation, using a computer is recommended.

The first set of rules states that in a system of 3 ascensionally ventilated parallel airways there is no danger of airflow reversal in airway 2 (fig. 62) as long as

$$p_{Ln2} > \frac{\gamma_a \Delta Z}{4}$$

and no danger of airflow reversal in airway 3 as long as

$$\frac{p_{Ln2} + p_{Ln3}}{2} > \frac{\gamma_a \Delta Z}{4}$$

This formula follows from the above derived expression

$$\frac{1}{2} R_C Q_C^2 + R_{a1} Q_{a1}^2 > \gamma_a \frac{\Delta Z}{4} \quad \text{or} \quad \frac{1}{2} p_{LnC} + p_{Ln1} > \gamma_a \frac{\Delta Z}{4}$$

With

$$p_{Ln3} - p_{LnC} = p_{Ln2} = p_{Ln1}$$

or

$$\frac{p_{Ln3}}{2} - \frac{p_{LnC}}{2} = \frac{p_{Ln2}}{2} = \frac{p_{Ln1}}{2}$$

one obtains

$$\frac{p_{LnC}}{2} + p_{Ln1} = \frac{p_{Ln2}}{2} + \frac{p_{Ln3}}{2}$$

The second set of rules states that there is no danger of airflow reversal in airway 2 as long as

$$R_{n1}(Q_{n1} + Q_{n2})^2 > \gamma_a \frac{\Delta Z}{4}$$

and no danger of reversal in airway 3 as long as

$$(R_{nC} + R_{n1})\,(Q_{n1} + Q_{n2} + Q_{n3})^2 > \gamma_a \frac{\Delta Z}{4}$$

B) Criteria for airflow reversals developed by BUDRYK

Besides trying to assess the influence of mine fires on neighboring airways, several attempts have been made by ventilation engineers to develop methods for the detection of unstable airways without having to perform a full network calculation (23, 35, 36, 98, 120,141). Although these methods, except for simple networks, can give only qualitative answers they can be of great importance. Besides indicating where and in which sequence airflow standstills or reversals occur, they can give valuable advice as to how threatened airways can be stabilized. The practical implications for escape ways for miners or advance routes for fire fighting teams are obvious.

The best known and widely applied of these methods was developed in Poland by Budryk. It was recently studied by the Committee on Mine Ventilation of the ECSC (35) and extended to the treatment of descensional ventilation (23, 120).

The closed ventilation plan or Budryk plan has been discussed in chapter V.E.a. Some additional comments are necessary to introduce terms, which are used in connection with the "Budryk method". The airway, whose stability is to be investigated or maintained, is the boundary between the external and internal subnetworks. The external subnetwork contains all normal pressure sources p_E, the internal subnetwork the fire p_I. The path connecting the airway at fire over the intake and return airways with the surface is called main circle, airways being the part of the main circle are being called branches, all other airways side branches. As an example, the simple network used by Hartman (44, fig. 7-10) in his textbook on ventilation has been transformed into a budryk plan (fig. 63). One pressure source to simulate the fire has been added.

If the fire is located in an ascensionally ventilated airway, its natural draft will have a tendency to move the air in this airway and in the main circle in the same direction as the external pressure source. The main branches are stable, the side branches instable.

If the fire is located in a descensionally ventilated airway, its natural draft will have a tendency to move the air in this airway and along the main circle in the opposite direction as the external pressure source. The main branches are instable, the side branches stable. Ascensional and descensional ventilation shall therefore be discussed separately.

a) Application on ascensional ventilation

The most simple example of a closed ventilation plan, where a fire in an ascensionally ventilated airway can cause airflow standstill or reversal, comprises two parallel airways plus pertinent intake and return airways (fig. 64a). If the fire develops the natural draft p_{Nf} in airway 3, airflow standstill in airway 4 will occur when

$$p_F = R_1 Q_1^2 + R_2 Q_2^2 \qquad \text{and}$$

$$p_{Nf} = R_3 Q_3^2$$

If the pressure sources p_F and p_{Nf} are called p_E and p_I (fig. 64b), since they are part of the external or internal subnetworks and if the resistance of the subnetworks is expressed by

$$R_E = R_1 + R_2 \quad \text{and} \quad R_I = R_3$$

the standstill condition is

$$p_E = R_E Q_E^2 \quad \text{and} \quad p_I = R_I Q_I^2 \quad \text{or}$$

$$\frac{p_E}{p_I} = \frac{R_E}{R_I} \qquad \text{since } Q_I = Q_E$$

Airflow reversal in airway 4 will be avoided for

$$\frac{p_E}{p_I} > \frac{R_E}{R_I}$$

it will occur for

$$\frac{p_E}{p_I} < \frac{R_E}{R_I}$$

The means to stabilize airway 4 are consequently to keep p_E and R_I as large and p_I and R_E as small as possible.

With several parallel or overlapping airways and several pressure sources in the external and internal subnetworks one has to modify these relations. Since pressure losses and fan pressures are

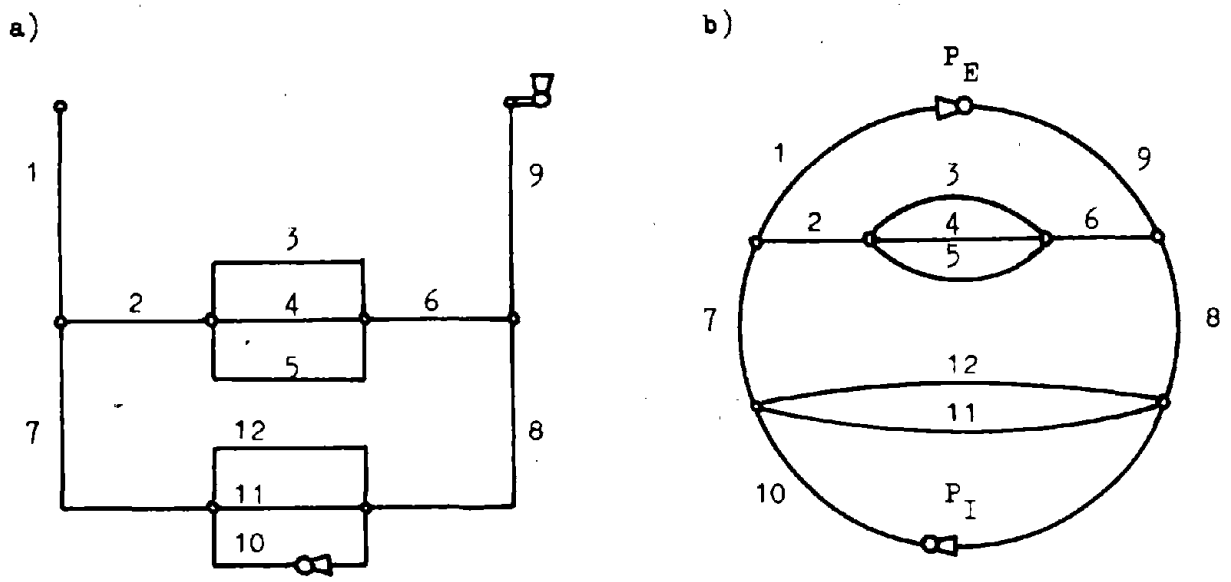

Fig. 63. Transformation of a Ventilation Plan (a) into a Budryk Plan (b)

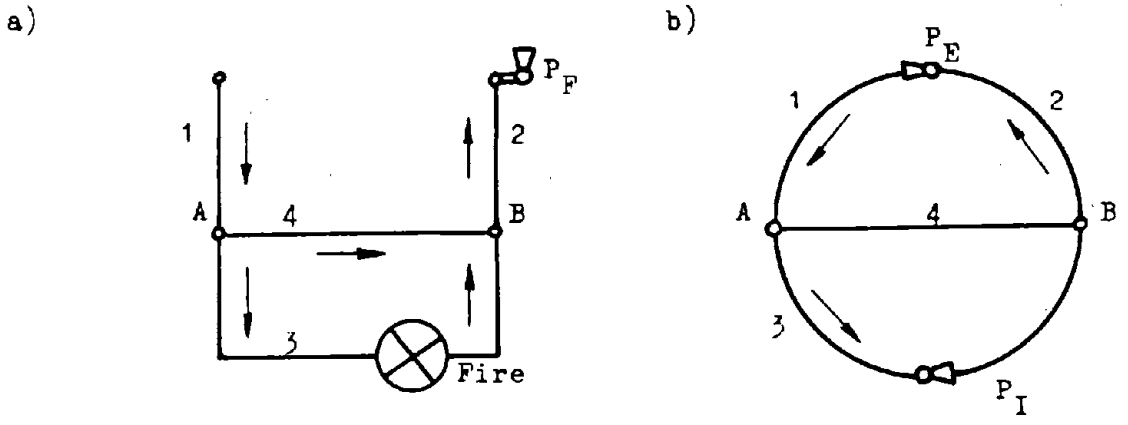

Fig. 64. Simple Example for the Derivation of the Budryk Criteria (35)

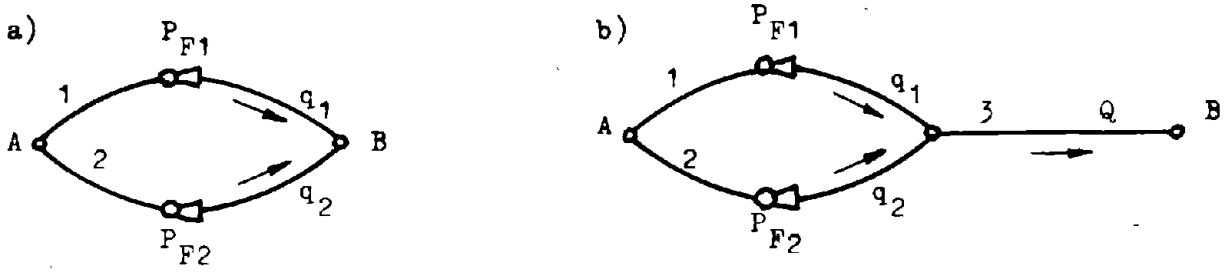

Fig. 65. Derivation of Equivalent Resistances $\mathcal{R}$ and Weighted Mean Pressures P_M

energies per unit volume or powers per unit volume flowrate and since the mesh equations, on which the above stability criteria are based are applications of the energy equation, to setting up an energy balance suggests itself.

The resistance factor $R = p_L/Q^2$ can be considered as a proportionality factor between energy per unit volume (pressure loss) and volume flowrate squared, or, with $R = p_L * Q/Q^3 = \bar{P}/Q^3$, between power and volume flowrate cubed. Using the ventilating potential P one can express the power necessary to provide the flowrate Q from point A to point B along an airway with the resistance R and pressure sources with the individual pressures p_F as

$$((P_B - P_A) + \sum p_F)\, Q = \bar{P} = R\, Q^3$$

If several air currents q_i flow from A to B and are exposed to different sources (fig. 65a) the total power necessary to transport $Q = \sum q_i$ from A to B is

$$((P_B - P_A)\sum q_i + \sum p_{Fi}\, q_i = \bar{P} = \sum \bar{P}_i = \sum R_i\, q_i^3$$

Applied to two parallel airways one obtains

$$((P_B - P_A)(q_1 + q_2) + p_{F1}\, q_1 + p_{F2}\, q_2 = R_1\, q_1^3 + R_2\, q_2^3 = \bar{P}_1 + \bar{P}_2$$

If an airway now is shared by several air currents q_i with the total airflow Q_i the required power will depend on the load of the airway and is

$$((P_A - P_B)\sum q_i + \sum p_{Fi}\, q_i = \bar{P} = \sum \bar{P}_i = \sum R_i\, Q_i^2\, q_i$$

Applied to two parallel airways with a third airway in series (fig. 65b) this is

$$((P_A - P_B)\,(q_1 + q_2) + p_{F1}\, q_1 + p_{F2}\, q_2 = R_1\, q_1^2 + R_2\, q_2^2 + R_3\, Q_3^2 (q_1 + q_2)$$
$$= \bar{P} = \bar{P}_1 + \bar{P}_2 + \bar{P}_3$$

If an equivalent resistance

$$\mathcal{R} = \frac{\sum R_i\, Q_i^2 q_i}{(\sum q_i)^3}$$

and a weighted mean pressure of the pressure sources

$$p_M = \frac{\sum p_{Fi}\, q_i}{\sum q_i}$$

is introduced, this equation becomes

$$P_B - P_A + p_M - \mathcal{R}(\sum q_i)^2 = 0$$

Applied to the external and internal subnetworks with q_E and q_I being the airquantities q_i which enter and leave the subnetworks at A and B one obtains

$$P_A - P_B + p_{ME} - \mathcal{R}_E q_E^2 = 0$$

$$P_A - P_B + p_{MI} - \mathcal{R}_I q_I^2 = 0$$

Airflow standstill is obtained in the critical airway A-B, forming the border between external and internal subnetworks, for $P_A = P_B$. In this case the last two equations again yield, with $q_E = q_I$, as standstill condition

$$\frac{p_{ME}}{p_{MI}} = \frac{\mathcal{R}_E}{\mathcal{R}_I}$$

Since no assumptions concerning the network configuration have been made, this equation is valid for all networks as long as p_{ME}, p_{MI}, $\mathcal{R}_E$ and $\mathcal{R}_I$ have been determined in the indicated way.

Physically, p_{ME} and p_{MI} are the energies per unit volume transferred by the external and internal pressure sources on q_E and q_I. $\mathcal{R}_E$ and $\mathcal{R}_I$ are the resistances of airways through which, when exposed to a pressure p_{ME} and p_{MI} the air quantities q_E and q_I would flow if all the other airways of the network did not exist.

$\mathcal{R}_E$ and $\mathcal{R}_I$ are functions of the network configuration and the airway resistances. For the simple case of fig. 64 they coincide with the resistance factors R_E and R_I. Since in this case

$q_E = \sum q_E = Q_E$ and $\sum p_{FE} = p_E$ one obtains

$$p_{ME} = \frac{\sum p_{FE}\, q_E}{\sum q_E} = p_E$$

$$P_A - P_B + p_{FE} = \mathcal{R}_E Q_E^2 = p_{LE} = R_E Q_E^2 \quad \text{or} \quad \mathcal{R}_E = R_E$$

Analogously: $\mathcal{R}_I = R_I$

$\mathcal{R}_E$ and $\mathcal{R}_I$ are however more difficult to determine if the subnetworks contain side branches. If for the network shown in fig. 63 the standstill conditions for airway 2-6 shall be determined (fig. 66a), one obtains again for the external subnetwork

$$p_{ME} = p_E, \quad \mathcal{R}_E = R_E = R_1 + R_9$$

For the internal subnetwork is

$$q_I = \sum q_I = q_7 = q_8 \qquad \sum p_{FI} = p_{FI} \qquad p_{MI} = \frac{\sum p_{FI} * q_I}{q_I} = p_I$$

$$\mathcal{R}_I = \frac{R_7 q_7^3 + R_{10} Q_{10}^2 q_7 + R_8 q_8^3}{q_{7,8}^3}$$

$$= \frac{R_7 q_7^2 + R_{10} Q_{10}^2 + R_8 q_8^2}{q_{7,8}^2} = \frac{p_{L7} + p_{L10} + p_{L8}}{q_{7,8}^2}$$

$$\mathcal{R}_I = \frac{p_I}{q_I^2}$$

The air quantity q_I, which is the air quantity in the airways 7 and 8 when the internal subnetwork is short circuited at A and B, has to be calculated by an ordinary network calculation. This is already unpleasant for little networks like the one under consideration. For large and complex networks it is a job which is difficult to accomplish without the help of computers. If computers are employed, there seems to be little sense in using them as auxiliary tools for the manual Budryk method. This is very true, but the Budryk method, although it has the capability, is little used for quantitative predictions. Its real value and importance is that it gives relatively simple and logical rules as how to stabilize certain airways in case of a fire.

Before these rules are discussed it will be shown how $\mathcal{R}_E$ and $\mathcal{R}_I$ can be changed. Both are functions which depend on the resistance of the main branches as well as on the airflow through these main branches. Simplified: $\mathcal{R}_E$ and $\mathcal{R}_I$ become the larger for given pressure sources p_{ME} or p_{MI} the smaller the air quantities q_E and q_I, exchanged by the two subnetworks are. The latter decrease with increasing resistance of the main branches and decreasing resistance of the side branches. As an example $\mathcal{R}_I$ has been calculated (fig. 66b) for the internal subnetwork of fig. 66a.

$$\mathcal{R}_I = \frac{p_I}{q_I^2} = \frac{p_I}{q_{10}^2} \frac{q_{10}^2}{q_I^2}$$

$$\frac{q_{10}}{q_I} = \frac{q_I + q_{11/12}}{q_I} = 1 + \sqrt{\frac{R_{7/8}}{R_{11/12}}}$$

$$\frac{p_I}{q_{10}^2} = R_I = R_{10} + \frac{1}{\left(\frac{1}{\sqrt{R_{11/12}}} + \frac{1}{\sqrt{R_{7/8}}}\right)^2} = R_{10} + \frac{R_{7/8}}{\left(1 + \sqrt{\frac{R_{7/8}}{R_{11/12}}}\right)^2}$$

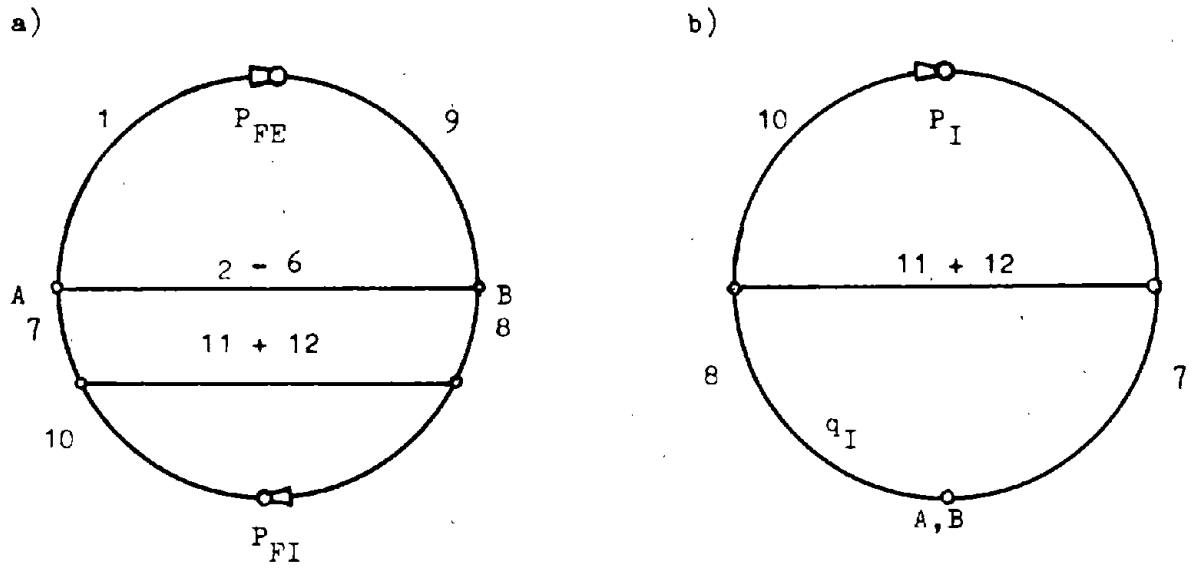

Fig. 66. Derivation of Standstill Conditions for Airways 2 - 6 (a) and of $\mathcal{R}_I$ (b)

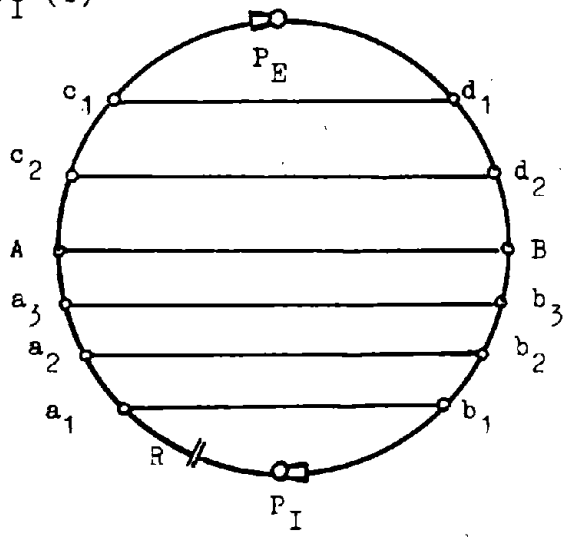

Fig. 67. Discussion of Means to Stabilize an Airway (120)

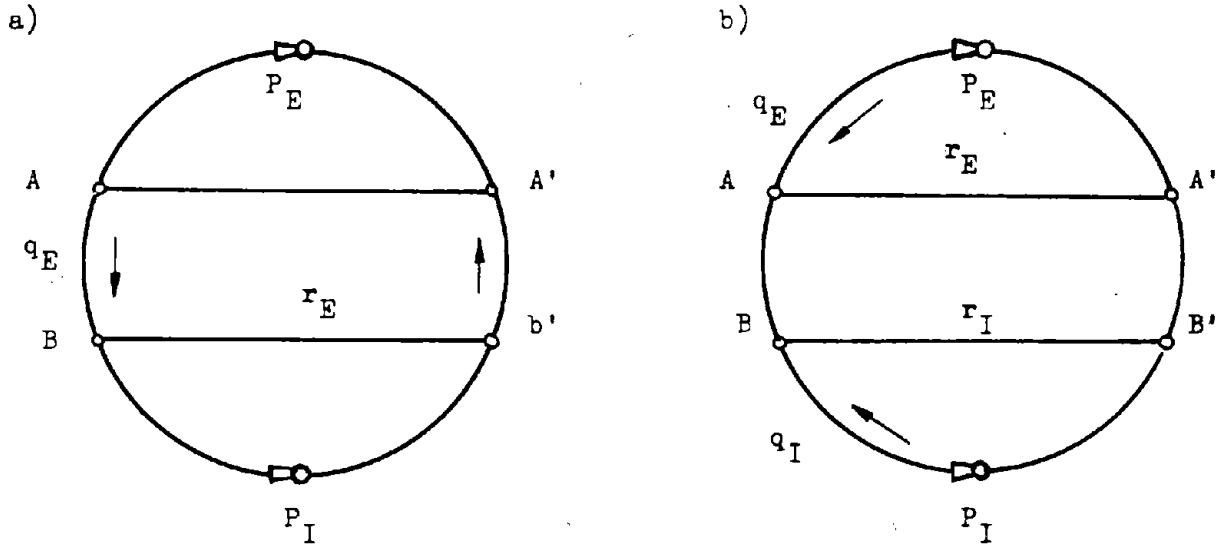

Fig. 68. Derivation of Budryk Criteria for Descensional Ventilation (23)

$$\mathcal{R}_I = \left(R_{10} + \frac{R_{7/8}}{\left(1 + \sqrt{\frac{R_{7/8}}{R_{11/12}}}\right)^2}\right)\left(1 + \sqrt{\frac{R_{7/8}}{R_{11/12}}}\right)^2$$

$$= R_{10}\left(1 + \sqrt{\frac{R_{7/8}}{R_{11/12}}}\right)^2 + R_{7/8}$$

It can be seen that the numerators in this expression contain only resistances of the main branches whereas the denominator contains the resistance of a side branch. The same result would be obtained for subnetworks of any size. A prerequisite, however, is that the airflow in the side branches of the internal subnetwork has already been reversed under the influence of internal pressure sources.

In complex networks, "bridges" between external and internal subnetworks can exist. It is difficult to predict how resistance changes in such bridges effect $\mathcal{R}_E$ or $\mathcal{R}_I$ except for the case that such bridges are a dominant part of one of the subnetworks. One should, therefore, not use such bridges for stabilizing measures but should watch them carefully in case of a fire and, if necessary, seal them.

1) Means for stabilizing an airway

According to Budryk's equation for air standstill

$$\frac{p_{MI}}{p_{ME}} = \frac{\mathcal{R}_I}{\mathcal{R}_E}$$

the stability of an airway against airflow reversals can be increased by increasing $\mathcal{R}_I$ and p_{ME} or by decreasing $\mathcal{R}_E$ and p_{MI}. For the following discussion of these choices, a simple example (fig. 67) shall be chosen (120).

Increase of $\mathcal{R}_I$

The optimal method to increase $\mathcal{R}_I$ is to install a regulator R in the airway at fire. Besides increasing $\mathcal{R}_I$ such a regulator reduces the air supply of the fire and, with the conventional axialflow fans, increases the fan pressure and therefore p_{ME}.

Regulators between a_1-a_2, a_2-a_3, a_3-A would increase $\mathcal{R}_I$ too and consequently have a beneficial effect on the stability of airway A-B. They would, however, reduce the stability of the internal side branches located between regulators and p_I. Regulators in those internal side branches, where the airflow still maintains its original direction, will increase $\mathcal{R}_I$. They will, however, increase the air aupply of the fire too and after a reversal reduce $\mathcal{R}_I$ and the stability of the airway A-B. Since such regulators are difficult to remove after a reversal, one should refrain right from the beginning from throttling internal

side branches. On the contrary, those ventilation doors or regulators which might exist in internal side branches between the fire and the location of the planned regulators in the main branches should be opened or removed.

Decrease of $\mathcal{R}_E$

$\mathcal{R}_E$ can be reduced by decreasing the resistance of the main branches and increasing the resistance of the side branches in the external subnetwork. If the main branches are part of other ventilation systems, as is frequently the case with intake shafts, a reduction of the air quantity flowing through these main branches to the other ventilation systems will decrease $\mathcal{R}_E$ too.

Increase of p_{ME}

The pressures of the fans in the external subnetwork should at least be kept in their normal range or should even be increased. The increase should, however, be accompanied by a simultaneous increase in $\mathcal{R}_I$ since otherwise the air supply of the fire and the fire intensity is increased, too.

Decrease of p_{MI}

p_{MI} can be decreased by decreasing the intensity of the fire. If direct fire fighting measures are no longer possible, this is done by reducing the air supply of the fire. The most effective way to accomplish this is a regulator in the airway at fire, which at the same time increases $\mathcal{R}_I$, too. It is a measure which is always correct as long as the formation of explosive mixtures due to excessive throttling is avoided.

b) Application on descensional ventilation

As discussed above fires in descensionally ventilated airways have a tendency to stop or reverse the airflow in the main branches of a closed ventilation plan. The side branches remain stable, although they might be filled with fumes.

The stability criteria are different from those for ascensional ventilation. If in the example of the simple network shown in fig. 68a the airway r_E be kept clean of fumes and is, therefore, made the boundary between external and internal subnetworks, standstill in the airway at fire results in

$$p_I = r_E q_E^2 , \qquad p_E = (\mathcal{R}_E + r_E) q_E^2 , \qquad \frac{p_I}{p_E} = \frac{r_E}{\mathcal{R}_E + r_E}$$

The airway is clean as long as

$$\frac{p_I}{p_E} < \frac{r_E}{\mathcal{R}_E + r_E}$$

After the airflow in the airway at fire has been reversed the airway A-B is threatened by a standstill or reversal next. With the terms used in fig. 68b, airflow standstill in airway A-B results in

$$p_I = (\mathcal{R}_I + r_I)\, q_I^2 , \quad p_E = (\mathcal{R}_E + r_E)\, q_E^2$$

$$r_I\, q_I^2 = r_E\, q_E^2 , \quad \frac{p_I}{p_E} = \frac{r_E}{\mathcal{R}_E + r_E} \cdot \frac{\mathcal{R}_I + r_I}{r_I}$$

The airway r_E is clean as long as $\frac{p_I}{p_E} < \frac{r_E}{\mathcal{R}_E + r_E} * \frac{\mathcal{R}_I + r_I}{r_I}$

Since functions $\mathcal{R}_E$ and $\mathcal{R}_I$ can be derived for networks of any size, the above derived standstill conditions are of general validity. If more than one pressure source is acting in the subnetworks, p_E and p_I have to be replaced by p_{ME} and p_{MI}.

1) Means for stabilizing an airway

From $\frac{p_{MI}}{p_{ME}} < \frac{r_E}{\mathcal{R}_E + r_E}$ it follows that the stability of descensionally ventilated airways at fire against airflow standstills or reversals can be increased by increasing p_{ME} and r_E or by decreasing p_{MI} and $\mathcal{R}_E$. $\mathcal{R}_I$ is not contained in this inequality but regulators in the airway at the fire will decrease the fire intensity and consequently p_{MI}.

From $\frac{p_{MI}}{p_{ME}} < \frac{r_E}{\mathcal{R}_E + r_E} * \frac{\mathcal{R}_I + r_I}{r_I}$ it follows that the stability of intake airways to a descensionally ventilated airway at fire against airflow standstills or reversals can be increased by increasing p_{ME}, $\mathcal{R}_I$ and r_E and by decreasing p_{MI}, $\mathcal{R}_E$ and r_I.

One sees that the necessary means to avoid airflow standstills or reversals for descensional ventilation are more or less the same as those for ascensional ventilation. The only difference is that the resistances of the side branches r_E and r_I, separating the external and internal subnetworks, now have an influence since standstills or reversals threaten the main branches.

c) Practical example

The fire at the mine Roche-la-Molière has been described above (fig. 45) and open and closed ventilation plans for this fire were discussed (fig. 47 and 48). The reported action to fight the fire was to set a regulator in airway 3-4, a correct but insufficient measure. Additionally the side branches of the external subnetwork 1-9, 9-10, 10-11 and the bridge 4-9 should have been throttled to decrease $\mathcal{R}_E$ (35).

d) Future prospects

The Budryk method in the form presented here does not take volume expansion and resistance increase with temperature rises into account. This can, however, easily be done by applying appropriate correction factors (23).

After some 30 years of its application in the Polish mines and more than 10 years of thorough study in West European countries the Budryk method has become very sophisticated. It is beyond the scope of this report to dwell on all of its aspects. It has only been tried to present its foundations and the general conclusions to be obtained from its application.

C) Mathematical description of ventilation networks for computer application

Computers execute mathematical operations without questioning their justification. If the mathematical description of a problem assigned to a computer is incorrect, the solution will necessarily be incorrect too.

Several possibilities exist for describing ventilation networks mathematically and each one has certain advantages and disadvantages. Unfortunately they are quite frequently not properly used by ventilation engineers. Before discussing computer applications it seems therefore advisable to give a short characterization of the mathematical descriptions.

Ventilation networks are usually considered to be in a steady state. This is justified since it takes only a short time until a new equilibrium is reached or a state, which is for practical purposes close enough to the new equilibrium, is achieved after a change in the ventilation system has taken place. Although mathematical descriptions of ventilation networks as non-steady state systems and even analog and digital computer (127) simulations exist, they have not yet found any larger application.

Mine fires are in principle non-steady state processes although, after being fully developed, they can reach a quasi-steady state. The same applies to the thermal forces exerted by them on the ventilation, although they too can reach a quasi-steady state or can right from the beginning be approximated as developed in steady state processes. In any case, these forces do not change very rapidly so that inertia forces of the air can be neglected and the response of the ventilation system can be considered as a sequence of equilibrium states, to which the steady state mathematical description of the network applies.

Steady state ventilation networks can mathematically be described by groups of three different types of equations: resistance equations, junction equations and mesh equations.

Resistance equations

The resistance equations are based on Darcy's equation

$$dh_L = f \frac{dL\ P}{4\ A} \frac{V_a^2}{2g}$$

where V_a is the average velocity of the air flowing through the cross section A. The headloss in an airway of the length L is consequently

$$h_L = \int f \frac{P}{4\ A} \frac{V_a^2}{2g}\, dL \quad \text{or, with } V_a = \frac{Q}{A} = \frac{G\ v}{A}$$

$$h_L = \int f \frac{P}{8\ g\ A^3} v^2\ G^2\ dL$$

For constant airway dimensions A and P and a constant mass flow this becomes

$$h_L = f \frac{P}{8\ g\ A^3} G^2 \int v^2\ dL$$

and if a mean square specific volume $v_{msq}^2 = \frac{1}{L}\int v^2\ dL$ and, based on this mean square volume, a resistance factor R_G is introduced, one obtains as one possible form of the resistance equation

$$h_L = f \frac{L\ P}{8\ g\ A^3} v_{msq}^2\ G^2 = R_G\ G^2$$

Under ordinary ventilation conditions without excessive volume changes, such as caused by fires, the approximation

$$v_{msq}^2 \approx v_m^2 \quad \text{with } v_m = (v_1 + v_2)/2$$

v_1 = specific volume at beginning of airway

v_2 = specific volume at end of airway

causes only negligible errors. They amount to less than 1% for shafts of 3000 ft depth for horizontal airways to even less (41).

In the above equations the headloss has the dimension "height of air column". Many ventilation engineers prefer to express headlosses in equivalent pressures p_{LS} based on a standard specific weight γ_S as $p_{LS} = h_L * \gamma_S$.

The massflow is equally expressed by an equivalent volume flow Q_S based on the same standard specific weight γ_S as $Q_S = G/\gamma_S$.

With this, the resistance equation can be written in another form as

$$p_{LS} = f \frac{L\ P}{8\ g\ A^3}\ \gamma_S^3\ v_{msq}^2\ Q_S^2 = R_S\ Q_S^2$$

If instead of the headloss the pressure loss p_L shall be used, one obtains from

$$dh_L = f\ \frac{P}{8\ g\ A^3}\ v^2\ G^2\ dL \qquad \text{with } dp_L = dh_L\ /v$$

$$dp_L = f\ \frac{P}{8\ g\ A^3}\ v\ G^2\ dL \qquad \text{and for constant A, P, and G}$$

$$p_L = f\ \frac{P}{8\ g\ A^3}\ G^2 \int v\ dL$$

If a mean specific volume $v_m = \frac{1}{L} \int v\ dL$ is used, this becomes

$$p_L = f\ \frac{L\ P}{8\ g\ A^3}\ v_m\ G^2$$

and if a mean volume flow $Q_m = G * v_m$ and a resistance R is introduced

$$p_L = f\ \frac{L\ P}{8\ g\ A^3}\ \frac{1}{v_m}\ Q_m^2 = R\ Q_m^2$$

Under ordinary ventilation conditions without excessive volume changes, the approximations

$$v_m \approx \frac{v_1 + v_2}{2} \quad \text{and} \quad v_m \approx \frac{1}{\gamma_m} = \frac{2}{\gamma_1 + \gamma_2} \qquad \text{are frequently used}$$

and the resistance equation, based on pressure losses and volume flows, is written in the form

$$p_L = f\ \frac{L\ P}{8\ g\ A^3}\ \gamma_m\ Q_m^2 = R\ Q_m^2$$

If the air is considered to be incompressible with the specific weight γ_S the second form of the resistance equation $p_{LS} = R_S\ Q_S^2$ and the third form $p_L = R\ Q_m^2$ coincide.

Junction equations

The junction equations are based on the law of mass conservation. The mass flow entering an airway or a junction is equal the mass flow leaving. This is mathematicall expressed as $\sum G = 0$.

For incompressible air the mass flow G and the volume flow Q are related by a constant γ and from $\Sigma G = 0$ follows $\Sigma Q = 0$.

If the mass flow is expressed by an equivalent volume flow with a constant γ_S one obtains from $\Sigma G = 0$ consequently $\Sigma Q_S = 0$.

If air of different specific weights is mixed in junctions, as well $\Sigma G = 0$ as, according to Amagat's law, $\Sigma Q = 0$ holds. If the air changes its specific weight along an airway, however, only $\Sigma G = 0$ is valid, the volume flow follows $\Sigma Q \neq 0$. The volume flow entering an airway is not equal the volume flow leaving and in network calculations, based on volume flow, a suitable allowance has to be made.

When methane, water vapour, compressed air, combustion products etc. enter an airway between junctions or when leakage leaves it, a genuine change of the mass flow takes place. This mass flow change has to be considered as being caused by a different airway (e.g. compressed air pipes) joining the airway under consideration or branching off from it.

As long as only one quantity G per airway is used to describe the mass flow, the equation $\Sigma G = 0$ is in every airway automatically satisfied and has to be applied to junctions only, hence the name.

Mesh equations

The mesh equations are based on the energy equation, which in the form

$$v\,dp + \frac{dV_a^2}{2g} + dZ + dh_L - dh_F = 0$$

applied to a mesh or loop results in

$$\oint v\,dp + \oint dh_L - \oint dh_F = 0 \quad \text{or}$$
$$\Sigma h_L - \Sigma h_F - h_N = 0$$

If the heads are converted into equivalent pressures by multiplying them with a constant standard density γ_S one obtains

$$\Sigma p_{LS} - \Sigma p_{FS} - p_{NS} = 0$$

From the energy equation in the form

$$dp + \frac{\gamma}{2g} dV_a^2 + \gamma\,dZ + \gamma\,dh_L - \gamma\,dh_F = 0$$

one obtains, applied to a loop, with the close approximation

$$\oint \frac{\gamma}{2g} dV_a^2 = 0$$

$$\oint \gamma \, dZ + \oint \gamma \, dh_L - \oint \gamma \, dh_F = 0 \quad \text{or}$$

$$\Sigma p_L - \Sigma p_F - p_N = 0$$

If the air is considered to be incompressible ($\gamma = \frac{1}{v}$ = constant) one obtains

$\oint v \, dp = - h_N = 0$ and $\oint \gamma \, dZ = - p_N = 0$ and with the assumption of $\gamma_S = \gamma$

$p_{LS} = p_L$ and $p_{FS} = p_F$

Summing up, the three types of equations, describing a ventilation network, resistance-, junction- and mesh equations, can be written in different forms. If energies are expressed as heads in heights of air columns and airflows in unit weights they read

$$h_L = R_G \, G^2$$
$$\Sigma G = 0$$
$$\Sigma h_L - \Sigma h_F - h_N = 0$$

If energies are expressed as pressure heads and airflows in unit volumes based on standard densities they can be written as

$$p_{LS} = R_S \, Q_S^2$$
$$\Sigma Q_S = 0$$
$$\Sigma p_{LS} - \Sigma p_{FS} - p_{NS} = 0$$

If energies are expressed as pressures and airflows in unit volumes, they can be written as

$$p_L = R \, Q_m^2$$
$$\Sigma Q = 0$$
$$\Sigma p_L - \Sigma p_F - p_N = 0$$

The resistance factors in these equations are

$$R_G = f \frac{L \; P}{8 \; g \; A^3} \, v_{msq}^2$$

$$R_S = f \frac{L \; P}{8 \; g \; A^3} \, \gamma_S^3 \, v_{msq}^2$$

$$R = f \frac{L \; P}{8 \; g \; A^3} \, \frac{1}{v_m}$$

All three possibilities for describing a ventilation network mathematically have the same justification, all three give the same results in network calculations and all three are used by ventilation engineers. By far the most popular one is the third possibility;

the second is preferred where larger density changes occur; the first one is little used since ventilation engineers seem to dislike to work with heads and mass flows. Unfortunately, quite frequently the second and third possibility are blended in an uncorrect manner.

In applying the third possibility it must be borne in mind that $\sum Q = 0$ is valid for junctions only and that Q can change within an airway even when no changes in the mass flow take place. The specific properties of p_N (chapter IV.B.a.) have to be taken into account too.

If the ventilation network contains
N_b airways
N_j junctions
N_m independent meshes
the network is described by 2 N_b equations:
N_b resistance equations
$N_j - 1$ junction equations
$N_m = N_b - N_j + 1$ mesh equations

D) Analog computers

a) Present use

Since half of the equations describing a ventilation network, the resistance equations, are square equations, direct analytical methods can be employed usefully to networks comprising airways in series and parallel only. Airways in series share all the same air quantities, airways in parallel all the same head or pressure losses. Insertion of square equations into other square equations is thus avoided.

For other more complicated networks approximation methods have been developed. However, they require so much work that ventilation engineers in the early 1940's began to develop special analog computers and, after they became available in the mid-1950's, started to use electronic digital computers for ventilation network calculations.

Analog computers are physical models and it is not surprising that flowmodels, working either with water or compressed air have been used for ventilation network calculations (5). They are, however, too difficult to handle and only a few models in Italy and Germany became known.

The similarity of Kirchhoff's rules for electrical networks and the junction and mesh equations for ventilation networks suggests the use of electric models. If the electric current I is used to simulate the airflow Q or G and the electric voltage V to simulate heads h or pressures p, mesh and junction equations are properly satisfied in electrical networks. Difficulties arise with the square resistance equation, which has to be simulated by

$V \propto R\ I^2$ (R = airway resistance). These difficulties are overcome in different ways.

The simplest electric analog computers use linear variable resistors as airway simulators, whose ohmic resistances ϱ are manually made proportional the product R I. The voltage drop across such a resistor is then $V = \varrho\ I \propto R\ I^2$ and shows thus the desired square relationship between V and I. Since I is not known in advance but is the result of the network calculation, one starts out from estimated values I_o and sets the resistors on initial values $\varrho_o \propto R\ I_o^2$. The actual flowing currents I_1 are then measured, the resistances adjusted to improved settings ϱ_1 (which could for instance be $\varrho_1 \propto \frac{R}{2}\ (I_o + I_1)$) and the procedure is repeated until further adjustment no longer effects any significant changes in I. Analog computers of this type were introduced in Great Britain in 1952 and are in use in most mining countries. Their advantage is their low price, their disadvantage the considerable amount of manual work necessary for the adjustment of the resistors. In Belgium and France (97) electrical ancillaries were developed, which allow the iterative adjustment without any manual calculations.

Complete electrical analogs of ventilation networks can be constructed with nonlinear resistors with a square V-I relationship. It was found (74) that ordinary filament lamps showed this relationship over a certain range and so-called "filament lamp models" were in use in Germany and in The Netherlands in the early 1950's. The disadvantage of this type of computer was the limited working range of the filament lamps and their changing characteristic due to aging. which required frequent checks. In the USA an attempt was made to overcome these difficulties with low voltage tungsten filament lamps, "Fluistors," and analog computers using these Fluistors are known as "fluid network analyzers."(78)

The fact that Fluistors, although built in a progressive series of relative resistance values ranging from 0.05 to 500 in nominal 5% steps, allow no stepless resistance variation, their low maximal voltage of 2.5 - 3 V, their exponent n = 1.85 instead of the wanted 2 in the voltage - current function $V = C\ I^n$, and their comparatively high price led to the design of two different types of analog computers. One type, built in the fifties in Germany and Russia and since discontinued, uses for every airway simulation an electro-mechanical element called a servomultiplicator, which sets an electrical resistor with the help of a servomotor on the product $\varrho \propto R\ I$ (39). The other type, built since the late fifties in France, Germany and Japan uses as airway simulations electronic function generators, which approximate the V-I parabola sectionwise by linear segments (9, 124).

Analog computers have, since the advent of the electronic digital computers, more and more been replaced by the latter. Being single purpose computers for the solution of sets of linear and square equations, every improvement in computing and handling

speed makes it harder to find enough work for them, except at central research and consulting offices.

b) Simulation of mine fires

Mine fires can influence the airflow distribution in a mine in different ways:
through physical changes of airways;
through the additional mass flow of the combusion products;
through air dentisy changes, which in turn effect volume flow and airway resistance changes and create natural drafts.

1) Airway- and mass flow changes

Physical changes of airways can be caused by rockfall, damaged ventilation doors, regulators and other ventilation equipment. The possibility of changes of this type depends very much on the local circumstances and defies a general discussion. They can be reduced by fireproof supports and installations. There is in principle no difficulty in considering them in a network calculation. For the frequent case of ventilation doors pushed open by airflow reversals and thus acting like valves, some of the electromechanical and electronical analog computers even provide special simulating elements.

The composition of gaseous combustion products has been discussed in chapter II.C.a. To estimate the order of magnitude of density and mass flow changes, a dry composition of 5% CO_2, 0.5% CO, 16% O_2, 78.5% N_2 shall be assumed for oxygen rich timber fires (106) and of 19% CO_2, 7% CO, 3% H_2, 1% O_2, 70% N_2 for fuel rich timber fires (104). The calculation delivers for density and mass flow increases 2 and 2.5% for the oxygen rich fires and 4.5 and 18% for the fuel rich fires. Baltajtis and Markovic (7) in their experiments measured 8 - 10% mass flow increases, Voskobojnikov (131) 5 - 11%, the Committe on Mine Ventilation of the ECSC (35) recommends, depending on fire extension and intensity, working with 5 - 15%.

Mass flow increases can be simulated by a separate path, discharging from the surface into the airway at the fire. Mass flow increases are usually not large enough to effect substantial changes in the airflow distribution of the network. Since they have a tendency to counteract the ventilation disturbances caused by the fire in neighboring airways, they are quite frequently neglected by ventilation engineers in emergency plans and considered as an additional safety.

Air density changes occur, contrary to physical airway changes, without delay after a fire starts. They are, at least during the first stage of the fire and frequently during its whole duration, the main source of ventilation disturbances. Their proper consideration in fire emergency plans is therefore very important, since emergency plans try to take the surprise out of a fire and aim at suggesting fast fire fighting and rescue measures. It has been shown that air density changes are caused less by changes in the composition of the air than by temperature changes.

2) Volume flow and resistance changes

Volume flow changes, if they are caused by density changes, have to be taken into account only in the third of the three discussed possibilities to describe networks mathematically. The other two possibilities are based on mass flows. In analog computers volume flow changes can, in the same way as mass flow changes, be simulated by a separate path connecting the point where the changes occur with the surface and adding to or subtracting from the flow.

If the volume flow changes steadily along an airway it is usually simulated by a mean flow

$$Q_m = \frac{1}{L} \int Q \, dL = \frac{1}{L} G \int v \, dL = G \, v_m$$

in order to keep the number of feed- and draw points and airway simulations in tolerable limits. This method requires one feed- and one draw point per airway. If the volume flow changes are caused by temperature changes, the equation of state delivers v/T = constant and v_m can be determined from

$$v_m = \frac{v_1}{T_1} \frac{1}{L} \int T \, dL = \frac{v_2}{T_2} \frac{1}{L} \int T \, dL$$

An expression for $\frac{1}{L} \int T \, dL$ for steady state heat exchange between air and airway walls has been derived in chapter III. A.

Another frequently used method is to simulate the influence of density changes on volume flow and resistance factors simultaneously. This method requires only one feed point or draw point per airway at either its beginning or end. With the subscripts 1 and 2 denoting beginning and end of the airway, the pressure loss in the airway is

$$p_L = f \frac{L}{8 g A^3} \frac{P}{v_m} Q_m^2 = f \frac{L}{8 g A^3} \frac{P}{v_1} Q_1^2 \frac{v_m}{v_1}$$

$$= f \frac{L}{8 g A^3} \frac{P}{v_2} Q_2^2 \frac{v_m}{v_2} = R_m Q_m^2 = R_1 Q_1^2 \frac{v_m}{v_1} = R_2 Q_2^2 \frac{v_m}{v_2}$$

The volume flow in the airway which receives from its starting junction the quantity Q_1 can either at its end or at its beginning be changed to Q_2. In the first case the resistance factor has to be made equal

$$R = f \frac{L}{8 g A^3} \frac{P}{v_1^2} \frac{v_m}{v_1^2}$$ or, if R_1 is the resistance factor the airway would have with air of the specific volume v_1

$$R = R_1 \frac{v_m}{v_1}$$

In the second case the resistance factor has to be made equal

$$R = f \frac{L\ P}{8\ g\ A^3} \frac{v_m}{v_2^2} = R_2 \frac{v_m}{v_2}$$

If the volume flow changes are caused by temperature changes, the factors

$\frac{v_m}{v_1}$ and $\frac{v_m}{v_2}$ can be replaced by $\frac{T_m}{T_1}$ and $\frac{T_m}{T_2}$.

The method just described is the one used by Voskobojnikov (131) in deriving equivalent resistance factors (chapter IV. A.). The Committee on Mine Ventilation of the ECSC (35) suggests its use, too, and recommends in emergency plans an assumption for ascensionally ventilated airways at fire T_m being twice the ordinary temperature since with this value the greatest disturbances occur (chapter VI.A.b.).

The influence of density changes on the 3 different resistance factors, which can be used for network calculations, is obvious from their definitions.

$$R_G = f \frac{L\ P}{8\ g\ A^3} v_{msq}^2$$

$$R_S = f \frac{L\ P}{8\ g\ A^3} \gamma_S^3 v_{msq}^2$$

$$R = f \frac{L\ P}{8\ g\ A^3} \frac{1}{v_m}$$

If the density changes are caused by temperature changes the equation of state yields, with $\frac{v}{T}$ = constant.

$$v_{msq}^2 = \left(\frac{v_1}{T_1}\right)^2 \frac{1}{L} \int T^2\, dL = \left(\frac{v_1}{T_1}\right)^2 (T_{msq})^2$$

$$v_m = \frac{v_1}{T_1} \frac{1}{L} \int T\, dL = \frac{v_1}{T_1} T_m$$

Expressions for T_m and T_{msq}^2 have been derived for steady state heat exchange between airway walls and air in chapter III.A.

3) Problems associated with the simulation of natural drafts

It has been explained that natural drafts are caused by the conversion of heat into mechanical energy and that they can originate only in loops of the ventilation network. The mechanical energy provided by natural drafts, expressed per unit weight of air

circulating in the loop under consideration, is

$$h_N = - \oint v \, dp$$

Per equivalent volume $\frac{1}{\gamma_S}$ of the unit weight it is

$$p_{NS} = - \gamma_S \oint v \, dp$$

and per unit volume of the air circulating in the loop under consideration it is

$$p_N = - \oint \gamma \, dZ$$

Like fan pressures or heads, natural drafts are simulated by power sources in electric analog computers. In flow models they could be simulated by pumps or compressors, but no such simulation has been reported.

Ventilation networks contain $N_m = N_b - N_j + 1$ independent meshes and their complete mathematical description must contain N_m mesh equations. They are, for the three discussed possibilities to describe networks

$$\sum h_L - \sum h_F - h_N = 0$$
$$\sum p_{LS} - \sum p_{FS} - p_{NS} = 0$$
$$\sum p_L - \sum p_F - p_N = 0$$

If the ventilation networks are simulated by analog computers, there is no difficulty in assigning head- or pressure losses and fanheads or fanpressures to the pertinent airways. There is however no fixed location for natural ventilation heads or pressures in a mesh. All the information the mesh equations provide is about their magnitude, not the location.

In simulating natural ventilation heads or pressures in analog computers therefore only one condition has to be met: that the mesh equations be satisfied. There is no rule on where to place the power sources, which represent the natural ventilation heads or pressures.

As an example, fig. 69 a shows the simplified isometric ventilation plan of a smaller potash mine (40). The natural ventilation heads p_{NS} (mm WG) are indicated for every one of the seven independent meshes. Fig. 69 b and c show two extreme possibilities for simulating these heads with one power source per mesh and one power source per airway. Both possibilities satisfy the same mesh equations and both consequently give the same results in a network calculation.

The work of finding out how many independent meshes a network contains and how many mesh equations have to be satisfied is tedious. Many ventilation engineers therefore consider every non-horizontal airway as part of an imaginary mesh closed by a corresponding vertical airway, which all meshes have in common, and by connecting

horizontal airways. The common corresponding vertical airway can either be one of the intake shafts or an imaginary air column of defined properties, preferably of a constant specific weight or temperature. Since the natural ventilation head can be approximated by

$$h_N = -\oint v \, dp \approx \frac{1}{T_m} \oint T \, dZ$$

and the natural ventilation pressure is

$$p_N = -\oint \gamma \, dZ$$

the temperature or density changes in the connecting horizontal airways are without influence on the size of h_N or p_N and do not have to be considered. These horizontal connections do not even have to exist.

Fig. 69 d shows the simulation of the natural ventilation heads in the meshes formed by the non horizontal airways and the intake shaft. Comparison of fig. 69 a with fig. 69 d shows that the mesh equations are satisfied.

The complete simulation of all natural ventilation heads or pressures in an electric analog computer requires at least as many power sources as the ventilation network has independent meshes. Since most analog computers don't provide this many power sources, ventilation engineers usually follow two different practices in their treatment of natural drafts. One practice is to consider only natural ventilation heads or pressures above a certain magnitude and neglect the smaller ones altogether. The other practice is to simulate the effect of the smaller natural ventilation heads or pressures by modifying the airway resistances. This latter method is the more popular one since the measurement of airway resistances can be accompanied by such large errors that many ventilation engineers prefer to check the accuracy of their results by performing a network calculation with the measured resistances. The agreement between the measured and the computer indicated airflow distribution serves as the criterion for the quality of the measurements. If disagreements exist they are removed by checking and varying the measured resistances.

Both methods have serious handicaps. As long as powerful fans provide airflows that make the head or pressure losses in the airways large compared to the natural drafts, the errors in neglecting the latter will not be too significant. They will, however, rarely be tolerable, if, as is frequently the case in emergency plans, reductions in fanheads or pressures or even fan failures have to be simulated.

The second practice gives more accurate results if in a ventilation planning the changes in the existing network parts are not too large. When, however, greater changes in the airflow distribution occur, the deviation of the airflow resistances from the reality will cause additional errors.

Fig. 69.

a)

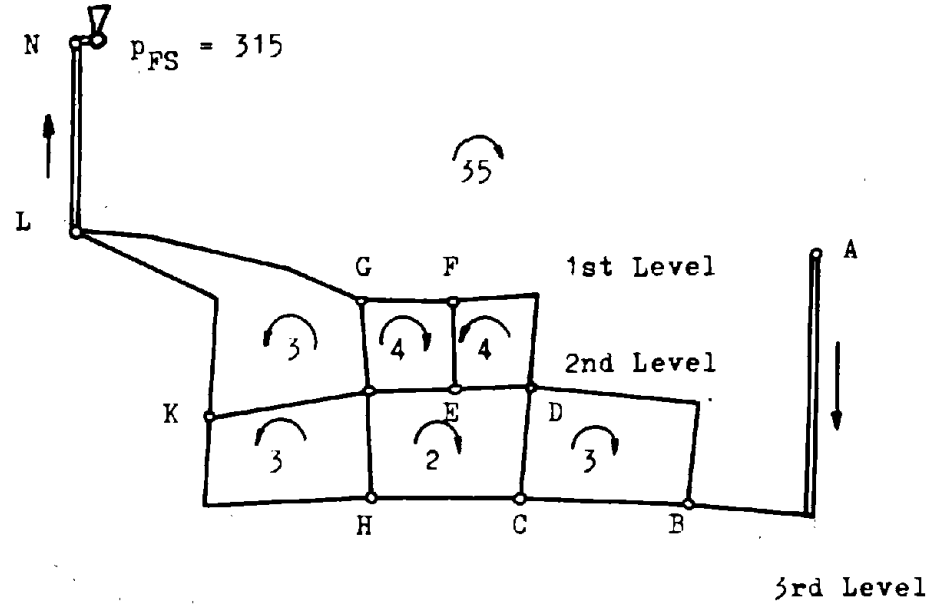
N
p_{FS} = 315
35
L
G
F
1st Level
A
3
4
4
2nd Level
K
E
D
3
2
3
H
C
B
3rd Level

b)

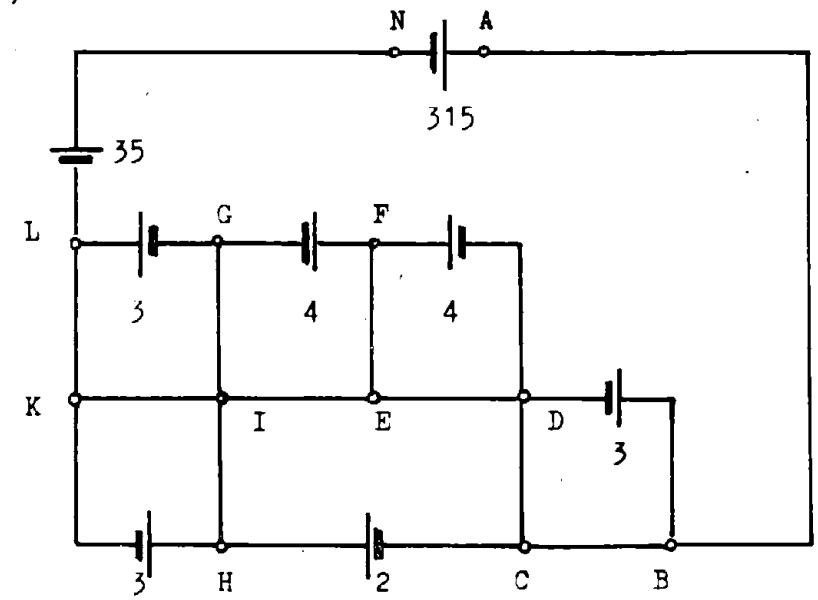
N
A
315
35
L
G
F
3
4
4
K
I
E
D
3
3
H
2
C
B

c)

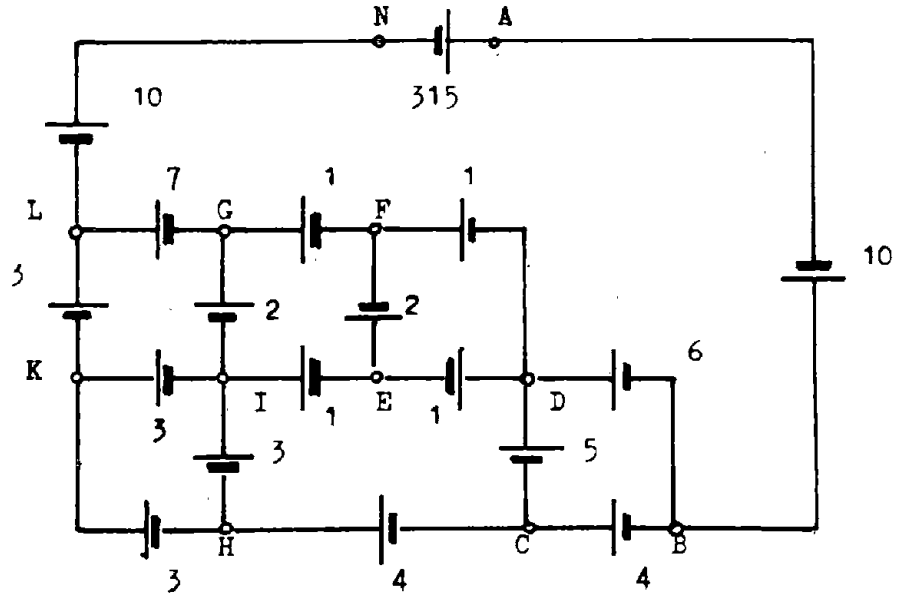
N
A
315
10
7
1
1
L
G
F
10
5
2
2
K
6
I
E
D
3
1
1
3
5
3
H
C
B
3
4
4

d)

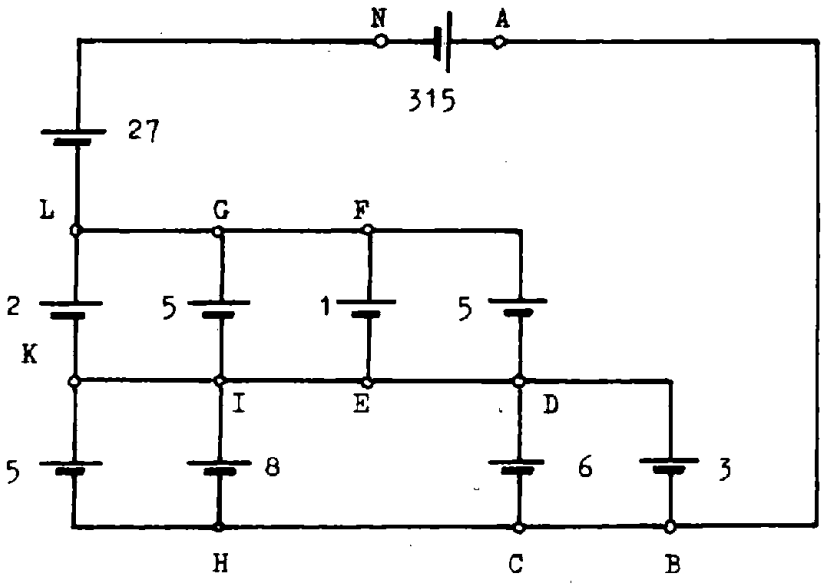

Fig. 69. Different Ways of Simulating Natural Drafts in an Electric Analog Computer (40)

As an example, table 19 shows for the network of fig. 69 a a comparison of the airflows obtained, when in network calculations all the natural ventilation heads except for the one of p_{NS} = 35 mm WG in mesh A-B-D-F-G-L-N-A are neglected with the airflows obtained when all natural ventilation heads have been considered. It must be admitted that this is a malignant example since the airway D-E contains a cooling plant. As long as the powerful fan with p_{FS} = 315 mm WG operates, the discrepancies don't seem to be too large, except for airway E-F. When, however, the fan is stopped the neglect of the small natural ventilation heads in the underground meshes precludes useful results (40).

4) Simulation of natural drafts caused by fires

All one has to do in simulating the additional natural draft caused by fires is to calculate for those meshes, where the fire has caused density changes, the new natural ventilation heads or pressures and to incorporate them in network calculations. Most ventilation engineers prefer to make every non-horizontal airway with a density change part of a new individual mesh (closed by a corresponding vertical air column and connecting horizontal airways) and to simulate the additional natural drafts in these meshes by one additional power source per mesh, located in the non-horizontal airway.

Since natural drafts generated by a fire will change the airflow distribution, an iterative method of successive density and natural draft precalculations and ventilation network calculations has to be used for the proper simulation of a fire. If larger changes in the operating points of the fans take place and the network calculations are based on pressures, the particular nature of p_N (chapter IV.B.a.) has to be considered too. In order to keep the work for the design of fire emergency plans in tolerable limits, ventilation engineers are usually content to find, with the help of their network calculations, the largest possible ventilation disturbances which could be caused by a fire. The Committee on Mine Ventilation of the ECSC (35) suggests therefore that an additional natural ventilation head or pressure based on twice the ordinary air temperatures in this airway be assumed in ascensionally ventilated airway at a fire. It has been shown (chapter VI.A.b.) that at such a temperature the largest disturbances occur. The present practice in the West German mines in investigating the danger of airflow reversals in descensionally ventilated airways is to assume for the natural draft a value which has been calculated from the empirically determined and with a generous safety factor supplied formula (chapter IV.B.c. and V.C.)

$$p_N = 0.133 \, \Delta \, Z \, (t_m - t_a)$$

c) Future prospects of analog computer application

Analog computers have been proven to be very valuable tools for performing ventilation network calculations. The majority of them do not, however, allow the complete simulation of all mesh

Table 19. Relative Results Obtained by Network Calculations with Neglection of Natural Drafts (40)

Airway	Airflow Ratio (%) Fan Operating	Fan Stopped
A - B	99.9	99.3
B - C	98.8	98.2
B - D	103.6	155.9
C - D	96.4	76.9
D - E	104.4	181.3
D - F	96.1	73.7
E - F	164.5	-39.7
F - G	103.9	150.5
C - H	99.8	95.4
E - I	94.5	70.4
H - I	96.3	70.4
I - G	93.3	61.4
H - K	103.6	148.3
I - K	97.2	78.4
G - L	99.4	95.4
K - L	100.3	103.1
L - N	99.9	99.3

Table 20a. Junction Temperatures and Elevations of Mine Shown in Fig. 70

Junction No	Temperature °F	Elevation ft	Junction No	Temperature °F	Elevation ft
1	50.0	+ 114	38	80.1	-2473
2	66.4	-2462	40	85.6	-2786
16	86.3	-2245	41	82.7	-2185
17	76.5	-2462	42	81.2	-2452
18	64.4	-2463	43	79.2	-2463
21	73.7	-2462	44	75.8	-2466
22	82.2	-1938	45	68.5	-2467
23	80.1	-2787	46	77.2	-2787
24	78.0	-2785	47	87.3	-2247
25	77.6	-2785	48	68.2	-2465
26	84.5	-2465	52	66.6	-2465
27	82.6	-1942	54	66.2	-2235
28	85.1	-2467	56	80.1	-2240
35	79.5	-2238	57	79.2	-1943
36	79.3	-2235	58	64.9	+ 88
37	66.7	-2466	59	79.2	-2239

equations and their network simulation is therefore only an approximation. If they allow a complete simulation, the mesh equations have to be manually established, which requires considerable work. The simulation of mine fires, with the necessary calculations of mass flow and density changes, the subsequent introduction of new conductors and power sources and the adjustment of airway resistances calls for so much additional work, that most ventilation engineers are content to detect the maximal ventilation disturbances.

It seems in principle not to be too difficult to develop analog computers, which are better suited for the simulation of mine fires and which would not require any manual calculations. Their chances to compete economically with the electronic digital computers seem, however, to be extremely slim.

E) Digital computers

a) Existing programs for ventilation network calculations

Analog computers for ventilation network calculations found their widest application in the hot and gassy Continental European coal mines. Around 1960 13 of the large electromechanical and electronic computers, each at a purchasing price of between $50,000 and $100,000 were used in West Germany alone. Their high cost induced European ventilation engineers immediately to test the usefulness of electronic digital computers, once the latter appeared on the market. The first ventilation network calculations with digital computers seem to have been conducted 1958 in Belgium and West Germany (27, 38). The programs used contained little more than the straightforward application of a method of successive approximation by balancing heads, suggested 1936 by H. Cross (28). Since this is by far the more popular one of the two methods developed by Cross, the other one working with balancing flowrates, it is usually referred to as "the Cross method". Its description can be omitted since it is contained in nearly all earlier papers on the use of digital computers for ventilation network calculations.

It became soon obvious that the then still slow digitial computers could match the performance of the well established analog computers only when an optimal rate of convergence of the Cross method was assured. Although several other iteration methods were tried (73) the programs which finally emerged in West Germany in 1960 were based on the Cross method with the loop selection done by the computer in such a way that the airways with high resistance factors (76) or high products R * Q appeared in a few loops as possible. From 1961 on it became customary furthermore to include for accurate calculations the natural ventilation heads in every loop and to have the computers calculate these heads from information on temperature and elevation of every junction (41, 30). Since then, ventilation network calculations with these programs have become routine for most German ventilation engineers and little need for their improvement has been felt to be necessary. Only lately some work has again started on faster mesh selection procedures and on new programs not based on the Cross method, which sacrifice speed for considerable

savings in storage requirements. Programs for ventilation network calculations for many years have been included in the program libraries of computer manufacturers and were freely issued to interested engineers in other countries. It has been reported (141) that in 1969 of the total of 28 West German coal mining companies 18 conducted their ventilation network calculations with the help of digital computers.

A computer program designed by French ventilation engineers in 1961 (25) is based on the Cross method, too. They report (113) that this program could on an IBM 704 computer perform 50 network calculations for networks with up to 207 branches and 39 independent meshed within 30 minutes.

More recently a new program was developed by the French CERCHAR (43, 141) which is different from the conventionally used Cross method and shall therefore be described in more detail. It is similar to Cross' method of successive approximation by balancing flowrates (28). In this less known method, to every airway is initially assigned such a pressure loss that the mesh equations are satisfied. The airflow calculated from the resistance equation $p_L = R\,Q^2$ will then not satisfy the junction equations $\sum Q = 0$. From the deviation obtained for a particular junction a pressure loss correction Δp_L for all airways sharing this junction is derived, which for the simple case of airways without fans would be (76).

$$\Delta p_L = -\frac{2\sum Q_i}{\sum \frac{Q_i}{p_{Li}}} = -\frac{2\sum \text{sign}(Q_i)\sqrt{\frac{|p_{Li}|}{Ri}}}{\sum \frac{1}{\sqrt{R_i\,|p_{Li}|}}}$$

The two squareroots make the calculation of Δp_L and, therefore, the whole method slow and for this reason it is not much favored.

The new CERCHAR program assigns a ventilation potential P to every junction and satisfies in this way the mesh equations. If a junction 0 has the potential P_o and is connected by n airways with n junctions having the potentials P_1, P_2, ... P_n, the sum of all air quantities entering and leaving this junction is a function of P_o and can be calculated from

$$\sum Q_{P_o} = \sum_{i=1}^{n} - \text{sign}(P_i - P_0)\sqrt{\frac{P_i - P_0}{R_i}} = \sum \frac{P_0 - P_i}{\sqrt{R(P_i - P_0)}}$$

For one and only one value of $P_0 = P_{0C}$ one will obtain $\sum Q_{Poc} = 0$ and satisfy the junction equation. To avoid the correction of P_0 with the above given expression for Δp_L, which is slow to handle, $\sum Q_{Po}$

is considered to be a linear function of P_0. An improved value P_0 can then be obtained from

$$P_0' = \frac{P_i \sum Q_{PO} - P_0 \sum Q_{Pi}}{\sum Q_{PO} - \sum Q_{Pi}}$$

The advantage of this program is seen in less storage requirements than other programs have. A network of 380 branches with 255 junctions requires only 6000 addresses. A disadvantage is a longer computing time and a less convenient preparation of the input data.

Russian ventilation engineers are using the Cross method also (1). Other iteration methods are tried, however, (34, 130). It is claimed that several of them (34) have a better convergence than the Cross method when the latter is not supported by a convergence accelerating loop selection. They require estimated values for the airflow distribution, which are not too distant from the real values. If they are not available, a preliminary network calculation based on linear relations between head- or pressure losses and air quantities is recommended.

Although the Cross method was, in 1951 in Great Britain (109), modified for its application to mine ventilation networks and convergence criteria were established, little work on computer programs for network calculations became known. In 1964 a program which still required a manual mesh assembly (80) and in 1966 an improved version with the mesh assembly done by the computer (79) were described in the literature. In 1967 the National Coal Board issued a manual for the users of their computer services (88) describing the then introduced standard program for ventilation network calculations. It is, except for the organization of input and output which must accommodate the local conditions, very similar to the programs used in West Germany and to the program used at Michigan Technological University, which is later described in more detail.

Judging from the literature, Japanese ventilation engineers started to conduct network calculations with digital computers in 1961 (47) and several programs have since been described (3, 48, 93). All of them seem to be based on the Cross method. The last program (3) provides a convergence improving mesh assembly done by the computer in such a way, that high resistance branches appear in as few meshes as possible and it provides a calculation of the natural ventilation pressure from the specific weight of the air in each junction. Furthermore it has been combined with a program for the precalculation of the wet- and drybulb temperatures of the air as function of depth, heat exchange between rock and air, water evaporation and seasonal surface temperature changes.

In the USA considerable work was devoted to the design of ventilation network programs by the Department of Mining, Pennsylvania State University. A first program (46) designed to prove the use-

fulness of digital computers was described in 1963. An improved version of this program (126), allowing the inclusion of fan characteristics as second order polynomials was discussed in 1964. Both programs still require that the assembly of the meshes and the balancing of airflows at junctions be done manually.

In 1967 a paper on a much more sophisticated program was published (137) where mesh assembly and assignment of initial airflow values was done by the computer. The procedure followed is similar to the one used by European ventilation engineers (76) with the difference that not only airways with high resistance factors but also airways with fans are made to appear in as few meshes as possible. Natural ventilation pressures can be included as constant pressure sources in non-horizontal airways. Fan characteristics are now described by polynomials of up to the 6th order. It is emphasized that, in applying the Cross method, the corrections to the branch flows are made immediately after the corrections have been obtained for a mesh. This has always been European practice, too (38). The calculation of an example with 203 branches, 146 junctions, 58 meshes 3 constant pressure sources and 3 fans on an IBM 7074 computer in 264 seconds is described, which required 154 iterations.

A new version of the program was described in 1970 (138). Its main difference is the introduction of so called fixed quantity airways, which do not follow a parabola $p_L = R\,Q^2$ but the function Q = constant. The assumption of such airways is a valuable planning aid and was always a feature in larger analog computers (9,39,124). Consequently, they were provided in most programs aimed at replacing analog by digital computers too (30,76).

The Department of Mining Engineering, Virginia Polytechnic Institute, in 1968 published a program for ventilation network calculations under the name VPI-OCR-Ventsim Program (16). It is based on the Cross method also and provides several possibilities not contained in other programs, such as calculation of friction factors, regulator dimensions, fan speed and blade positions for a minimum horsepower. The mesh assembly is, however, done in a unique way, whose quality is hard to judge since the program description (16) does not contain the actual program statements. The computer traces paths through the network from atmosphere to atmosphere. Pairs of paths are then compared to eliminate duplicate airways. Those airways remaining, unduplicated, constitute a loop. To support this procedure the input data for the airways must be entered in an order which indicates these paths, otherwise "detrimental overlap" can occur with the result that the junction equations for certain junctions are violated. It can happen that an airway is not included in a loop in which case a warning message is printed out and the user has to decide whether this airway should or should not have been included.

Apart from the inconvenience of helping the computer to trace paths by suggesting them manually, this method of mesh assembly seems to have serious deficiencies. For a network calculation mesh equations for all independent meshes which exist in the network and

whose number is $N_m = N_b - N_j + 1$ have to be used, otherwise the mathematical description of the network is incomplete and a solution is impossible. The fact that each airway is included in at least one loop does not guarantee that all independent mesh equations have been established. The fact that airways are not included in loops always indicates that the mathematical description of the network is incomplete and one should not proceed with the calculation. The possibility of incorrect junction equations should not exist in a mathematically sound program.

The VPI-OCR-Ventsim program does not provide for natural ventilation pressures, although this could certainly be done and is not such a handicap as the unhandy and most probably imcomplete mesh assembly.

A complete different program for network calculations was developed by Wang and Pana (139). It applies the linear programming technique to networks with a prescribed airflow in every branch (controlled splitting). The aim is to find for a given number and location of fans the fan pressures as well as the location and pressure losses of the necessary regulators in such a way that a minimum fan power is required. Although this is a type of network calculation very often used in coal mines, it is not capable of determining airflow distributions. They are prescribed and enforced with regulators.

Michigan Technological University has used, since 1967, a program which is based on the programs of German ventilation engineers and, as mentioned above, is very similar to the standard program of the British NCB issued in 1967. Because it did not constitute a genuine novelty, the author saw no reason to describe it in a publication especially since meanwhile more than 100 copies have been distributed to interested persons. Two versions of this program were written to suit Michigan Tech needs and facilities. One version comprises only the core program and allows one network calculation per computer run. It is mainly used by students. The other program allows an unlimited number of network calculations per computer run and serves research and consulting needs.

The judgement of computer programs depends very much on customs and personal preferences. With all the accumulated experience they are, moreover, so fast to change that any argument about special merits of a program, as long as it gives the correct results, makes little sense. The author feels, however, that the Michigan Tech program offers certain advantages, which make it handy to use. It provides, of course, all the features of modern programs, such as mesh assembly and balancing of airflows at junctions, four types of airways, namely normal airways, fixed quantity airways, constant pressure fans, and fans operating on a characteristic described by a polynomial. Besides this, it has a very good convergence since the meshes are chosen in such a way that airways with high products R * Q are made "basic" or "Primary" branches (76, 137) and appear in as few meshes as possible. If the computer finds that the convergence is poor, new primary branches are calculated with values

for Q, which have been obtained by the computer in the meantime. Fans are made secondary branches and there is no limitation in their number. The necessary number of iterations rarely exceeds 10 - 20, even in large networks.

The natural ventilation heads can be calculated by the computer from information on temperature and elevation of every junction. The formula

$$p_{NS} = \frac{\gamma_S}{T_m} \oint T \, dZ$$ is for this purpose approximated by (30,88)

$$p_{NS} = \gamma_S \frac{n \sum (T_s Z_f - T_f Z_s)}{\sum (T_s + T_f)}$$

where n = number of airways in loop

T_s, Z_s = temperature and elevation of starting junction of airways in loop

T_f, Z_f = temperature and elevation of finishing junction of airways in loop

This approximation assumes a linear change of temperature with elevation. If this is not the case, intermediate junctions can be introduced. Network calculations can be performed with and without consideration of the natural ventilation heads by the computer. If preferred, the natural ventilation can be simulated by fictitious fans in non-horizontal airways, too.

The airway cards do not have to be arranged in any specific sequence. Consequently they do not need rearrangement after changes of the network have been performed. The output is limited to those data which the ventilation engineer needs for his work.

The version of the Michigan Tech program, which allows the calculation of an unlimited number of network calculations in one computer run, checks if the input data are complete and, as far as the computer can decide, correct. If a network whose data are stored in the computer is to be modified, only the changes have to be read in. The computer checks the input data and, in order to keep a log of what has been done, prints these changes together with the results of the network calculation out.

If only the order of magnitude or tendencies of the results are of interest, the network calculation can be performed without consideration of natural ventilation heads or fan characteristics to increase the speed. Fan characteristics, once read into the computer, are stored and not erased if momentarily not used. This facilitates the comparison of different fans for a certain ventilation job.

All fixed quantity airways can be converted into regular airways with the resistance they had in the last network calculation. This

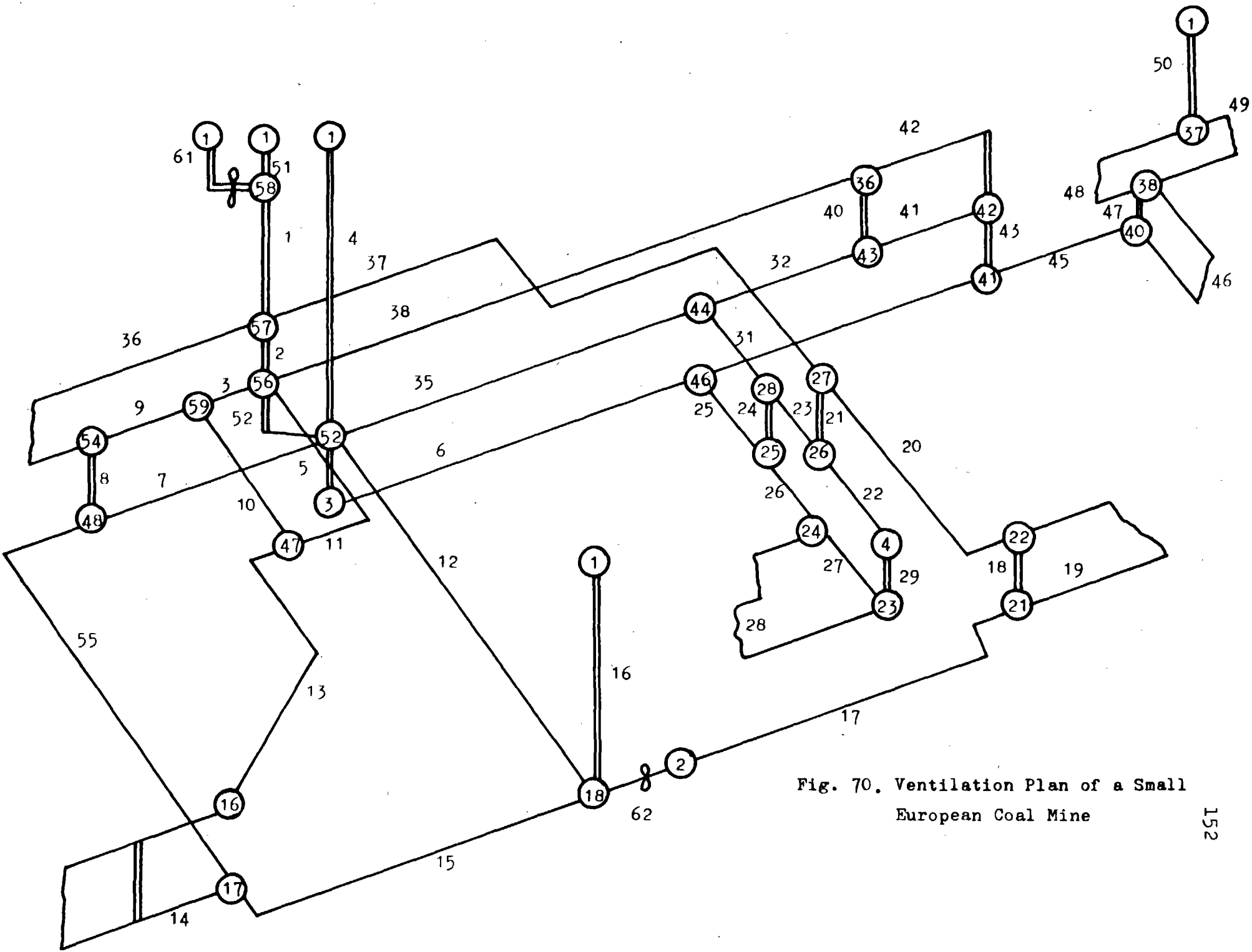

Fig. 70. Ventilation Plan of a Small European Coal Mine

Table 20b. Network Calculation for the Mine Shown in Fig. 70, Both Fans Working

REGULAR AIRWAYS

AIRWAY	FROM	TO	TYPE	RESISTANCE	AIRFLOW	PRESSURE LOSS
1	57	58	0	0.359	323718.	3.762
2	56	57	0	0.072	233695.	0.393
3	59	56	0	0.854	68139.	0.397
4	1	52	0	0.156	169479.	0.448
5	52	3	0	0.048	49325.	0.012
6	3	46	0	0.360	49325.	0.088
8	48	54	0	1.066	93599.	0.934
9	54	59	0	1.260	63759.	0.512
10	47	59	0	1.385	4380.	0.003
11	47	56	0	3.630	33168.	0.399
12	52	18	0	2.400	30053.	0.217
13	16	47	0	18.360	37548.	2.588
14	17	16	0	5.572	37548.	0.786
15	18	17	0	4.324	95698.	3.960
16	1	18	0	0.479	124535.	0.743
17	2	21	0	2.307	58891.	0.800
18	21	22	0	1888.233	3982.	2.994
19	21	22	0	9.923	54909.	2.992
20	22	27	0	3.239	58891.	1.123
21	26	27	0	4.000	1292.	0.001
22	4	26	0	3.772	28825.	0.313
23	26	28	0	1.108	27533.	0.084
24	25	28	0	474.065	4924.	1.149
25	46	25	0	0.821	33748.	0.094
26	25	24	0	1.437	28825.	0.119
27	24	23	0	124.385	5005.	0.312
28	24	23	0	5.500	23819.	0.312
29	23	4	0	3.900	28825.	0.324
31	28	44	0	2.047	32457.	0.216
32	44	43	0	2.285	46050.	0.485
35	52	44	0	77.702	13593.	1.436
36	54	57	0	14.000	29840.	1.247
37	27	57	0	20.002	60183.	7.245
38	36	56	0	6.265	91327.	5.225
40	43	36	0	2.966	51215.	0.778
41	42	43	0	3.500	5166.	0.009
42	42	36	0	4.931	40112.	0.793
43	41	42	0	4.565	45278.	0.936
44	46	41	0	41.490	15576.	1.007
45	40	41	0	0.475	29701.	0.042
46	38	40	0	13.375	26901.	0.968
47	38	40	0	1234.019	2800.	0.968
48	37	38	0	14.500	14851.	0.320
49	37	38	0	14.500	14851.	0.320
50	1	37	0	0.995	29701.	0.088
51	1	58	0	441.000	16136.	11.482
52	52	56	0	46.882	41063.	7.905
55	17	48	0	5.450	58150.	1.843

FIXED QUANTITY AIRWAYS

AIRWAY	FROM	TO	TYPE	RESISTANCE	AIRFLOW	PRESSURE LOSS
7	52	48	-1	47.918	35449.	6.022

FANS

AIRWAY	FROM	TO	TYPE	CONST. PRESS.	AIRFLOW	FAN PRESSURE
61	58	1	1	10.000	339854.	11.482
62	18	2	1	4.000	58891.	4.077

THE FOLLOWING FANCHARACTERISTICS ARE STORED

AIRWAY	Q	P	Q	P	Q	P
61	100000.	13.10	200000.	13.20	280000.	12.32
62	20000.	3.60	40000.	3.97	55000.	4.08

Table 20c. Network Calculation for Reduced Resistance of Upcast Shaft

THE FOLLOWING AIRWAYS HAVE BEEN CHANGED

AIRWAY	FROM	TO	TYPE	RESISTANCE	AIRFLOW
1	57	58	0	0.032	400000.
2	56	57	0	0.024	300000.

NEW NO OF AIRWAYS 51 NEW NO OF JUNCTIONS 32

REGULAR AIRWAYS

AIRWAY	FROM	TO	TYPE	RESISTANCE	AIRFLOW	PRESSURE LOSS
1	57	58	0	0.032	366334.	0.429
2	56	57	0	0.024	268349.	0.173
3	59	56	0	0.854	78140.	0.521
4	1	52	0	0.156	192133.	0.576
5	52	3	0	0.048	58960.	0.017
6	3	46	0	0.360	58960.	0.125
8	48	54	0	1.066	103705.	1.146
9	54	59	0	1.260	73090.	0.673
10	47	59	0	1.385	5050.	0.004
11	47	56	0	3.630	38022.	0.525
12	52	18	0	2.400	33926.	0.276
13	16	47	0	18.360	43072.	3.406
14	17	16	0	5.572	43072.	1.034
15	18	17	0	4.324	111328.	5.359
16	1	18	0	0.479	139348.	0.930
17	2	21	0	2.307	61947.	0.885
18	21	22	0	1883.233	4185.	3.308
19	21	22	0	9.923	57761.	3.311
20	22	27	0	3.239	61947.	1.243
21	26	27	0	4.000	5423.	0.012
22	4	26	0	3.772	34880.	0.459
23	26	28	0	1.108	29458.	0.096
24	25	28	0	474.065	5915.	1.658
25	46	25	0	0.821	40795.	0.137
26	25	24	0	1.437	34880.	0.175
27	24	23	0	124.385	6059.	0.457
28	24	23	0	5.500	28821.	0.457
29	23	4	0	3.900	34880.	0.474
31	28	44	0	2.047	35372.	0.256
32	44	43	0	2.285	51716.	0.611
35	52	44	0	77.702	16344.	2.076
36	54	57	0	14.000	30615.	1.312
37	27	57	0	20.002	67370.	9.078
38	36	56	0	6.265	104730.	6.872
40	43	36	0	2.966	58697.	1.022
41	42	43	0	3.500	6981.	0.017
42	42	36	0	4.931	46033.	1.045
43	41	42	0	4.565	53014.	1.283
44	46	41	0	41.490	18165.	1.369
45	40	41	0	0.475	34850.	0.058
46	38	40	0	13.375	31564.	1.333
47	38	40	0	1234.019	3286.	1.333
48	37	38	0	14.500	17425.	0.440
49	37	38	0	14.500	17425.	0.440
50	1	37	0	0.995	34850.	0.121
51	1	58	0	441.000	15595.	10.711
52	52	56	0	46.882	47458.	10.559
55	17	48	0	5.450	68256.	2.539

FIXED QUANTITY AIRWAYS

AIRWAY	FROM	TO	TYPE	RESISTANCE	AIRFLOW	PRESSURE LOSS
7	52	48	-1	65.071	35449.	8.177

FANS

AIRWAY	FROM	TO	TYPE	CONST. PRESS.	AIRFLOW	FAN PRESSURE
61	58	1	1	10.000	381918.	10.711
62	18	2	1	4.000	61947.	4.068

THE FOLLOWING FANCHARACTERISTICS ARE STORED

AIRWAY	Q	P	Q	P	Q	P
61	100000.	13.10	200000.	13.20	280000.	12.32
62	20000.	3.60	40000.	3.97	55000.	4.08

Table 20d. Network Calculation for Reduced Temperatures in Intake Airways

THE FOLLOWING JUNCTIONS HAVE BEEN CHANGED

JUNCTION	TEMPERATURE	ELEVATION
1	32.00	114.
3	59.30	-2467.
17	73.50	-2462.
18	59.30	-2463.
37	58.90	-2466.
46	73.00	-2787.
52	58.80	-2465.

REGULAR AIRWAYS

AIRWAY	FROM	TO	TYPE	RESISTANCE	AIRFLOW	PRESSURE LOSS
1	57	58	0	0.032	375730.	0.452
2	56	57	0	0.024	275262.	0.182
3	59	56	0	0.854	79873.	0.545
4	1	52	0	0.156	199793.	0.623
5	52	3	0	0.048	61273.	0.018
6	3	46	0	0.360	61273.	0.135
8	48	54	0	1.066	105875.	1.195
9	54	59	0	1.260	74570.	0.701
10	47	59	0	1.385	5302.	0.004
11	47	56	0	3.630	38875.	0.549
12	52	18	0	2.400	37271.	0.333
13	16	47	0	18.360	44179.	3.583
14	17	16	0	5.572	44179.	1.088
15	18	17	0	4.224	114605.	5.679
16	1	18	0	0.479	139853.	0.937
17	2	21	0	2.307	62521.	0.902
18	21	22	0	1888.233	4223.	3.367
19	21	22	0	9.923	58298.	3.372
20	22	27	0	3.239	62521.	1.266
21	26	27	0	4.000	6642.	0.018
22	4	26	0	3.772	36363.	0.499
23	26	28	0	1.108	29721.	0.098
24	25	28	0	474.065	6161.	1.799
25	46	25	0	0.821	42523.	0.148
26	25	24	0	1.437	36363.	0.190
27	24	23	0	124.385	6323.	0.497
28	24	23	0	5.500	30039.	0.496
29	23	4	0	3.900	36363.	0.516
31	28	44	0	2.047	35882.	0.264
32	44	43	0	2.285	52841.	0.638
35	52	44	0	77.702	16959.	2.235
36	54	57	0	14.000	31306.	1.372
37	27	57	0	20.002	69162.	9.568
38	36	56	0	6.265	107668.	7.263
40	43	36	0	2.966	60328.	1.079
41	42	43	0	3.500	7487.	0.020
42	42	36	0	4.931	47341.	1.105
43	41	42	0	4.565	54828.	1.372
44	46	41	0	41.490	18749.	1.459
45	40	41	0	0.475	36079.	0.062
46	38	40	0	13.375	32677.	1.428
47	38	40	0	1234.019	3402.	1.428
48	37	38	0	14.500	18040.	0.472
49	37	38	0	14.500	18040.	0.472
50	1	37	0	0.995	36079.	0.130
51	1	58	0	441.000	15446.	10.521
52	52	56	0	46.882	48847.	11.186
55	17	48	0	5.450	70427.	2.703

FIXED QUANTITY AIRWAYS

AIRWAY	FROM	TO	TYPE	RESISTANCE	AIRFLOW	PRESSURE LOSS
7	52	48	-1	69.391	35449.	8.720

FANS

AIRWAY	FROM	TO	TYPE	CONST. PRESS.	AIRFLOW	FAN PRESSURE
61	58	1	1	10.000	391175.	10.521
62	18	2	1	4.000	62521.	4.067

THE FOLLOWING FANCHARACTERISTICS ARE STORED

AIRWAY	Q	P	Q	P	Q	P
61	100000.	13.10	200000.	13.20	280000.	12.32
62	20000.	3.60	40000.	3.97	55000.	4.08

Table 20e. Network Calculation for the Case of a Failure of Both Fans

THE FOLLOWING AIRWAYS HAVE BEEN CHANGED

AIRWAY	FROM	TO	TYPE	RESISTANCE	AIRFLOW
61	58	1	0	0.010	150000.
62	18	2	0	0.010	15000.

NEW NO OF AIRWAYS 51 NEW NO OF JUNCTIONS 32

REGULAR AIRWAYS

AIRWAY	FROM	TO	TYPE	RESISTANCE	AIRFLOW	PRESSURE LOSS
1	57	58	0	0.032	145267.	0.068
2	56	57	0	0.024	107969.	0.028
3	59	56	0	0.854	31938.	0.087
4	1	52	0	0.156	81874.	0.105
5	52	3	0	0.048	30694.	0.005
6	3	46	0	0.360	30694.	0.034
7	52	48	0	69.390	13688.	1.300
8	48	54	0	1.066	40696.	0.177
9	54	59	0	1.260	29655.	0.111
10	47	59	0	1.385	2283.	0.001
11	47	56	0	3.630	15554.	0.088
12	52	18	0	2.400	11083.	0.029
13	16	47	0	18.360	17837.	0.584
14	17	16	0	5.572	17837.	0.177
15	18	17	0	4.324	44846.	0.870
16	1	18	0	0.479	48989.	0.115
17	2	21	0	2.307	15227.	0.053
18	21	22	0	1888.233	1026.	0.199
19	21	22	0	9.923	14201.	0.200
20	22	27	0	3.239	15227.	0.075
21	26	27	0	4.000	11031.	0.049
22	4	26	0	3.772	18630.	0.131
23	26	28	0	1.108	7599.	0.006
24	25	28	0	474.065	3089.	0.452
25	46	25	0	0.821	21719.	0.039
26	25	24	0	1.437	18630.	0.050
27	24	23	0	124.385	3243.	0.131
28	24	23	0	5.500	15387.	0.130
29	23	4	0	3.900	18630.	0.135
31	28	44	0	2.047	10688.	0.023
32	44	43	0	2.285	18053.	0.074
35	52	44	0	77.702	7365.	0.421
36	54	57	0	14.000	11041.	0.171
37	27	57	0	20.002	26257.	1.379
38	36	56	0	6.265	41433.	1.076
40	43	36	0	2.966	22886.	0.155
41	42	43	0	3.500	4833.	0.008
42	42	36	0	4.931	18547.	0.170
43	41	42	0	4.565	23380.	0.250
44	46	41	0	41.490	8975.	0.334
45	40	41	0	0.475	14405.	0.010
46	38	40	0	13.375	13047.	0.228
47	38	40	0	1234.019	1359.	0.228
48	37	38	0	14.500	7203.	0.075
49	37	38	0	14.500	7203.	0.075
50	1	37	0	0.995	14405.	0.021
51	1	58	0	441.000	-688.	-0.021
52	52	56	0	46.882	19045.	1.701
55	17	48	0	5.450	27009.	0.398
61	58	1	0	0.010	144578.	0.021
62	18	2	0	0.010	15227.	0.000

NETWORK CONTAINS NO FIXED QUANTITY AIRWAYS

NETWORK CONTAINS NO FANS

THE FOLLOWING FANCHARACTERISTICS ARE STORED

AIRWAY	Q	P	Q	P	Q	P
61	100000.	13.10	200000.	13.20	280000.	12.32
62	20000.	3.60	40000.	3.97	55000.	4.08

is a valuable aid since the conversion is an absolute necessity for emergency plans. The program provides, furthermore, for a stated number of copies of the output as are usually needed for reports written by the ventilation engineer.

The Michigan Tech program does not contain any provisions for the determination of airway resistances, since separate programs are used for this purpose. The precalculation of resistance factors from stated friction factors and airway dimensions could easily be added, if desired.

As an example, the output of 4 consecutive network calculations for a small network comprising 49 airways and 2 fans will be given. Fig. 70 shows the isometric ventilation plan for the mine, a small Continental European coal mine working 7 longwall faces. Table 20a shows the input list of temperatures and elevations for the junctions, from which the natural ventilation heads are determined. This list is not printed out with every single network calculation, only changes are printed. Table 20 b shows the results of a network calculation, when both fans are working according to their fan characteristic and the airways have the indicated resistance factors. For the results in Table 20 c it has been assumed that the buntons in the ventilation shaft have been removed and the resistance of airways 1 and 2 has consequently decreased. Table 20 d shows how a drop of the surface temperature from 50.0 to 32.0°F and the subsequent temperature changes in the intake airways effects the ventilation. And Table 70 e shows the airflow distribution when at this surface temperature both fans fail. Note that the fixed quantity airway 7 has been converted into a regular airway. The 3 points indicated for every stored fan characteristic serve to identify the characteristic only. The stored number of points is usually 5 - 10 per fan.

b) Simulation of mine fires

All three methods discussed in chapter VI.C. to describe ventilation networks can be used for ventilation network calculations with digital computers. The first method, however, finds little favor with ventilation engineers, who seem to dislike the use of head and mass flow units. The third method, which is frequently favored in network calculations with analog computers is not too advantageous, since it requires a consideration of density changes as well for the volume flows as for the resistance facts. Moreover, if correctly applied, the calculation of the natural ventilation pressure is not easy since it is considerably influenced by pressure loss and fan pressures. The compromise between the methods 1 and 3, method 2, which is based on heads and mass flows but expresses them as pressures and volume flows by applying a constant density as conversion factor, seems to be the method best suited for digital computers.

It is hard to judge if the existing programs have consciously been based on this method or if they use method 3 and simply neglect density changes. All of them use pressure and volume flow units and

only a few (129) contain any special provisions to accommodate the volume flow changes with air density. The terminology used is generally that of the 3rd method. As long as the air density changes are not too large, the errors resulting from their neglect quite frequently go undetected and the ventilation engineer is under little pressure to use the correct network description.

This is, however, no longer the case when the influence of mine fires on ventilation systems are to be investigated. In any case, there is no reason not to apply correct formulas when their use is as easy as that of the wrong ones.

Only the second method to describe ventilation networks will be discussed for fire emergency plans, since the author feels that this is the best suited method. It uses three types of equations, the resistance equation

$$p_{LS} = R_S Q_S^2 \qquad \text{with } R_S = f \frac{L\ P}{8\ g\ A^3} \gamma_S^3 v_{msq}^2$$

the junction equations

$$\sum Q_S = 0 \qquad \text{with } Q_S = G/\gamma_S$$

and the mesh equations

$$\sum p_{LS} - \sum p_{FS} - p_{NS} = 0$$

$$\text{with } p_{NS} = -\gamma_S \oint v\, dp \approx \frac{\gamma_S}{T_m} \oint T\, dZ$$

All newer programs can either handle these equations or can be easily modified to handle them.

As discussed in chapter VI.D.b. mine fires can:

physically change airway characteristics,
add to the mass flow,
change the air density, which in turn effects volume flow, resistance factors and creates natural drafts.

No simulation of physical airway changes has become known so far, but if they can be described mathematically there is no difficulty in including them in a network calculation.

Increases in mass flow can be simulated in digital computers in the same way as in analog computers by a separate path leading from the surface to the point where the increase occurs. The order of magnitude for these increases and the fact that they are quite frequently neglected as an additional safety factor has been discussed.

Volume flow changes due to density changes do not have to be considered since the network description is based on mass flows.

Resistance factors are proportional to the mean square specific

volume

$$v_{msq}^2 = \frac{1}{L} \int v^2 \, dL$$

of the air in the airway under consideration. As discussed in chapter D.b.2 the latter can be expressed by

$$v_{msq}^2 = \left(\frac{v_1}{T_1}\right)^2 \frac{1}{L} \int T^2 \, dL = \left(\frac{v_1}{T_1}\right)^2 (T_{msq})^2$$

Although a mathematical expression for T_{msq}^2, at least under the assumption of a steady state heat exchange between air and airway wall, is easy to derive (chapter III.A.), no computer program with automatic adjustments of the resistance factors has become known. T_{msq}^2 is either obtained from charts and manually fed into the computer or the increase of the resistance factor by fires, the throttling effect, is neglected altogether as an additional safety factor. Frequently, for fires in non-horizontal airways, the throttling effect is contained in the data used for the simulation of the natural draft in this airway.

Almost all newer computer programs contain provision for consideration of natural drafts but several require that these be calculated manually and the pertinent program descriptions give no guidelines on how to do it. If, as here recommended, the second method of network description is used, the correct way to calculate the natural draft is to employ the formula

$$p_{NS} = -\gamma_S \oint v \, dp$$

The precalculation of γ, v, and p is cumbersome and possible only when the pressure distribution in the network is known. Computer programs, which calculate the natural draft from input data prefer, therefore, with few exceptions (3, 141), the approximation

$$p_{NS} \approx \frac{\gamma_S}{T_m} \oint T \, dZ$$

This approximation is especially handy when natural drafts developed by mine fires are to be considered since it is not too difficult to make halfway reasonable assumptions on the temperature changes caused by the fires. Computer programs working with this approximation found immediate application for fire emergency plans. The temperatures are obtained from charts as functions of airway dimensions and air quantities and fed manually into the computer or such temperatures, which have the worst possible effect on the ventilation, are assumed. Some ventilation engineers follow the same practice they are accustomed to from the analog computers. Manually prepared charts of heads or pressures developed by fires as functions of the air quantity are fed into the computer and used in the network calculation like fan characteristics.

Although the preparation of fire emergency plans with digital computers became routine in the early sixties (129) all methods used

to simulate throttling effects and natural drafts are still very crude and rely on manual support. No program of general validity became known which calculates the temperatures and other air properties for all airways affected by a fire. Such programs would require repeated alternating network calculations, temperature precalculations and, if the nature of the fire makes it sensible, a precalculation of fire properties. That such a superimposed iterative procedure for network calculations and temperature precalculations shows a reasonable convergence is proven by the fact that a similar program for ordinary ventilation conditions needed reportedly (3) only 2 - 3 cycles until a satisfying result was achieved.

c) Concluding remarks

Digital computers do not suffer from any mathematical limitations. They have become more accessible and cheaper than equivalent analog computers for ventilation network calculations and have widely replaced them. In the 15 years of their application a greater number of programs have been developed which allow complete simulations of ventilation networks and provide all necessary service comfort. These programs have been used for more than 10 years in several countries to investigate routinely the influence of mine fires on the ventilation system of mines and to work out fire emergency plans. Since they were written for planning purposes under ordinary ventilation conditions, they need considerable support by manual calculations for the simulation of fires. The full potential of digital computers has in this respect not yet been exploited.

It seems possible without excessive work to adjust existing programs to the simulation of ventilation networks with internal fires. Since the temperature changes caused by the fire are mainly responsible for influences on ventilation, it seems advantageous to make this adjustment for use of those programs which already contain an automatic consideration of natural drafts based on temperatures.

BIBLIOGRAPHY

1. Abramov, F. A., Bojko, V. A. and Bulach, G.I., The Application of Fast Electronic Computers for the Calculation of the Mine Ventilation. Izvestija AN SSR, OTN, Metallurgija i Gornoe Delo 1963, No. 2, pp. 161-68.

2. Abramov, F. A.,Mosin, I. M. and Kremnev, O. A., Ventilation in Coal Mines at Fire. Ugol Ukrainy 6 (1962), No. 2, pp. 41-42.

3. Amano, K. and Shigeno, S., An Underground Ventilation Network Analysis and Estimation of Temperatures of Air Currents. A Decade of Digital Computing in the Mining Industry, pp. 433-57, AIME, New York, 1969.

4. Aprile, G., The Pneumatic Model of the Institute of Mineral Engineering Palermo for the Solution of Ventilation Networks. Rivista Min. Siciliana, March-April 1960.

5. Aprile, G., A Pneumatic Model for Solving Mine Ventilation Problems. Journ. Mine Vent. Soc. of S.A. 13 (1960), No. 12, pp. 207-09.

6. Baboin, M., Fire in the Plant Combes of the Coal Mine Roche-la-Molière. Annales des Mines Memoires, Vol. VI, 1934.

7. Baltajtis, V. J. and Markovic, M. J., Methods to Determine Some Properties of Mine Fires from the Composition of the Fumes. Izvestija VUZ, Gornyj Zurnal 10 (1967), No. 9, pp. 46-51.

8. Batzel, S., Determination of Thermal Properties in Mine Workings and Their Use for the Mathematical Solution of Climatic Problems. Bergbau-Archiv 13 (1952), H. 3/4, pp. 15-34.

9. Belugou, P. and Bertard, C., Concept and Execution of a Ventilation Computer at CERCHAR. Centre d'Etudes et Recherches des Charbonnage de France, Paper No. 1261, 1962.

10. Bogojavlenskij, V. A., The Specifics of Nonsteady-State Heat Transfer in Faces of Deep Mines. Izvestija VUZ, Gornyj Zurnal 1961, No. 9, pp. 85-91.

11. Boldizsar, T., The Influence of the Temperature Field of the Earth Crust on the Heating of Air in Deep Mines. Bany. Lap. 1956, No. 9-10, pp. 1-24.

12. Boldizsar, T., A Numerical Graphical Method for the Calculation of Temperature Changes of Mine Air. Bergbau-Archiv 21 (1960), H. 2, pp. 17-27.

13. Both, W., New Insights for Fighting Open Mine Fires in Ascensional and Descensional Ventilation. Internat. Congress on Mine Ventilation. Joachimsthal (CSR) 1968.

14. Both, W., Experience with CO-Recorders for the Early Detection of Mine Fires. Glueckauf 1968, pp. 135-138.

15. de Braaf, W., Heating of Air in Shafts and Intake Airways. Geologie en Mijnbouw 1951, pp. 117-154.

16. Bucklen, E. P., Prelaz, L. J., Suboleski, S. C. and Lucas, J.R., Computer Applications in Underground Mining Systems, Vol. 5, Ventsim Program. Department of the Interior, Research and Development Report No. 37 (1968).

17. Budryk, B., Fires and Explosions in Mines. Polish Publishing House for Mining and Metallurgy (WHG), Katowice 1956.

18. Bystron, H., Canonical Ventilation Plans. Przeglad Gorniczy 1959, No. 3, pp. 228-233.

19. Bystron, H., Theory of the Airflow Direction During a Mine Fire. Annales des Mines de Belgique, 1965, No. 5.

20. Bystron, H., The Potential Plan. Przeglad Gorniczy 1959, No. 2, pp. 73-91.

21. Carslaw, H. S., Jaeger, J. C, Some Two-Dimensional Problems in Conduction of Heat with Circular Symmetry. Proc. London Math. Soc. 1940, p. 361.

22. Carslaw, H. S. and Jaeger, J. C., Conduction of Heat in Solids. 2nd Ed., Oxford 1959, Clarendon Press.

23. Champagnac, G, Extension of Budryk's Theory on Descensional Ventilation. ECSC, Doc. 1276/69d.

24. Carrier, W. H., Air Cooling in the Gold Mines on the Rand. AIME Techn. Publication No. 970, Sept. 1938.

25. Chaineaux, L. and Seeleman, D., Solution of Ventilation Problems by Computation. Revue de l'Industrie Minerale, 1961, pp. 517-531.

26. Committee on Mine Ventilation (British): The Assessment of Environmental Hazards in High Productivity Mining. The Mining Engineer 130 (1970-71) pp. 772-95.

27. Crombrugghe, O. and Remacle, J., Mine Ventilation Calculation of Networks with Meshes. Annales des Mines de Belgique 1958, pp. 875-97.

28. Cross, H., Analysis of Flow in Networks of Conduits or Conductors. Bulletin 286, 1936, Illinois University Engineering Experimental Station.

29. Dougherty, J. J., Control of Mine Fires. West Virginia University, 1969.

30. Duerr, H. G., The Calculation of Ventilation and Compressed Air Networks Based on Energy Princ Under Consideration of Thermal Energies with the Help of Electronic Digital Computers. Bergbau-Wissenschaften 10 (1963) No. 4, pp. 73-84.

31. Egorov, V. A. and Kondratenko, I.D., The Concentration of Gases and Their Occurrence in Mine Air During Fires, Explosions and Coal and Gas Outbursts. Ugol Ukr. No. 1, 1970, pp. 46-48.

32. Eisner, H.S. and Shepherd, W.C.F., Recent Research in Mine Fires. Transactions, The Inst. of Mining Engineers 113 (1953/54), pp. 1057-84.

33. Eisener, H. S. and Smith, P. B., Convection Effects from Underground Fires: The Backing of Smoke Against the Ventilation. SMRE Res. Rep. 96 (1954).

34. Evdakimov, A. G. and Jalovkin, B. D., Analysis of Methods for the Discreet Model Simulation of Stationary Flow Distribution Processes in Mine Ventilation Networks with Electronic Digital Computers. Izvest. VUZ, Gornyj Zurnal 1966, No. 3, pp. 101-108.

35. ECSC Publication Service, Stabilization of Mine Ventilation Systems During Open Fires. Doc. 13797/1/67/1.

36. Fluegge, G., Pressure Gradients for Judging the Stability of Ventilation Currents. Glueckauf-Forschungshefte 30 (1969), No. 3, pp. 135-45.

37. Goch, D. C. and Patterson, H. S., The Heatflow into Tunnels. Journ. Chem. Soc. S.A. 1940/41, pp. 117-28.

38. Greuer, R., Calculation of Ventilation Networks by Electronic Digital Computers. Glueckauf 1959, pp. 769-73.

39. Greuer, R., The Analog Computers "Ventilation Network Models" and Their Importance for the Mining Industry. Nachrichtentechnische Fachberichte, Fernwirktechnik III, Vol. 16 (1959), pp. 85-87.

40. Greuer, R., The Importance of Ventilation Pressure Surveys and the Presentation of Their Results. Glueckauf 1961, No. 18, pp. 1076-85.

41. Greuer, R., Natural Ventilation. Bergbau Archiv 1964, No. 3, pp. 39-59.

42. Greuer, R., The Natural Ventilation of Mines. Wharve, Graduate Study at Michigan Technological University, 1971, pp. 16-21.

43. Gunther, J., A New Method to Calculate Ventilation Networks. Rev. Ind. Miner. 49 (1967), No. 11, pp. 797-802.

44. Hartman, H. L., Mine Ventilation and Air Conditioning. The Ronald Press Company, New York, 1961.

45. Hartmann, I., Nagy, J., Barnes, R. W. and Murphy, E.M., Studies With High Expansion Foams for Controlling Experimental Coal Mine Fires. USBM Rep. Invest. 5419 (1958).

46. Hartman, H. L. and Trafton, B. O., Digital Computer May Find New Use in Determining Mine Ventilation Networks. Mining Engineering 1963, pp. 39-42.

47. Hashimoto, B., Analysis of Mine Ventilation Distribution Networks by Digital Computer. Waseda U. Bull. Sci. Eng. Res. Lab. No. 17 (1691), pp. 18-29.

48. Hashimoto, B., Asaeda, E. and Takakashi, K., Analysis of Mine Ventilation Networks by Digital Computer, Journ. Min. Metall. Inst. Japan 82 (1966), pp. 8-16.

49. Heerden, Van C., A Problem of Unsteady Heatflow in Connection with the Air Cooling of Collieries. Proceedings of the General Discussion on Heat Transfer. London. Institution of Mechanical Engineers 1951, p. 283.

50. Heise, F. and Drekopf, K., The Heat Equalization Mantle and Its Importance for Keeping Deep Mines Cool. Glueckauf 1923, pp. 81-88, 109-113.

51. Heise, F. and Drekopf, K., The Forming of Mine Temperatures and Possibilities to Influence Them. Glueckauf 1924, pp. 582-90, 608-14.

52. Hiramatsu, Y. and Kokado, J., An Investigation on the Cooling of Mines by Their Air Currents. Bergbau-Archiv 19 (1958), H. 1/2, pp. 16-40.

53. Hitchcock, J. A. and Jones, C., Heatflow into a New Mine Roadway. Colliery Engineering 1958, pp. 73-76, 117-122.

54. Hinsley, F. B., A Reappraisal of the Problems Concerned with the Reversal of the Ventilation Flow in an Emergency. The Mining Engineer, March 1967.

55. Hottel, H. C. and Mangelsdorf, H. G., Heat Transmission by Radiation From Non-Luminous Gases. Experimental Study of Carbon Dioxide and Water Vapor. Transaction Am. Inst. Chem. Engrs. 31 (1935), pp. 517-549.

56. Hottel, H. C. and Egbert, R. B., Radiant Heat Transmission from Water Vapor. Transaction Am. Chem. Engrs. 38 (1942), pp. 531-68.

57. Hrbác, J. and Tesar, J., Interdependence of Ventilation Pressure and Thermal Draft in Mine Shafts. International Congress on Mine Ventilation, Joachimsthal (CSR) 1968.

58. Jakob, M., Heat Transfer. John Wiley & Sons, Inc., New York-London 1959.

59. Jaeger, J. C., Heat Flow in the Region Bounded Internally by a Circular Cylinder. Proc. Roy. Soc. Edinb. (A) 61, 1942, pp. 223-28.

60. Jaeger, J. C. and Clarke, M., A Short Table of etc. Proc. Roy. Soc. Edinb. (A) 61, 1942, pp. 229-30.

61. Jordan, D. W., The Numerical Solution of Underground Heat Transfer Problems - I. Method Relating to Dry Roadways. Int. Journ. Rock Mech. Min. Sci. 2 (1965) pp. 247-70.

62. Jordan, D. W., Sharp, D. F. and Moore, B., II. Details of Numerical Calculations Relating to a Static Roadway and to an Advancing Roadway in a Dipping Seam. Int. Journ. Rock Mech. Min. Sci. 2 (1965), pp. 341-63.

63. Jordan, D. W., III. The Calculation of Temperature Distribution in Dry and Wet Force Ventilated Headings. Int. Journ. Rock Mech. Min. Sci. 2 (1965), pp. 365-87.

64. Kappelmeyer, O. and Mundry, E., About the Solution of the Heat Conductivity Equation. Kali und Steinsalz 1963, pp. 359-62.

65. Keenan, C. M., Coal Mine Fires and Gas and/or Dust Ignitions Since Enactment of the 1952 Federal Coal Mine Safety Act. USBM Inf. Circ. 7967.

66. Kennedy, M. and Taylor, G., Temperature Distribution Downwind of Stationary Mine Fires. Brit. J. Appl. Phys. 18 (1967) pp. 349-56.

67. Kingery, D. S., Introduction to Mine Ventilation Principles and Practice. USBM Bull. 589, 1960.

68. Klinger, K., Large Scale Mine Fire Experiments to Test Measures to Stop Open Mine Fires. Glueckauf 1955, pp. 329-337.

69. Koenig, H., Mathematical Investigation of the Mine Climate. Bergbau-Archiv 13 (1952), H. 3/4, pp. 1-14.

70. Kremnev, O. A. and Koslov, E. M., Coefficient of Non-Steady Heat Exchange in Mine Workings with an Aircurrent Temperature Variable in Time. Dop. Akad. Nauk Ukr. RSR 1961, pp. 307-10.

71. Kremnev, O. A. and Mosin, I. M., The Theoretical Foundations of the Calculation of Temperature Conditions in Mine Workings at Fire. Dop. AN Ukr. RSR 1961, pp. 1487-89.

72. Leech, W. A., Carbonization of Coal and Gas Making. Marks' Standard Handbook of Mechanical Engineers. McGraw-Hill Book Company, New York 1967.

73. Lenz, O., Methods of Ventilation Network Calculations. Bergbau-Archiv 22 (1961), No. 1, pp. 11-25.

74. Maas, W., An Electrical Analogue for Mine Ventilation and its Application to Ventilation Planning. Geologie en Mijnbouw 12 (1950), No. 4, pp. 117-23.

75. Maas, W. and Sadée, C., Reversal of Airflow by a Fire. Geologie en Mijnbouw 45 (1966), No. 3, pp. 59-69.

76. Massen, F., Ventilation Calculations by Digital Computer. Bergbauwissenschaften 1962, pp. 179-90.

77. McCrodan, P. B., Underground Fire at McIntyre Porcupine Mines Ltd., Canad. Min. Journ. 1965, Sept., pp. 66-75.

78. McElroy, G. E., A Network Analyzer for Solving Mine Ventilation Distribution Problems, USBM Inf. Circ. 7704.

79. McPherson, M. J., Ventilation Network Analysis by Digital Computer. The Mining Engineer, Oct. 1966, pp. 12-28.

80. McPherson, M. J., Mine Ventilation Network Problems: Solution by Digital Computer. Colliery Guardian 209, Aug. 1964 pp. 253-59.

81. Mitchell, M. and Nagy, C., Practical Aspects in Fighting a Fire of a Mining Machine. International Meeting of the Directors of Mine Safety Institutes. Warsaw 1961.

82. Mitchell, D. W., Fighting Mine Fires. Transact. SME 223 (1962), pp. 218-24.

83. Mundry, E., About the Solution of the Heat Conduction Equation: Mathematical Treatment of the Problem. Kali and Steinsalz 1963, H. 11, pp. 363-71.

84. Mundry, E., A Method to Calculate Air Temperatures in Wet Mines. Kali und Steinsalz 1964, H. 2, pp. 37-41.

85. Myers, J. W., Goldberg, S. A. and Smith, R. W., Calculation of Theoretical Temperatures in Furnaces. Transact. ASME 80 (1958), pp. 202-16.

86. Nagy, J., Hartmann, I. and Howarth, H. C., Tests on the Control of Coal Mine Fires in the Experimental Coal Mine. USBM Rep. Inv. 4685.

87. Nagy, J., Murphy, E. M. and Mitchell, D. W., Controlling Mine Fires with High Expansion Foams. USBM Rep. Inv. 5632.

88. National Coal Board (UK): Solution of Mine Ventilation Networks. Finance Department - Computer Services, 1967.

89. Neumann, W., Plasche, F. and Sonnemann, G., Mine Ventilation and Fighting of Mine Fires. VEB Deutscher Verlag fuer die Grundstoff-industrie, Leipzig, 1963.

90. Nicholson, J. W., A Problem in the Theory of Heat Conduction. Proc. Roy Soc. (A), 1921, pp. 226-40.

91. Nottrot, R. and Sadée, C., Cooling of Homogeneous Isotropical Rock Surrounding a Circular Airway by Air of Constant Temperature. Glueckauf-Forschungshefte 1966, H. 4, pp. 193-200.

92. Oberbergamt Dortmund, Regulations for the Coal Mines in the Administrative District of the Oberbergamt Dortmund, Dec. 18, 1964.

93. Oka, Y., Kiyama, H. and Hiramatsu, Y., Analyzing Ventilation Network Problems by a Digital Computer. Journ. Min. Metal. Inst. Japan 83 (1967) No. 945, pp. 1-7.

94. Osipov, S. N. and Zadan, V. M., Progress of a Fire in a Horizontal Mine Roadway. Ugol Ukrainy 11 (1967) No. 9, pp. 35-38.

95. Osipov, S. N. and Zadan, V. M., Simplified Method to Determine the Stability of Air Currents in Case of Mine Fires. Ugol 44 (1969) No. 7, pp. 57-61.

96. Parker, A. S. and Hottel, H. C., Combustion Rate of Carbon. Industrial & Eng. Chemistry 28 (1936) pp. 1334-41.

97. Patigny, J., Investigation of the Ventilation of Mines with Electrical Analogues. Revue Universelle des Mines, Vol. XIV, No. 11, 1958.

98. Rabstyn, J. and Bystron, H., Air Potential and Safety in Mines. Intern. Conf. Mine Safety Tokyo, 1969.

99. Ramsay, H. T., Presidential Address to the Midland Institute of Mining Engineers, The Mining Engineer 130 (1970-71), pp. 311-16.

100. Roberts, A. F. and Kennedy, M., Modeling of Mine Roadway Fires. SMRE Research Report 239, 1965.

101. Roberts, A. F., Clough, G. and Blackwell, J. R., A Model Duct for Mine Research. SMRE Research Report 243, 1966.

102. Roberts, A. F. and Clough, G., Model Studies of Heat Transfer in Mine Fires. SMRE Research Report 247, 1967.

103. Roberts, A. F. and Clough, G., The Propagation of Fires in Passages Lined with Flammable Material. Combustion and Flame 1967, No. 5, pp. 365-76.

104. Roberts, A. F., and Blackwell, J. R., The Possibility of the Occurrence of Fuel Rich Mine Fires. The Mining Engineer 1969, pp. 699-709.

105. Roberts, A. F., Fires in the Timber Lining of Roadways: A Comparison of Data from Reduced-Scale and Large-Scale Experiments. SMRE Research Report 263, 1970.

106. Roberts, A. F., Fires in Ducts Under Forced Ventilation Conditions. Fire Technology 1970, No. 1, pp. 13-21.

107. Scerban, A. N. and Kremnev, O. A., The Scientific Basis of Calculations and Control of Climatic Conditions in Deep Mines. AN Ukrain. R.S.R., Kiev 1959.

108. Scerban, A. N., Kremnev, O. A. and Zuravlenko, V. J., Manual for Heat Calculations of Mines and for the Planning of Air Cooling Plants. Gosgartechizdat, Moscow 1960.

109. Scott, D. R. and Hinsley, F. B., Ventilation Network Theory. Colliery Engineering 28 (1951), pp. 67-61, 159-66, 229-35, 497-500.

110. Scott, D. R., Hudson, R. F. and Hinsley, F. B., A Calculator for the Solution of Ventilation Network Problems. Transact. Inst. Min. Engrs. 112, 1952-53, pp. 624-37.

111. Scott, D. R., The Cooling of Underground Galleries. Transact. Inst. Min. Engrs. 118 (1959), pp. 355-79.

112. Scott, J. L., Marovelli, R. L. and Yancik, J., Status Report on the Bureau's Fire and Explosion Program. Coal Age 77 (1972), pp. 92-99.

113. Seelemann, D., Calculation of Ventilation Networks. Chapter V of the Handbook Mine Ventilation. Revue de l'Industrie Minerale, 1962.

114. Schmidt, W., Calendar for Mine Officials in Coal Mines 1963. Karl-Marklein-Verlag, Duesseldorf 1963.

115. Schmidt, W., Instabilities in Descensional Ventilation. International Congress for Mine Ventilation. Joachimsthal (CSR) 1968.

116. Schmidt, W., Document No. 4179/70d, Expert Group Ventilation, ECSC 1970.

117. Schmidt, W., Ventilation Stability and Stabilizing Possibilities. 14. International Conference of Mine Safety Institutes, Doniezk 1971.

118. Schmidt, W. and Grumbrecht, K., Influence of Fires on Descensional Ventilation. Unpublished Report, 1971.

119. Smith, L. P., Heat Flows in an Infinite Solid Bounded Internally by a Cylinder. J. App. Physics 1937, pp. 441-48.

120. Simode, E., Contribution to the Stabilization of Ventilation Systems During Mine Fires. ECSC Doc. 3532/70d.

121. Skotschinski, A. A. and Komarov, W. B., Mine Ventilation. Ugletechizdat, Moscow-Leningrad 1951.

122. Starfield, A. M., Tables for the Flow of Heat into a Rock Tunnel with Different Surface Heat Transfer Coefficients. J. S.A. Inst. Min. Metall. 1966, pp. 692-94.

123. Stokes, B. and Cernik, B., The Fight Against High Mine Temperatures. J. Springer, Berlin 1931.

124. Suzuki, T., Analytical Studies on Ventilation Networks for Preventing Coal Mine Explosions. 10th International Conference of Directors of Mine Safety Institutes, Pittsburgh 1959.

125. Tesar, J. and Suchen, S., Report of the Mine Catastrophe at the Mine Dukla. Actualities from Mining Research, Tisk 04, Prerov (CSR).

126. Trafton, B. O. and Hartman, H. L., The Use of Digital Computers for Mine Ventilation Problems. Transact. Soc. Min. Engrs. AIME 229 (1964), pp. 313-19.

127. Trutwin, W., Use of Digital Computers for the Study of Non-Steady States and Automatic Control Problems in Mine Ventilation Networks. Int. J. Rock Mechanics Min. Sci. 9 (1972), pp. 289-323.

127a. Trutwin, W., Modelling of Non-Steady States in Mine Ventilation Networks by Means of Analog Computers. Scientific Bull. Acad. Min. Metall. No. 230, pp. 1-83, Cracow 1968.

128. Trutwin W., Estimation of the Natural Ventilating Pressure Caused by Fires. Int. J. Rock Mechanics Min. Sc. 9 (1972) pp. 25-36.

129. Uhrig, E., Practical Application of the Digital Computer for Ventilation Planning. Bergbauwissenschaftern 11 (1964) No. 8, pp. 173-75.

130. Volkov, A. A. and Evdokimov, A. G., Mathematical Description of Steady State Flow Distribution Processes in Mine Ventilation Networks. Izvestija VUZ, Gornyj Zurnal 1965 (No. 2).

131. Voskobojnikov, V. I., Determination of a Favorable Ventilation When Fighting a Mine Fire by Using an Electric Analog Computer. Ugol Ukrainy 4 (1960) No. 7, pp. 16-20.

132. Voss, J., Contribution to the Precalculation of the Heat and Vapor Absorption of Air in Coal Mines. Glueckauf-Forschungshefte 26 (1965) No. 4, pp. 187-98.

133. Voss, J., A Method to Determine the Heat and Vapor Emission of Coal and Backfill in Haulage Roads and Faces. Glueckauf-Forschungshefte 26 (1965) No. 3, pp. 153-67.

134. Voss, J ., Determination of Thermal Properties from Measurements of the Heating of the Air and Cooling of the Rock in Intake Airways. Glueckauf-Forschungshefte 28 (1967) No. 2, pp. 67-80.

135. Voss, J ., A New Method for Climatic Precalculations in Coal Mines. Glueckauf-Forschungshefte 30 (1969) No. 6, pp. 321-31.

136. Voss, J., Climatic Precalculations for Producing Coal Faces. Glueckauf 1971, No. 11, pp. 412-18.

137. Wang, Y. J. and Hartman, H. L., Computer Solution of Three-Dimensional Mine Ventilation Networks with Multiple Fans and Natural Ventilation. Int. J. Rock Mech. Min. Sci. 4 (1967), pp. 129-54.

138. Wang, Y. J. and Saperstein, L. W., Computer Aided Solution of Complex Ventilation Networks. Transact. Soc. Min. Engrs. AIME 247 (1970), pp. 238-50.

139. Wang, Y. J. and Pana, M. T., Solution of Ventilation Network Problems by Linear Programming. AIME Meeting, New York, 1971.

140. Weaver, H. F., Cause Analysis of Coal Mine Fires and Ignitions. Safety Newsletter, Coal Mining Section, National Safety Council, August 1960.

141. Wehr, R. and Hennigsen, U., The Present State of Digital Computing Technique in the Field Mine Ventilation in the German Coal Mines. Glueckauf 106 (1970) No. 13, pp. 641-58.

142. Wilde, D. G., Fire Retardant Treatments for Mine Timber. The Mining Engineer 131 (1971-72) pp. 281-90.

143. Wiles, G. G., Cylindrical Heat Flow into a Tunnel. J. Chem. Soc. S.A. 1947, pp. 114-18.

144. Wiles, G. G., Theory Underlying Temperatures in Horizontal Airways. Journ. Chem. Met. Min. Soc. S.A. 1954, p. 133.

145. Wiles, G. G., Wet Bulb Temperature Gradients in Horizontal Airways. Journ. S.A. Inst. Min. Met. 1959, pp. 339-59.

146. Woropajew, A. F., Discussion of a Self-Produced Airflow Reversal When a Mine Fire Starts. Ugol 32 (1957) No. 3, pp. 27-30.

147. Zeidler, U., CO Measuring and Warning Instruments in the German Coal Mines. Glueckauf 1972, pp. 797-805.